UNIVERSITÄT BAYREUTH

Ups and downs of staying quiet underwater:

Characterization of the flooding-induced transcription factors RAP2.2 and LBD41 in *Arabidopsis thaliana*

Dissertation

to achieve the academic degree of

Doctor of Natural Sciences (Dr. rer. nat.)

submitted by

Marvin Cedric Hönle

born 25.06.1992 Augsburg, Germany

Bayreuth, March 2025

Die vorliegende Arbeit wurde in der Zeit von März 2019 bis August 2024 in Bayreuth am Lehrstuhl Pflanzengenetik unter Betreuung von Frau Professor Dr. Angelika Mustroph angefertigt.

Vollständiger Abdruck der von der Fakultät für Biologie, Chemie und Geowissenschaften der Universität Bayreuth genehmigten Dissertation zur Erlangung des akademischen Grades eines Doktors der Naturwissenschaften (Dr. rer. nat.).

Form der Dissertation: Monographie

Dissertation eingereicht am: 05.08.2024

Zulassung durch die Promotionskommission: 14.08.2024

Wissenschaftliches Kolloquium: 20.01.2025

Amtierender Dekan: Prof. Dr. Cyrus Samimi

Prüfungsausschuss

Prof. Dr. Angelika Mustroph (Gutachterin)

Prof. Dr. Stephan Clemens (Gutachter)

Prof. Dr. Gerrit Begemann (Vorsitz)

Prof. Dr. Andreas Möglich

Abstract

Consequential of a man-made climate change, our environment is subjected to rising ocean levels and increased frequency of extreme weather events. Among them, storm floods can cause a high stress situation for most established crop plants. To ensure a stable food supply of the future, natural mechanisms of tolerance require detailed understanding. Against flooding, *A. thaliana* utilizes a quiescent response strategy, including an upregulation of hypoxia responsive genes (HRGs) through the transcription factors GVIIERFs RAP2.2, RAP2.12 and RAP2.3. Differences between these three proteins were investigated here. Importance during flooding was studied in the context of HRG transcription and resulting activity, as well as survival during submergence. Here, a higher impact of RAP2.12 was measured, with a near-identical function of RAP2.2 and minor importance of RAP2.3. When studying plant responses to reocurring hypoxia, a potential memory effect is recorded.

Found among the HRGs induced by the GVIIERFs is the transcription factor LBD41. This protein promotes a repressive transcriptional effect on various seemingly unrelated target genes. Through studying KO and OE variant lines of LBD41, further characteristics of this elusive transcription factor are defined. Additional to its induction through hypoxia, increased activation of LBD41 was found in connection with germination, maturation and salt stress. The consequences of combined salt and low oxygen stress was investigated, where an overlap to LBD41 regulated genes could be found. Furthermore, a substantially reduced survival rate to submergence is recorded through misregulated overexpression. Additionally, the previously postulated post-translational modification of LBD41 could be detected in *A. thaliana* and when expressed in *N. benthamiana*. This modification with likely a single SUMO1 appears as the dominant proteoform, independent of hypoxia. Further modification is detected in heterologous *N. benthamiana* expression and the implications on activity and survival discussed. Potential orthologs of LBD41 in *N. benthamiana*, and conserved putative modification sites were identified. Further regulatory mechanisms influencing the activity of LBD41 are proposed.

Kurzfassung

Als Folge des menschengemachten Klimawandels ist unsere Umgebung steigenden Meeresspiegeln und erhöhter Frequenz an extremen Wetterereignissen ausgesetzt. Sturmfluten stellen eine besonders stressvolle Situation für die meisten Kulturpflanzen da. Um eine sichere Lebensmittelversorgung in der Zukunft zu gewährleisten, müssen natürliche Toleranzmechanismen im Detail verstanden werden. Bei Überflutung führt *A. thaliana* eine ruhende Antwortstrategie aus, einschließlich der Hochregulation von Hypoxie-responsiven Genen (HRGs) durch Transkriptionsfaktoren GVIIERFs RAP2.2, RAP2.12 und RAP2.3. Unterschiede zwischen diesen drei Proteinen wurden untersucht. Die Relevanz dieser Proteine während Überflutung wurde im Zusammenhang mit Transkription von HRGs und deren resultierende Aktivität, sowie dem Überleben unter Wasser betrachtet. Die wichtigste Rolle wurde für RAP2.12 gemessen, mit nahezu identischer Funktion von RAP2.2 und nur geringer Wichtigkeit von RAP2.3. Durch Untersuchung von wiederkehrendem Sauerstoffmangel konnte eine möglicher Erinnerungseffekt festgehalten werden.
Innerhalb der von GVIIERFs induzierten HRGs befindet sich der Transkriptionsfaktor LBD41. Dieses Protein führt einen repressiven Effekt auf mehrere scheinbar unzusammenhängende Zielgene aus. Durch Betrachtung von KO und OE mutanten Pflanzenlinien, können weitere Eigenschaften dieses komplexen Transkriptionsfaktors aufgedeckt werden. Zusätzlich zur Induktion durch Hypoxie, konnte erhöhte Aktivierung in Zusammenhang mit Keimung, Reifung und Salzstress festgestellt werden. Die Folgen von kombiniertem Salzstress und Sauerstoffmangel wurden untersucht, wodurch eine Überschneidung der regulierten Gene gefunden wurde. Zusätzlich verursachte Überexpression einen wesentlichen Einbruch des Überlebens bei Überflutung. Des Weiteren konnte die zuvor postulierte post-translationale Modifikation von LBD41 in *A. thaliana* detektiert werden. Diese Modifikation findet durch vorraussichtlich ein einzelnes SUMO1 statt, und stellt die dominante Form des Proteins dar. Weitere Modifikationen wurden durch heterologe Expression in *N. benthamiana* entdeckt, sowie potenzielle *N. benthamiana* Orthologe von LBD41 identifiziert. Konservierte SUMOylierungsstellen sowie weitere putative Regulationsmechanismen der Transkriptionsantwort werden diskutiert.

List of abbreviations

ADH	Alcohol dehydrogenase
ANOVA	Analysis of Variance
AOX1D	Alternative oxidase 1 D
AP2	Apetala 2
APS	Ammonium persulfate
ATE	Arginyl-tRNA:protein-arginyltransferase
ATP	Adenosine triphosphate
Col-0	Columbia-0
DNA	Deoxyribonucleic acid
dNTP	Deoxynucleotide triphosphate
DTT	Dithiothreitol
EAR	ERF-associated amphiphilic repression
EF-1α	Elongation factor 1 α
EIN3	Ethylene insensitive 3
GFP	Green fluorescent protein
GGT4	Gamma glutamyl transpeptidase 4
GVIIERF	Group VII Ethylene responsive factors
HA	Human influenza hemagglutinin
HADLH	Haloacid dehalogenase-like hydrolase
HDAC	Histone deacetylase
HIF1a	Hypoxia inducible factor 1 α

HRA	Hypoxia response attenuator
HRE	Hypoxia responsive ERF
HRG	Hypoxia responsive gene
HRPE	Hypoxia responsive promoter element
HS	Hoagland Salt medium
KO	Knockout
LB	Lysogeny broth
LBD	Lateral organ boundaries domain (containing protein)
LOES	Low oxygen escape syndrome
LOQS	Low oxygen quiescence syndrome
Luc	Luciferase
MAP	Met-Aminopeptidase
MS	Murashige-Skoog
MW	Molecular weight
NAD	Nicotinamide adenine dinucleotide
OE	Overexpression
ON	Over night
PAGE	Polyacrylamide gel electrophoresis
PAM	Protospacer adjacent motif
PAP1	Production of anthocyanin pigment 1
PBS	Phosphate-buffered saline
PcG	Polycomb group
PCR	Polymerase chain reaction
PCO	Plant cysteine oxidase
PDC	Pyruvate decarboxylase
PGDH	3-Phosphoglycerate dehydrogenase

Phy	Phytochrome
PIF	Phytochrome interacting factor
PTA	Protoplast transactivation assay
PUP10	Purine permease 10
PVDF	Polyvinylidene fluoride
qPCR	Quantitative polymerase chain reaction
RAP2	Related to APETALA 2
RNA	Ribonucleic acid
ROS	Reactive oxygen species
RT	Room temperature
RT-PCR	Reverse transcription polymerase chain reaction
SDS	Sodium dodecyl sulfate
SLAH3	Slac1 homologue 3
SUMO	Small ubiquitin like modifier
TPL	Topless
UAS	Upstream activation sequence
Ub	Ubiquitin
VP16	Virus protein 16
WT	Wild type
YEB	Yeast extract beef
40 41 42	LBD40 LBD41 LBD42

Contents

CHAPTER 1

Introduction

1.1 A brief history of oxygen and humans

All advanced lifeforms as we know them require oxygen in some capacity, but it was not always this available. In the first 1.5 - 2 billion years of our planet's estimated 4.5 billion years existence, Earth's atmosphere was nearly completely devoid of oxygen (Kump, 2008) (Zahnle et al., 2010). Only through the evolution of photosynthesis by cyanobacteria approximately 2.5 - 3 billion years ago, aerobic life became possible (Chen et al., 2022) (Large et al., 2022) (Schirrmeister et al., 2015). Since then, oxygen levels have fluctuated multiple times, reaching 150 % of our current atmospheric content during the Jurassic period (Borzenkova et al., 2009). However, by the time the first apes or *Hominidae* originated 20 million years ago, oxygen made up around 21 % of our atmosphere as it does today (Mills et al., 2023).

The human path towards civilization was fundamentally changed with the agricultural growing of crop plants, named the neolithic period. Only for about 10,000 - 12,000 years has humanity been actively cultivating plants and slowly adapted to a more sessile lifestyle (Barker, 2006) (Oras et al., 2023) (Zeder, 2011). The practice of controlling which plants are regrown and protecting them from harm proved more effective than foraging. Over time, the first settlements began further influencing plant life around them by selectively breeding crops for favorable traits (Fuller et al., 2014). Through the millennia since then, agriculture all over the world evolved through ages of yield optimization by different methods of planting, pest control, fertilization, or irrigation. However, as humanity faces a rapidly changing climate and exponential population growth, new advancements from multiple fields of research need to be employed quicker than ever before.

1.2 Population growth and its food demand

One of humanity's biggest challenges moving forward is expanding and evolving its food supply to match the needs of a globally growing population (Dijk et al., 2021) (Sadigov, 2022). The human population explosion which occurred within the last two centuries encompasses a massive scale. Of the roughly 117 billion *Homo sapiens* estimated to have ever existed on Earth in the last 192,000 years, around 6.8 % are alive at this moment (Kaneda et al., 2022). This growth would not be possible without ever increasing food availability, oftentimes resulting from agricultural innovations. Just within the 20th century alone, the global population increased from approximately 1.6 billion to 6 billion. This growth was fueled in large parts through the discovery of ammonia generation for synthetic fertilizers by Fritz Haber in 1908 (Erisman et al., 2008) (Smil, 1999) (Stewart et al., 2005).

With a current population of around 8.1 billion, this exponential human growth is expected to further shape the 21st century. Current estimations project a global population of around 10 billion by the year 2050, possibly over 14 billion by 2100 (O'Sullivan, 2023) (U.N. Department of Economic and Social Affairs Population Division, 2022). It is most likely that traditional farming practices will not be sufficient to sustain this surge in food demand (Food and Agriculture Organization of the United Nations, 2023) (Molotoks et al., 2018). Therefore, it is crucial that we explore multiple approaches to secure our plant-based food production. From the use of alternative growing techniques such as hydro- or aeroponics, to more yield efficient and stress resistant crops (FAO United Nations, 2023) (Ranganathan et al., 2018). For the foreseeable future, the majority of crops will be grown traditionally on fields. Here they are subjected to fluctuating conditions, including an increasing occurrence of extreme weather events.

1.3 Climate change and water

For at least 70 years scientists have warned about a human caused climate change, which is agreed upon in 99 % of peer-reviewed literature (Lynas et al., 2021). Especially the increase of atmospheric greenhouse gases was shown as a major cause of concern (Sawyer, 1972). These emissions of mainly CO_2, methane and N_2O were reported as strong contributors to a global

warming effect because of their infra-red trapping properties (Anderson et al., 2016) (Jain, 1993) (MacKay et al., 2000) (Tavassoli et al., 2023). With a rise in global mean surface temperature, the atmospheric water-holding capacity also increases. With a 1 °C rise in air temperature already increasing the water vapor content by 7 % (Coumou et al., 2012) (Santer et al., 2007). As a result of this atmospheric change, some regions will face a higher prevalence of drought. These areas will be affected by an increasing demand for artificial irrigation to maintain agriculture and the likely disappearance of species with a high water demand (Balting et al., 2021) (Gamelin et al., 2022).

Simultaneously, in other geographic regions, this leads to a high frequency of strong precipitation events. Such heavy rain almost inevitable leads to increased flooding (Fischer et al., 2015) (Santer et al., 2007) (Tabari, 2020). Furthermore, ocean levels are projected to continue rising, endangering coastal regions (Mimura, 2013). While these natural catastrophes already pose a threat to human lives directly, their effect on crop yield and food availability entails far-reaching consequences. In 2021, record rainfall of up to 150 L/m^2 within 24 h led to flooding that affected large parts of Rhineland Palatinate, North Rhine-Westphalia, Bavaria and Saxony. Additionally to over 180 people which lost their lives, these floods caused at least 200 M€ in agricultural damage alone (Bundesministerium des Innern und für Heimat et al., 2022). Such floods cannot be fully prevented, thus we need to find ways to minimize the damage they cause. To protect our crops from devastating effects, we need to understand how they themselves respond to such events. By studying traits of successful adaptations to flooding, the same principles might be applicable for future crops.

1.4 The flooding environment

When they are subjected to flooding, plants experience a multitude of changes in their environment. Firstly, the overabundance of water leads to a displacement of nearly all surrounding air. Under standard conditions air contains 20.95 % oxygen. However, even when still saturated with air, water contains less than 1 % oxygen (Kutty, 1987). If oxygen content drops below the normal air levels or normoxia, this state of low oxygen is called hypoxia, while a complete absence of oxygen is named anoxia (Sasidharan et al., 2017). Adjacent to this

drastic difference in oxygen content is the movement of gases within a liquid. For oxygen specifically, the diffusion coefficient in water of 1.90 x 10^{-9} m^2/s is 10,000 times lower than in air with 1.98 x 10^{-5} m^2/s (Armstrong, 1980) (Jackson, 1985) (Schachtschabel et al., 1998). Other gases such as nitric oxide (NO) and CO_2 can also be limited underwater, depending on soil composition and water depth. Compared to the modern 420 ppm in air, CO_2 content in water ranges from air-equal levels to under 10 ppm (Friedlingstein et al., 2022) (Mitchell et al., 2010) (Someya et al., 2005). With the erosion of soil combined with hypoxic conditions, the distribution of minerals also changes. Under low oxygen, microorganisms reduce Fe^{3+}-Phosphorus complexes, leading to the release of P and Fe^{2+} (Maranguit et al., 2017).

Figure 1: Flooding changes the plant environment

Overview of factors involved in flooding and their effect on plants. Arrows indicate changes in environmental and cellular composition. Picture was taken near Bayreuth, Germany.

Another key factor affecting survival underwater is the availability of light. Fortunately for submerged organisms, water mostly absorbs far-UV light and far-red above 650 nm, allowing most light wavelengths between 300-600 nm to pass through. Even at a depth of 10 m, around 80 % of blue light at 450 nm is still available (Pope et al., 1997) (Wozniak et al., 2006). However, flooding water is usually not clear. Instead, the water masses quickly erode their surrounding soil and sediment. A murky and darkened water increases the absorption of light, while decreasing its availability for plants. Without sufficient light, PHOTOSYSTEM II is unable

to supplement the plant through oxygenic photosynthesis, further intensifying the state of hypoxia (Pedersen et al., 2018). Furthermore, while plants usually need to protect themselves constantly from air- and soil-borne pathogens and pests, in a flooded environment they are now more susceptible to water-based bacteria and fungi (Cameron et al., 1978) (Francioli et al., 2022). Therefore, a submerged plant needs to adjust to a new microbiome while already stressed by reduced light and oxygen availability.

1.5 A plant's oxygen needs

As one of life's most essential building blocks, the element Oxygen is required by all aerobe organisms including plants. In a flooding environment, a substantial limitation of plants is their lack of a circulative oxygen transportation system. Many animals evolved effective methods of allocating oxygen to tissue through heart- or heart-like muscles (Stephenson et al., 2017). For example, transport via blood of an average human male results in a total oxygen delivery rate of 0.997 L/min, with 98 % bound as oxyhemoglobin (Dunn et al., 2016) (Kaufman et al., 2023). Plants however, possess no active gas transportation mechanisms and rely entirely on passive diffusion for oxygen distribution (Farquhar et al., 1989). While this type of oxygenation is sufficient when most of the plants surface is in contact with air, its effectiveness drops drastically under water. As a terminal electron acceptor, plants require oxygen for chemical energy production in the form of ATP, through the mitochondrial electron transport chain (mETC) (Lambers et al., 2005) (Tcherkez et al., 2017).

Under limited oxygen, the mETC process of oxidative phosphorylation at the CYTOCHROM C OXIDASE is missing its key substrate and becomes inactive (Taylor et al., 2010). With an ineffective mETC, ATP can only be supplied through glycolysis, which in turn requires a supply of oxidized NAD^+ (Rees, 1985). To now produce sufficient amounts of NAD^+ without oxidative respiration, the plant turns to ethanol and lactate fermentation. This is achieved by up-regulating pyruvate decarboxylase (PDC) and alcohol dehydrogenase (ADH), despite the cellular toxicity of their products (Loreti et al., 2020). While this mechanism allows for further production of ATP, it is exceptionally inefficient. Under normal oxygen availability, a single molecule of Glucose is used to produce 38 molecules of ATP throughout its catabolic process.

With fermentation however, a Glucose molecule only yields 2 molecules of ATP, showcasing how plants quickly run out of energy without fresh air (Jardine et al., 2023) (Tadege et al., 1998). Besides ATP production, many plant processes involve oxygen as a powerful electron donor in enzymatic reactions (Jabłońska et al., 2019) (Romero et al., 2018). Also among some of the oxygen dependent mechanisms are biosynthesis of short-lived phytohormones such as gibberellic- and abscisic acid or ethylene (Pattyn et al., 2021). Oxygen also serves as a signal in the form of reactive oxygen species (ROS), involved in a variety of stress signaling (Kohli et al., 2019) (Mansoor et al., 2022) (Noctor et al., 2016). Therefore, while a certain demand for oxygen is ubiquitously present within plants, the immediate oxygen need varies depending on biotic and abiotic factors.

1.6 Hypoxia in plants

While flooding events are the strongest initiators of hypoxic stress, severity of the resulting energy crisis depends on how much of the plant is underwater. If only the roots and parts of the stem are submerged, the environment is described as waterlogging, which still allows gas exchange through the upper parts of the plant and most leaves (Sasidharan et al., 2017). While still a hypoxic stress, waterlogging usually does not lead to a full depletion of oxygen or CO_2 (Pan et al., 2021). Some plant varieties like the common watercress *Nasturtium officinale* or the marsh yellowcress *Rorippa palustris* even adapted to a highly water-saturated environment (Akman et al., 2014) (Müller et al., 2021). However, in the case of full submergence the entire organism is below the surface, resulting in a high stress situation that threatens the plants survival. This overabundance of water leads to a drastically reduced gas exchange and depending on its duration, a full depletion of oxygen and CO_2 (Fukao et al., 2019). Even as the water retreats and re-oxygenation takes place, survival of the plant remains uncertain. The quick burst of oxygen combined with increased light creates an overabundance of ROS, potentially damaging cells severely (Jethva et al., 2022) (León et al., 2021) (Pucciariello et al., 2021).

However, not all occurrences of hypoxia in plants are the result of unfavorable conditions. When short term, transient low-oxygen occurs it is referenced as acute hypoxia and mostly provides a stressful situation for the plant (Loreti et al., 2020). Contrary, so-called chronic hypoxia is confined to specific tissue types and utilized as a developmental signal. A hypoxic niche

is even required to complete leaf organogenesis in shoot apical meristems (SAM) as well as induce growth in lateral root primordia (LRP). There, oxygen gradients are used to induce directional growth (Le Gac et al., 2019) (Weits et al., 2019). Another example of chronic hypoxia is found in some seeds, where low oxygen creates a protective gas-impermeable layer (Borisjuk et al., 2009). It is unclear if these hypoxic niches are established through an increase in oxygen consumption, or a still undiscovered diffusion barrier. Nevertheless, most plant tissue will suffer adverse effects of prolonged hypoxia. As without a terminal electron acceptor for mitochondrial respiration, energy homeostasis suffers greatly.

1.7 Flooding stress-induced plant adaptations

When looking at the response to flooding in plants, two distinct strategies of tolerance were identified: Escape or Quiescence. While generally behaviour of a plant under hypoxia can be classified in one of these strategies, mechanisms of acclimation are not exclusive to either strategy.

The low-oxygen escape syndrome (LOES) is mostly executed through morphological and anatomical changes. Simply put, these plants attempt to reduce the effects of flooding stress on their metabolism by escaping a low-oxygen environment (Bailey-Serres et al., 2008) (Nakamura et al., 2020). These anatomical changes serve in improving the plants oxygen supply, either by increasing air surface area or improving internal gas distribution. The most prominent among these morphological escape changes are the elongation of leaf and stem regions to reach the surface. Additionally, development of adventitous roots for increased gas exchange, as well as aerenchyma formation, which increases internal aeration through controlled cell death, are found frequently (Jia et al., 2021). If successful, these acclimations lead to an increased oxygen availability, allowing for a vastly extended survival duration. When these changes however do not suffice in achieving an improved aeration, the plant will have used up most of its energy reserves on growth instead of survival. Another issue arises at the end of the flooding stress and the following withdrawal of water, as the now acclimated plants can be structurally deficient to support their own weight (Bailey-Serres et al., 2012) (Voesenek et al., 2015).

The second strategy of tolerance called low-oxygen quiescent syndrome (LOQS), mainly

revolves around the concept of outlasting flooding events (Bailey-Serres et al., 2008). With flooding resulting from heavy precipitation, hypoxia events are mostly temporary. While essential functions need to be maintained to allow for later recovery, reduced ATP production requires switching to an energy-conserving state. To facilitate this quiescence, a variety of metabolic acclimations take place. Leaf growth is mostly stopped and carbohydrate metabolism altered. These plants also induce fermentation to maintain NAD^+ electrochemistry and sustain essential functions. Simultaneously however, ATP-intensive processes such as lipid synthesis, secondary metabolism, as well as most redox-regulation mechanisms are downregulated to preserve energy (Ismond et al., 2003) (Jethva et al., 2022) (Klok et al., 2002) (Dongen et al., 2009) (Xie et al., 2021). While these mostly biochemical acclimations are well suited for short term stress survival, prolonged flooding will eventually lead to starvation.

The model organism mouse-ear cress *Arabidopsis thaliana* is considered moderately flooding tolerant and enacts a mostly quiescent syndrome. Even without morphological changes, *A. thaliana* survives submerged conditions for up to one month, depending on lighting availability (Vashisht et al., 2011). While no elongation of stem regions takes place underwater, *A. thaliana* exhibits an uplifting of leaves called hyponastic response (Eysholdt-Derzsó et al., 2019) (Lee et al., 2011).

1.8 Low-oxygen sensing

For a directed and controlled acclimation during flooding events, the low-oxygen state must first be sensed by a plant. While strategies of hypoxia acclimation can vary even between closely-related ecotypes, cellular identification of the low-oxygen state appears strongly conserved. While no biological oxygen sensor can be found that directly quantifies a low-oxygen state, higher organisms sense hypoxia through a combination of factors. Even both plants and animals posses a technique to measure oxygen indirectly, similar in its functionality (Holdsworth et al., 2020) (Licausi et al., 2020) (Masson et al., 2019). Many representatives of the plant kingdom, including *Arabidopis thaliana*, constitutively express the transcription factors GROUP VII ETHYLENE RESPONSIVE FACTORS (GVIIERFs) which could directly induce drastic changes of flooding acclimation (Giuntoli et al., 2018).

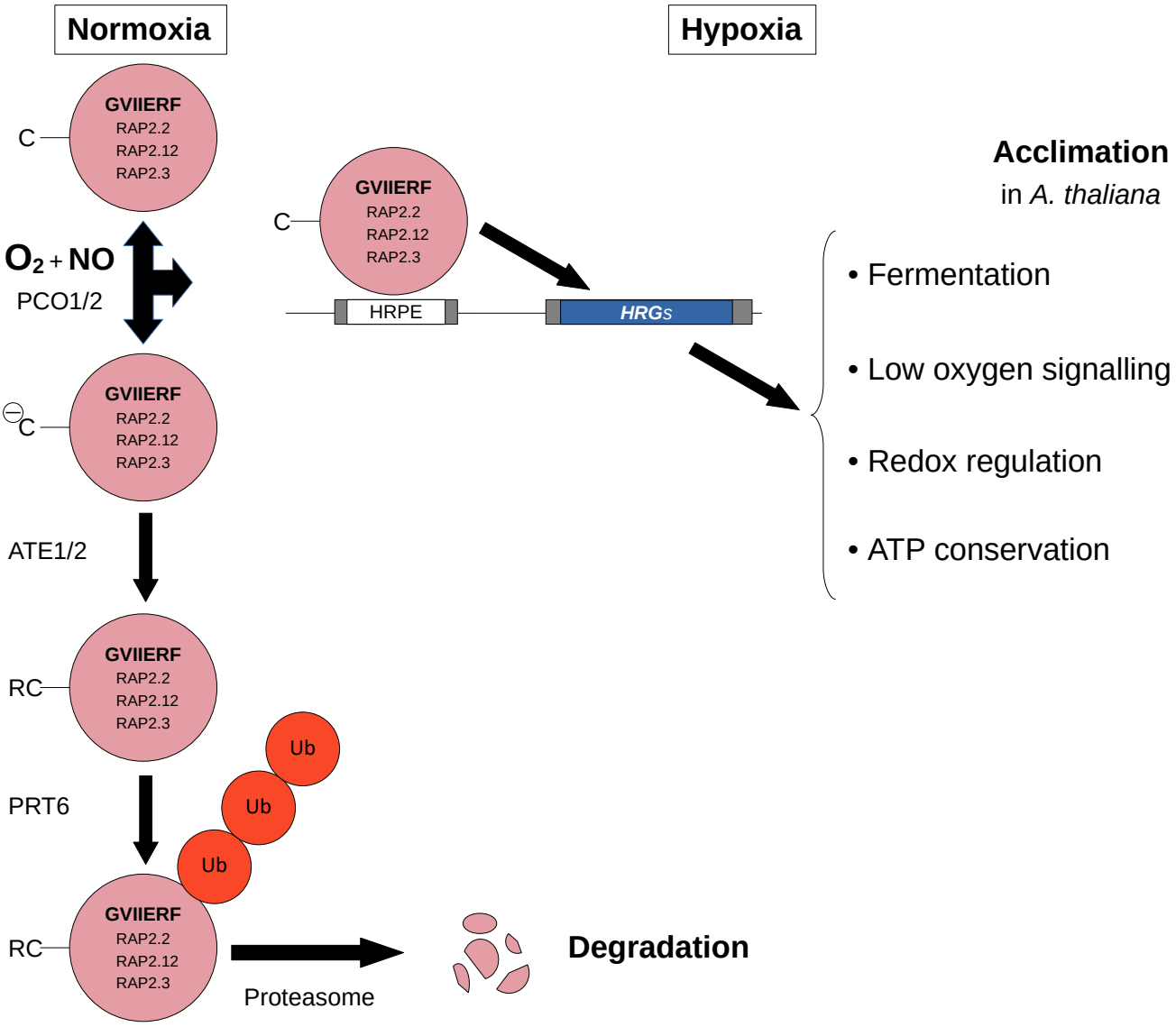

Figure 2: N-degron pathway regulates oxygen sensing

Depiction of the N-degron pathway mediated oxygen sensing through the GVIIERFs (RAP2.2, RAP2.12, RAP2.3, also HRE1 and HRE2, not depicted). Depending on O_2 and NO availability, the GVIIERFs are either degraded or allowed to accumulate. After the initial N-terminal methionine is cleaved off (not depicted) the exposed cysteine is oxidized by PCO1/2. This charged cysteine is then arginylated by ATE1/2. Following this step is a poly-UBIQUITINation through PRT6, leading to proteasomal degradation of GVIIERFs. Under Hypoxia, accumulated GVIIERFs bind to the HRPE motif and transcriptionally induce HRGs, activating low-oxygen acclimation.

However, to ensure that hypoxia acclimation only takes place in the event of flooding, the GVIIERFs are immediately processed for degradation under air. Despite their name, these proteins are not regulated by ethylene but rather the presence of O_2 and NO. This regulation mechanism is performed by the Cys branch of the N-degron pathway, through the conserved N-terminal MC residues of the GVIIERFs (Gibbs et al., 2011) (Licausi et al., 2011) (Sasidharan et al., 2011). Here, the N-terminal methionine is at first cleaved off by MET-AMINOPEPTIDASES (MAP1/2) and the now exposed cysteine is oxidized by PLANT CYSTEINE OXIDASES (PCO1/2). The GVIIERFs are further processed by adherence of arginine to the N-terminus through arginyl-tRNA:protein-arginyltransferases (ATE1/2). Following this step, the PROTEOLYSIS6 (PRT6) ligase interacts with the GVIIERFs, leading to ubiquitination and eventually degradation by the 26S proteasome (Fig. 2) (Dissmeyer, 2019) (Holdsworth et al., 2020). Therefore, even though the GVIIERFs are always expressed, there is no hypoxic acclimation under normoxia as the transcription factors are immediately broken down. A similar mechanism was also found in animals, through oxygen dependent degradation of HYPOXIA INDUCIBLE FACTOR 1α(HIF1a) (Ratcliffe et al., 1998) (Schofield et al., 2004).

Now if O_2 and NO levels go down under flooding conditions, the N-terminal cysteine is not oxidized or processed, which leads to the accumulation of GVIIERFs. The before-mentioned reduced gas diffusion underwater, also leads to accumulation of the gaseous phytohormone ethylene. As ethylene builds up resulting from limited gas exchange, the hormonal signal activates a first response even before cellular hypoxia occurs (Hartman et al., 2019). Within just 1 h of submergence the ethylene transcriptional regulator EIN3 accumulates. High levels of EIN3 lead to an increased expression of the NO scavenger PHYTOGLOBIN1, resulting in decreased NO-availability for degradation of GVIIERFs. While this pre-adaptation allows for faster changes once oxygen levels drop, the ethylene signal alone is not sufficient in activating most hypoxic genes (Hartman et al., 2021). This limitation is likely because fluctuating ethylene levels occur outside of flooding events, such as during root growth (Růžička et al., 2007).

1.9 Hypoxia acclimation by RAP2.2/2.12/2.3

In *A. thaliana* five GVIIERFs were identified, HYPOXIA RESPONSIVE ERF (HRE) homologs HRE1 and HRE2, as well as RAP2.12, RAP2.2 and RAP2.3 the RELATED TO APETALA2 (RAP) proteins of the APETALA family (Giuntoli et al., 2018). They are characterized by an AP2 domain as well as a highly conserved MCGGAII/L motif at the N-terminus. While they are all involved in hypoxic acclimation, HRE1 and HRE2 appear to induce only secondary regulation, however their individual characteristics have not been fully identified (Gibbs et al., 2015) (Licausi et al., 2010) (Phukan et al., 2017). Additionally to the N-degron pathway driven post-translational regulation, the GVIIERF RAP2.2 was found to be transcriptionally activated by WRKY33 and WRKY12 under hypoxia (Tang et al., 2021).

As oxygen levels drop and the N-degron pathway is disabled, the GVIIERFs accumulate and start executing their transcriptional activity. By binding to a 12 bp hypoxia responsive promoter element (HRPE) they activate the transcription of a multitude of hypoxia responsive genes (HRG) (Gasch et al., 2016) (Lee et al., 2021). Although the total induced transcripts vary depending on different plant organs, there is an overlap of 49 enriched mRNAs independent of cell type (Mustroph et al., 2009). This extensive change of the transcriptome named the core hypoxia response encodes for complex signalling, metabolic changes and also appears largely conserved (Mustroph et al., 2010). Most of the identified genes directly influence a survival mechanism, such as ADH1 based fermentation. However, the acclimation process is further regulated by at least three transcription factors (Mustroph et al., 2009) (Mustroph et al., 2014) (Sasidharan et al., 2011).

1.10 Transcriptional regulation in the core response

The first transcription factor induced through the hypoxia core response is HRE2, which as a GVIIERFs is itself involved in activating the hypoxia-responsive and ethylene-mediated GCC motif. While HRE2 was also linked with salt stress, it has been found to mostly regulate root functions (Lee et al., 2015) (Seok et al., 2014) (Seok et al., 2022). HRE2 was later confirmed as a main regulator of adventitious root formation under hypoxia (Eysholdt-Derzsó et al., 2019).

As both low oxygen and increased osmosis will affect lower plant parts first, a different transcriptional response in roots seems likely. However, the exact role of HRE2 requires future characterization. Also induced by the core response is the transcription factor HYPOXIA RESPONSE ATTENUATOR1 (HRA1). Instead of propagating the low oxygen response, HRA1 induces a negative feedback loop by downregulating transcription of RAP2.12 (Giuntoli et al., 2014) (Giuntoli et al., 2017). This regulation, which indirectly impacts the intensity of the core response, likely allows transcriptional fine-tuning of HRG regulation to prevent overshooting. Therefore, out of the three transcription factors induced in the core response, two are involved in a feedback loop. The third transcription factor ubiquitously expressed in all cell types under hypoxia, and major focus of this work, is the LOB-domain containing protein 41 (LBD41, AT3G02550).

1.11 The LBD protein family and LBD41

As an important class of transcription factors formally known as ASYMMETRIC LEAVES2-LIKE, the LATERAL ORGAN BOUNDARIES DOMAIN (LBD) protein family regulates various aspects of tissue differentiation (Shuai et al., 2002) (Zhang et al., 2020). They serve as essential controllers in plant organ development and growth, but have also been found to play a part in pathogen defense as well as abiotic stress responses (Thatcher et al., 2012) (Xu et al., 2016). All 42 LBD proteins identified in *A. thaliana* contain a conserved N-terminal LATERAL ORGAN BOUNDARIES (LOB) domain with a zinc finger-like $CX_2CX_6CX_3C$ motif for DNA binding. However their remaining sequence can differ strongly, dividing this family into two classes (Iwakawa et al., 2002).

With 36 members in *A. thaliana*, LBD proteins of Class I carry a leucine-zipper-like coiled-coil motif which has been associated with activity regulation by dimerization (Majer et al., 2011) (Pandey et al., 2018). This class is further divided into I-A with functions mostly in aboveground organ formation, while I-B and I-C LBD Proteins are primarily involved in root and tracheary development (Soyano et al., 2009).

LBD proteins in Class II however, do not contain a complete leucine-zipper motif or were found to functionally dimerize. Their LOB domain contains a CNGCRVLRKGCSE N-terminal

consensus sequence (Shuai et al., 2002). They are also classified by a conserved C-terminal ERF-associated amphiphilic repression (EAR) domain. Although this short domain varies in sequence, a LXLXL consensus could be identified. This motif has been found to transmit a repressive signal by first interacting with TOPLESS (TPL) proteins (Plant et al., 2021). They in turn recruit histone deacetylases (HDACs), resulting in heterochromatin formation and repression of targets through polycomb group (PcG) complexes (Baile et al., 2021) (Kagale et al., 2011). Additionally to their mechanistic differences, no essential roles during development were discovered for LBD proteins of Class II, and instead their involvement in biotic- and abiotic-stress responses have been reported. While LBD37, LBD38 and LBD39 are mostly involved with nitrogen starvation, LBD40, LBD41 and LBD42 are associated with hypoxic regulation (Zhang et al., 2020).

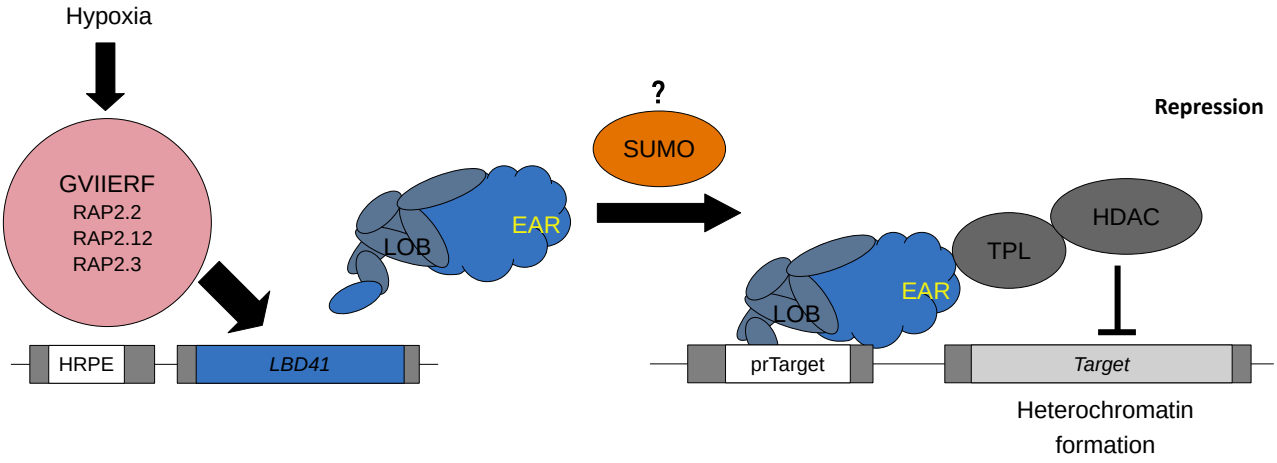

Figure 3: Regulation of LBD41, status quo

Current knowledge on the regulation of LBD41. Transcription is activated through binding of the GVIIERFs to the HRPE motif. The protein LBD41 is characterized by a N-terminal α-helix-heavy LOB domain, and C-terminal EAR motif. After LOB-mediated target promoter recognition, the EAR motif is recognized by TOPLESS (TPL). Responding to TPL binding, HISTON DEACTEYLASES (HDAC) are recruited. Activity of HDACs then leads to a formation of heterochromatin and the repression of target genes. A putative post-translational regulation through SUMO is speculated.

As a member of Class II within the LBD family, LBD41 displays nearly no basal transcription under control conditions. After a few hours of low oxygen, transcription of this 28 kDa protein was strongly induced. A hypoxic induction of possible LBD41 orthologs appears conserved not only within close relatives of *A.thaliana*, but also in rice, poplar and possibly maize (Gasch et al., 2016) (Mustroph et al., 2010) (Tamura et al., 2022). To further determine the function of LBD41, the effect of a T-DNA knockout line *lbd41* was studied previously in a semi-quantitative RT-PCR (Bäumler, 2020) (Gasch, 2015). Surprisingly, no difference in transcript level of possible target genes was measured upon hypoxia in *lbd41*, compared to the wildtype Col-0. Instead, the transcript level of LBD40 (AT1G67100) was increased in the absence of LBD41. This indicates a possible functional complementation of LBD41's repressive activity by LBD40. For LBD42 (AT1G68510), no detectable induction under hypoxia was measured in Col-0 or *lbd41*, however its sequential similarity suggests a possible redundancy for all three proteins. The occurrence of two potential backup copies of LBD41, further insinuates the importance of its regulation (Láruson et al., 2020) (Wagner, 1996).

1.12 LBD41 as a transcriptional repressor

While the exact biological role of LBD41 could not be discerned so far, the identified EAR domain highly suggests that it serves as a transcriptional repressor. In line with this proposed regulatory function, no trans-activating activity was discovered in a GAL4-UAS protoplast assay. In further characterizations of LBD41's function, the EAR domain was replaced with a VP16 domain from Herpes simplex to create a transactivating mutant (Gasch, 2015). This mutant was then expressed in mesophyll protoplasts under a 35S promoter, and its effect on the transcriptome analyzed in a RNA microarray.

Compared with native LBD41 overexpressed under the same conditions, multiple significantly differentially-expressed genes were shown. From the overlap of genes significantly downregulated by pr35S:LBD41 and simultaneously upregulated by pr35S:LBD41ΔEAR:VP16, at least 8 putative target genes were identified (Bäumler, 2020). The proposed target genes include LOB DOMAIN CONTAINING PROTEIN 39 (LBD39, AT4G37540), PRODUCTION OF ANTHOCYANIN PIGMENT 1 (PAP1, AT1G56650), ALTERNATIVE OXIDASE 1D (AOX1D,

AT1G32350), 3-PHOSPHOGLYCERATE DEHYDROGENASE (PGDH, AT1G17745), HALOACID DEHALOGENASE-LIKE HYDROLASE (HADLH, At5G02230), ZINC-BINDING ALCOHOL DEHYDROGENASE PROTEIN (At5G42250), LONG-CHAIN FATTY ALCOHOL DEHYDROGENASE PROTEIN (At4G28570) and POLY-PEPTIDE 28 of the CYTOCHROME P450 Family 71 B (At1G13090).

Additionally, GAMMA GLUTAMYL TRANSPEPTIDASE 4 (GGT4, AT4G29210) showed significant induction by p35S:LBD41ΔEAR:VP16, but no repression through pr35S:LBD41, marking it as another possible target gene. Concurrently, the gene PURINE PERMEASE 10 (PUP10, AT4G18210) displayed the reverse behavior, with significant repression by pr35S:LBD41 but unaffected by the VP16 construct. Differential expression was also measured for SLAC1 HOMOLOGUE 3 (SLAH3, AT5G24030). While functions for some of these putative target were recently identified, their effects on flooding acclimation remains elusive.

1.13 Ocurrence of LBD41 in other stress conditions

While LBD41 displays low basal expression under control conditions, it is likely that flooding is not the only factor that could influence its expression. Increased levels of LBD41 transcripts were previously detected during seed ripening and germination, possibly involved in the previously mentioned hypoxic niche (Klepikova et al., 2016). Furthermore, differential regulation of LBD41 upon infection with certain fungi pathogens was recorded. The most pronounced induction was detected for the Oomcyete *Phytophthora parasitica* (Thatcher et al., 2012). While *P. parasitica* itself is a terrestrial pathogen, many members of the genus *Oomycete* or water molds prefer highly humid conditions (Beever et al., 2012). Therefore, it might be possible that an increased occurrence of *Oomycete* in connection with hypoxia led to a specialized response for such a combination of abiotic and biotic stress.

Another influential candidate that could affect LBD41 is high salinity, which induces osmotic oxidative stress. Generally in a soil-grown environment, flooding with fresh water has the potential to dissolve and dilute salt clusters. By reducing the local osmotic effect of salinity, flooding can have an antagonistic effect on salt stress. In line with this, some of the proposed targets downregulated by LBD41 were shown to be involved with oxidative stress, namely

AOX1D, PGDH and PAP1 (Rosa-Téllez et al., 2020) (Lee et al., 2016) (Oh et al., 2022). Most of their mechanisms reduce ROS-based cellular damage, one of the central factors of osmotic stress (Kesawat et al., 2023) (Castillo et al., 2018) (Manbir et al., 2022). In this context, a hypoxia-induced repression of oxidative stress responses appears beneficial.
Contrary to this however, water intrusion from oceans can produce salt-water flooding in coastal regions. These increasingly occurring events create a combination of high salt and low oxygen conditions (Cantelon et al., 2022) (Mahmoodzadeh et al., 2019) (Taylor et al., 2019). Furthermore and not limited to coastal regions, the erosion of mineral reservoirs by flooding can introduce higher salinity to previously unaffected plants (Nones, 2019) (Panchuck, 2021). Overall, limited information about combined salinity and hypoxia stress conditions is known. However, with the currently rising ocean levels such conditions are expected to increase, and require further research.

1.14 Putative regulation of LBD41 by SUMO

The hypoxic upregulation of LBD41 by GVIIERFs has been identified in previous studies, along with its low basal expression level under non-stress conditions (Bäumler, 2020) (Gasch, 2015). Additionally to this hypoxic transcriptional activation, available data points towards further post-translational modification (PTM) with SMALL UBIQUITIN LIKE MODIFIER (SUMO). In a proteome-wide study, LBD41 was identified as an interaction target with SUMO modifying enzymes ESD4 and SCE1, as well as SUMO1 and SUMO3 (Elrouby et al., 2010). Using the prediction tool GPS-SUMO, possible interaction sites for SUMOylation were identified (Zhao et al., 2014). With this knowledge, a co-immunoprecipitation of LBD41 and SUMO1 detected a potentially poly-SUMOylated state (Bäumler, 2020). Part of the UBIQUITIN-like protein family, the roughly 100 amino acid and 11.5 kDa sized SUMO proteins exist in multiple isoforms.
Of the 8 isoforms encoded in the genome of *A. thaliana*, only SUMO1, SUMO2, SUMO3 and SUMO5 are actively expressed, and engage with their targets through a SUMO-interacting motif (SIM) (Clark et al., 2022) (Park et al., 2011). Of these four isoforms, SUMO1 and SUMO2 are the dominant forms, SUMO5 has minimal characterization so far and SUMO3 has previously only been associated with pathogen defense (Castaño-Miquel et al., 2011) (Ingole et al., 2021) (Rytz

et al., 2023). However, as LBD41 and other members of the LBD Group II family have displayed induction in reaction to fungal infections, SUMO3 might be involved (Thatcher et al., 2012).
The general impact of SUMOylation was discovered to affect many pathways, including those of abiotic stress resistance (Han et al., 2021) (Park et al., 2011) (Singh et al., 2022). However, in spite of its frequent occurrence in altering proteomic functions, its individual implications on the protein of interest are not trivial. The most commonly observed regulation by SUMOylation is serving as a signal for UBIQUITINation, with subsequent degradation through the proteasome (Benlloch et al., 2018) (Park et al., 2011) (Tatham et al., 2008). However, the regulation imposed by SUMOylation can not only decrease a proteins availability, but also increase it, influence its stability, structure, solubility or affect localization (Péter et al., 2021). Thus, LBD41's potential SUMOylation could affect its activity and organism-wide effects in a multitude of ways.

1.15 Aim

Humanity is facing an accelerated climate change including rising ocean levels. As a consequence, our agriculture is increasingly threatened with extreme weather events. To ensure a stable food supply of the future, stress-tolerance mechanisms of crop plants require in-depth understanding. Multiple morphological and metabolic contributors in flooding adapted species were already uncovered in the last decades. However, our knowledge is still limited when considering the various environmental factors involved in flooding. Simultaneously, not all genes involved in low-oxygen acclimation are fully characterized.
The GVIIERFs RAP2.2, RAP2.12 and RAP2.3 were identified as major regulators in the induction process of HRGs in *A. thaliana*. While they appear redundant in hypoxic acclimation, their individual regulation requires additional evaluation. Multiple transcriptional and phytohormonal factors which affect their combined or individual activity were recently identified. Further potential differences between these transcription factors will be studied here. By investigating the effect of *rap2.2* and *rap2.12* KO mutants, nuances in regulation are discussed. Differences in hypoxic acclimation will be studied in a transcriptional and translational context, including an impact on flooding survival. Additionally, also a potential influence of repeated hypoxic stress on acclimation intensity is discussed here.

Induced by the core hypoxia response, the transcriptional repressor LBD41 is expected to play a significant role in flooding acclimation. However, the detailed regulation and role of this protein remains elusive. Due to potential redundancy through homologs LBD40 and LBD42, the impact of a *lbd40 lbd41 lbd42* genotype is investigated. Furthermore, misregulation is studied through constitutive expression of native LBD41 or LBD41ΔEAR:VP16. Through these lines, transcriptional changes of LBD41 and putative targets are explored in the context of low oxygen. An impact of LBD41 misregulation on flooding survival is examined with varying stress intensity. Different protein variants of LBD41 are investigated, and changes in target repression activity recorded. Furthermore, the regulation imposed by LBD41 is potentially not limited to flooding acclimation.

A putative synergistic effect of salt stress and hypoxia is studied, and their impact on fitness and survival evaluated. Additionally, a potential role of LBD41 during germination and maturation is discussed. Moreover, although the hypoxic transcriptional induction of LBD41 is well documented, data on post-transcriptional regulation is limited. Previously, LBD41 was identified as a potential target for SUMOylation. However, the location, frequency and purpose of this post-translational modification requires exploration. Through removal of putative SUMO-binding sites in LBD41, consequences to its regulatory activity are analyzed. Most importantly, the influence of oxygen availability on this post-translational modification is studied.

CHAPTER 2

Materials and methods

2.1 General materials

2.1.1 Chemicals and water

All chemicals used within the confines of this work will be listed in this publication. These substances were of analytical purity and purchased by licensed providers such as Thermo Fisher Scientific (Waltham, USA), Carl Roth (Karlsruhe, Germany), New England Biolabs (Ipswich, USA), Duchefa (Haarlem, Netherlands), Sigma-Aldrich (Burlington, USA) and Invitrogen (Waltham, USA). All water for buffers, media, reactions and assays was purified through an Advantage A10 or Reverence A+ Mili-Q deionizer (Millipore, Burlington, USA). Waterlogging survival experiments were performed with demineralized water (Central Tech Department, University Bayreuth), while tap water was used for regular watering of plants and full submergence.

2.1.2 Growth media

The different media used for proliferation and selection of bacteria, as well as germination of seedlings is listed in Table 1.

2.1.3 Plasmids and oligonucleotides

The different types of plasmids used in this work are listed in Table 2. Additionally, complete lists of all used plasmids and oligonucleotides are found in the supplementary section (Table 4 and Table 5).

Table 1: Growth medium composition and usage

Medium	Composition / L	Usage
MS	4.4 g MS-salts, 10 g sucrose, pH adjusted 5.7 with KOH, 10 g agar (plant) if solid	*A. thaliana* germination and seedling growth assays
Hoagland	0.975 g MES, 10 g sucrose, 0.2 ml 1.4 M $Ca(NO_3)_2$, 0.2 ml 0.5 M $(NH)_4H_2PO_4$, 0.2 ml 1 M $MgSO_4$, 0.2 ml 3 M KNO_3, 0.5 ml 10 mM Fe-HBED, pH adjusted 5.7 with KOH, 10 g agar (plant)	*A. thaliana* seedling growth assays and salt stress phenotype experiments
LB	10 g tryptone, 10 g NaCl, 5 g yeast extract, 15 g agar if solid	*E. coli* proliferation and transformation
YEB	10 g peptone, 5 g sucrose, 1 g yeast extract, 0.492 g $MgSO_4$ H_2O, 15 g agar if solid	*A. tumefaciens* proliferation and transformation

2.2 Plants and growth conditions

2.2.1 Plant lines

All *in vivo* and *in vitro* plant experiments were conducted using *Arabidopsis thaliana*, except for the transient overexpression of LBD41 variants, performed in *Nicotiana benthamiana*. For all experiments with *A. thaliana* the ecotype Columbia-0 (Col-0) was used as wild type and background for mutant lines. Genetically modified plant lines were a *rap2.12* line (Gasch et al., 2016), two *rap2.2* Crispr lines B/C and double mutants of *rap2.2 rap2.12* (Judith Bäumler, Plant Genetics, University Bayreuth). Furthermore a triple mutant *lbd40 lbd41* lbd42* comprised of a Transfer- (T-DNA) insertion line of *lbd41* (SALK_144556) crossed with Crispr/Cas disabled *lbd40* and *lbd42* was used. Further lines were a pr35S:HA'LBD41'GFP overexpression line OE(N) as well as the activating-mutant pr35S:LBD41ΔEAR:VP16 lines (VP16-1/2/3) (Bäumler, 2020).

2.2.2 Germination and growth chambers

All plants were grown in isolated growth chambers in accordance with the S1 security level for genetically modified organisms. Seeds of *A. thaliana* were surface-sterilized with chlorine gas for 45 min (5 ml 37 % HCl, 10 ml 12 % sodium hypochlorite). For germination, seeds were distributed on sterilized medium and placed under cold and dark stratification at 4 °C (Rivero L. et al., 2014). Then, after 3 d of stratification, seeds were transferred to illuminated growth chambers. Germination of seeds was always performed under long day conditions, except plants for protoplast isolation. Transference of stratified seeds to a growth chamber is defined as the first day of germination. Growth chambers were ventilated and tempered at 23 °C, as well as illuminated with canopy lighting at PAR PPFD of around 100 µmol/ m^2s (Lumilux Cool White L36W/840, Osram, Munich, Germany). Lighting cycles within the chambers were kept at either short day (8 h light / 16 h dark) or long day (16 h light / 8 h dark) conditions.

2.2.3 Soil composition

Two different soil compositions were used for growing plants throughout this work. Both were comprised of 3 parts standard soil, 3 parts pricking soil (Ökohum GmbH, Herbetingen, Germany) and 1 part vermiculite (Nr. 4, Dämmstoff-Fabrik Klein GmbH, Bubenheim, Germany). However, the type of standard soil used varied between these two mixtures. Composition 1 contained standard soil CL Ton Kokos (Patzer Erden GmbH, Sinntal, Germany) while composition 2 had standard soil CL ED73 (Patzer Erden GmbH, Sinntal, Germany). The main difference being the addition of coconut fiber in CL Ton Kokos. The first was used for PTA with 100 mM NaCl and assays with single K105R mutants. Additionally, it was used for *rap2.2* / *rap2.12* survival and ADH experiments. All other experiments involving soil were performed with composition 2.

2.3 Bacterial work

2.3.1 Strains of bacteria

The *Escherichia coli* strain DH10B (Grant et al., 1990) was used for standard cloning procedures and the propagation of pHBTL and pBT10 vectors. Furthermore, the *E. coli* strain DB3.1 (Bernard et al., 1992) was employed in this work for Gateway cloning. The *Agrobacterium tumefaciens* strain GV3101 (Koncz et al., 1984) was utilized for transient transformation of *Nicotiana benthamiana* and stable transformation of *A. thaliana*. Additionally, for heterologous expression in *N. benthamiana*, the *A. tumefaciens* strain 19k (Voinnet et al., 2003) provided removal of gene silencing in heterologous expression. Competent *A. tumefaciens* were created prior to this work, as described in (Müller, 2020).

2.3.2 Creation of chemically competent *E. coli*

To create aliquots of chemically competent DH10B, a bacterial stock was plated out in a dilution separation on LB agar. A single colony was later used to inoculate a 2 ml LB culture and incubated ON at 37 °C and 180 rpm (Innova44, New Brunswick, Edison, USA). Of this small culture, 1 ml was then added to a 100 ml of LB in a baffled Erlenmeyer flask and the cultures incubated again at 37 °C and 180 rpm. When the cultures reached an OD_{600} = 0.4, further growth was halted by placing the flasks in an ice bath for 10 min. Subsequently the culture was divided into pre-cooled 50 ml conical Greiner tubes and the cells pelleted through centrifugation in a swing-out rotor (3000 rcf, at 4 °C, for 20 min). After centrifugation, the medium supernatant was discarded and the cell pellets carefully resuspended in 20 ml of TFB1 (30 mM $KC_2H_3O_2$, 100 mM KCl, 10 mM $CaCl_2$, 50 mM $MnCl_2$, 15 % (v/v) Glycerol, adjusted pH 5.8 with acetic acid). Following another incubation on ice for 5 min, the previous centrifugation step was repeated and the resulting supernatant discarded again. The cell pellets were then resuspended in 2 ml TFB2 (10 mM MOPS, 10 mM RbCl, 75 mM $CaCl_2$, 15 % (v/v) glycerol, adjusted to pH 6.6 with KOH) followed by 15 min of incubation on ice. Using a pre-cooled widened pipette tip, aliquots of 100 µl were added to cooled 1.5 ml Eppendorf tubes, immediately frozen in liquid nitrogen and stored at -80 °C.

Table 2: Plasmid usage and origin

Name	Usage	Published by
pHBTL	Effector expression for PTA	(Kuhlmann et al., 2003)
pK7FWG2	Binary vector, stable *A. thaliana* / transient *N. benthamiana* transformation	(Karimi et al., 2002)
pDONR221	Donor plasmid for Gateway cloning	(Invitrogen, 2003)
pKSE401	Binary vector, CRISPR/Cas gene editing	(Xing et al., 2014)
pBT10	Luciferase (Firefly / Renilla) expression for PTA	Firefly (Wehner et al., 2011) Renilla (Bäumler, 2020)
pBin19	Binary vector, heterologous expression helper, P19 anti-silencing	(Voinnet et al., 2003)

2.3.3 Transformation of bacteria

To transform competent bacteria, frozen tubes with 50 µl *E. coli* or 100 µl *A. tumefaciens* aliquots were at first thawed on ice. The transformation process was started with the addition of 1 µl plasmid DNA (around 20 ng) for both organisms.

Competent *E. coli* were then incubated on ice for 30 min, followed by a 45 s heat shock at 42 °C. After another 2 min on ice, 1 ml of LB medium was added and the suspension incubated at 37 °C and 300 rpm for 1 h (Thermomixer comfort, Eppendorf, Hamburg, Germany). For competent *A. tumefaciens*, the aliquots were re-frozen in liquid nitrogen after addition of the plasmid DNA. A heat shock was then performed at 37 °C for 5 min, followed by the addition of 1 ml YEB medium. Incubation of the transformation reaction took place at 28 °C and 300 rpm for 3 h (Thermomixer comfort, Eppendorf, Hamburg, Germany). After final incubation, both *E. coli* and *A. tumefaciens* transformants were plated on LB or YEB agar, respectively. These agar plates contained specific antibiotics for selection, depending on the resistance provided by the transformed vector.

2.4 Nucleic acid methods

2.4.1 Isolation of plasmid DNA from *E. coli*

To proliferate *E.coli* strains carrying plasmid DNA, inoculated 3 ml (Miniprep) or 250 ml (Mediprep) LB cultures were incubated ON at 37 °C and 180 rpm (Innova44, New Brunswick, Edison, USA) The isolation of plasmid DNA from cultures was performed using a GeneJET Plasmid Miniprep or Mediprep kit (Thermo Scientific, Waltham, USA), following the provided protocol.

Table 3: Antibiotics and their concentration

Antibiotic	**Working concentration (µg/ml)**	**Solvent**
Ampicilin	100	H_2O
Kanamycin	50	H_2O
Spectinomycin	100	H_2O
Gentamicin	20	H_2O
Rifampicin	50	DMSO
Chloramphenicol	50	Ethanol

2.4.2 DNA extraction *A. thaliana*

To extract genomic DNA from plant tissue, the frozen samples (seedlings or leaves) were ground in a ball mill (30 Hz) under liquid nitrogen cooling. The samples were brought to RT, after which 500 µl of Quickprep extraction buffer (200 mM Tris-Cl pH 7.5, 250 mM NaCl, 25 mM EDTA, 0.5 % (w/v) SDS) was added. To combine the pulverized tissue with the buffer, all tubes were inverted 4 times and then centrifuged (13,000 rcf, at RT, for 5 min). After the insoluble tissue components were pelletized, 300 µl of the supernatant was transferred to a new 1.5 ml Eppendorf tube, to which 300 µl of RT isopropanol were added. Afterwards, the tubes were inverted twice and centrifuged again (13,000 rcf, at RT, for 5 min) to precipitate all

gDNA. The supernatant was then fully removed and the pellets dried at RT for 15 min. After the isopropanol had evaporated, 40 µl of dd H_2O were added to each pellet and the samples incubated at 60 °C for 5 min. Tubes were then directly transferred to ice and incubated for 2 min followed by a final centrifugation step (13,000 rcf, at RT, for 1 min). Of the dissolved gDNA supernatant, 30 µl were transferred to a new tube and stored at 4 °C.

2.4.3 RNA extraction and reverse transcription

To isolate RNA, frozen plant tissue was ground in a ball mill with liquid nitrogen cooling. Then 500 µl of TRIsure (Bioline, Germany) were added to the pulverized samples, which were subsequently vortex-mixed for 1 min and then incubated at RT for 5 min. After briefly vortex-mixing the samples a second time, 100 µl of Chloroform were added before shaking the tubes vigorously for 30 s, followed by incubation at RT for 2 min. The samples were then centrifuged (13,000 rcf, 15 min, 4 °C) after which 250 µl of the supernatant was transferred to a new tube. This supernatant was combined with 250 µl of isopropanol before inverting the tubes 5 times and subsequent incubation for 10 min at RT.

After incubation, the samples were centrifuged again (13,000 rcf, 10 min, 4 °C), followed by fully discarding the supernatant, and washing the pellet with 750 µl of 75 % (v/v) ethanol. The sample tubes were then centrifuged again (6,000 rcf, 5 min, 4 °C), before discarding the supernatant and drying the pellet at RT for 15 min. By adding 50 µl dd H_2O, the pellets were dissolved and then frozen at -20 °C. The extracted RNA was later incubated at 60 °C for 10 min before determining the concentration with a Nanodrop-photometer. To reverse transcribe cDNA from the isolated RNA, 2 µg of genetic template was diluted in a volume of 11.5 µl. To this, 1 µl of oligo dT (100 µM) were added and the samples incubated at 65 °C for 5 min. Then 4 µl of 5x RT buffer (Thermo fisher), 2 µl dNTPs (10 mM), 1 µl reverse transcriptase (200 U/µl) and 0.5 µl RNAse inhibitor (40 U/µl) were added to the samples. The reverse transcription reaction was performed at 42 °C for 60 min, followed by 10 min at 70 °C. The resulting cDNA was then stored at 4 °C.

2.4.4 Standard PCR and sequencing

A polymer chain reaction was performed for the amplification of gDNA, cDNA and plasmid DNA. Amplifications of these polynucleotides was conducted in a Labcycler 48 (SensoQuest, Göttingen, Germany). These reactions were mainly performed at a volume of 25 µl. Here 1 µl of template DNA (concentrated at 1–5 ng/µl) was combined with 2.5 µl of a 10x concentrated PCR buffer (100 mM Tris pH 9, 500 mM KCl, 15 mM $MgCl_2$, 0.1 % (v/v) Triton X-100). Oligonucleotide primers were diluted with H_2O to a concentration of 10 µM and then added as matching forward and reverse primers at a volume of 0.5 µl each, followed by 0.5 µl of dNTPs (10 mM each). To amplify a genomic template for sequencing or detection on an agarose gel, in-house made Taq polymerase was added at a volume of 0.25 µl. The volume was then adjusted with dd H_2O.

After initial denaturation at 93 °C for 3 min, samples were amplified in 32 cycles of 3-steps. The first step included a 30 s denaturation at 93 °C, followed by 30 s hybridization at primer dependent temperatures and then a elongation step of 72 °C for 1 to 3.5 min depending on product length. Ideal primer hybridization temperatures were calculated with the Tm Calculator Web tool of Thermo Fisher, based on (Allawi et al., 1997). At the end of the cycles, a final elongation step was performed at 72 °C for 5 min, followed by cooling to 14 °C. Confirmation by sequencing was performed externally by Macrogen Europe (Amsterdam, Netherlands) using the Ez-Seq service.

2.4.5 Quantitative PCR (qPCR)

For qPCR, the at 100 µM dissolved primer stocks were mixed into a 0.5 µM primer mix of target-matching forward and reverse oligos diluted with bidest. H_2O. The recently reverse transcribed cDNA was then diluted 1:50 with bidest. H_2O. A master mix consisting of 1:2 primer mix to iQ SYBR Green Supermix, was then prepared on ice. In each well of a 96-well plate, 7.5 µl of this master mix was pipetted on ice, then removed the plate from ice and added 2.5 µl of the diluted cDNA per well. The final reaction mix contained a total of 1 M betaine for improved amplification of GC regions. For each combination of primers and templates, three technical replicates were set up and measured. After addition of the cDNA template the

96-well plate was sealed with a microseal film. The plate was briefly centrifuged for 20 s at 1000 rcf to remove droplets from the film, and then placed in a qPCR cycler (CFX Connect Real-Time PCR Detection System, Bio-Rad Laboratories Inc., Hercules, USA).
After initial denaturation for 3 min at 95 °C, the samples were amplified in a 3-Step program for 40 cycles: 95 °C for 10 s, 60 °C for 30 s and 72 °C for 30 s. To validate the quality of this amplification, a melting curve from 65 to 95 °C was also performed. After another initial denaturation at 95 °C for 10 s, the temperature was increased by 0.5 °C every 5 s. To confirm an exponential reaction with a newly designed set of qPCR primers, testing was performed by amplification of a 5-step 1:5 cDNA dilution series. To ensure purity of reactions, three water (null) reactions for each primer combination were additionally measured on each plate. The relative transcript level (RTL) of specific genes within samples was referenced against ELONGATION FACTOR 1-α (EF1a) using the formula 2-ΔCT (Livak et al., 2001).

2.5 *In vivo* plant experiments

2.5.1 Survival assays

For all survival experiments, the plants were at first germinated under long day conditions (16 h light / 8 h dark). At the age of 1 week, the seedlings were transferred to soil and then further grown under short day conditions (8 h light / 16 h dark). For submergence experiments with *rap2.2* and *rap2.12* mutants, seedlings were pricked into a 2:1 mixture of soil to sand, using soil composition 1. Submergence experiments with mutant lines of LBD41 were transferred in a 3:1 soil to sand mixture with soil composition 2. After another 2 weeks of growth for RAP experiments or 3 weeks for LBD41 waterlogging and submergence, the plants were transferred to their respective stress environment. Survival experiments were performed under a short day light cycle.

2.5.1.1 Waterlogging

For waterlogging stress treatments, plants of each genotype were either placed in demineralized water with added starch (1 g/L), or pure demineralized water up to the upper soil level.

Another 2 plants of each genotype were kept under control conditions and were watered normally. Both waterlogging stress conditions were topped of with demineralized water twice a week, to offset uptake and evaporation and maintain the waterlogged effect. After 2 weeks of stress treatment, the waterlogging condition was removed, the plants transferred to fresh containers and their appearance documented. After documentation, the plants were kept under short day conditions for another 2 weeks while being watered normally. After which they were photographed a second time to document the recovery process.

2.5.1.2 Full submergence

For full submergence treatments, at a total of 3 (RAP) or 4 weeks (LBD) old, the plants were submerged in clear plastic tubs filled with tap water. These tubs were filled 24 h prior to the stress treatments beginning, to allow for temperature equilibration and the dispersion of air within the water. Both the submergence and desubmergence were performed in the morning, roughly 90 min after the beginning of a light period. On the day of submergence 28 plants of each genotype were carefully lowered into the water, slightly tilting during the process to disperse the water pressure at the moment of crossing the surface. The plants were randomly and equally distributed to 4 water filled tubs in an effort to minimize local effects and contaminations.

Starting from 3 weeks after the beginning of the stress treatment, 1/4 of randomly selected plants were removed from submergence and transferred to fresh containers. At 3 additional time points, precisely 24, 28 and 31 days of stress treatment, additional plants were removed. These plants were then further kept under short day conditions and allowed to recover for 2 weeks with normal watering. After this recovery period, the plants were documented photographically, and their survival rate captured. The survival of an individual plant was determined by its ability to form new leaves within the recovery period.

2.5.2 Hypoxia treatment with nitrogen

For both seedlings and adult plants (*A. thaliana*or *N. benthamiana*), hypoxia treatments were performed in an enclosed desiccator for 2, 4 or 8 hours. For the stress-treated plants, the

desiccator was constantly flushed with pure Nitrogen gas to allow dispersion of all oxygen from the system. For the control plants, normal air was pumped from the plant chamber into the desiccator. In both cases, the inflow of gas was adjusted to a similar intensity through observing the frequency of bubbles exiting the desiccator through a small amount of water. After the treatment, seedling or leaf samples were swiftly harvested and frozen in liquid nitrogen to avoid re-acclimation to normoxic levels. In the case of recovery treatments, another set of plants were stressed in a third desiccator with nitrogen. After the stress treatment, these plants were transferred to a new tray and left at normoxic room conditions for 1 h before harvesting the samples. While seedlings of *A. thaliana* were harvested as a whole, for adult plants three leaves of equivalent size were combined from individual plants of the same genotype, and then frozen in liquid nitrogen. In the case of infiltrated *N. benthamiana* leaves, three leaf discs (Ø 8 mm) were cut out of the plants after stress treatment and frozen immediately.

2.5.3 Salt stress root growth and phenotype

Either Hoagland or MS agar medium was prepared with the addition of 25 to 100 mM NaCl and poured into square petri dishes. Using a toothpick, sterilised seeds were laid onto the solidified medium while maintaining about 1 cm distance between the seeds. After stratification at 4 °C for 3 days, the petri dishes were transferred to long day growing conditions. The seedlings were then grown for 7 or 14 days, followed by photographic documentation and measurement of root length by hand.

For the phenotypic separation of seedlings, seeds were germinated on Hoagland medium with 50 mM NaCl added. At the age of 6 d, the seedlings were separated based on their appearance. While still remaining on the same agar petri dish, the plants displaying a green leaf color and little to no stress phenotype were grouped as the tolerant seedlings. Contrasting this, the plants with clearly decreased size and yellowish leaf color were gathered as the sensitive seedlings. At the following day, the now 7 d old seedlings were treated with nitrogen or air for 8 h.

2.6 *In vitro* plant experiments

2.6.1 Studies of anthocyanin content

2.6.1.1 Growth conditions for anthocyanin measurements

Seeds of Col-0 or pr35S:LBD41ΔEAR:VP16 were germinated on MS medium either with (solid) or without (liquid) agar added. Medium with agar added was poured into standard round petri dishes, while the liquid medium was added to 6-well plates. The seeds were sterilized using chlorine gas (5 ml of 37 % HCl, 10 ml of 12 % sodium hypochlorite) for 45 min before spreading them on the solidified / liquid medium. These plates were then stratified for 3 days at 4 °C in the dark, before transferring them to a long day growth chamber. At either 3, 4, 5 or 6 days the plates were removed from the growth chamber, harvested with tweezers and dried off any surface medium using cell paper. After the fresh weight was determined, the seedlings were frozen in 2 ml centrifuge tubes using liquid nitrogen, followed by storage at -80 °C.

2.6.1.2 Anthocyanin extraction and quantification

To extract and determine the anthocyanin content, the frozen seedlings were ground in a ball mill for 1 min (30 Hz) while cooling with liquid nitrogen. After bringing the tubes to RT, 300 µl of extraction solution (methanol with 1 % HCl) were added to each tissue sample. Subsequently, samples were vortex-mixed for 15 sec, incubated at RT for 5 min, vortex-mixed again for 5 sec and then centrifuged (14,000 g, at 4 °C, for 10 min). Of the supernatant, 200 µl were transferred to a new 1.5 ml tube, to which 200 µl of purified deionized water and 500 µl of chloroform were added. Samples were then vortex-mixed for 10 sec, before centrifugation (17,900 rcf, at 4 °C, for 15 min). Following centrifugation, the supernatant was moved to a fresh 1.5 ml tube and kept on ice. To determine the anthocyanin content within the extracts and a blind sample, absorption was then measured at both 538 and 630 nm. Anthocyanin content was quantified as A_{538}-A_{630} / g of tissue fresh weight.

2.6.2 ADH activity determination

2.6.2.1 Protein extraction for activity measurements

For a total protein extract from seedlings, frozen samples were ground in a cooled ball mill for 1 min (30 Hz) and then stored on ice. Freshly prepared extraction buffer (50 mM HEPES pH 6.8, 5 mM Mg-acetate, 15 % (v/v) Glycerin, 1 mM EDTA, 1 mM EGTA, 5 mM β-mercaptoethanol, 0.1 mM Pefabloc protease inhibitor) was added to the pulverized plant samples with a ratio of 1 ml buffer for 200 mg of sample fresh weight. The samples were then vortex-mixed for 10 s each, before being centrifuged for 15 min (13000 rcf, 4 °C). After centrifugation, the supernatant was transferred to a new 1.5 ml tube and stored on ice until the measurement.

2.6.2.2 Protein content by Bradford

To determine the protein concentration of tissue extracts, a standard calibration curve was measured at BSA concentrations of 0.1, 0.5, 1 and 2.5 mg/ml. At first, the required amount of Bradford reagent (ROTI Quant, Roth) was diluted 1:5 with pure water. Of the BSA standards 10 µl were added to a polystyrene cuvette filled with 1 ml of diluted Bradford reagent, then mixed thoroughly. After incubating the samples for 10 min at RT, the absorption was measured at 595 nm. Following the BSA standards, tissue protein extracts were also added at a ratio of 10 µl/ml Bradford reagent and measured just the same. Total protein content of samples was then determined using the calibration slope (Bradford, 1976).

2.6.2.3 ADH activity assay

Enzymatic ADH activity of tissue protein extracts was measured indirectly, through the conversion of the co-substrate NADH to NAD+ and the resulting shift in absorption. For the photometric measurement inside a cuvette, 970 µl of buffer (50 mM TES adjusted pH 7.5 with KOH) were combined with 10 µl of 17 mM NADH and the addition of 10 µl protein extract. Samples were then incubated for 5 min at RT, before measuring the baseline absorption at 340 nm for 5 min in a spectrophotometer (Specord 200 Plus edition 2010, Analytik Jena GmbH, Jena, Germany). The enzymatic reaction was then started, by adding 10 µl of 10 mM Acetaldehyde to the cuvette and mixing the sample by inversion. Using the same wavelength

of 340 nm, the sample's absorption was measured immediately after addition of the substrate Acetaldehyde and over the course of the next 5 min. To determine the activity of ADH, the difference in slope of the baseline absorption, to the slope after substrate addition, was calculated. Based on this difference in slope, the activity was determined in nmol per min and mg of protein.

2.6.3 Protoplast promoter studies

2.6.3.1 Isolation of *A. thaliana* protoplasts

For the transformation of protoplasts with varying reporter and effector constructs, *A. thaliana* plants of the ecotype Col-0 or the genotype *lbd40 lbd41* lbd42* were germinated under short day conditions on normal soil. At the age of 4-6 weeks, roughly 30 randomly selected leaves were cut into short pieces (1 mm^2) and transferred to a small beaker. To the leaf fragments, 5 ml of enzymatic solution (500 mg cellulase (1 U/mg), 100 mg macerozym (0.5 U/mg), 0.4 M mannitol, 20 mM KCl, 20 mM MES, 10 mM $CaCl_2$, pH 5.7) were layered on top. Enzymatic digestion of the cellular membrane was initiated by applying a vacuum for 10 s, followed by incubation at RT for 4 h. Individual cells were released from the tissue by light shaking for 5 min, followed by filtering through a steel net (63 µm). The protoplasts were then centrifuged for 2 min (120 rcf, swing-out rotor, slow acceleration and braking), supernatant discarded and the resulting pellet resuspended in 5 ml W5 buffer (5 mM KCl, 2 mM MES, 154 mM NaCl, 125 mM $CaCl_2$, pH 5.7). After repeating the centrifugation step (1 min) and subsequent resuspension in 5 ml W5, the cells were pelleted again through centrifugation and finally resuspended in 2-5 ml MMg buffer (0.4 M mannitol, 4 mM MES, 15 mM $MgCl_2$, pH 5.7) depending on pellet size.

2.6.3.2 Transient transformation of protoplasts

To perform a protoplast transactivation assay, the previously detached cells were transformed with various vectors. Here, each 200 µl of this protoplast suspension was combined with 0.5 µg of Renilla normalization plasmid (pBT10:rLUC), 2 µg of effector plasmid (pHBTL) and 4 µg of the Firefly reporter plasmid (pBT10:fLUC). Placed in rounded Eppendorf tubes and

combined with 220 µl PEG buffer (40 % (w/v) PEG_{4000}, 0.2 M mannitol, 0.1 M $CaCl_2$), the mixture was swiftly inverted 15 times and then incubated at RT for 20 min. Afterwards, the reaction was diluted through the addition of 800 µl W5 buffer (5 mM KCl, 2 mM MES, 154 mM NaCl, 125 mM $CaCl_2$, pH 5.7) then inverted once and centrifuged for 1 min (RT, 150 rcf, slow acceleration and braking). As the protoplasts were pelleted, the supernatant was discarded and the cells resuspended in 300 µl WI buffer (0.5 M mannitol, 20 mM KCl, 4 mM MES) followed by incubation under long day conditions for 16 h.

2.6.3.3 Protoplast transactivation assay

To measure the influence of co-expressed effectors on the transcription of pBT10:fLUC reporter constructs, the luminescence signal of samples was detected with a GloMax 96 microplate luminometer. As the transformed protoplasts had sedimented after the previous long day incubation step, the buffer supernatant was discarded and the pellet resuspended in lysis juice (PJK GmbH, Kleinbittersdorf, Deutschland) and vortex-mixed for 10 s. Of the resulting lysed samples, aliquots of 20 µl were transferred to opaque 96-well reader plates. After addition of the firefly substrate D-luciferin or its Renilla substrate counterpart (Renilla juice and Coelentherazin 50:1) at 50 µl per sample, their luminescence signal was measured individually for each sample.

2.6.4 Heterologous overexpression of LBD41 variants

2.6.4.1 Transient transformation of *N. benthamiana*

Seeds of *N. benthamiana* were germinated on soil at long day conditions. At 7 days the seedlings were separated into new soil pots and returned to a long day chamber. After 3 weeks of growth, the leaves were co-infiltrated with *Agrobacterium tumefaciens* strains carrying either a pBin19 helper plasmid, or a pK7FWG2 vector for constitutive expression of a AtLBD41 variant. Prior to infiltration, the *A. tumefaciens* cultures were resuspended in a freshly prepared infiltration buffer (10 mM MES pH 5,2, 10 mM $MgCl_2$). Then, 10 ml infiltration cultures were prepared at an OD_{600} = 1, and incubated at room temperature for 2 h at a gentle rolling motion. After incubation, equal volumes of P19 and pK7FWG2 cultures were combined

and mixed through gentle inversion. Using a syringe without a nozzle, the cultures were infiltrated into one separate leaf of three different plants, with a maximum of three constructs for each plant. Those infiltrated plants were then incubated at long day conditions for 65 h.

2.6.4.2 Protein separation and SDS-PAGE

To detect the presence and size of LBD41 protein variants, samples of infiltrated *N. benthamiana* leaves were extracted and separated by SDS-polyacrylamide gel electrophoresis (PAGE). The frozen leaf discs (Ø 8 mm) were pulverized in a ball mill (1 min, 30 Hz) while cooling the components with liquid nitrogen. Subsequently, the samples were brought to room temperature. Then, 200 µl of freshly prepared and 60 °C tempered extraction buffer (8 M Urea, 50 mM Tris-HCl pH 6.8, 30 % (v/v) Glycerol, 4 % (w/v) SDS, 50 mM DTT) was added to each sample. The first two replicates were however extracted with an alternative extraction buffer (4 M Urea, 100 mM Tris-HCl pH 7.4, 150 mM NaCl, 5 mM EDTA, 10 % (w/v) SDS, 10 mM DTT). After 20 min of incubation at 60 °C, the samples of only N'HA LBD41 C'GFP were diluted 1:100 with additional extraction buffer.

Then, 20 µl of all extracts was transferred to a new tube. For mass-based separation of proteins, an acrylamide gel was prepared (3 % Stacking gel: 0.3 ml acrylamide/bis-acrylamide (30/0.8 % (w/v), 0.75 ml 0.5 M Tris-HCl pH 6.8, 1.9 ml H_2O, 30 µl 10 % SDS, 15 µl 11 % (w/v) APS; and a 10 % Separating gel: 2 ml acrylamide/bis-acrylamide, 1.5 ml 1.5 M Tris-HCl pH 8.8, 2.4 ml H_2O, 60 µl 10 % SDS, 30 µl 11 % (w/v) APS). To each aliquot of protein extract, 5 µl of a 5x Loading buffer (150 mM Tris-HCl pH 6.8, 60 % (v/v) glycerol, 5 % SDS, 500 mM DTT) were mixed into the sample, before directly transferring 20 µl into the gel pockets. To each gel, 6 µl of PageRuler prestained protein ladder (Thermo Fisher Scientific Inc., Waltham, USA) was added as a standard molecular weight marker. Electrophoresis was performed at 45 V and constant current for 70 min, followed by another 80 min at 100 V (PowerPac HC, Bio Rad, Hercules, USA).

2.6.4.3 Western Blot

After size separation through electrophoresis, the acrylamide gel was laid onto a PVDF membrane (Roti-Fluoro, Carl Roth, Germany), which was previously incubated in methanol for 20 min. Blotting of separated proteins was performed at 100 V for 1 h. After transferal onto the PVDF membrane, it was gently washed with 15 ml of PBS-T buffer (10 mM Na_2HPO_4, 137 mM NaCl, 2.7 mM KCl, 1.8 mM KH_2PO_4, pH 7.4, 0.1 % (v/v) Tween-20). Then, membranes were incubated in 25 ml Blocking buffer (5 % (w/v) powdered milk in PBS-T) over night at 4 °C and under constant motion. On the following day the blocking solution was discarded, and the blotted membrane washed with 15 ml of PBS-T for three times and 10 min each. After discarding the final wash, 10 ml of primary antibody dilution (1:3000 of α-HA or α-GFP in blocking buffer) was poured over the membrane and then incubated at RT on a roll shaker for 1 h. After removal of the primary antibody, the previous washing step with 15 ml PBS-T was repeated three times.
Then 10 ml of the secondary antibody (1:10,000 anti-mouse-HRP (HORSERADISH PEROXIDASE) in blocking buffer) were added to the membrane, followed by subsequent incubation at RT for 1 h on a roll shaker. After removal of the secondary antibody and thrice repeated washing with PBS-T, the membrane was transferred to a clear plastic foil. For the detection of adhered antibody complexes, the Amersham ECL Prime Western Blotting Detection kit was utilized. Here, 500 µl of a 1:1 mix of both provided solutions was used for each membrane, followed by immediate detection of signals for 10 min with sequential image integration. Imaging was performed with a chemiluminescent detector (Intas Science Imaging Instruments GmbH, Göttingen, Germany).

2.7 Generation of new constructs

2.7.1 High-fidelity mutagenesis PCR

When creating new constructs or amplifying sequences for cloning, a high fidelity PCR was performed. To introduce point mutations in vector sequences, complementary primers were designed with an intentional mismatch at the center. In both cases, the forward and reverse

primers were then diluted to 10 µM and added to 0.1 ml tubes at 2.5 µl each. Now, 1 µl of template DNA was combined with 10 µl of 5x Phusion HF buffer. Finally, 0.5 µl of 10 mM dNTPs and 33 µl H_2O were included before addition of 0.5 µl Phusion high-fidelity polymerase. For the amplification reaction in a Labcycler 48 (SensoQuest, Göttingen, Germany) an initial denaturation was performed at 98 °C for 2 min. A 3-step PCR was carried out in 38 cycles, starting with a 30 s denaturation at 98 °C. Then, a hybridization was performed for 45 s at the ideal temperature calculated with the Tm calculator web tool (Thermo Fisher, based on (Allawi et al., 1997)). As the third step within the cycle, polymerisation was executed at 72 °C for 2 to 3.5 min depending on product length. At the end of the cycles, a final polymerisation step was performed at 72 °C for 10 min, followed by cooling down to 14 °C.

2.7.2 Gateway cloning

To clone a new construct into an existing destination vector, either LBD41 or a target promoter sequence were first amplified with an overhang corresponding to the matching overhang of attB adapter primers. The resulting fragment was then amplified with the attB adapter primers through a two-step PCR (5 cycles of 45 °C annealing temperature, 20 cycles at 55 °C annealing temperature) followed by purification of the product by a PCR cleanup kit (Thermo Fisher Scientific, Waltham, USA).

To create the gateway entry clone with a BP reaction, 1 µl of the attB-PCR product was combined with an equal concentration and volume of Donor vector (pDONR221), 8 µl of TE buffer (10 mM Tris pH 8, 0.1 mM EDTA) and 2 µl of thawed and briefly vortexed BP clonase II mix. The reaction was incubated for 1 h at 25 °C, before stopping the reaction through the addition of 1 µl Proteinase K, followed by subsequent incubation at 37 °C for 10 min. The resulting vector was transformed into competent DH10B cells, followed by plasmid extraction and confirmation by sequencing. To clone the construct from its Donor plasmid into the destination vector (pHBTL), 1 µl of both vectors were combined at an equal concentration, along with 8 µl of TE buffer, as well as 2 µl of thawed and briefly vortexed LR clonase II mix. The reaction was again incubated for 1 h at 25 °C and afterwards stopped with 1 µl Proteinase K and subsequent incubation at 37 °C for 10 min.

2.7.3 Crispr/Cas based genome editing

For the introduction of mutations based on the Crispr/Cas system, potential targets within a sequence were identified through proximity to a protospacer adjacent motif (PAM). Using the scoring system of Geneious Prime 2022 (Doench et al., 2016), potential PAM sites with a NGG motif and their surrounding sequence were evaluated. Sequences were checked for off-target sites in the genome of *A. thaliana*. A forward and reverse strand consisting of 24 nucleotides was then designed for each position, including overhang restriction sites for BsaI. These oligonucleotides coding for the guide RNA (gRNA) were diluted in bidest H_2O and combined at 1 µM each. Annealing was performed at 65°C for 5 min to create double stranded oligos. The binary vector pKSE401 (Xing et al., 2014) was then prepared through digestion with BsaI for 1 h at 37 °C, followed by inactivation for 20 min at 65 °C. To create the Crispr vector, double stranded fragments were ligated into the digested vector in an overnight reaction at 16 °C (3 µl vector, 1 µl gRNA oligo, 0.5 µl T4 Ligase, 2 µl 10x ligation buffer, 2 µl 50 % PEG4000). Ligated Crispr vectors were then transformed into competent *E. coli* DH10B, followed by amplification and sequencing. After conformation of the sequence, the crispr vectors were transformed into *A. tumefaciens*, with subsequent transformation of *A. thaliana* by floral dip.

2.7.4 Stable transformation of *A. thaliana*

Permanently inserting a new genetic sequence into the genome of *A.thaliana* was performed through floral dip. Here, *A. tumefaciens* aliquots of the strain GV3101 were transformed with 1 µg of either a pKSE401 or pK7FWG2 vector. The cells were then re-frozen in liquid nitrogen, heat-shocked for 5 min at 37 °C and allowed to recover for 3 h at 28 °C and light shaking after the addition of 1 ml YEB medium. Confirmed transformants were then used to inoculate a 2 ml ON culture of YEB medium and relevant antibiotics. After growth at 30 °C, 1 ml of each ON culture was transferred to 200 ml LB medium, which were again incubated ON at 30 °C. Roughly 1 h before the floral dip was performed, 5 % (w/v) sucrose were added to the culture, which was then further incubated at 30 °C. To each culture 0.2 % (v/v) Silwett-77 were added to increase the surface tension, followed by submerging the inflorescence of flowering *A. thaliana* upside down into the cultures. Plants were then covered in clear foil tubes and incubated ON

in the dark at RT. On the following day, the transformed plants were transferred to long day growing conditions until the seed pods were ripe for harvesting.

2.7.5 Crossing of *A. thaliana* genotypes

To create new *A. thaliana* strains through crossing, plants were grown under long day conditions until they reached the flowering phase. Using a magnifying glass and precision tweezers, individual flowers had their sepals, petals and stamen carefully removed. The now exposed stigma of the pistil was gently chafed with the stamen of a flower carrying the genotype to be crossed with. All flowers used in the crossing process were labeled for later identification of F1 seeds. The plants were placed back into a long day growth chamber for optimal seed generation and ripening.

CHAPTER 3

Results

3.1 Studies of GVIIERFs *At*RAP2.12 and *At*RAP2.2

As major activators under hypoxia in *A. thaliana*, the GVIIERF transcription factors RAP2.2, RAP2.12, and RAP2.3 induce acclimation to flooding. Their abundance and the resulting intensity of acclimation is mainly controlled post-translationally, with oxygen availability through the N-degron pathway. Nevertheless, further transcriptional regulation has been uncovered recently, which appears to affect mainly RAP2.12. Such individual regulations imply that these three transcription factors are not entirely identical in their function or regulation. Whether they share identical target specificity, or induce a more individual response remains to be explored. Considering their importance in flooding acclimation, the impact of their individual activity requires investigation through selective mutagenesis studies. Therefore, prior to this work, a knockout *rap2.12* line (Gasch et al., 2016) was crossed with two Crispr/Cas mutated *rap2.2* lines (Judith Bäumler, University Bayreuth). Both utilized *rap2.2* lines introduced an early STOP codon, with Crispr B containing a very early STOP, and Crispr C a STOP at around 60 % of the wild type sequence in Col-0.

3.1.1 HRG expression in RAP mutant seedlings

To assess the capacity to activate a core hypoxic response, seedlings of Col-0, *rap2.12*, *rap2.2* Crispr B, *rap2.12 rap2.2* B, and *rap2.12 rap2.2* C were exposed to low-oxygen conditions. At the age of 7 days, seedlings grown on MS agar plates were fumigated with either nitrogen or air for 4 h. After treatment, samples were frozen and subsequently had their RNA extracted. To measure transcript levels, the isolated RNA was reverse transcribed to cDNA and quantified in

a qPCR. As two genes highly upregulated under hypoxia, the transcripts of ADH1 and LBD41 were both analyzed and referenced to a housekeeping gene transcript. For this, ELONGATION FACTOR 1α (EF-1α) (AT5G60390) was selected, an essential subunit of aminoacyl-tRNA transport to the ribosome.

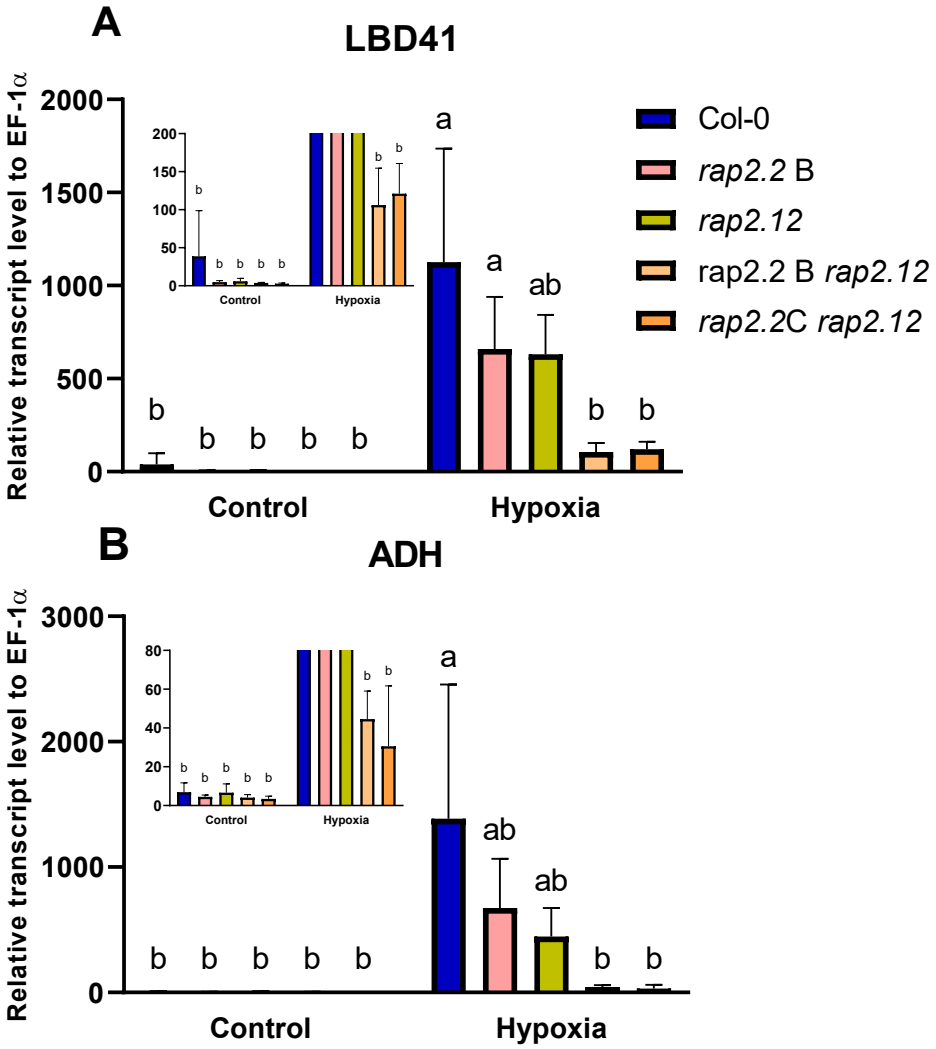

Figure 4: Induction of hypoxic response genes in rap mutant qPCR

Hypoxic fumigation of 7-day-old seedlings for 4 h with either air (control) or N_2 (hypoxia). Different single and double GVIIERF mutant lines (*rap2.2* B / C, *rap2.12*, *rap2.2 rap2.12* or Col-0) were grown on MS agar medium under long-day conditions. All RNA was extracted and reverse transcribed to cDNA, then measured by qPCR. Transcript level of LBD41 (A) and ADH (B) was calculated in reference to EF-1α. Graphs show the average with standard deviation of 3 biological replicates. Letters indicate significant differences $p < 0.05$ calculated in a statistical analysis (Two-way ANOVA, Tukey post-hoc).

Indispensable for protein synthesis, EF-1α makes a suitable reference for stress acclimation (Chen et al., 2013) (Chen et al., 2019). Here, both HRGs LBD41 and ADH display a clear induction upon hypoxia, with a low baseline expression at normoxic control conditons (Fig. 4). This difference is most pronounced in the wild type and reduced in mutants. The single mutants *rap2.2* Crispr B and *rap2.12* already show a decreased induction of the transcript levels for both targets, however not significantly (Two-way ANOVA, Tukey post-hoc). For both double mutants, an even stronger reduction of the transcript levels takes place. In direct comparison of control and hypoxic conditions, the double mutants still show an induction of both LBD41 and ADH. However, the HRG transcript levels under hypoxia are significantly reduced in *rap2.12 rap2.2* from those of Col-0.

3.1.2 ADH activity

While the hypoxia treatment with nitrogen was shown to induce transcriptional responses, it does not confirm if the acclimation signal is also translated into an enzymatic response. When induced by GVIIERFs as part of the core response, ADH should directly enact a reaction which strongly influences carbohydrate metabolism. This activity of converting acetaldehyde to ethanol requires electrons from a co-substrate NADH. When the generation of oxidized NAD^+ is limited under hypoxia, this fermentation allows the electrochemical oxidation of NADH to NAD^+ even in the absence of oxygen. This conversion of NADH to NAD^+ is captured in a spectral shift of light absorption at 340 nm, and herein interpreted as ADH activity.

3.1.2.1 ADH activity singular

From the identical set of 7-day-old seedlings treated for the RNA transcript levels of ADH (3.1.1), further samples were taken. These for 4 h N_2 (Hypoxia) or air (Control) treated seedlings had their total protein content extracted and quantified through Bradford. After which protein extract samples were measured at 340 nm over 5 min, first for a baseline activity and again after addition of the substrate Acetaldehyde. With the difference in slope, an activity was calculated based on the total protein content. This first set of measurements, however, did not reveal any differences to the hypoxic treatment or between the genotypes (Supplementary,

Fig. 30). With 4 h of nitrogen treatment not inducing fermentation activity in *A. thaliana*, variations of stress application might be required.

3.1.2.2 ADH activity double fumigation and transcript memory

It has been previously observed that when subjecting plants to stress events, future iterations of this stress type show a decreasing negative effect on these individuals. Recently, multiple studies uncovered epigenetic modifications, which regulate such memory mechanisms for abiotic stress (Crisp et al., 2016) (Oberkofler et al., 2021) (Ramakrishnan et al., 2022).
It is possible that a similar genetic imprinting mechanism is applied for reoccurring hypoxia stress. To test for increased hypoxia acclimation with repeated stress, 7 day old seedlings grown on MS medium were fumigated for 6 h, with either N_2 (hypoxia) or air (control). After treatment, some seedlings were frozen as samples and others transferred to soil. At the age of 28 days, these now adult plants were then fumigated with N_2 or air for a second time. This resulted in plants that were stressed as both seedlings and adults, stressed only as either seedlings or adults, and plants that were never subjected to a hypoxic stress. After protein extraction, the ADH activity was photometrically measured and then referenced to the total protein content.
For the seedlings and unlike to the first set of measurements, an overall induction of activity could be measured (Fig. 5 A). Here, an increase in activity after hypoxia was measured for Col-0 as well as the single mutants, although no significant difference could be calculated under control conditions. In case of the double mutants, no visible induction of activity could be measured. When looking at the activity of adult plants, a generally reduced induction compared to seedlings can be detected. In comparison to adult plants which were hypoxia-stressed for the first time, seedlings display a 5-fold increase in activity induction (Fig. 5 A and B). While in seedlings the first hypoxic stress seems sufficient to induce ADH activity, this does not seem to be the case for adults. On the other hand, adult plants that were previously stressed as seedlings still show a slightly elevated activity level, even when fumigated with air (Fig. 5 C and D).

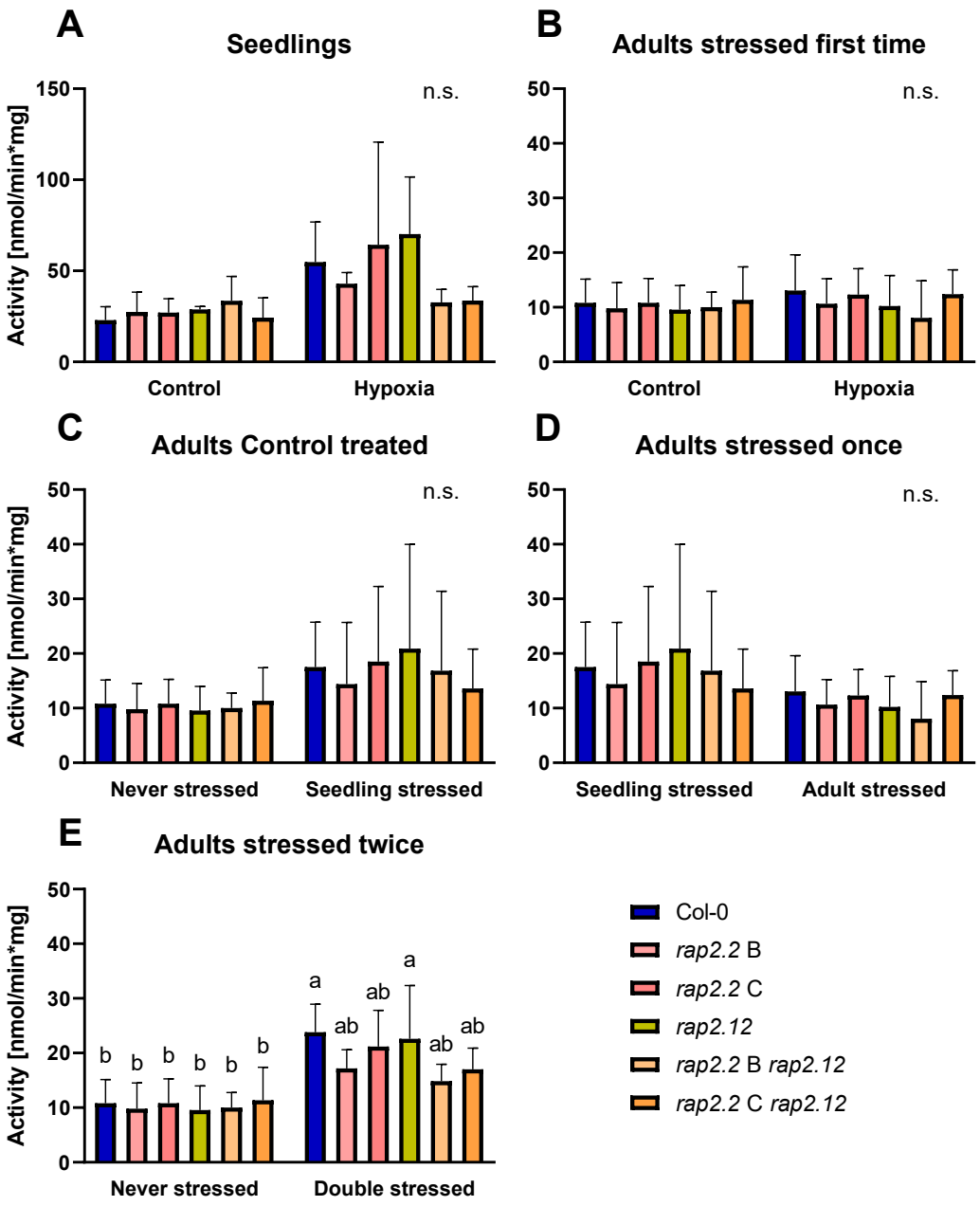

Figure 5: ADH activity of hypoxia treated GVIIERF mutant plants

Seedlings of Col-0, *rap2.2* Crispr B and C, *rap2.12* and their double mutants were fumigated for 6 h with either air (Control) or N_2 (Hypoxia). Seedlings were germinated on MS medium, grown under long-day conditions and then stressed at 7 d old (A). The seedlings were transferred to soil and stressed again at the age of 28 d. Shown are the activity of plants which were stressed only as adults and control treated as seedlings (B), plants that were stressed only as seedlings and control treated as adults (C), stressed as either seedlings or adults (D) and comparing never stressed to double stressed (E). Protein leaf samples were extracted, quantified by Bradford and the ADH activity measured. Graphs show the average with standard deviation of 5 biological replicates. Letters indicate significant differences $p < 0.05$ calculated in a statistical analysis (Two-way ANOVA, Tukey post-hoc). Data was collected by Alina Hieber.

Only for adult plants that were subjected to hypoxic stress both as seedlings and as adults, a significant difference in activity could be measured (Fig. 5 E). While the data shows increased activity for all genotypes, only Col-0 and *rap2.12* display significant differences to control conditions.

3.1.3 Survival of RAP mutants

As the RAP proteins are key players in activating flooding acclimation, it can be assumed that their absence would severely impact a plants ability to survive low-oxygen environments. To test whether the decrease of GVIIERFs in *rap2.2* and *rap2.12* lines directly translates into impaired acclimation, survival throughout prolonged flooding was determined. For this, seedlings were pre-grown on MS Agar plates for 7 days, then transferred to soil and grown under short-day conditions. Plants were subjected to a full submergence stress treatment at the age of 3 weeks old, which lasted for 21 to 31 days. Respectively at 3 weeks (21 d), 3.5 weeks (24 d), 4 weeks (28 d) or 4.5 weeks (31 d) one fourth of the plants were removed from the treatment and allowed to recover for 14 d at normoxic short-day conditions. After recovery, plants were documented on appearance and survival rate. Individual plants were classified as alive if they were able to develop new leaves within the recovery period.
Beginning with the first time point, nearly all plants were able to recover from 3 weeks of submergence with no visible differences between the lines (Fig. 6 A) (Supplementary, Fig. 31). At the second time point just 3 days later, the plants did not appear observably different then before. However, in some replicates increased algae growth led to visibly decreased survivability already by this time point. At 24 d, the survival rate after recovery of the various mutants had already dropped substantially compared to the first time point. Here the mutants show an average survival rate of around 80 %, while Col-0 still displays a 96 % survival rate (Fig. 6 B). Both single and double mutants of *rap2.2* with the late STOP Crispr C, exhibited the lowest survival rate at this time point. By the third time point at 28 d of submergence, this difference between wildtype and mutants is still present (Fig. 6 C). While around 50 % of Col-0 plants were able to recover after 4 weeks of submergence, the average survival rate among the mutants was only 33 %. The average survival rate of mutants shows the lowest deviation

at this point. A final time point was taken at 31 d of submergence, with a survival rate of less than 40 % across all plant lines (Fig. 6 D). Here, Col-0 shows survival with an average 33 % rate, while *rap2.2* B, *rap2.2* C single mutants and *rap2.2* C *rap2.12* show even lower survival with 20 to 30 %. Surprisingly however, *rap2.12* and *rap2.2* B *rap2.12* display a slightly higher average survival rate than Col-0 at this time point.

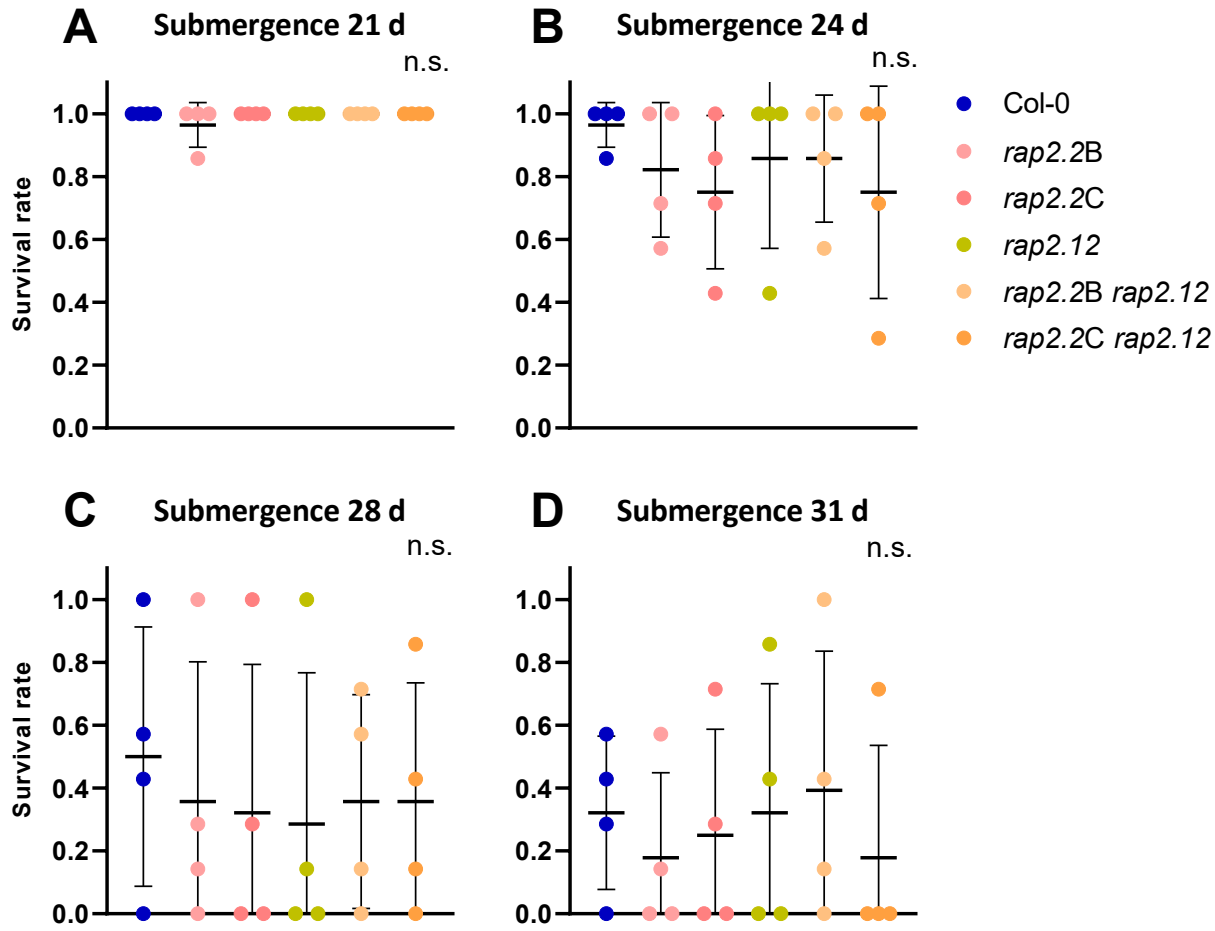

Figure 6: Survival rate of RAP KO mutants under full submergence

Short-day grown 3 w old plants of Col-0, *rap2.2* (Crispr B and C), *rap2.12* or their double mutants were subjected to 21 d (A), 24 d (B), 28 d (C) or 31 d (D) of full submergence followed by 14 d of recovery. Both stress and recovery were performed under short-day conditions. Plants were placed in clear tubs filled with tap water. The survival rate was calculated by the ratio of plants showing new growth after recovery to the total number of plants. Data shows individual replicate ratios and average rate ± standard deviation of 4 biological replicates with 7 plants each. No significant differences $p<0.05$ were revealed in a statistical analysis (One-way ANOVA, Tukey post-hoc).

3.2 Characterizing the transcriptional repressor *At*LBD41

As one of the transcription factors involved in the core flooding response of *A. thaliana*, the ubiquitous induction of LBD41 suggests an important role in the acclimation process to hypoxia. With HRE2 and HRA1 appearing more involved in finetuning the total acclimation response, LBD41's putative targets were only discovered preceding this work (Bäumler, 2020). However, those of its target genes with known functions appear mostly unrelated to hypoxia. While the general function as a transcriptional repressor has been uncovered for LBD41, the exact purpose of this hypoxia-induced transcriptional repression remains mostly unknown. By downregulating nonessential genes and reducing ATP consumption underwater, LBD41 might be a key player of the quiescent survival strategy.

3.2.1 LBD41:VP16 mutant lines

To determine the effect of this repressive transcription factor, creation of a mutated version with reversed function was performed prior to this work. Removal of the identified EAR motif was combined with an exchange to a viral VP16 activation domain from *Herpes simplex* (Gasch, 2015). The VP16 domain is expected to interact with histone deacetylases through TATA Box binding proteins. As this signal cascade has been formerly shown to enable promoter-specific euchromatin formation, activation of previously repressed genes is made possible (Arnosti et al., 1993) (Bensmihen et al., 2004). This mutant LBD41ΔEAR:VP16 variant was at first tested through transient overexpression in protoplasts, followed by detection of differentially expressed genes in a microarray (Bäumler, 2020).

This led to the discovery of multiple putative target genes, which were also downregulated by overexpressed native LBD41. To then further explore the function of LBD41 and possible consequences of its malfunction, the VP16 mutant was previously inserted stably into a Col-0 background. This pr35S:LBD41ΔEAR:VP16 construct was integrated randomly into the genome through pK7FWG2 mediated T-DNA insertion (Bäumler, 2020). The cultivation and selection of stable VP16 mutants was begun prior to this work and allowed the identification of three homozygous lines. These VP16 lines do not show visual differences to Col-0, with the exception of a seed and silique phenotype of line VP16-2 (Supplementary, Fig. 32 A, B and D).

3.2.1.1 LBD41 ΔEAR:VP16 mutant expression

To confirm a constitutive expression of LBD41ΔEAR:VP16 in these new lines, transcript levels were analyzed in a qPCR. At first, seedlings of Col-0, VP16-1, VP16-2 and VP16-3 were germinated and grown on MS agar plates for 7 d, then subjected to hypoxia treatment with nitrogen fumigation for 8 h. After treatment, seedlings were frozen immediately and later had their total RNA extracted. Subsequently, the extracted RNA was reverse transcribed to cDNA. For transcript quantification of LBD41 the cDNA was measured in a qPCR, using EF-1α as a reference. The selected primers were complementary to an early part of the coding sequence, allowing quantification of combined mutant and native transcripts.

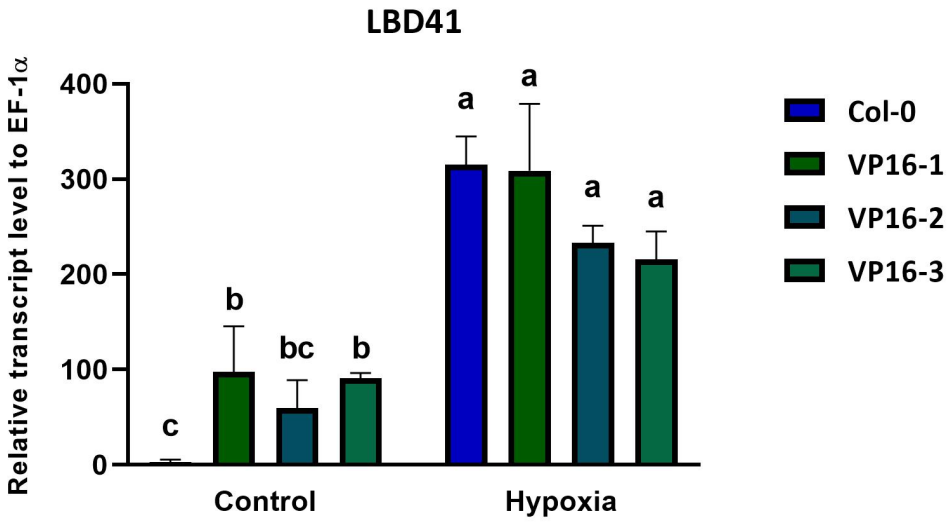

Figure 7: LBD41 transcript changes to hypoxia of VP16 mutants

Quantification of total LBD41 RNA transcripts by qPCR. Seedlings of 7 d old Col-0 or pr35S:LBD41ΔEAR:VP16 lines 1, 2 and 3 were treated with hypoxia. Plants were fumigated with air (control) or N_2 (hypoxia) for 8 h and directly frozen. All RNA was extracted and reverse transcribed to cDNA. Transcript level of LBD41 was determined relative to EF-1α. The graph shows average with standard deviation of 3 biological replicates. Letters indicate significant differences $p<0.05$ calculated from a statistical analysis (Two-way ANOVA, Tukey and Sidak post-hoc).

Here, all three mutant lines could be confirmed to constitutively express the LBD41ΔEAR:VP16 construct (Fig. 7). Unlike the total LBD41 transcript levels of Col-0, which were nearly undetectable under normoxic control conditions, the mutant lines already display elevated levels. Through the hypoxia treatment, an induction of LBD41 could be recorded in Col-0 and

VP16 lines alike. The total transcript levels in VP16 lines during hypoxia however, did not represent levels substantially higher than wildtype despite their already normoxic elevation. Furthermore the transcript levels found in mutant lines under normoxia are relatively low when compared to the hypoxic induction in Col-0.

3.2.1.2 Anthocyanin content during germination

Biosynthesis of anthocyanins is often linked with various stress responses, including low phosphorus, oxidative or salt stress acclimation. Besides their signalling roles, the chemical properties of anthocyanins make them powerful ROS scavengers. Within a long term flooding environment the abundance of ROS is limited, substantially reducing the need for antioxidants. With the putative repression of PRODUCTION OF ANTHOCYANIN PIGMENTS1 (PAP1) by LBD41, anthocyanin biosynthesis is potentially downregulated to preserve energy. Simultaneously, a constitutive expression of LBD41ΔEAR:VP16 should then also result in elevated anthocyanin levels.

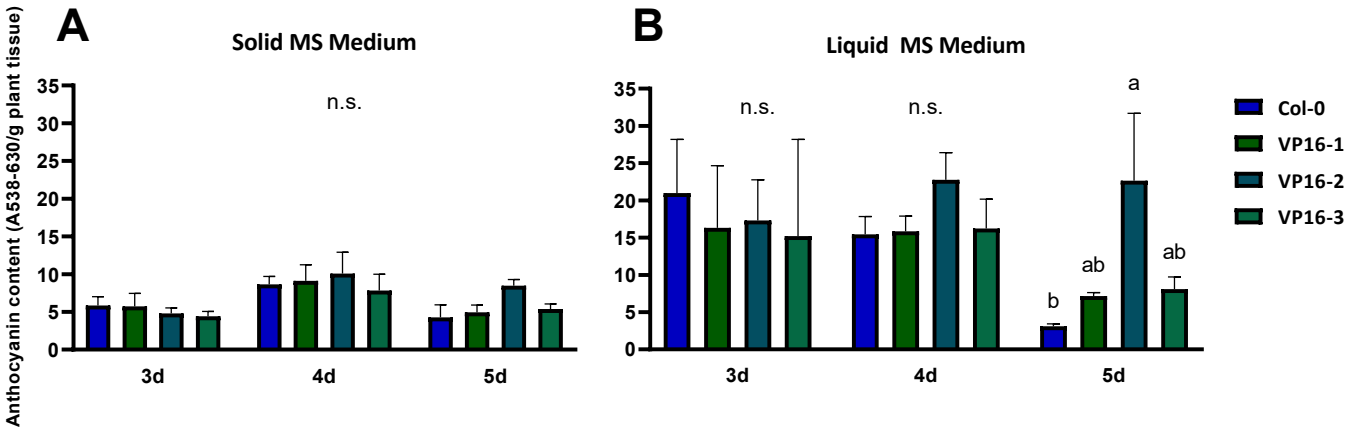

Figure 8: Anthocyanin content of LBD41-VP16 seedlings during germination

Seedlings of Col-0 or three independent pr35S:LBD41ΔEAR:VP16 lines 1, 2 and 3 were germinated on solid MS medium (A) or in liquid MS medium (B). All growth took place under long-day conditions. Samples were harvested at 3, 4 or 5 d after transferal to long-day growth conditions, followed by determination of their fresh weight. Anthocyanin content was calculated from photometrically measured difference of A_{538}-A_{630}, per g of tissue fresh weight. Graphs show the average with standard deviation of 3 biological replicates. Letters indicate significant differences ($p<0.05$) calculated from a statistical analysis (One-way ANOVA, Tukey post-hoc test).

When homozygous stable LBD41ΔEAR:VP16 expressing seedlings were grown on normal MS agar medium and normoxic conditions, no phenotypic difference could be detected. However when growing the seedlings in liquid MS medium, a darker coloring was detected within the first days of germination (Supplementary, Fig. 32 C). This phenotype, however, disappeared by the time the seedlings reached an age of 7 days. To test if the color difference stems from seedlings carrying an increased level of anthocyanins, seedlings of pr35S:LBD41ΔEAR:VP16 were germinated on either MS Agar Medium or liquid MS medium at pH 5.7. At different ages, the seedlings were harvested, their fresh weight determined and their anthocyanin content measured.

Despite the constitutive expression of pr35S:LBD41ΔEAR:VP16 lines, the seedling did not contain elevated anthocyanin levels during normoxia (Fig. 8 A). Overall, the anthocyanin content is elevated by about four-fold when germinating in liquid medium compared to solid MS. (Fig. 8 B) This increase is also present in Col-0 at the beginning, although, by day 5 the anthocyanin content of liquid germinated seedlings is at the same level as WT grown on solid medium. However, the anthocyanin content of all VP16 lines remained elevated on day 5, but only significantly different to Col-0 in the line VP16-2. This difference between WT and VP16 lines was only pronounced at day 5, with minimal difference remaining by day 6 (Supplementary, Fig. 33).

3.2.2 Triple knockout *lbd40 lbd41 lbd42*

Attributable to gene redundancy in many organisms including *A. thaliana*, it is common for some single knockout mutants to not show a clear phenotype. Previous work has shown that a *lbd41* knockdown displays a stronger transcriptional induction of LBD40, presumably rescuing the missing regulation. A similar behavior is postulated for LBD42, however finding a condition in which LBD42 is induced has not been successful so far. With the goal of fully disabling the function of LBD41, as well as potential homologous backup proteins LBD40 and LBD42, a triple mutant *lbd40 lbd41 lbd42* was created prior to this work. The genes of LBD40 and LBD42 were altered through the Crispr/Cas system, providing an early STOP codon and resulting in a dysfunctional protein (Bäumler, 2020). However, the mutant *lbd41* was

created through a T-DNA insertion (SALK_144556) which was presumably located upstream of the important EAR motif. These single mutants were then crossed into a Col-0 background, supposedly resulting in a *lbd40 lbd41 lbd42* knockdown . After a homozygous triple mutant line was selected, it was discovered that the T-DNA insertion of *lbd41* starts downstream of the EAR motif. To determine if the protein resulting from this shortened version is still capable of transducing a repressive activity, the *lbd41* single mutant sequence was reconstructed in a pHBTL vector. It was then tested if this shortened variant (*lbd41**) would behave differently than native LBD41.

3.2.2.1 Repressive activity of *lbd41**

To measure the transcriptional activity of LBD41, its variants and homologs, their regulatory function on putative target genes was studied *in vitro*.

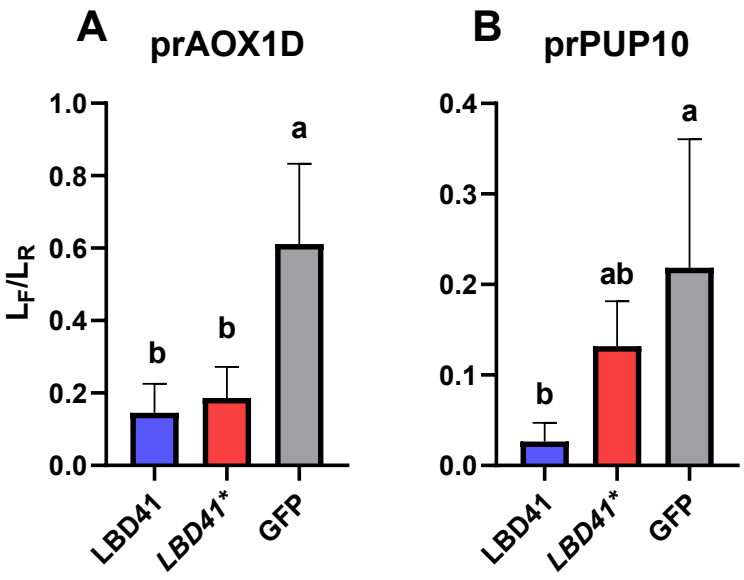

Figure 9: Protoplast transactivation assay of mutant *lbd41*

Leaves of 4 week old short-day grown Col-0 were harvested. Protoplasts were then isolated and transformed with prTarget:Luc_F, pr35S:LBD and pr35S:Luc_R vectors at 16 h prior to the measurement. Overexpressed effectors (pHBTL:pr35S) were a GFP baseline control, native LBD41 or shortened mutant *lbd41**. Target promoters were tested with vectors for AOX1D (A) and PUP10 (B). Graphs show the average with standard deviation of 3 biological replicates, with 2 technical replicates each. Letters indicate significant differences $p<0.05$ calculated in a statistical analysis (One-Way ANOVA, Tukey post-hoc).

For this purpose, the protoplast transactivation assay was selected, which allows for indirect detection of promoter interaction activity (Wehner et al., 2011). Through co-transformation of pHBTL:pr35S:LBD41 and a prTarget:FireflyLuciferase pBT10 vector, increased repression through the overexpressed factor is detectable through comparison to the baseline luciferase activity. This baseline activity is recorded by overexpression of a non-transcriptionally active null-effector (pr35S:GFP). Normalization of the luciferase signal was achieved through co-expression of a pBT10 pr35S:RenillaLuciferase construct. Measured here for both putative target promoters prAOX1D and prPUP10, a significant repression of the luciferase signal is detected for overexpressed native LBD41 compared to GFP (Fig. 9). Similarly, the shortened mutant version (*LBD41**) still shows a significant signal reduction compared to GFP for prAOX1D, and a clearly decreased signal for prPUP10. In these measurements the mutant variant displays a reduced repression capability compared to its native counterpart. However, this mutant construct still shows a mostly viable signal transduction.

3.2.2.2 Crispr/Cas mediated *lbd41* knockout

As the previously used *lbd41* mutant contained a T-DNA insertion that only started downstream of the EAR motif, the resulting protein could still display repressing capabilities. After this was confirmed in a PTA, new *lbd41* KO lines were created using the Crispr/Cas system. Sites were selected using the prediction tool of Geneious2021, based on (Doench et al., 2016) and later confirmed with CCTop (Stemmer et al., 2015). All selected sites show at least a medium efficacy score, and produce no off-target matches within *A. thaliana*. To ensure the inability to emit a repressive function, three different Crispr sites were chosen and introduced through a pKSE401 vector. Mutations were introduced into a Col-0 background using floral dip with transformed *A. tumefaciens*. Crispr1 and Crispr3 sites are located within the first half of the LOB domain, after the LOB consensus motif but within the first exon. Crispr2 is located in the second exon, near the end of the predicted LOB domain, and upstream of the EAR motif. Crispr1 and Crispr3 are located on the non-coding-strand, Crispr2 on the coding-strand (Fig. 10).

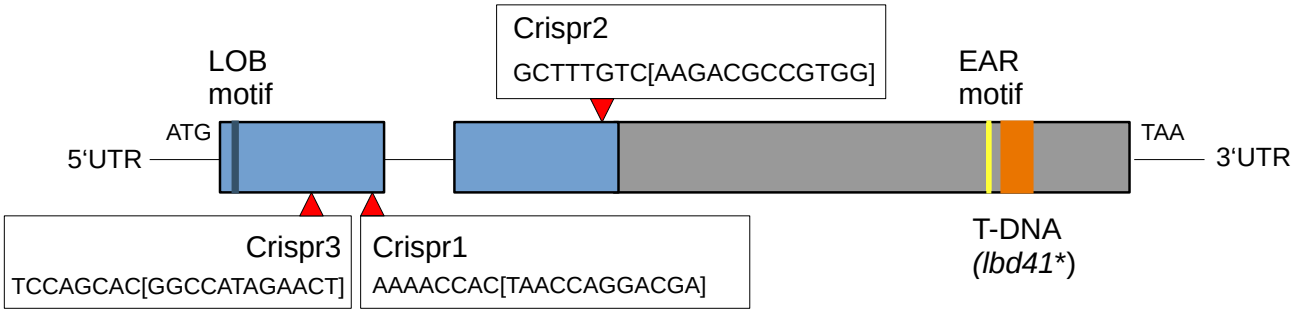

Figure 10: Representation of selected Crispr/Cas sites in *LBD41*

Figure depicts the genetic structure of *LBD41* and the selected Crispr/cas sites. The blue part symbolizes the LOB DNA binding domain, separated by an intron. Highlighted are the sequences coding for the LOB consensus motif (dark blue) or the EAR motif (yellow). Schematic display the location of the previous T-DNA insertion (SALK_144556) downstream of the EAR motif. Selected Crispr-editing sites and their approximate location are indicated. Sequence in brackets represents the predicted editing site by CCTop.

Homozygous LBD41 Crispr knockout lines were selected for but only tested briefly. These preliminary qPCR were performed with RNA extracted from 7 day old seedlings, stressed with Hypoxia (N_2) for 8 h. The results show no clear difference in the transcription of LBD41, but displayed an increased transcript for LBD40 under hypoxia. When evaluating the transcript level of the putative target gene PUP10, a trend towards increased transcript levels under hypoxia was measured for mutant seedlings (Supplementary, Fig. 34). Reproducibility of these results is not ensured, as only a single replicate could be performed due to time constraints. To determine their effect, further transcriptomal data on LBD41 homologs and their targets has to be collected in these new mutant lines.

3.2.3 LBD41 transcriptional effect studies

3.2.3.1 Hypoxia stress on target transcript abundance

With a *lbd40 lbd41* lbd42* line that features reduced promoter activity of LBD41 and deactivation of its homologs, this knockdown of the imposed regulation is studied. Simultaneously, the pr35S:LBD41ΔEAR:VP16 lines express an activator variant already under normoxia, which allows study of this misregulation. To investigate the effects of these mutations, changes to the

transcriptome upon hypoxia were analyzed. By comparing transcript levels of putative targets to those found in wild type plants, differences in regulation are revealed. For this, seedlings of Col-0, *lbd40 lbd41* lbd42* and the three VP16 lines were germinated and grown on MS agar for 7 days. These plants were then put under hypoxic stress through N_2 or air fumigation for 8 h. Samples were extracted from the treated seedlings in the form of RNA, which was then reverse transcribed and later analyzed in a qPCR. Transcript levels of target genes were relativized to the reference gene EF-1α.

Additionally to transcripts of previously mentioned putative targets LBD39, PUP10, AOX1D, PAP1 and HADLH, here SLAH3 (AT5G24030) was also tested. SLAH3 or SLAC1 HOMOLOGUE 3 encodes an anion channel that helps maintain NO_3^- and K^+ homeoostasis during flooding (Lehmann et al., 2021) (Liu et al., 2023). Among all results, the *lbd40 lbd41* lbd42* mutant and the VP16-activating lines showed generally higher transcript levels of all observed target genes than the WT (Fig. 11). Even though this trend was ubiquitously present under both normoxic and hypoxic conditions, target transcript levels of the mutant lines were rarely significantly higher than that of Col-0. Independently of the differences between the genotypes, the transcriptional changes that occur upon hypoxic stress vary greatly between the putative target genes. Here, the transcript levels of PAP1, PUP10 as well as SLAH3 seem unaffected by the decreasing oxygen levels. However, the remaining genes show a significantly different hypoxic response. While both LBD39 and HADLH display a clear repression under hypoxia, the transcript levels of AOX1D shows a strong induction within the same samples. Here, AOX1D under hypoxia presents the strongest difference between wild type and mutant seedlings, with elevated transcript level in *lbd40 lbd41* lbd42* and two out of three VP16 lines.

3.2.3.2 Evaluating VP16-activity in protoplasts

When originally tested in protoplasts, the pr35S:LBD41ΔEAR:VP16 constructs displayed substantial effects on target regulation (Bäumler, 2020). Therefore, a similar outcome was expected when testing the stable expression lines. However, with only limited changes with pr35S:LBD41ΔEAR:VP16 and *lbd40 lbd41* lbd42* genotypes on stress dependent transcriptional changes, their activity required isolated investigation.

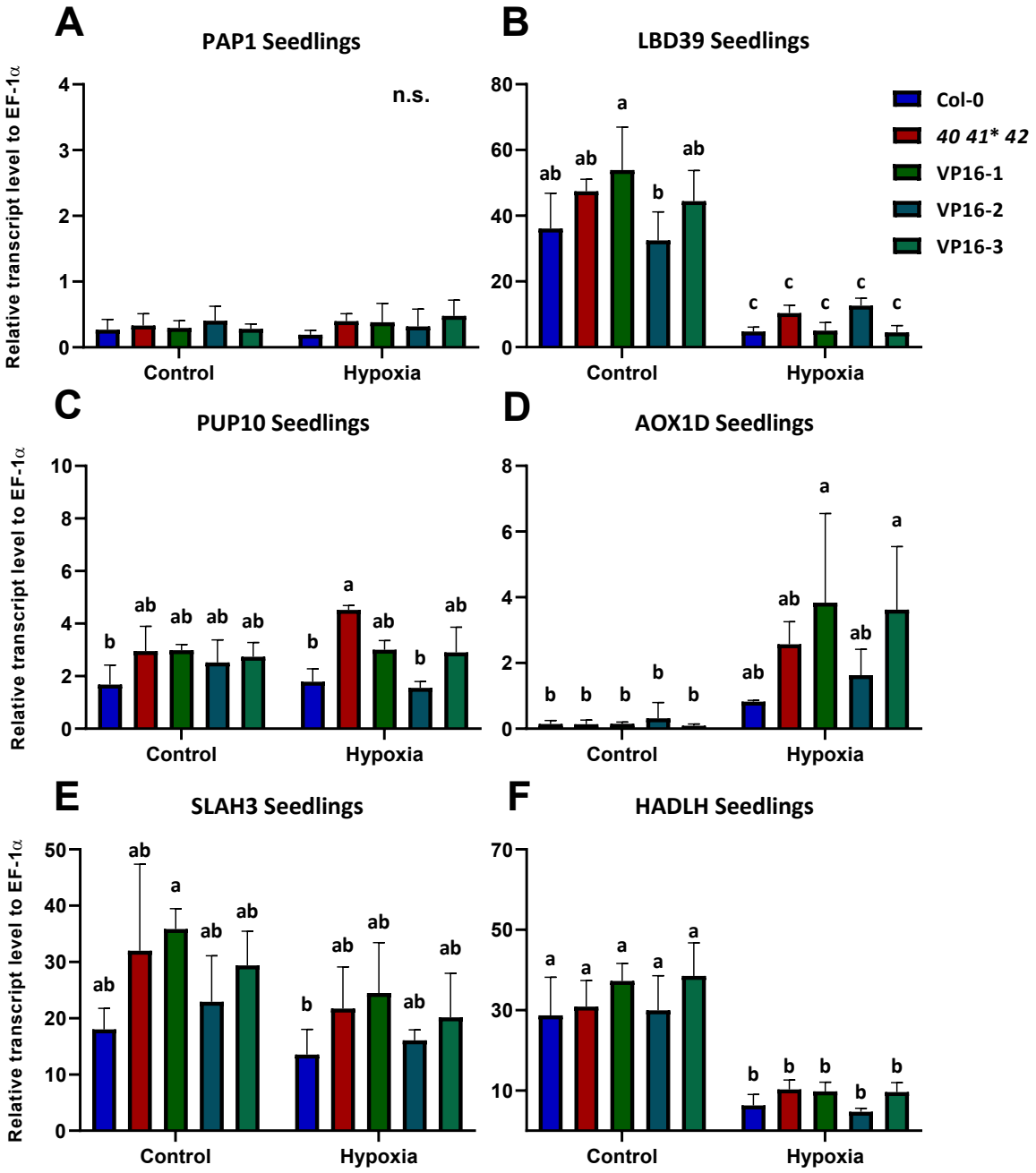

Figure 11: Quantitative PCR of target transcripts in LBD41 mutant lines

Seedlings of Col-0, lbd40 lbd41 lbd42 triple mutant (*40 41* 42*) or pr35S:LBD41ΔEAR:VP16 lines 1, 2 and 3 were germinated on MS medium and grown under long-day conditions until 7 d old. For the hypoxia treatment, plants were fumigated with air (control) or N2 (hypoxia) for 8 h before harvesting samples. All RNA was extracted and transcribed to cDNA. Transcript level of putative targets genes was determined through qPCR, relative to the reference EF-1α. Quantification was performed for PAP1 (A), LBD39 (B), PUP10 (C), AOX1D (D), SLAH3 (E) and HADLH (F). Graphs show the average with standard deviation of 3 biological replicates, each with 3 technical replicates. Letters represent significant differences $p<0.05$ provided by statistical analysis (Two-way ANOVA, Tukey post hoc).

Therefore, differences were also studied in the protoplast transactivation system. Previous experiments revealed the potential redundancy of the transcription factors LBD40, LBD41 and LBD42 in their capability to enact a similar regulatory activity on identical target genes. This homology is studied further through the repressive function of LBD40, LBD41, LBD42 and activating activity of their VP16 counterparts on target promoters. The promoter sequence of putative target AOX1D was analyzed first, as it previously showed substantial transcriptional changes to overexpression of LBD41. Therefore, protoplasts were transformed with pBT10:prAOX1D:Firefly Luciferase and overexpressed homolog mutant variants of pHBTL:pr35S:LBD41.

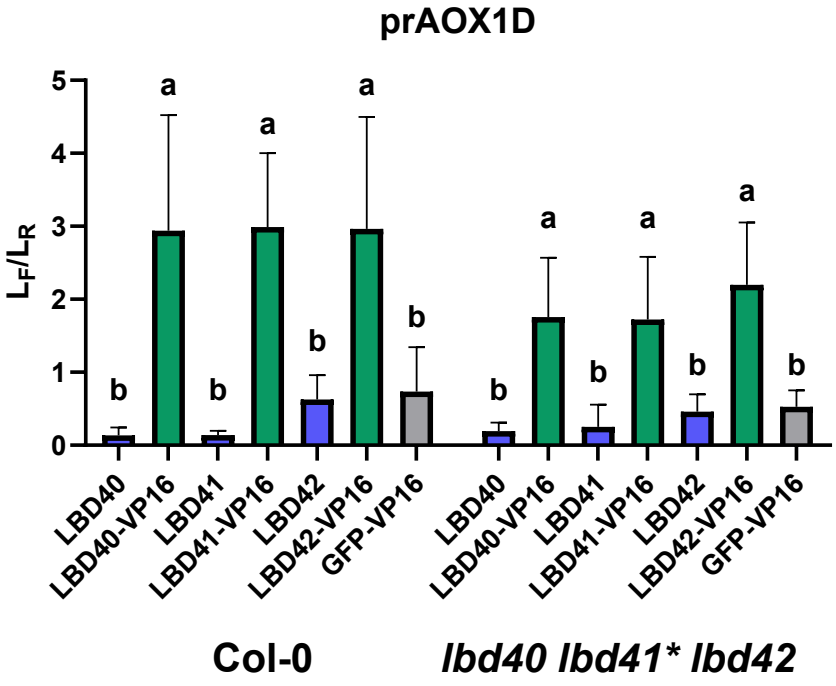

Figure 12: AOX1D promoter transactivation of LBD41 homologs and VP16-mutants
Protoplasts were isolated from 4-6 w old Col-0 or *lbd40 lbd41* lbd42* plants grown under short-day conditions. Cells were transformed with prTarget:Luc_F, pr35S:LBD and pr35S:Luc_R vectors at 16 h prior to the measurement. Target reporter pBT10:prAOX1D:Luc_F. Variants of LBD include LBD40, LBD41, LBD42, their respective ΔEAR:VP16 mutants or GFP-VP16 control. Luminescence signal of LucF and LucR was measured and L_F/L_R determined for each sample. Graphs represent the average with standard deviation of 3 biological replicates, with 2 technical replicates each. Letters indicate significant differences $p<0.05$ calculated in a statistical analysis (Two-way ANOVA, Tukey post-hoc).

Additionally to protoplasts isolated from Col-0, plants from the triple mutant *lbd40 lbd41* lbd42* were also utilized to study a potential impact of dampening the wild type background expression. When comparing the relative luciferase activity of overexpressed native LBD40/41/42 to the baseline GFP control, a non-significant repressive activity is detected. Additionally, the mutant VP16 variants all displayed an activating activity on the prAOX1D:Firefly Luciferase construct (Fig. 12). When comparing the results in Col-0 protoplasts to those isolated from *lbd40 lbd41* lbd42*, they were unexpectedly decreased. Contrasting the expected increased activation of prAOX1D in the mutant background, the VP16 mutant activation capability seems reduced. Albeit all three LBD homolog VP16 variants show decreased activation of prAOX1D in the mutant background, this difference is not significant. As a potentially new target of LBD41, trans-regulatory activity of the SLAH3 promoter was also measured for LBD41 homologs and variants. Interestingly, unlike other putative targets, prSLAH3 showed no increased activation through LBD41ΔEAR:VP16 or LBD40ΔEAR:VP16. However, a significant induction through LBD42ΔEAR:VP16 was detected (Supplementary, Fig. 35).

3.2.4 Salt stress and LBD41

With increased dilution of salt molecules by excessive water, ionic and osmotic stress should potentially decrease through flooding. Interestingly, the osmotic stress caused by high salinity usually affects plants in a similar way to drought stress (Chen et al., 2010). Unlike drought stress however, high salinity and flooding can occur simultaneously. Whether salt and hypoxic stress exhibit antagonistic or combined effects on plants is not fully understood. Similarly, the effect of salt stress on hypoxia acclimation and vice versa cannot be predicted easily. With some of LBD41's putative target genes potentially involved in osmotic salt stress acclimation, their hypoxic downregulation should result in reduced viability under high salt. To further investigate this hypothesis, the *lbd40 lbd41* lbd42* and pr35S:LBD41ΔEAR:VP16 constructs and lines were examined for differences in phenotype, fitness and transcriptional activity under varying intensities of salt stress.

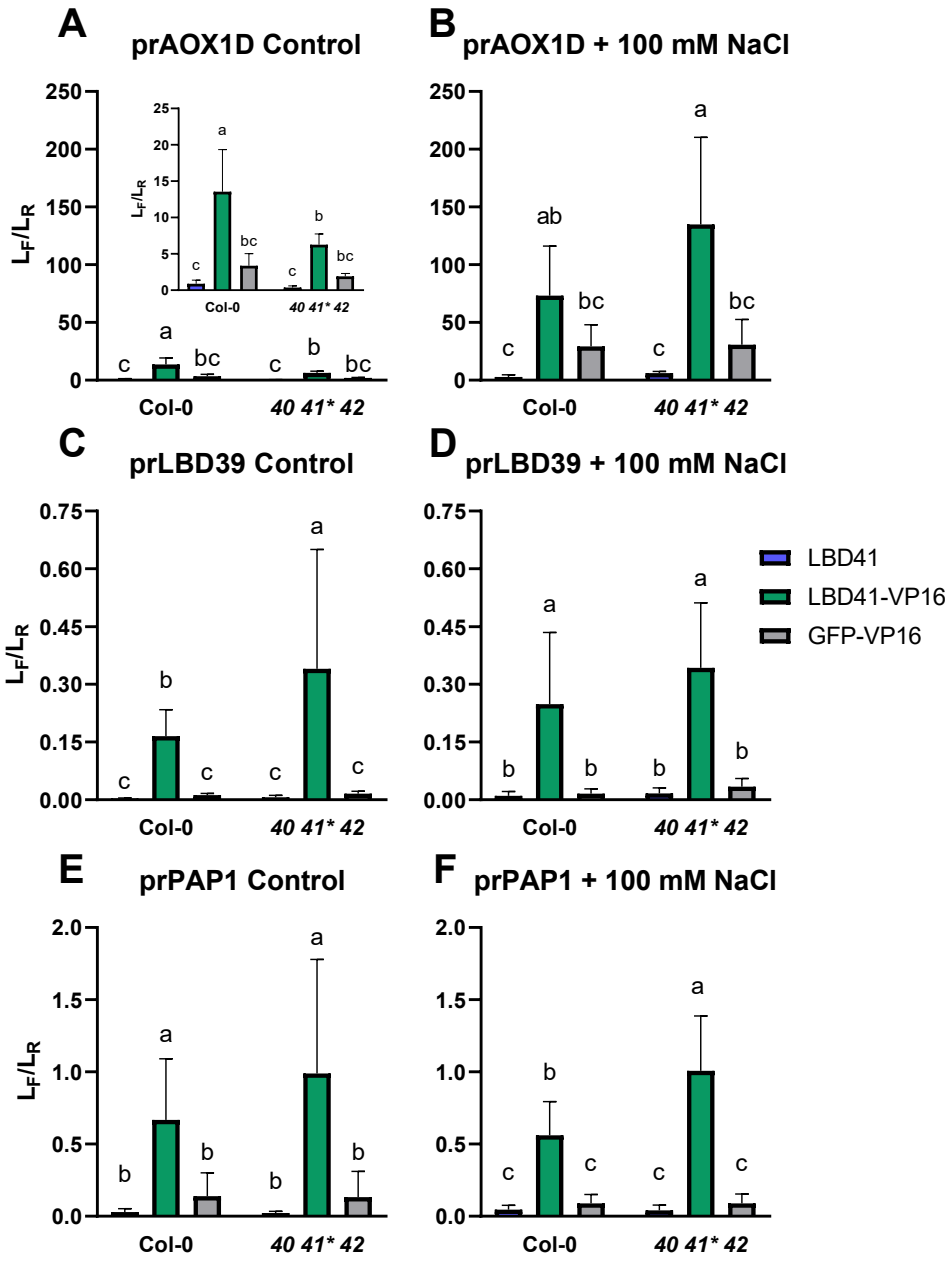

Figure 13: Promoter regulatory changes to salt in PTA

Protoplasts were isolated from 4-6 w old Col-0 or *lbd40 lbd41* lbd42* plants grown under short-day conditions. Cells were transformed with pBT10:prTarget:Luc_F, pHBTL:pr35S:LBD and pBT10:pr35S:Luc_R vectors at 16 h prior to the measurement. Optional 100 mM NaCl was added after transformation. Target reporter vectors were tested with promoters of AOX1D (A and B), LBD39 (C and D) or PAP1 (E and F). Overexpressed effectors were native LBD41, LBD41ΔEAR:VP16, or null effector GFP. Luminescence signal of Luc_F and $Luc_R$was measured and L_F/L_R determined for each sample. Graphs represent the average with standard deviation of 3 biological replicates, with 2 technical replicates each. Letters indicate significant differences $p<0.05$ calculated in a statistical analysis (Two-way ANOVA, Tukey post-hoc). Data was collected by Hayat Kopkin (A and B) and Max Bauer (C, D, E and F).

3.2.4.1 Salt stress on promoter activity in protoplasts

To study first effects of salt stress on the regulation of LBD41's putative targets, the protoplast environment was utilized further. In principle, targets of LBD41 that are also regulated by salt stress, should show either enhanced or decreased promoter activity in salinated buffer. By optionally adding 100 mM NaCl to already transformed protoplasts, followed by ON incubation, effects on promoter activity are subsequently studied. Activity measurements were then performed with the promoters of putative targets AOX1D, LBD39 and PAP1. Alongside those isolated from Col-0, protoplasts of *lbd40 lbd41* lbd42* were also utilized to further investigate their background effect.

In line with previous measurements (Fig. 12), prAOX1D shows reduced activation by LBD41-VP16 in *lbd40 lbd41* lbd42* protoplasts. Here, measurements even include a significantly reduced promoter activity of LBD41-VP16 in triple mutant protoplasts, compared to the wild type (Fig. 13 A). When incubated with 100 mM NaCl containing buffer, two major changes on the regulation of prAOX1D occur. Firstly, the overall induction of this promoter causes a 5x increase of the fluorescent signal in Col-0 protoplasts overexpressing LBD41-VP16 or GFP (Fig. 13 B). Secondly, the previously measured repressing nature of the triple mutant background appears reversed with salt stress. Activation through LBD41-VP16, combined with reduced repression in *lbd40 lbd41* lbd42* protoplasts and increased induction with salt stress, even causes a 10x signal increase. Separately obtained results for the reporter constructs prPAP1:Firefly and prLBD39:Firefly, showed no difference in regulation to addition of 100 mM NaCl. They however display a repression through overexpressed native LBD41, activation by LBD41-VP16, and overall increased activation in the triple mutant background (Fig. 13 C, D, E and F).

3.2.4.2 Growth and germination on salt-containing medium

With a potential overlap of salt and hypoxic regulation as seen for AOX1D, the physiological impact of *lbd40 lbd41* lbd42* and the VP16 lines was studied further. To get an overview if general differences in growth or fitness exist between the lines, mutant and wild type seeds were germinated on MS medium for optimal growth. To add osmotic salt stress, the previous

addition of either 50 mM, 70 mM or 100 mM NaCl was performed. Seedlings were then grown to an age of 7 days, at which point their root length was determined. Seeds that did not germinate were no included in root length evaluation. Already with control medium, VP16-2 and VP16-3 display significantly reduced root length from the other lines. As expected, the root length of all lines then decreased, as the concentrations of NaCl increased.

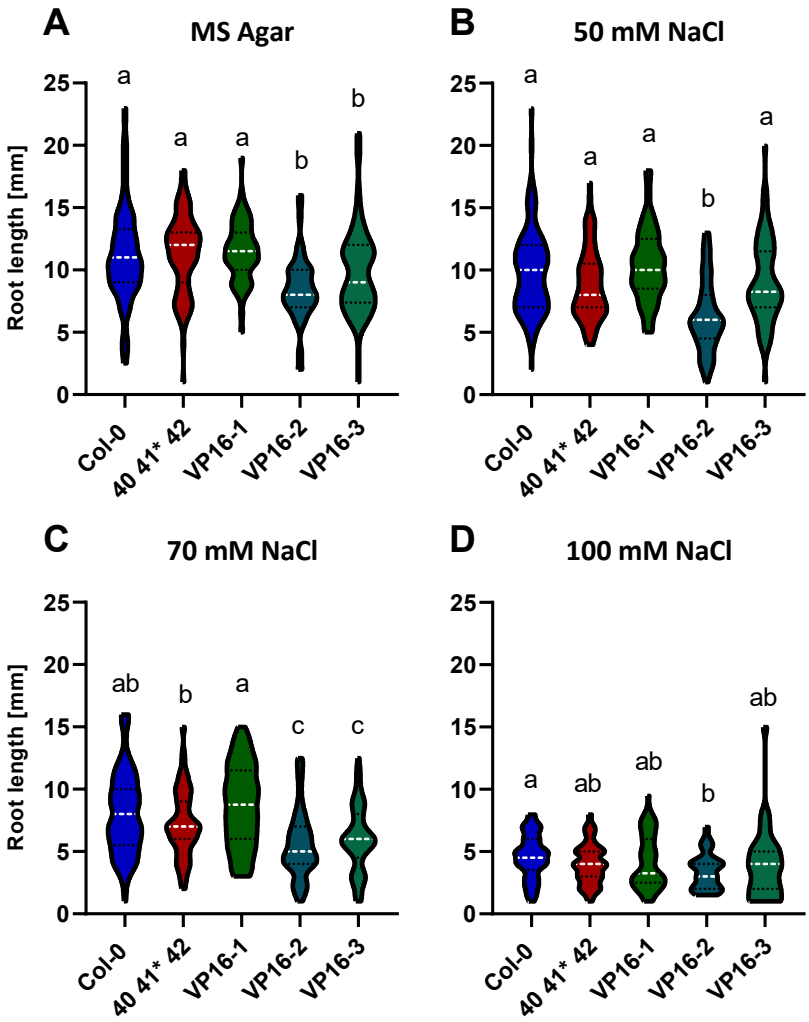

Figure 14: Root length of salt stressed LBD41 mutants on MS medium

Seedlings of Col-0, lbd40 lbd41 lbd42 triple mutant (40 41* 42) and VP16 mutant lines 1, 2 and 3 were germinated on MS agar medium. Seeds were placed on either regular MS medium (A) or with 50 mM (B), 70 mM (C) or 100 mM NaCl added (D), then grown under long-day conditions. The root length was determined when the seedlings were 7 d old. Graphs show the average (white line) with standard deviation (black lines) as well as distribution of 10-18 biological replicates, with 8 seeds each. Letters indicate significant differences $p<0.05$ calculated in a statistical analysis (One-way ANOVA, Tukey post-hoc). Data collected by Christina Zwinge.

Here, the average length of Col-0 roots on control MS was more than halved with the addition of 100 mM NaCl. Overall, correlating to salt concentration a similar reduction in root length is recorded, with no discernible differences visible between the lines (Fig. 14).

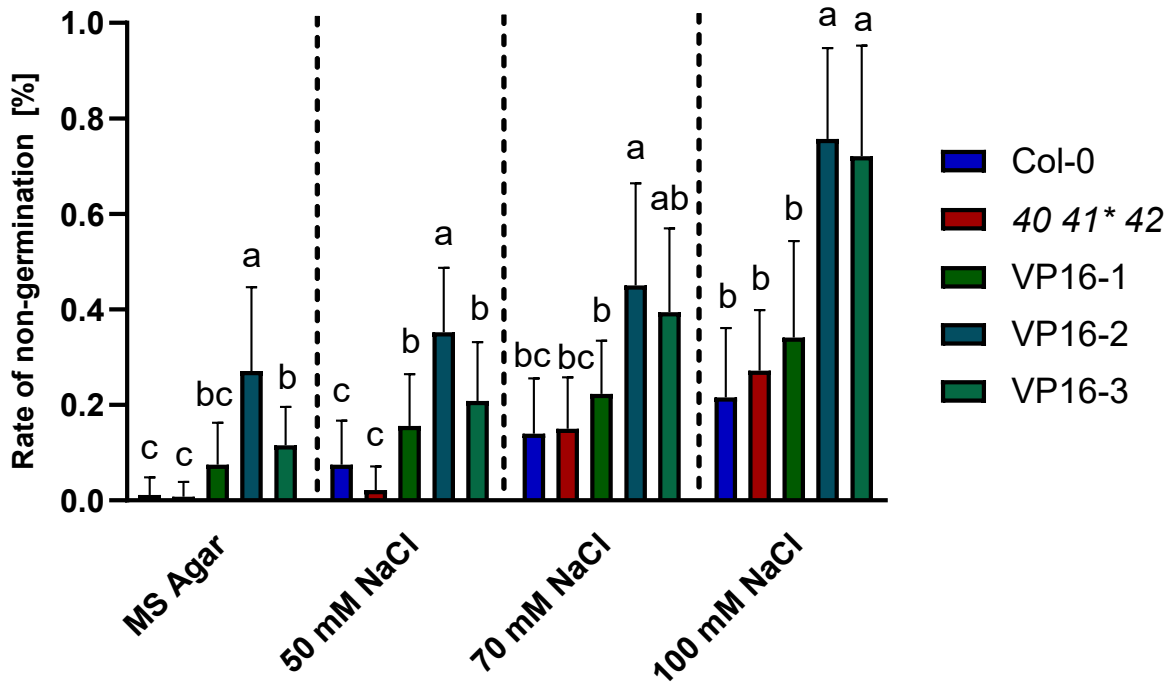

Figure 15: Non-Germination of LBD mutant seedlings on increasing salt stress

Seeds of Col-0, *lbd40 lbd41* lbd42* and VP16 lines were germinated on MS medium containing increased NaCl content. Growth took place under long-day conditions on normal MS agar or with 50 mM, 70 mM or 100 mM NaCl added. Graphs display the rate of non-germinated seeds to the total number of seeds of 10-18 biological replicates, with 8 seeds each. Letters indicate significant differences $p<0.05$ calculated in a statistical analysis (One-way ANOVA, Tukey post-hoc). Data collected by Christina Zwinge.

When growing seedlings on MS medium with added NaCl, a decreased germination rate was observed for the VP16 mutants. By recording the number of seeds that did not germinate and the total number of seeds used, the germination rate could be determined. When viewing the rate of non-germination, the triple mutant *lbd40 lbd41* lbd42* shows similar ratios to Col-0 under control and salt stress. Here, both lines display a non-germination rate of less than 5 % under control conditions and a rate of around 20 % with the highest addition of 100 mM NaCl.

Contrasting this, the VP16 lines show increasing rates of non-germination, further intensifying with higher salt concentration. Of the VP16 mutant lines, VP16-2 shows the highest decrease in germination capabilities. With already an average non-germination rate of 25 % under control medium, an increase to 75 % non-germination is achieved with 100 mM NaCl. The mutant lines VP16-1 and VP16-3 display similarly increased rates of non-germination, albeit at lower intensity than VP16-2 (Fig. 15).

3.2.4.3 Varying intensity of salt stress on Hoagland medium

Previous plant studies often revealed substantial differences in seedling fitness, depending on the type of growth media used. While the MS medium generally used for *A. thaliana* germination provides an optimal supply of nutrients, this choice of medium might be less ideal for stress studies (Kittiwongwattana, 2019). A type of Hoagland medium was selected as an alternative, due to its frequent use in hydroponic based stress research (Delden et al., 2020). Further increasing the stress level, herein used solid Hoagland medium did not contain any of the trace elements copper, manganese, boron, molybdenum or zinc (Uraguchi et al., 2020). As possible differences might also not occur within the first week of germination, the duration of the growth assay was also increased to 14 days. Therefore, an involvement of LBD41 in salt stress was determined through root growth on Hoagland medium with either 25 or 50 mM NaCl.

Similar to results obtained with MS medium, the three VP16 lines already show different growth under control conditions. Here, *lbd40 lbd41* lbd42* and VP16-1 display similar root growth to Col-0. Similar to the results on MS, root growth of VP16-2 is significantly reduced from Col-0. Unlike VP16-3, which on Hoagland is even significantly increased from VP16-1 (Fig. 16 A). With 25 mM NaCl added to the medium, the average root length only showed small variations between the lines. Some roots still displayed control-like growth (Fig. 16 B). When increasing the salt concentration to 50 mM this effect persists, with little difference between the genotypic lines. However, a persistent occurrence are control-like seedlings alongside highly salt-stressed individuals. This is also represented within the root length, which under control conditions primarily follows a normal Gaussian distribution. However, with increasing salt

concentration the data appears to separate into a bimodal distribution. This effect was most prominent in Col-0 and the *lbd40 lbd41* lbd42* mutant, but also present to a lesser extent with the VP16 lines (Fig. 16 C).

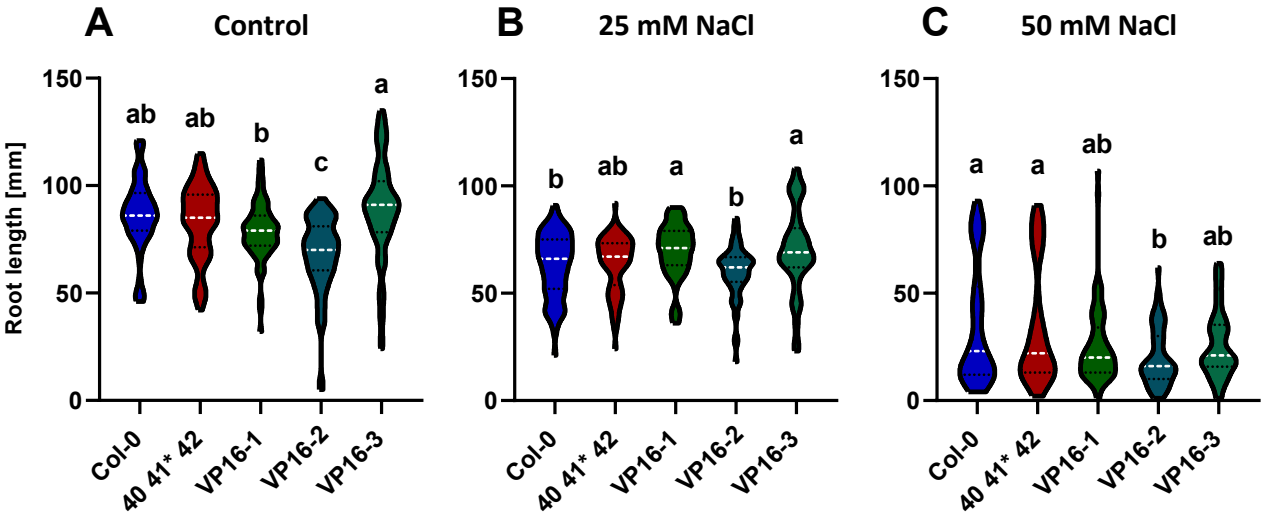

Figure 16: Root length on NaCl containing Hoagland medium

Seedlings of Col-0, *lbd40 lbd41* lbd42* triple mutant (40 41* 42) and pr35S:LBD41ΔEAR:VP16 were germinated on Hoagland agar medium. Plants were grown for 14 d under long-day conditions. Seeds were placed on either control Hoagland agar (A), and with 25 mM (B) or 50 mM NaCl (C) added. Graphs show the average (white line) with standard deviation (black lines) and distribution of 70-80 seedlings. Letters indicate significant differences $p<0.05$ calculated in a statistical analysis (One-way ANOVA, Tukey post-hoc). Data collected by Konrad Buchholz.

3.2.4.4 Seedling salt stress phenotype and separation

When seedlings were germinated under long-day conditions on Hoagland medium with 50 mM NaCl, a strong variance in seedling root length and phenotype occurs. While most seedlings display a salt-stressed sensitive phenotype with decreased root length and a more yellowish leaf color, other seedlings appear less affected. These salt tolerant phenotype seedlings show a normal saturated green leaf color and a healthy root length, while still showing slightly decreased fitness compared to control conditions (Fig. 17). With a reduced abundance of salt acclimated phenotypes in VP16 lines, the occurence of this separation was investigated further. To investigate reproducibility of this unusual phenomenon, seedlings were grown in larger numbers on Hoagland plates containing the additional 50 mM NaCl.

With the possibility of salt clusters forming during storage, medium was thoroughly heated and mixed prior to seed application. Nevertheless, these different salt stressed phenotypes appeared in every replicate. It was then investigated further if this phenotype affects LBD41 and its targets.

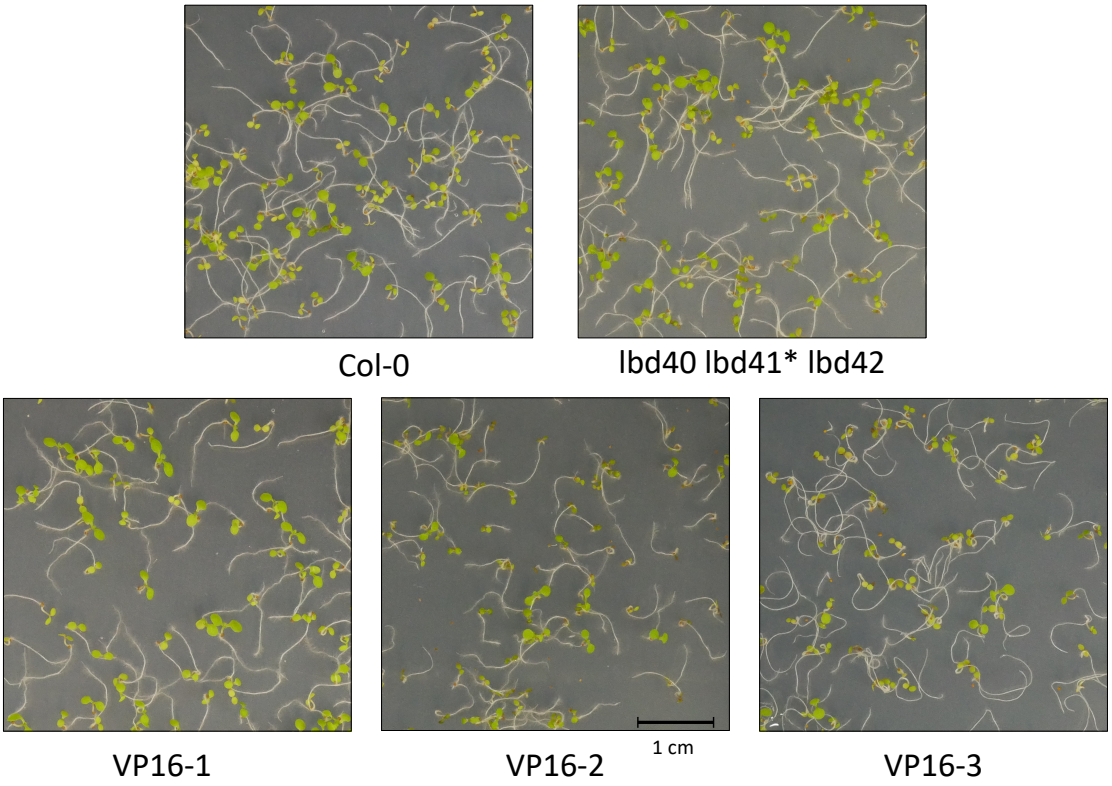

Figure 17: Phenotypic separation in salt-stressed seedlings

Under long-day conditions, seedlings were germinated on Hoagland agar medium with 50 mM NaCl. Pictures show seedlings 6 d after transferral to long-day, displaying different phenotypes. Plants that grew to a control-like appearance and color were considered **tolerant**, while seedlings with decreased size and yellowish hue were declared salt-stress **sensitive**. Both phenotypes appeared in all tested plant lines (Col-0, *lbd40 lbd41* lbd42*, pr35S:LBD41ΔEAR:VP16 lines 1, 2 and 3). Images are representative of 4 biological replicates.

Based on the differences in leaf appearances, the seedlings were sorted into tolerant and sensitive phenotypes at 6 days old and then returned to salt stress conditions. Similarly to the previous root length assay, both Col-0 and *lbd40 lbd41* lbd42* displayed a higher frequency of

developing the tolerant phenotype.

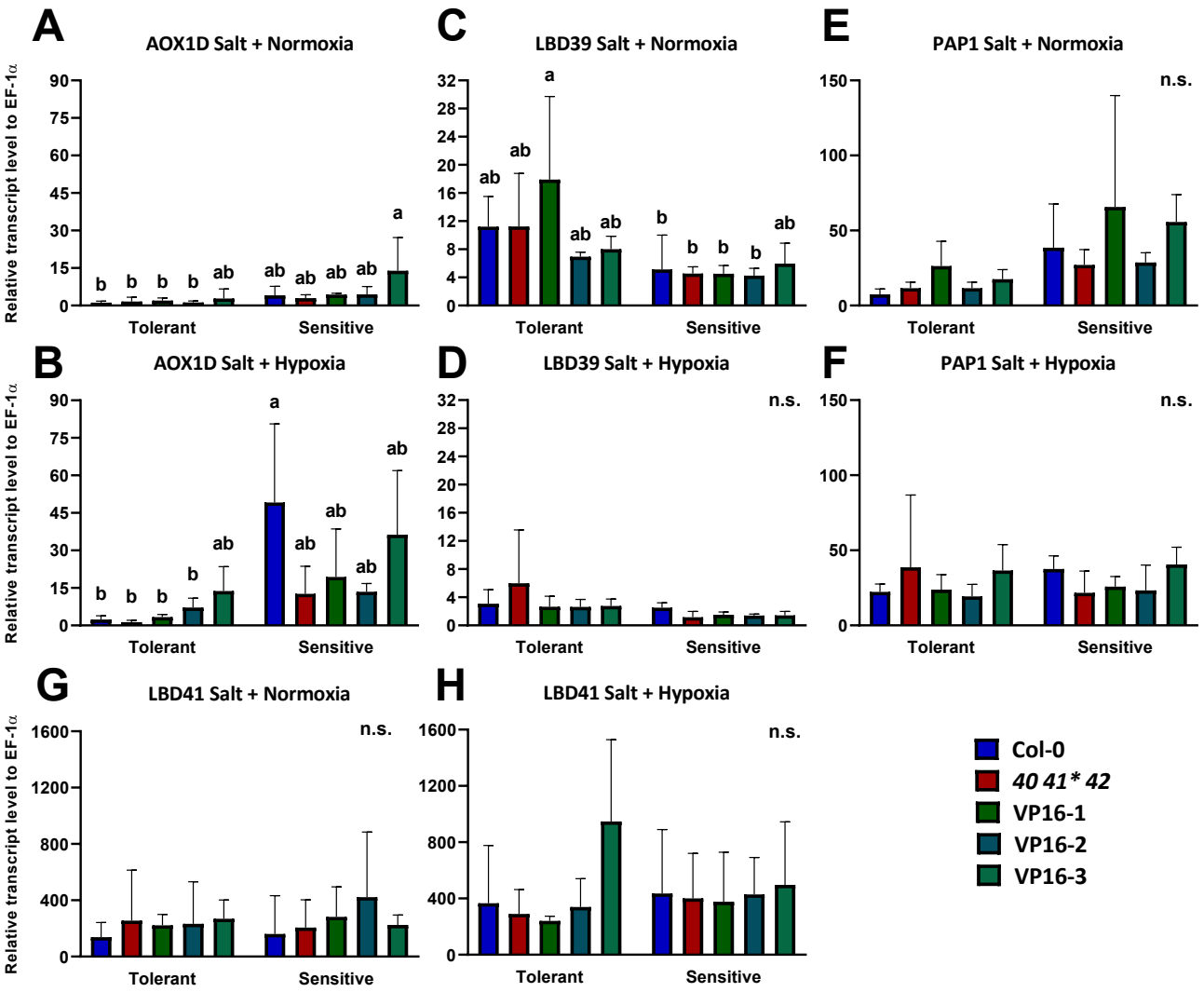

Figure 18: Transcriptional changes to hypoxia in salt-stressed phenotypes

Seedlings of Col-0, *lbd40 lbd41* lbd42* triple mutant (40 41* 42) and pr35S:LBD41ΔEAR:VP16 lines 1, 2 and 3 were germinated on Hoagland agar medium with 50 mM NaCl. After incubation under long-day conditions at 6 d old, seedlings were separated based on phenotype into sensitive and tolerant plants. Remaining under salt stress conditions At 7 d old the seedlings were fumigated with either air (control) or N_2 (hypoxia) and then harvested. All RNA was extracted from the samples and transcribed to cDNA, then measured by qPCR. Transcript levels LBD41 were calculated relative to EF-1α. These graphs display the average with standard deviation of 4 biological replicates. Letters indicate significant differences $p<0.05$ calculated by a statistical analysis (Two-way ANOVA, Tukey post-hoc).

While the lines VP16-2 and VP16-3 show an increased proclivity towards the more sensitive phenotype, in general the sensitive seedlings of VP16-2 appear especially affected (Fig. 17). To add the influence of hypoxic stress on already salt stressed plants, the then 7 days old seedlings underwent hypoxic stress treatment through N_2 fumigation. After 8 hours of treatment with N_2 or control air, seedlings were sampled and frozen. Samples then had their RNA extracted, reverse transcribed and analyzed through qPCR. To reveal an impact of salinity on hypoxic acclimation, transcript levels of LBD41 and some of its putative target genes were quantified. When observing some of LBD41's target genes, transcriptional differences between the two phenotypes become apparent. For AOX1D, the sensitive phenotype already displays elevated transcript levels under normoxia, when compared to their tolerant counterparts (Fig. 18 A). Under hypoxia this difference increases, with only a slight induction in tolerant seedlings but highly elevated in sensitive individuals (Fig. 18 B). In the case of LBD39 the opposite effect occurs, with the highest levels in normoxic salt tolerant seedlings (Fig. 18 C). Simultaneously, LBD39 is at its lowest in hypoxic salt sensitive plants (Fig. 18 D). For PAP1, slightly elevated levels could be detected in salt sensitive compared to tolerant seedlings (Fig. 18 E). However, this difference between the phenotypes was only detected under normoxia, and seemingly disappears under hypoxia (Fig. 18 F).

To measure whether salt stress already directly affects the regulation of LBD41, its transcript levels were also analyzed. Overall, LBD41 transcription appears the most similar between the two salt phenotypes. Surprisingly, even under normoxia, both phenotypes exhibit elevated levels of LBD41 (Fig. 18 G). The addition of hypoxia then only slightly increases induction of LBD41 (Fig. 18 H). Although the described phenotypes appear to have little effect on LBD41 transcripts, the 50 mM NaCl Hoagland condition already leads to LBD41 expression itself, when compared to control seedlings (Supplementary, Fig. 36).

3.2.5 Overexpression of native LBD41

3.2.5.1 Influence of protein tags on the activity of LBD41

To further inquire into the effects of misregulated LBD41, a stable overexpression of native LBD41 was added to the collection of studied genotypes. A construct generated and introduced

into Col-0 prior to this work was native LBD41 under 35S promoter control, but also tagged with N-terminal HA and C-terminal GFP (Bäumler, 2020). With the regulatory function of LBD41 involving N-terminal target promoter recognition and binding, N-terminal tagging could influence this activity. Furthermore, other variant lines used in this work express a C-terminally HA tagged construct. Therefore, the question arose how strongly protein tag location influences the target repressing activity of LBD41. To test this, the effect of LBD41 C'HA or LBD41 N'HA overexpression was compared in a PTA.

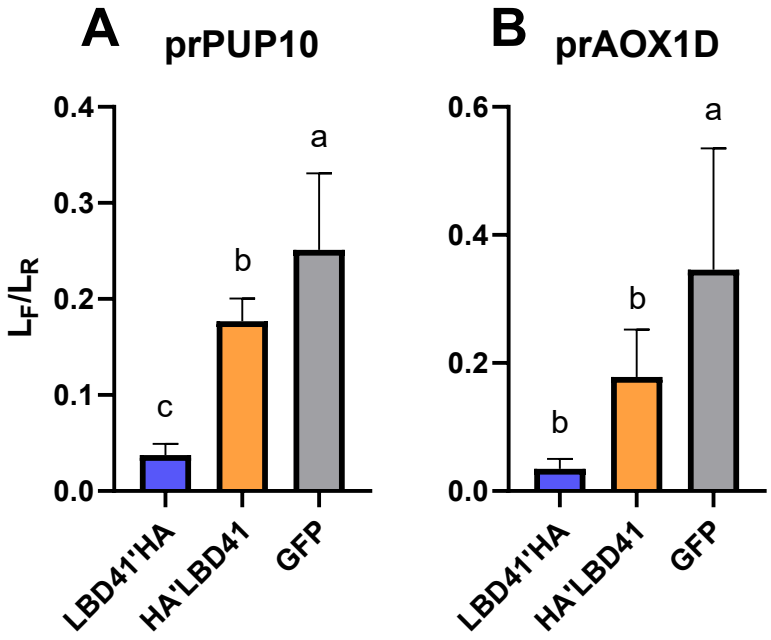

Figure 19: Influence of tag location on the activity of LBD41

Protoplasts were isolated from 4 w old Col-0 plants grown under short-day conditions. Cells were transformed with pr35S:LBD41 or pr35S:GFP expressing pHBTL vector. Overexpressed LBD41 was fused with either N-terminal or C-terminal HA-tag. For activity detection, protoplasts were cotransformed with pBT10 reporter and normalization vectors. Activity was tested with promoters of PUP10 (A) or AOX1D (B). Luminescence signal of LucF and LucR was measured and L_F/L_R determined for each sample. Graphs represent the average with standard deviation of 3 biological replicates, with 2 technical replicates each. Letters indicate significant differences $p<0.05$ calculated in a statistical analysis (Two-way ANOVA, Tukey post-hoc).

For detecting the influence of HA-tag location on target promoter interaction of LBD41, the target promoters prAOX1D and prPUP10 were used as reporter constructs. Protoplasts of Col-0 plants were isolated and transformed with the reporter constructs for prPUP10 and

prAOX1D. This measurement then shows a clear repression of promoter activity for both versions of LBD41, when compared to the baseline (GFP). However, the N-terminally tagged LBD41 (HA'LBD41) displays a decreased repressive activity compared to its C-terminally tagged counterpart. This distinction could be measured for both prAOX1D and prPUP10, but the statistical evaluation revealed a significant difference only in the case of prPUP10 (Fig. 19).

3.2.5.2 Overexpression lines

The construct pr35:HA'LBD41'GFP (OE(N)) was inserted into the background of Col-0 before this work, and a homozygous line with constitutive expression was selected (Bäumler, 2020). Interestingly, seeds of this line appeared enlarged compared to the wild type (Supplementary, Fig. 32 D). This size difference could be detected in seeds of two generations, however a detailed analysis was not performed. With the current overexpression lines featuring a construct with potentially reduced activity, regulatory differences are difficult to assign. Therefore, a new overexpression line was constructed through insertion of a C-terminal tagged pr35S:LBD41'HA construct into the Col-0 background. Genomic T-DNA insertion was performed through a pK7FWG2 vector, with *A. tumefaciens* mediated transformation by floral dip. From this insertion, four independent lines were propagated and genotype selected for two generations. Resulting from time constraints, no experiments with these new overexpression lines were conducted in this study. Future measurements are required to address phenotypical or transcriptomal differences to the wildtype.

3.2.6 Hypoxia acclimation of mature plants

3.2.6.1 Transcriptional regulation in adults

During the maturation process from a juvenile to an adult flowering state, plants undergo a multitude of transcriptional changes. While seedlings prioritize growth and survival, the main priority of mature plants shifts towards reproduction. In stress situations, acclimation mechanisms are often reduced in favor of flowering and seed maturation (Kazan et al., 2016) (Osnato, 2022) (Takeno, 2016). To determine if the regulation of LBD41 or its putative targets changes with age, transcriptional changes upon hypoxia were analyzed in adult plants. For

this, seedlings were germinated on MS and long-day conditions until 7 d old, then transferred to soil. Three clones per pot were then grown under short-day conditions until 4 w old. Plants were subjected to hypoxic treatment by nitrogen or control fumigation. Leaves were harvested after treatment and their RNA extracted. After reverse transcription, transcript levels of LBD41 and its targets were analyzed in a qPCR. When comparing the relative transcript level of LBD41 to those in seedlings, a stronger response can be detected in adults. Already Col-0 displays a stronger induction upon hypoxia in adults compared to seedlings, but also the constitutive expression of mutated LBD41 in pr35S:LBD41ΔEAR:VP16 yields higher transcript levels in adults (Fig. 20).

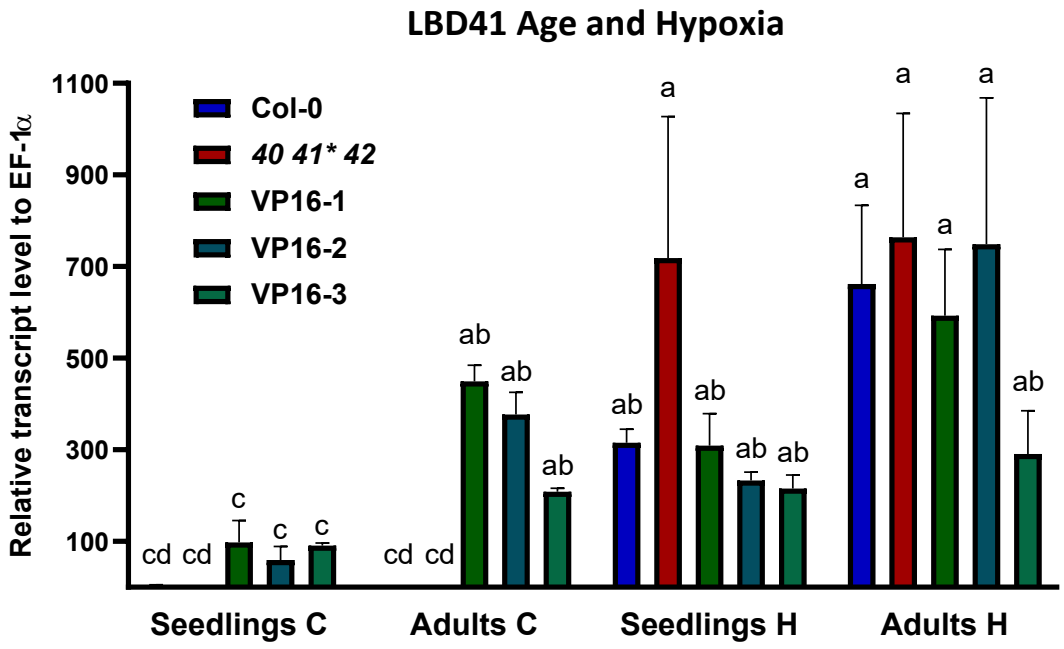

Figure 20: LBD41 transcript level in adult plants under hypoxia

At the age of 28 d plants of Col-0, triple mutant *lbd40 lbd41* lbd42* (40 41* 42) and pr35S:LBD41ΔEAR:VP16 mutant lines 1, 2 and 3 underwent hypoxic stress. The plants were fumigated with air (C) or N_2 (H) for 8 h. All RNA was extracted and transcribed to cDNA, then quantified by qPCR. Values represent the average with standard deviation of 3 biological replicates, each with 3 technical replicates. Letters indicate significant differences $p<0.05$ calculated by statistical analysis (Two-way ANOVA, Tukes post-hoc).

When looking at the various putative target genes, further alterations within the transcriptional response come to light. While in seedlings the putative target PAP1 showed no changes in response to hypoxic conditions, adult plants display a clear induction of PAP1 under

hypoxia. Here *lbd40 lbd41* lbd42* and the VP16 lines exhibit an even stronger induction of PAP1 than Col-0.

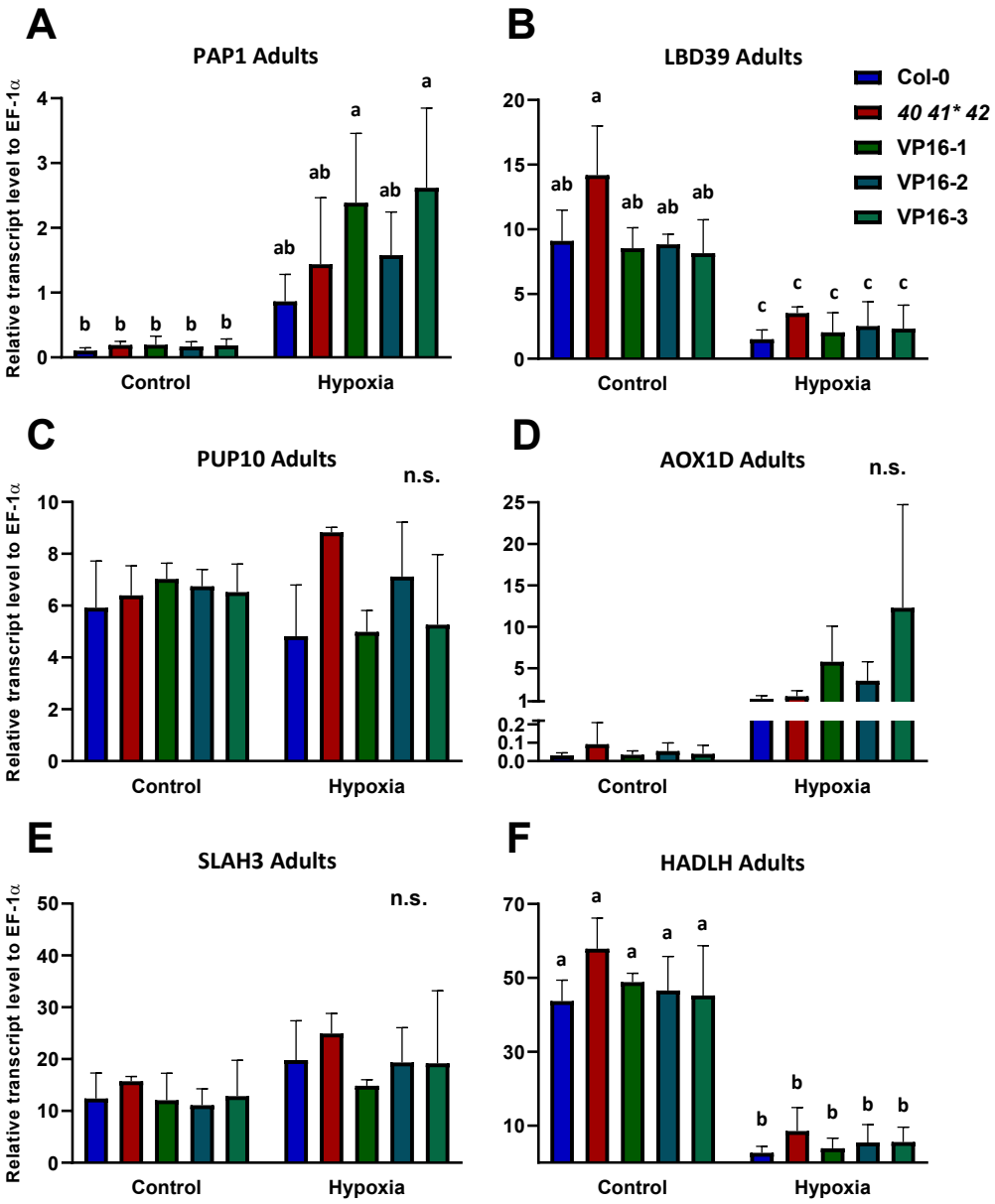

Figure 21: Target transcripts of adults under hypoxia

At the age of 4 w, plants of Col-0, triple mutant *lbd40 lbd41* lbd42* and the VP16 activator mutant lines 1, 2 and 3 underwent hypoxic stress. The adult plants were fumigated with air (control) or N_2 (hypoxia) for 8 h. RNA was extracted and transcribed to cDNA which was quantified in a qPCR. Values represent the mean with standard deviation of 3 biological replicates. Letters indicate significant differences $p<0.05$ in some of the datasets, calculated by statistical analysis (Two-way ANOVA, Tukey post-hoc).

The transcripts of LBD39 show a similar regulatory pattern as seedlings upon hypoxia, however total LBD39 transcripts are vastly decreased in adults (Fig. 21 A and B) (Supplementary, Fig. 36). For the targets PUP10 and SLAH3 no significant changes to hypoxia are recorded in adults (Fig. 21 C and E). These levels are similar to the transcripts previously recorded in seedlings (Fig. 11 C and E). Transcription of HADLH displays the same hypoxic repression and intensity in adults, as it does in seedlings (Fig. 11 F) (Fig. 21 F). Target AOX1D appears also unaffected by maturation, and is induced in adults under hypoxia (Fig. 21 D). This induction intensity is similar to seedlings, but still significantly reduced compared to combined salt and hypoxia (Supplementary, Fig. 36).

3.2.6.2 Waterlogging stress

A central factor of flooding acclimation is the intensity of its resulting hypoxia. If only lower parts are submerged, conditions are described as waterlogging. Here, light is less limited and gas exchange can still occur, albeit reduced. Therefore, the intensity of required acclimation should correspond with flooding severity. To understand how flooding intensity could impact the role of LBD41, adult plants were subjected to waterlogging stress. For this, plants of Col-0, *lbd40 lbd41* lbd42*, the three VP16 lines and LBD41 overexpression (OE(N)) were tested. Seedlings were first germinated on MS medium and transferred to soil after 1 week. Subsequently, plants were grown under short-day conditions until 4 w old and then subjected to waterlogging treatment. To simulate a more demanding stress environment, starch was optionally added to the waterlogging treatment at 1 g/L. The additional carbohydrate source enabled random microorganism growth within the treatment. Additionally to further intensifying the state of hypoxia through oxygen consumption, pathogen responses are also potentially induced in plants.

After 14 d of stress treatment, plants were allowed to recover for another 14 d before evaluation. Across all replicates, treatment with just demineralized water did not provide a lethal stress (Fig. 22 A). Independent of genotype, all plants survived 2 w of pure waterlogging. However, when introducing starch and subsequent microbial growth the stress level, clearly increases. Nearly all plant lines show some mortality after waterlogging with starch, with

the exception of *lbd40 lbd41* lbd42*. Under these conditions, overexpression lines of native HA'LBD41'GFP and VP16 activator mutants show slightly decreased survivablity than Col-0. Despite a noticeable difference, no statistically significant survival differences could be obtained within three replicates (Fig. 22 B). When comparing visual differences between the genotypes, control plants grown simultaneously without waterlogging treatment were also considered.

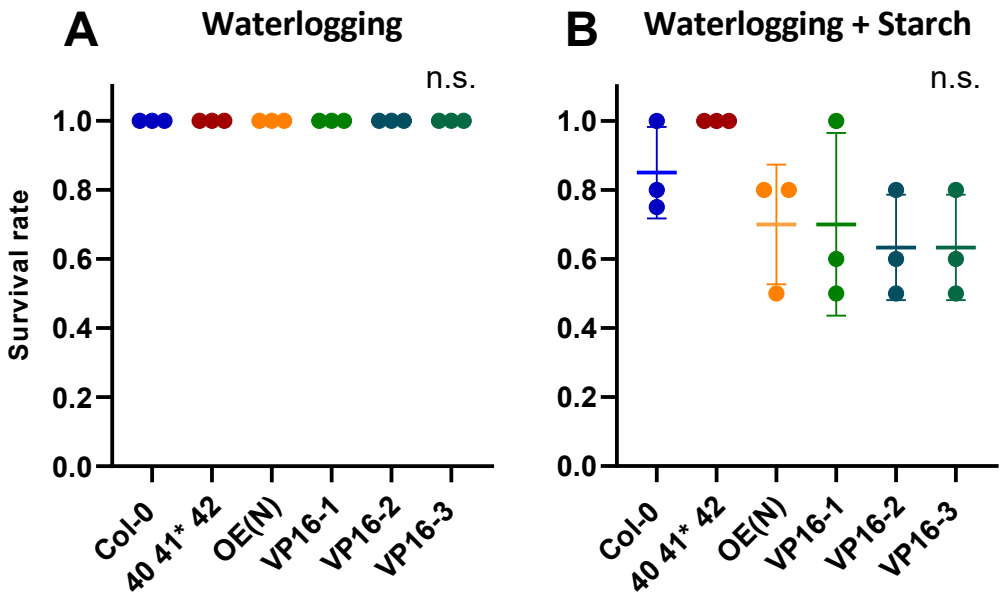

Figure 22: Survival rate of 2 weeks waterlogged plants

short-day grown 4 w old plants of Col-0, triple mutant *lbd40 lbd41* lbd42*, N-terminally HA-tagged overexpression line (OE(N)) or VP16 activation mutants 1, 2 and 3 subjected to 14 d of waterlogging followed by 14 d of recovery. Stress and recovery under short-day conditions. Plants were either waterlogged in clear dd H_2O (A) or with 1 g/L starch added (B). The survival rate was calculated by the ratio of plants showing new growth after recovery to the total number of plants. Data shows individual ratios and average rate ± standard deviation of 3 biological replicates with 5 plants each. No significant difference $p<0.05$ was revealed in a statistical analysis (One-way ANOVA, Tukey post-hoc).

Under these conditions, the *lbd40 lbd41* lbd42* and VP16 lines did not display a differential phenotype to wild type Col-0. However, the LBD41 overexpression line OE(N) exhibited a distinguishable phenotype, both under control conditions and waterlogging. Already under short-day control conditions, leaf lobes are turned inward, giving the leaves a rolled-in appearance.

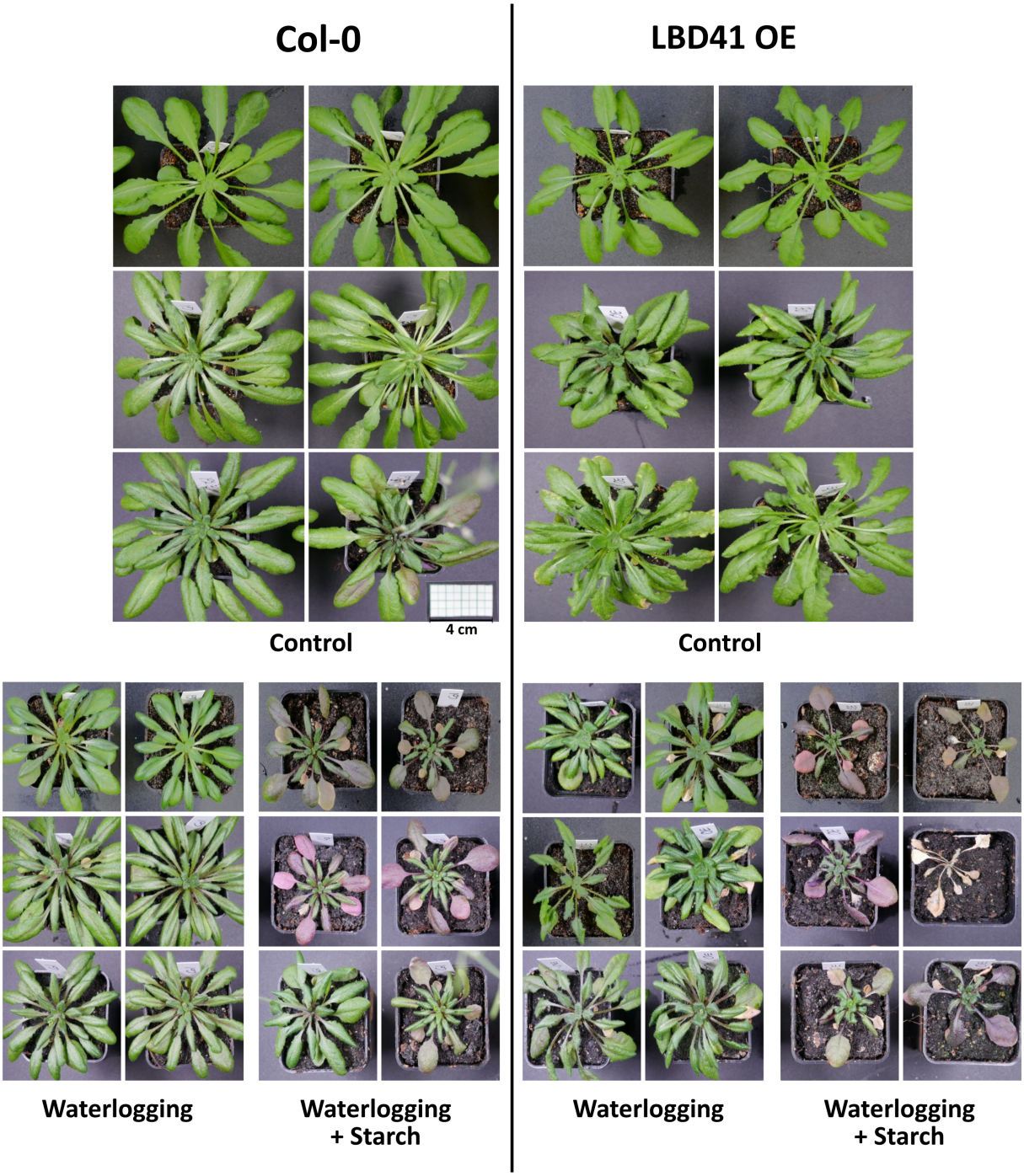

Figure 23: Waterlogging LBD41 overexpression phenotype

Comparison of wild type Col-0 and OE(N) plants during waterlogging. Seedlings were germinated on MS agar and transferred to soil at 7 d old. Plants were grown until 4 w old and then subjected to 14 d of waterlogging treatment followed by 14 d of recovery. Control plants were kept under short-day conditions. Waterlogging was performed with pure deionized water or with 1 g/L starch added. Pictures are representative of 3 biological replicates with 5 plants each.

At the same time, petioles appear slightly shortened and twisted, tilting the leaves to a more vertical state. This combined morphological change gives LBD41 OE plants a *turbine* appearing phenotype. When now comparing plants stressed with demineralized water, this phenotype becomes more apparent. While waterlogged Col-0 also display decreased petiole and leaf size than under control conditions, stress impact is visibly intensified in OE plants. Here the phenotypic difference is the most striking, with straight wildtype leaves and curved *turbine* leaves of LBD41 OE (Fig. 23).

With the addition of starch and increased stress intensity, plants feature decreased size compared to treatment with clear water. Also present in all starch-waterlogged plants are senescent older leaves which show red pigmentation. In line with a reduced survival rate, the OE line also shows decreased average size after starch-waterlogging compared to Col-0. Besides a size difference however, the leaf phenotype can not be clearly detected here. Under these increased stress conditions, all younger leaves appear to display a rolled-in shape independent of genotype.

3.2.6.3 Full submergence survival

From heavy rain soaked soil to prolonged deep flooding, hypoxic stress can come in a variety of conditions. Depending on the duration and amount of plant organs submerged, the requirements for acclimation change. While waterlogging treatment already showed pronounced differences, these plants only had their lower parts submerged. Under these conditions, gas exchange through the leaves was still possible and induction of HRGs likely less pronounced. If however plants are subjected to prolonged deeper submergence, their survival is threatened more severely. To test how the different mutant lines react to heavy flooding, full submergence treatment was imposed on adult plants for up to 31 d.

Seedlings were germinated on MS medium and long-day conditions, then transferred to soil at 7 d old. Plants were then grown under short-day conditions until 4 w old, before submergence in transparent plastic tubs. During treatment, plants were fully submerged, about 25 cm below the surface. After 21 d of treatment, one fourth of plants was removed from submergence and allowed to recover under short-day conditions.

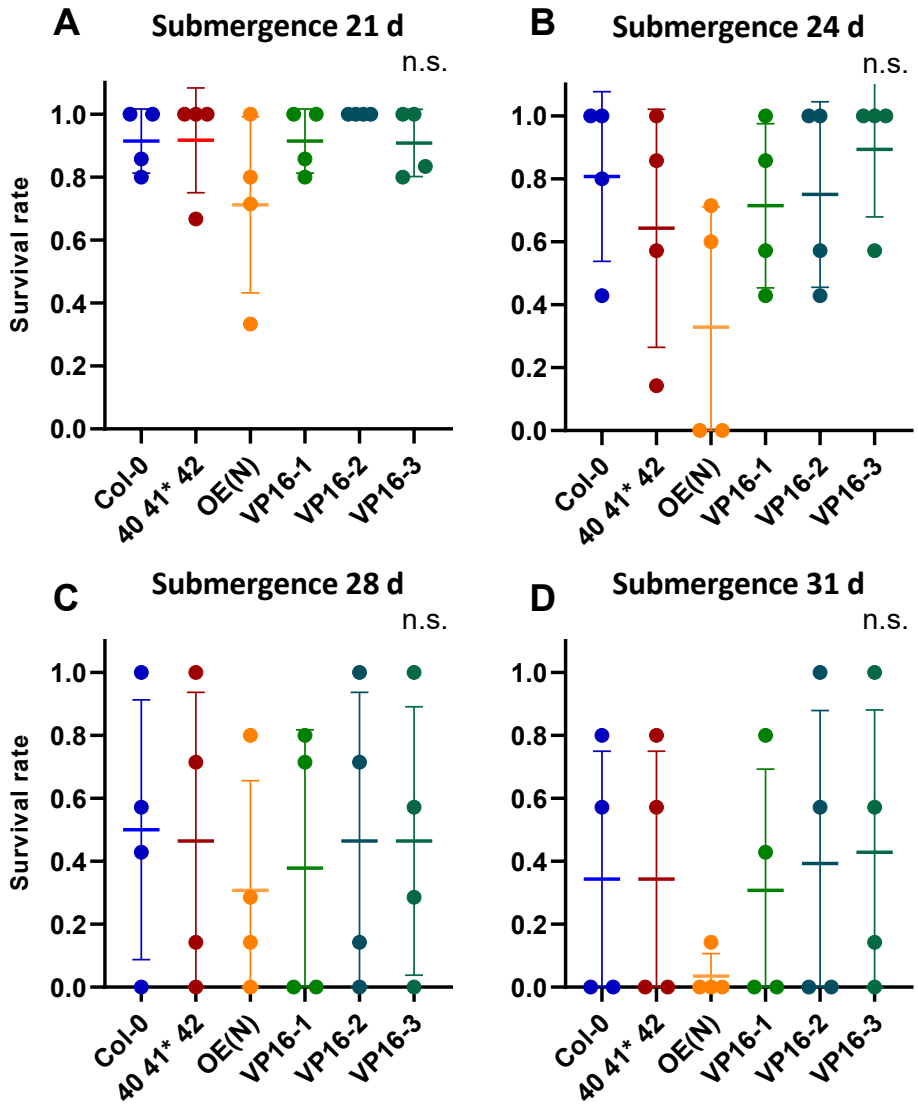

Figure 24: Survival rate of LBD41 mutant plants under full submergence

short-day grown 4 w old plants of Col-0, triple mutant *lbd40 lbd41* lbd42* (40 41* 42), N-terminally HA-tagged overexpression line (OE(N)) or VP16 activation mutants 1, 2 and 3 were subjected to 21 d (A), 24 d (B), 28 d (C) or 31 d (D) of full submergence followed by 2 w of recovery. Both stress and recovery were performed under short day conditions. Plants were placed in clear tubs filled with tap water. The survival rate was calculated by the ratio of plants showing new growth after recovery to the total number of plants. Data shows individual ratios and average rate +/- standard deviation of 4 biological replicates with 7 plants each. No significant differences $p<0.05$ were revealed in a statistical analysis (One-way ANOVA, Tukey post-hoc).

After 14 d of recovery, plants were documented and their survival rate recorded (Fig. 24 A). This process was repeated at 24, 28 and 31 d of submergence. Resulting from unfiltered tab water used for submergence experiments, natural algae started growing within the treatments.

This was noticeable through a green hue visible at about 2 w, progressing at 4 w into surface located algae patches. These green algae, likely of the *Zygnema* genus due to their filamentous shape, could affect both oxygen and light availability for submerged plants (Supplementary, Fig. 37 A). Additionally, visibly noticeable after around 3 w of treatment, undefined microorganisms started also growing within the top layers of soil. While at first only limited to the surrounding soil, this growth would eventually also affect and cover the *A. thaliana* genotypes (Supplementary, Fig. 37 B).

When comparing the different submergence durations after recovery, a majority of plants managed to acclimate to 3 weeks of submergence. Here, most lines display around 90 % survival rate after 21 d, between 60-80 % at 24 d, 40-60 % at 28 d and around 40 % at 31 d. This applies to Col-0, *lbd40 lbd41 lbd42* and the VP16 lines, however OE(N) shows decreased survivability under all time points. Already at 21 d OE(N) averages at only 70 % survival rate (Fig. 24 A), drops to 30-40 % at 24 d (Fig. 24 B) and 28 d (Fig. 24 C) and reaches near zero at 31 d (Fig. 24 D). After recovery, surviving individuals of OE(N) generally showed decreased size to other lines. However, the leaf phenotype displayed by OE(N) under waterlogging conditions did not occur during submergence (Supplementary, Fig. 38).

3.2.7 Post-translational regulation of LBD41

It could be shown that the transcription of LBD41 is not only induced by hypoxia but also potentially changes with age and salt stress. Additionally, preceding studies have hinted at further post-translational regulation of LBD41 through SUMOylation (Elrouby et al., 2010). This process is a covalent binding of SUMO to lysine (K) residues of target proteins. Such SUMOylation process likely influences the activity of LBD41 in a not yet characterized way. To study this additional layer of regulation, one such putative SUMOylation site lysine 105 was identified through the prediction tool GPS-SUMO, and deactivated through arginine (R) mutation prior to this work (Zhao et al., 2014). This K105 location was also chosen due to its close proximity to the DNA binding domain of LBD41. Furthermore, previous protein detection by western blot displayed a pattern of bands, hinting at potentially different poly-SUMOylated states (Bäumler, 2020).

3.2.7.1 Effect of SUMOylation on activity

One of the possible influences of SUMOylation is affecting the activity of its targets. This change in activity could have either decreasing or enhancing effects on target repression of LBD41. By mutating a potential binding site to arginine, SUMO binding is disabled while maintaining structural similarity in protein folding. With the overexpression of LBD41 displaying measureable repression of targets in protoplasts, this system should allow detection of activity changes through SUMOylation.

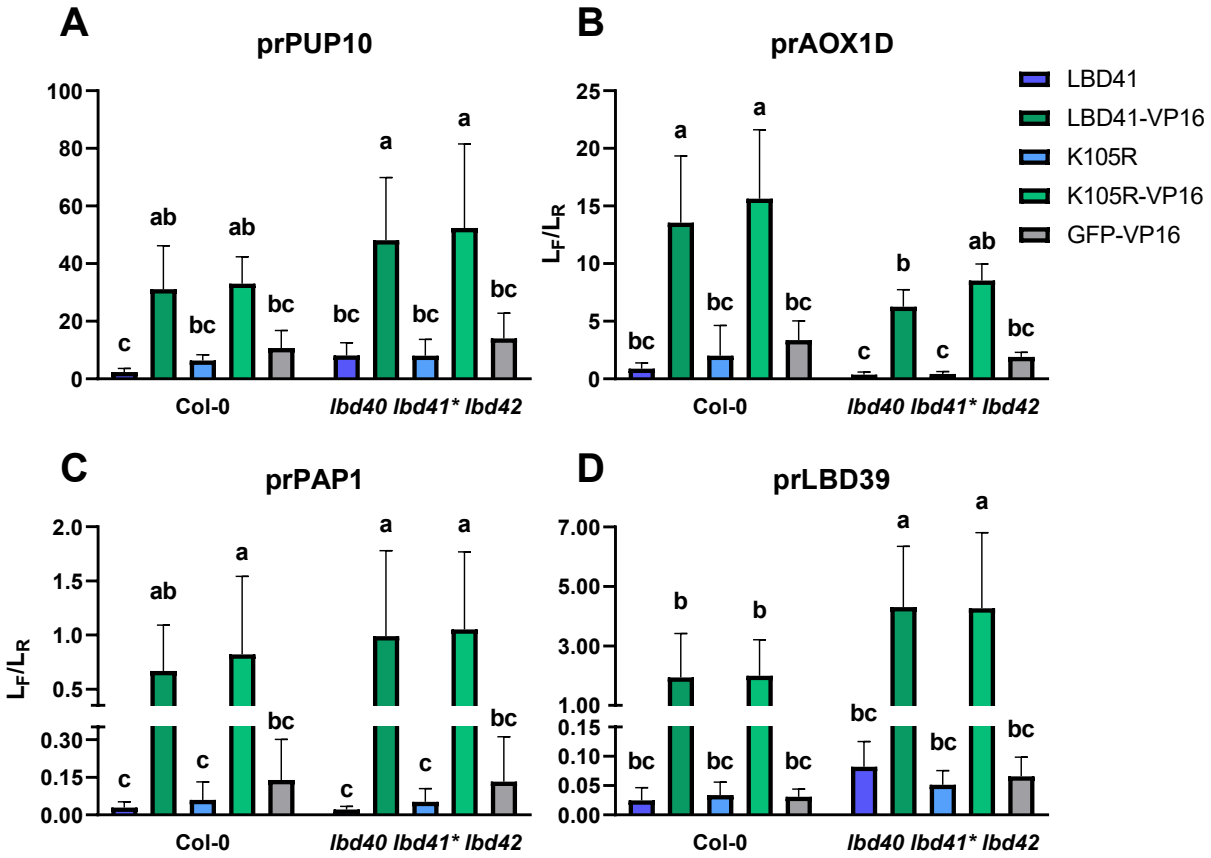

Figure 25: Protoplast transactivation assay of LBD41 K105R SUMO mutants

Protoplasts were isolated from 4-6 week old Col-0 or mutant plants grown under short-day conditions. Cells were transformed with prTarget:Luc_F, pr35S:LBD and pr35S:Luc_R vectors at 16 h prior to the measurement. Control overexpression of GFP is compared to native LBD41, LBD41ΔEAR:VP16 and their respective K105R mutants. Variants were tested with promoter reporter constructs of prPUP10 (A), prAOX1D (B), prPAP1 (C) and prLBD39 (D). Graphs represent the average with standard deviation of 3 – 4 biological replicates, with 2 technical replicates each. Letters indicate significant differences $p<0.05$ calculated in a statistical analysis (One-way ANOVA, Tukey post-hoc). Data collected by Hayat Kopkin and Kathrin Döhla.

When transiently transforming protoplasts with overexpressing LBD41 K105R or LBD41-VP16 K105R, they were compared on their regulatory activities on target promoters prAOX1D, prLBD39, prPUP10 or prPAP1 constructs. Additionally, because of the previously shown differential regulation in the *lbd40 lbd41* lbd42* knockdown background, mutant protoplasts were also used for testing. Here, similar to the PTA data collected for the influence of salt stress, the promoters of LBD39, PAP1 and PUP10 show increased activity in mutant protoplasts. As seen before, prAOX1D is less active in mutant protoplasts. However when comparing native LBD41 and its VP16 variant to their K105R mutant variants, no clear differences are detected. Here, only slight differences in altered repression of LBD41 or activation of LBD41ΔEAR:VP16 could be measured for their K105R mutants (Fig. 25).

Alongside lysine on position 105, additional potential SUMOylation sites were detected using the GPS-SUMO algorithm. These lysine residues located at positions 135, 172, 197, 221 and 253 were identified as potential binding sites within LBD41. Their potential influence on transcriptional activity of LBD41 was then explored further. Similar to the special location of position 105 in proximity to the LOB domain, position 221 is located right before the EAR motif. When testing single lysine to arginine mutants of all mentioned positions, promoters of AOX1D and PUP10 were utilized. These promoters showed higher baseline activation than prLBD39 or prPAP1, allowing for better detection of potential changes. After evaluation of all single mutants and a K105R K221R double mutant, no regulatory changes to native LBD41 could be recorded (Supplementary, Fig. 39). However, a potential multiple modification was detected prior to this work, which might be necessary for the imposed regulation.

Therefore, double and triple mutants of different lysine to arginine combinations were also tested for changes in transcriptional activity. With a total of 15 different combinations of double mutants alone, the initially studied mutants K105R was favored as basis for other mutations. When analyzing the activity of double mutants, the target promoters of PUP10 and AOX1D were used as further reference. However, no significant differences between native and SUMO mutant variants could be measured for double mutants (Fig. 26 A and B). When then moving on to triple mutants, the background K105R K221R was utilized. Here, variant K105 K197R K221R displays equal repression to native LBD41 for prAOX1D and prPUP10.

Triple mutants of K105R K221R with either K135R, K172R or K253R however, showed slightly elevated luciferase levels to native LBD41. Thus hinting at a reduced repression activity of target promoters by these mutants. Yet, these increased signals were not found to be statistically significantly different from the activity of native LBD41 (Fig. 26 C and D).

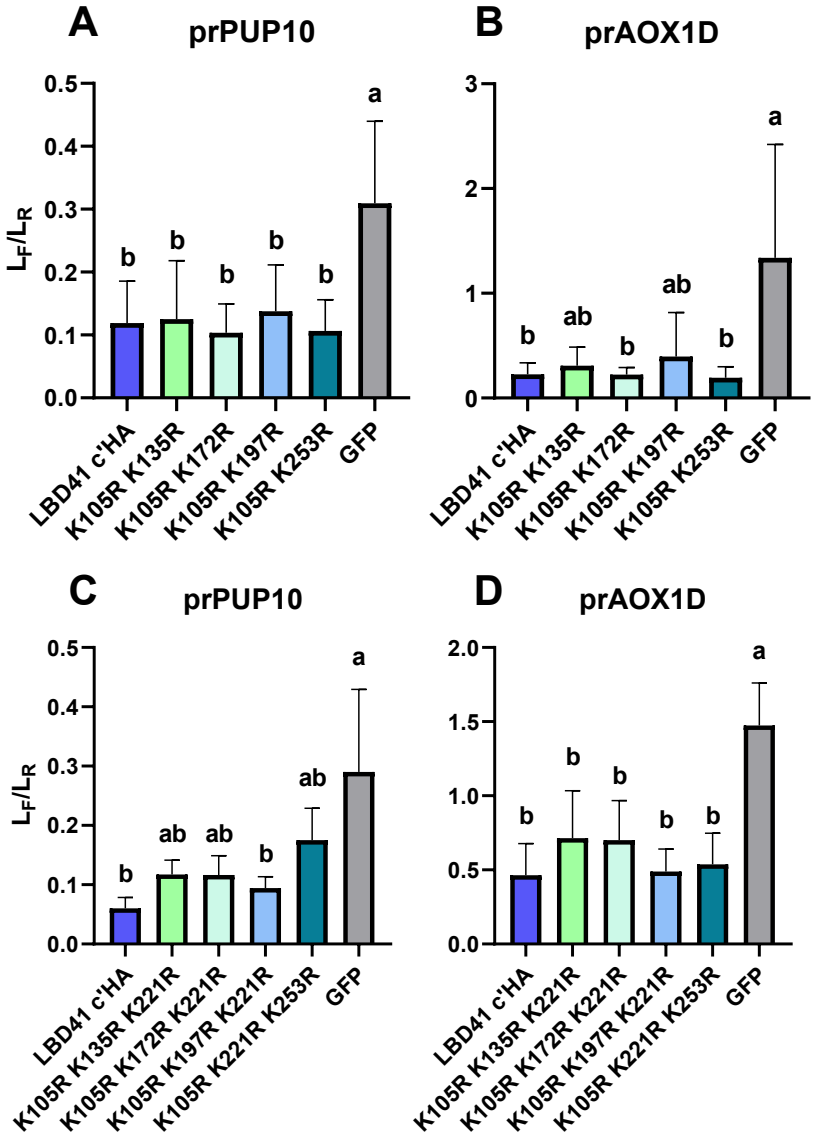

Figure 26: Protoplast activity assay of double and triple SUMO mutants

Protoplasts were isolated from 4-6 week old Col-0 plants grown under short-day conditions. Cells were transformed with pBT10:luc reporter and normalizations plasmids 16 h prior to the measurement. Co-transformation of pHBTL pr35S:LBD41 with various lysine to arginine mutations was tested against a GFP control. Target reporter vectors were tested with promoters of PUP10 (A and C) or AOX1D (B and D). Graphs represent the average ±standard deviation of 3 biological replicates, with 2 technical replicates each. Letters indicate significant differences $p<0.05$ calculated in a statistical analysis (One-way ANOVA, Tukey post-hoc).

3.2.7.2 Western blot unveils LBD41 in *N. benthamiana*

With the protoplast assays showing no significant differences in activity for the predicted SUMOylation sites, the protein availability of LBD41 needs further evaluation. Prior to this work, detection of LBD41 through western blot already displayed a distribution pattern of at least three different sizes. Their connection to hypoxia was therefore studied further. To detect the different proteoforms of pr35S-overexpressed LBD41, 7 d old seedlings were stressed with hypoxia. After 8 h of treatment with either air or nitrogen, some hypoxia stressed seedlings were allowed to reaerate for 1 h before harvest. Frozen seedlings then had their protein extracted and separated by SDS-PAGE. Using primary α-HA and secondary anti-mouse-HRP antibodies, separated samples were then detected through western blot. Here a detectable signal could not be obtained for the VP16 lines, however it was possible for OE(N) (pr35S:HA'LBD41'GFP) seedlings. For these samples, an equally strong signal at around 70 kDa could be obtained under all three conditions. Additionally, a signal at around 30 kDa was detected under control conditions and reaeration (Supplementary, Fig. 40).

To also study other variants of LBD41, an increased protein content was required than could be easily obtained from *A. thaliana*. Thus, variants of LBD41 were expressed heterologously in *N. benthamiana*. Tobacco plants were shown to synthesize high protein levels, even if stressed (Petre et al., 2016) (Norkunas et al., 2018). Constructs were transformed on a pK7FWG2 T-DNA vector, by infiltration with *A. tumefaciens*. All variants were expressed under control of pr35S. Through co-expression of RNA silencing suppressor P19, protein expression was previously shown to be enhanced **Jay2023AscpP19/scp**. Additionally, preliminary experiments have shown that co-expression of a P19 helper strain enhances the detectability of heterologously expressed LBD proteins. When transforming only pK7FWG2 vectors without pBin19, no detectable signals could be obtained. Then, around 65 h after co-infiltration, plants were subjected to 2 h of hypoxia treatment by nitrogen fumigation. Plants were placed compactly into the treatment desiccator chamber, leading to randomly overlapped leaves during treatment (Supplementary, Fig. 41 B). After treatment, half of the hypoxia stressed plants were re-aerated for 1 h before harvest. The variants tested here were native LBD41 with either C-terminal HA tag, C-terminal GFP tag, N-terminal HA and C-terminal GFP, LBD41ΔEAR:VP16 C'HA or

LBD40 C'GFP. Additionally, to also detect transcriptional differences between the constructs, treated tobacco samples were also RNA extracted and analyzed by qPCR (Supplementary Fig. 41 A). Here, the transcript level of *At*LBD41 was referenced against *Nb*Ube35, which is deemed suitable for bacterial infiltration studies (Pombo et al., 2019). However, the primers used here for quantification of *Nb*Ube35 (qPCR_NbUbe35_fw and qPCR_NbUbe35_fw) require future testing and optimization. Only a weak signal for *Nb*Ube35 transcripts was obtained, resulting in very high relative transcript levels for *At*LBD41.

Samples of co-infiltrated and hypoxia treated plants were then harvested, extracted and separated by SDS-PAGE. With the 3rd replicate of infiltration and treatment, the extraction buffer was optimized with increased urea. After gel separation, samples were blotted onto a PVDF membrane followed by antibody-based detection. Depending on the variants used, the blots were incubated with either α-GFP or α-HA primary antibodies, followed by anti-mouse secondary antibodies. Secondary antibodies carried HORSERADISH PEROXIDASE (HRP) which allowed for chemiluminescent detection. Here, various proteoforms could be detected for all observed overexpression constructs. However, signals of protein abundance showed a strong disparity between replicates. Despite differences within replicates, a reproducible effect of hypoxia treatment was not displayed. The various detected bands and reoccuring discernible patterns are herein discussed.

Across all variants of LBD41, the variant tagged with N-terminal HA and C-terminal GFP displayed massively increased protein content. While the transcript level of N'HA LBD41 C'GFP was equal to that of LBD41 C'HA, its protein abundance was highly increased. Only at a 100x dilution of N'HA LBD41 C'HA samples, was their signal comparable among the constructs. The strongest signal of this variant is found at around 70 kDa, which is present in all replicates. With the molecular weight of native LBD41 at 28 kDa and GFP at 27 kDa, this signal does not correlate with an unmodified proteoform. As the molecular weight of SUMO is at 11 kDa, this signal could represent a single SUMOylated form. In some of the samples, a smaller band at 50 kDa and another above 250 kDa could also be detected. However, in all replicates, the proteoform at 70 kDa stood out as the strongest signal of this variant (Supplementary, Fig. 42).

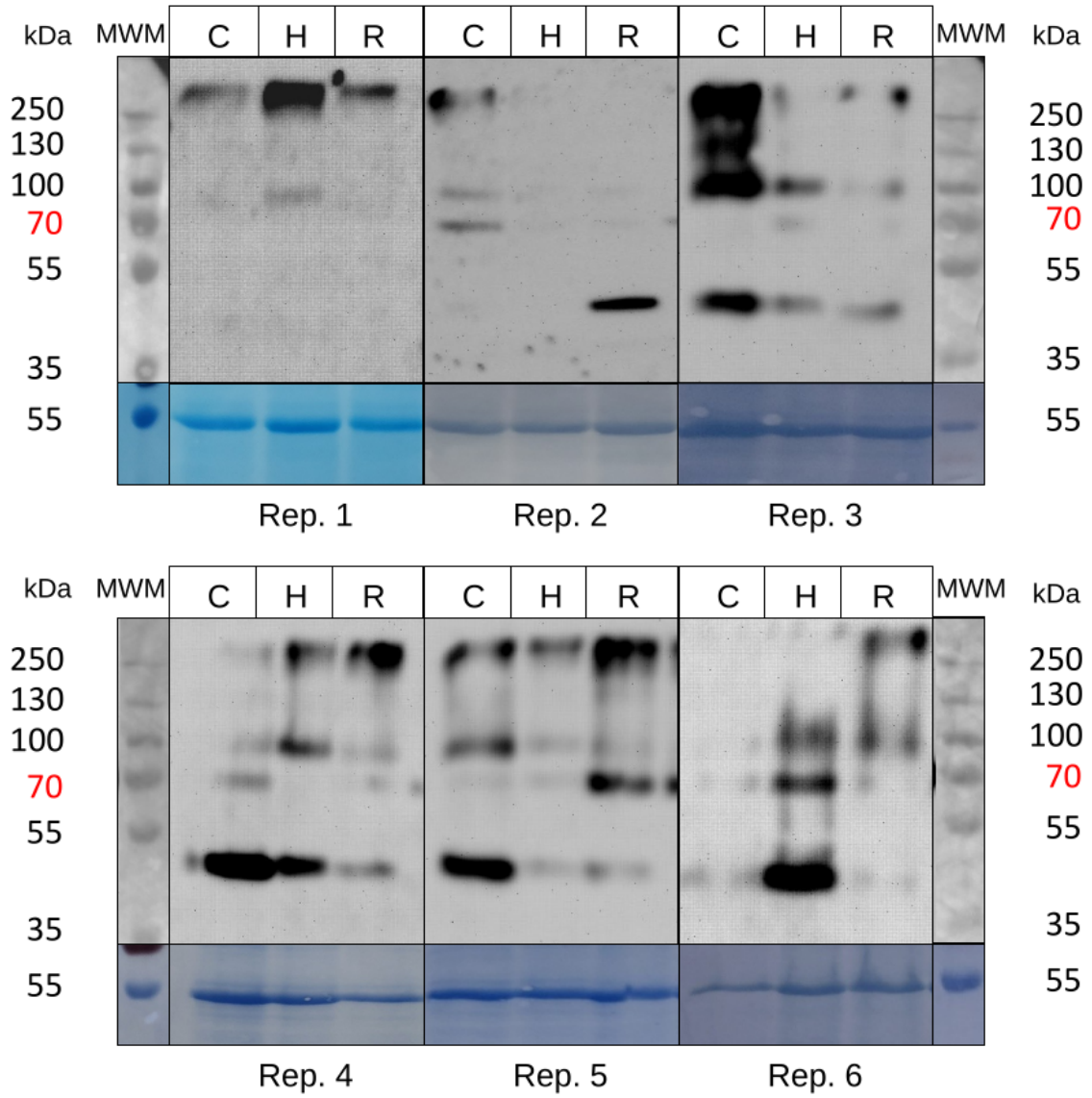

Figure 27: Western blot of heterologously expressed LBD41 C'HA

Leaves of 3 w old *N.benthamiana* were co-infiltrated using transformed *A.tumefaciens* carrying a pBin19 anti-silencing plasmid and pK7FWG2 expression vector. Heterologous expression of HA-tagged LBD41 performed with constitutive 35S promoter under long day conditions for 65 h. Plants were then subjected to 2 h of fumigation with air (C), N_2 (H) or N_2 followed by 1 h of reaeration with air (R). Random leaf shading during treatment. Proteins were extracted, separated by SDS-PAGE, and detected by western blot using α-HA primary and anti-Mouse-HRG secondary antibodies. Images represent 6 biological replicates for infiltration and treatment, with a different extraction buffer used after the second replicate. Detection of chemiluminescent signal was performed with 10 min exposure and sequential integration. Molecular weight marker (MWM) was applied as PageRuler Prestained Protein Ladder (Thermo Fisher Scientific Inc.) which contained standards for 250, 130, 100, 70, 55, 35, 25, 15 and 10 kDa. Blots were stained with coomassie brilliant blue after signal detection.

The variant expressed with only a C-terminal GFP also displayed a high protein abundance, although still vastly decreased compared to N'HA LBD41 C'GFP. While LBD41 C'GFP already shows significantly decreased transcript levels, it is not at the same scope of the resulting protein content. Also for this variant, a signal at around 70 kDa is detected in all replicates and oxygen conditions. In the last three replicates, two different signals between 35 and 55 kDa could also be obtained. These bands could represent GFP still fused to a partially degraded LBD41. Furthermore, a strong band above 250 kDa is detected, which in most replicates shows equal signal strength to the band at 70 kDa. Between the signals at 70 and 250 kDa, another weaker band at 100 kDa was obtained in most replicates (Supplementary, Fig. 43).
When evaluating the observed pattern for LBD40 C'GFP, a strongly decreased signal intensity is detected compared to LBD41 C'GFP. Despite being under control of the same 35S promoter, this difference in abundance was detected in all replicates. The transcript level of AtLBD40 was not analyzed within the confines of this work, making it unclear if the difference in expression is already present at RNA level. Interestingly, the main signal of LBD40 C'GFP is at 55 kDa, with another aggregate signal above 250 kDa. Although LBD40 theoretically has a size of 25 kDa, which is only slightly smaller than LBD41's 28 kDa, a noticeable size difference can be observed. This difference between LBD41 C'GFP and LBD40 C'GFP represents at least 10 kDa and is even detectable in the high MW aggregate bands. Furthermore, in all replicates LBD40 protein content was higher under control and reaeration condition than it was under hypoxia. With hypoxia, a signal for LBD40 is mostly only found in the high MW aggregate proteoforms (Supplementary, Fig. 43).
Detection of the variant LBD41 C'HA was performed, which was also integrated into Col-0 as a new overexpression line. Based on previous results on tag location, this variant is expected to behave the most native-like. Here, at least 4 different sized proteoforms could be detected, starting with the smallest at around 40 kDa. This signal represents a native LBD41 with 28 kDa and around 1 kDa for the HA tag, leading to another theoretical size difference of around 11 kDa. This signal of a putative single-SUMOylated form was again the strongest band in most of the replicates. Further signals for this variant could be obtained at around 70, 100 and above 250 kDa respectively. Additionally, within these samples, the transcript level of LBD41

C'HA was equal to that of N'HA LBD41 C'GFP, and significantly increased to LBD41 C'GFP. However the protein content of LBD41 C'HA is substantially decreased compared to N'HA LBD41 C'GFP, and also lower than LBD41 C'GFP. While LBD41 C'HA displays considerable proteoform differences to hypoxia treamtent, no replicable pattern could be obtained (Fig. 27). Lastly, overexpression of the mutant variant LBD41ΔEAR:VP16 C'HA yielded a strongly decreased availability. Within half of all samples, no signal for LBD41-VP16 could be obtained. When it could be detected, a substantially weaker signal compared to native LBD41 variants was displayed. The most frequent occurrence of LB41-VP16 signals was also found under control conditions. When comparing RNA transcript levels under these conditions, the VP16 mutant displays similar levels to those of LBD41 C'GFP. Despite their similar transcript levels, protein abundance of LBD41-VP16 C'HA appears vastly decreased. With 33 kDa, the VP16 mutant variant is theoretically slightly bigger than native LBD41, however no size difference can be discerned in these blots. Instead, for the VP16 mutant variant the main signal is also detected at around 70 kDa (Supplementary, Fig. 42).

After these experiments were performed, the genome of *N. benthamiana* was sequenced and published (Kurotani et al., 2023). This allows identification of potential orthologs of *At*LBD41. Using the NbenBase gene database, six possible orthologs were annotated to the sequence of *At*LBD41. Unlike the close proximity of *At*LBD40 and *At*LBD42, these orthologs are all located on different chromosomes. Those six (Nbe.v1.1.chr15g30010, Nbe.v1.1.chr03g40240, Nbe.v1.1.chr02g17130, Nbe.v1.1.chr19g42470, Nbe.v1.1.chr08g26640, Nbe.v1.1.chr18g40320) display a highly conserved LOB domain when comparing their protein sequence. Furthermore, a conserved LxLxL EAR motif is also found in most orthologs, with the exception of Nbe.v1.1.chr02g17130. From these, Nbe.v1.1.chr19g42470 shows the highest protein sequence similarity to *At*LBD41 when aligned individually (Fig. 28). When comparing the putative SUMOylation sites of *At*LBD41 to those in Nbe.v1.1.chr19g42470, all lysine residues downstream and including K172 were not conserved. However, the two lysine residues K105 and K135 were found to be conserved not only in Nbe.v1.1.chr19g42470, but also in Nbe.v1.1.chr08g26640 and Nbe.v1.1.chr18g40320. Furthermore, lysine residue K135 was even found to be conserved in all six putative orthologs.

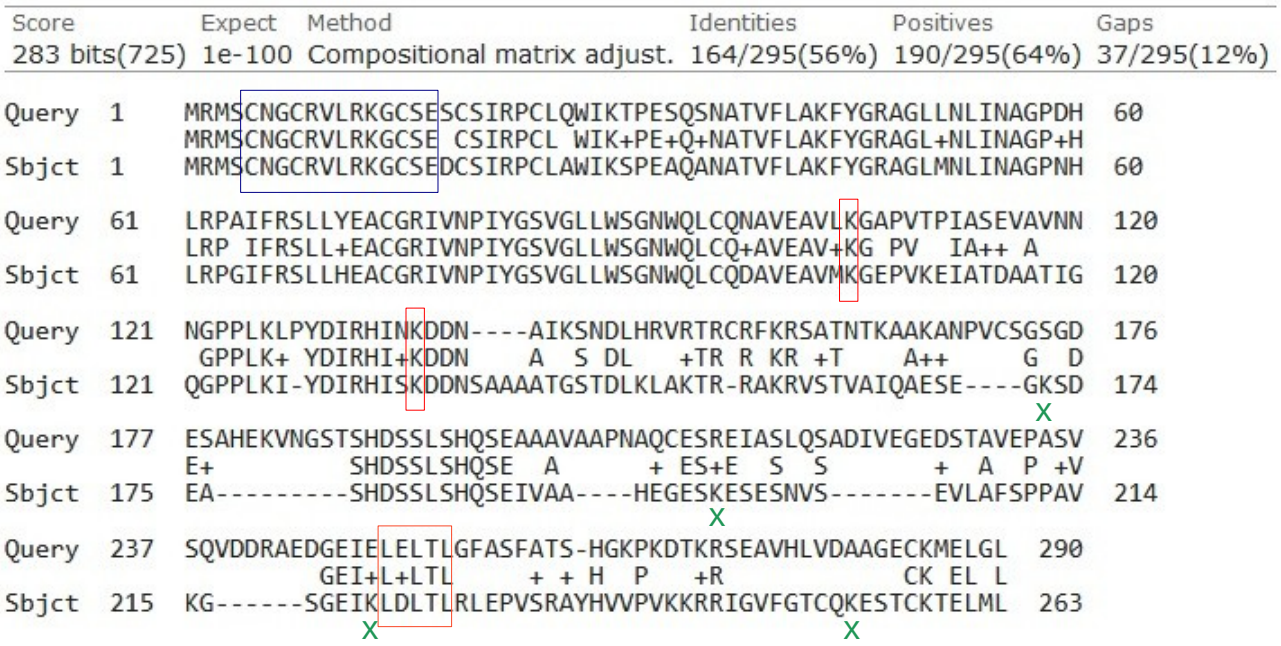

Figure 28: Alignment of *At*LBD41 with putative *Nb*LBD41

Protein sequence alignment of newly identified *N. benthamiana* ortholog (Nbe.v1.1.chr19g42470, Query) and LBD41 from *A. thaliana* (Subject). Indicated are the conserved regions of the LOB (blue) and EAR motif (orange). Putative SUMOylation lysine (K) residues of position 105 and 135 are conserved (red), while 172, 197, 221 and 253 are not. (green) Sequence alignment by NCBI, Protein BLAST, using the BLOSUM62 matrix and an expect threshold of 0.05.

Additionally, when aligning all six orthologs together with *At*LBD40, *At*LBD41 and *At*LBD42, additional sequence conservation is revealed. Another lysine residue of *At*LBD41 and not previously considered, K126 is also conserved in Nbe.v1.1.chr18g40320, Nbe.v1.1.chr08g26640 and *At*LBD40 (Supplementary, Fig. 44). Between the residues K126 and K135 of *At*LBD41, a DIRH motif is found in all compared sequences. Further residue conservation is found for the LDLTL EAR motif of *At*LBD41, which has the final leucine conserved in all nine proteins. Besides the highly conserved N-terminus, two C-terminal consensus sequences could be identified among the *N. benthamiana* homologs, all containing the LXLXL EAR motif. The first C-terminal consensus of Nbe.v1.1.chr18g40320, Nbe.v1.1.chr15g30010 and Nbe.v1.1.chr08g26640 is near identical to the EAR motif sequence of *At*LBD42. Finally, the second C-terminal consensus found in Nbe.v1.1.chr19g42470 and Nbe.v1.1.chr03g40240 can also be partially aligned to the C-terminus of *At*LBD41.

CHAPTER 4

Discussion

With a constantly progressing climate change, we are facing an increasing frequency of extreme weather events. Among them, heavy rain and subsequent flooding can lead to catastrophic outcomes. Such storm floods can bring about substantial damages to humans and our environment alike. While animals have the ability to flee, sessile plants had to evolve other ways of surviving such events. When studying flooding adapted species, two different acclimation strategies are described. Plants either escape hypoxia through morphological changes, or attempt to endure the flooding event. The later, called quiescence, mainly involves metabolic changes to maintain essential functions and outlast a stress event.

Model organism *A. thaliana* also exhibits a quiescent syndrome, induced as a low-oxygen response in all plant parts. Multiple transcriptional and enzymatic participants contained in this acclimation process were uncovered within the last years. However, the complexity of regulation continues to increase when considering all environmental and cellular factors involved in flooding. Many of the identified transcription factors also feature homologous proteins, with seemingly similar but not identical properties. Characterized as one of the main transcriptional regulators, GVIIERF RAP2.2 activates a wide range of genes in response to low oxygen. Part of this core response to flooding in *A. thaliana*, is a subsequent induction of the transcriptional repressor LBD41.

4.1 Induction of hypoxia acclimation by RAP2.2

Constitutively expressed and post-translationally regulated, GVIIERFs are the main activators of flooding acclimation. Without available oxygen for N-degron-based degradation, the GVIIERFs accumulate and induce a multitude of transcriptional changes. In *A. thaliana* five

members of this group were identified, HRE1, HRE2, RAP2.2, RAP2.12 and RAP2.3. Previous studies uncovered that core acclimation is mostly driven by the three RAP transcription factors, with secondary regulatory functions of HRE1 and HRE2. While the three RAP proteins appear to induce a similar response on the same targets, their own transcriptional regulation appears distinct. Previously, RAP2.12 was found to be transcriptionally activated by WRKY12 and WRKY33 (Tang et al., 2021). Simultaneously, RAP2.12 transcription was found to be downregulated by HRA1 (Giuntoli et al., 2014) (Giuntoli et al., 2017). Therefore, regulatory differences between RAP2.2 and RAP2.12 were investigated in the context of target activation and impact on survival.

4.1.1 Potential differences in RAP-mediated acclimation

The GVIIERFs RAP2.2, RAP2.12 and RAP2.3 accumulate concurrently to dropping oxygen saturation (Kosmacz et al., 2015). This rapid response is mostly achieved by constitutive expression and regulation through the N-degron pathway. By constantly flagging and processing GVIIERFs for degradation in the presence of oxygen, the core response activates in correlation to the severity of flooding. When submerged for a long time, the cellular oxygen levels can drop to near anoxia. This intense stress state was partially recreated here through nitrogen fumigation. By flushing seedling or adult plants with pure nitrogen gas, induction of low-oxygen acclimation is studied separately. However, this experimental setup does not capture factors encountered during flooding, other than low oxygen.

Recently, the role of ethylene for hypoxia acclimation was unveiled further. The reduced gas diffusion underwater and subsequent ethylene accumulation also leads to increased levels of PHYTOGLOBIN1 (PGB1). The abundance of PGB1 then leads to increased NO scavenging and reduces NO availability for N-degron based degradation (Hartman et al., 2019) (Hartman et al., 2021). In the experimental setup of nitrogen fumigation used in this work, this accumulation of ethylene is not possible. Treated plants are therefore directly transferred to oxygen conditions encountered only during prolonged flooding, but without the pre-acclimation state. Consequently, differences detected between *rap2.12* , *rap.2.2* or *rap2.12 rap2.2* likely do not represent a natural flooding environment. Here, distinctions in hypoxia acclimation were

investigated through quantification of the transcriptional activation of LBD41 and ADH1. After seedlings were subjected to 4 h of N_2-fumigation, all tested mutants displayed decreased capabilities in inducing ADH and LBD41. Single mutant lines *rap2.2* and *rap2.12* retained a similar capacity to induce transcription of LBD41 and ADH1, with slightly increased induction in *rap2.2* over *rap2.12* (Fig. 4).

These results mostly align with previously acquired transcript levels after 3 h of nitrogen fumgiation (Gasch et al., 2016). This further reinforces the idea that RAP2.2 and RAP2.12 take a nearly equally important role in HRG induction. The strong drop in target transcripts displayed in both double mutants, signifies an only secondary role of RAP2.3. While HRGs in the double mutants are still clearly increased under hypoxia, only a fraction of the wildtype induction remains. Simultaneously however, when comparing ADH activity the strong effect of the double KO disappears (Fig. 5). While an induction of activity was mostly weaker in *rap2.2 rap2.12* lines, the single mutants display equal activity to Col-0 under hypoxia. Despite the strong distinction in transcript levels of ADH1, no significant differences in activity could be measured between the genotypes. An explanation why the clear transcriptional effect does not translate into an enzymatic activity could be the experimental setup. Compared to traditional submergence, nitrogen fumigation causes cellular oxygen levels to deplete much more rapidly. In this state of low oxygen, protein synthesis might be limited, leading to reduced translation of the acclimation signal.

Possible differences between *rap2.2* and *rap2.12* genotypes were then also investigated for long-term submergence and survival. Here, the survival duration under light submergence was higher than expected. Previous studies of Col-0 plants showed a submergence median lethal time of around 20 d in the light, and 5 d in the dark (Vashisht et al., 2011). In the present study, Col-0 still displayed a 100 % survival rate at 21 d, and had only reached an average 50 % survival rate by 28 d (Fig. 6). Previous studies featured an experimental setup with water circulation, UV-light-based reduction of algae growth and a slightly longer short day of 9 h. Even with seemingly more stressful treatment, the higher survival rate recorded here could be the result of improved lighting conditions.

It was also investigated here which parts of the native sequence of RAP2.2 are required for its function. The variant Crispr C expressed in *rap2.2* C still contains more than half of the wildtype sequence. This variant should still include the predicted AP2/ERF domain (A0A178VM98-F1, AlphaFold). In contrast, the Crispr B variant features an early STOP upstream of this predicted AP2/ERF sequence. Here, only slightly increased ADH activity was measured in hypoxia stressed *rap2.2* C compared to *rap2.2* B. Additionally, no noticeable differences in target induction and survival were recorded between the two double mutant variants. From this, it can be concluded that the remaining sequence downstream of the AP2/ERF domain is necessary for target activation.
Overall, differences in target regulation between *rap2.2* and *rap2.12* are suggested to some degree. In these experiments, reduced transcript levels of HRGs, increased activity of ADH and higher survival rate of *rap2.12* was recorded. These differences were however not statistically significant, and will have to be investigated further. A higher acclimation in *rap2.12* could potentially result from the previously recorded increased induction of RAP2.2 by WRKY33 and WRKY12 and a possibly missing downregulation of RAP2.12 by HRA1 (Giuntoli et al., 2017) (Tang et al., 2021).

4.1.2 *A. thaliana* retains a memory of low-oxygen events

It has been previously recorded that prior stress acclimations can lead to higher tolerance against similar events in the future. This concept of a stress memory has received increasing attention within the last few years (Galviz et al., 2020) (Oberkofler et al., 2021) (Sharma et al., 2022). Just within the last year, studies revealed the impact of epigenetic modifications on reoccurring drought and heat stress (Charng et al., 2023) (Kambona et al., 2023). When considering anatomical changes in response to hypoxia, such as the formation of adventitous roots in *N. officinale*, the increased aeration continuously benefits this plant's hypoxia tolerance. The low-oxygen acclimation of *A. thaliana*, however, mostly relies on transient metabolic changes. Nevertheless, the possibility of such persistent acclimations was investigated here through subjecting seedlings of Col-0 and *rap2.2 rap2.12* single and double KO lines to re-occurring hypoxic stress. Plants were stressed in the seedling stage at 7 d after transference to the light. These plants

were then stressed again 21 d later, followed by quantification of their ADH activity.
In virgin adult plants, no measurable induction of activity was recorded after 6 h of near anoxic conditions (Fig. 5 B). In comparison, another study using nitrogen fumigation on *Z. mays* seedlings, already showed higher ADH activity after 6 h of hypoxia (Johnson et al., 1994). Furthermore, in previous measurements of ADH activity, induction after 2 d of submergence was only recorded in more tolerant species than *A. thaliana* (Müller, 2020). However, adults already subjected to hypoxia as seedlings now displayed a significant induction of activity compared to virgin plants (Fig. 5 E). These results provide only a first glimpse of a potential hypoxia stress memory in *A. thaliana*.
As the induced fermentation by ADH occurrs as part of the core hypoxia response, multiple steps of this process could promote this memory effect. An elevated activity level was already recorded in adults 21 d after the seedlings experienced hypoxic stress (Fig. 5 C). With no second stress event required, a putative euchromatin formation of the ADH gene is plausible (Hilker et al., 2019). Additionally, as this memory effect was measured in fumigated plants with constant gas exchange, an impact of ethylene or NO levels during treatment appears unlikely. Furthermore, the function of ADH1 is recycling NADH to NAD^+ through an electron transfer. It is therefore highly affected by the surrounding redox conditions (Dumont et al., 2018). However, whether increased ADH induction is facilitated by already stabilized GVIIERFs, epigenetic modifications and euchromatin formation, non-gaseous phytohormones or other factors remains unknown. Future experiments could investigate if nature-like flooding treatment also leads to increased transcription and activity levels. Furthermore, an impact of seedling hypoxia priming on the survival rate of submerged adults should also be studied.

4.2 The elusive transcriptional repressor LBD41

The escape and quiescence syndrome represent perfect examples of convergent evolution. Both acclimation strategies were previously found in the grasses *Poaceae* and the cabbage *Brassicaceae* family. While an escape syndrome was described in deepwater rice C9285 and *N. officinale* (Hattori et al., 2009) (Müller et al., 2021), the concept of quiescence is employed by rice cultivar FR13A and *A. thaliana* (Lee et al., 2011) (Xu et al., 2006). However, independent of growth,

plants are severely limited in their ATP production underwater. Therefore, energy is preserved through metabolic acclimations and downregulation of ATP-intensive processes. Linked to this mechanism of energy conservation, transcription factor LBD41 was identified as part of the core response to low oxygen. Conveyed through the C-terminal EAR motif, induction of LBD41 leads to repression of inessential genes. Although this hypoxia-based repression appears more associated with the quiescent syndrome, homologous proteins of LBD41 were also found in LOES species. With confirmed ortholog induction during flooding in *Oryza sativa* (OS01G0511000) and *N. officinale* (NoLBD41), its occurrence seems independent of the quiescent response (Müller, 2020) (Tamura et al., 2022).

4.2.1 Discerning the biological function of AtLBD41

While the transcriptionally repressive function of LBD41 could be revealed, discerning the exact purpose of this regulation remains complex. Although putative target genes were identified previously, they are associated with seemingly unrelated pathways. These potential targets appear mostly unconnected to growth, primary metabolism or developmental processes. When combining recent publications, most targets can now be associated to other stress response mechanisms.

Among them, the role of LBD39 in nitrogen starvation was already previously linked to regulation of NitRate Transporters (NRT) (Rubin et al., 2009). Furthermore, PUP10 is involved in cytokinin hormonal transport, possibly for heat or cold stress responses (Liu et al., 2020). The target GGT4 is involved in glutathione regulation, mostly used in pathogen defense and other biotic stress responses (Zechmann, 2020). For HADLH a role in flavin mononucleotide (FMN) availability is described, likely for photosynthetic regulation or phosphate starvation (Rawat et al., 2011) (Rouached et al., 2010). Additionally to AOX1D's well documented function during oxidative and salt stress (Oh et al., 2022), PGDH's role in serine biosynthesis was also linked to salt stress acclimation (Rosa-Téllez et al., 2020). Another potential target of LBD41 is PAP1, a central regulator of anthocyanin production. The plant-exclusive flavonoids anthocyanins were already identified to play vital roles in reproduction and pollination. Additionally however, their involvement in low phosporus, salt or drought stress have been described

recently (Dabravolski et al., 2023) (Lee et al., 2016). A downregulation of anthocyanin production through LBD41 was observed here, through the reverse effect in pr35S:LBD41ΔEAR:VP16 seedlings (Fig. 8).

Additionally, the chemical properties of anthocyanins make them powerful ROS scavengers (Cerqueira et al., 2023). While ROS are not unrelated to flooding, potentially harmful ROS bursts are mostly encountered during the first hours of submergence and upon reoxygenation, while induction of LBD41 is associated with prolonged hypoxia. Deducing from these recent findings, the role of LBD41 can be specified further. The repressive activity appears to deactivate specific steps of stress response pathways, which are not required during flooding. This includes response pathways to heat, drought, salt, biotic and potentially high-light stress. Future experiments into stress susceptibility of KO lines could further clarify this biological function.

4.2.2 Homology of LBD41 prevents loss-of-function

Across different model organisms, vital functions are often protected through multiple gene copies with identical or similar functions. This gene redundancy is likely evolutionary beneficial in higher organisms, as it provides a safety net for random loss of function mutations (Nowak et al., 1997) (Wagner, 1996). For most cases, gene duplications are believed to be the leading cause of this phenomenon, shown by high sequence similarity between redundant genes. The same is likely true for LBD41 and its homologs LBD40 and LBD42. Most notably, the genes *LBD40* and *LBD42* are connected by a close proximity on chromosome 1 and a 71 % identity score (E-value $3e^{-73}$, Protein sequence alignment, NCBI Blast) (Kerfeld et al., 2011). While LBD41 is located on chromosome 3 and only shares a 54 % sequence identity with LBD40, a homologous connection is highly suggested (E-value $6e^{-89}$).

Initially, the set of core genes induced during flooding in Col-0 includes LBD41 and not its homologes. However, previous experiments with *lbd41* knockdown identified an increased induction of LBD40 after 8 h of hypoxia. Simultaneously, an equal target repression capacity of overexpressed LBD40 and LBD42 to LBD41 was recorded in protoplasts (Bäumler, 2020). This homologous promoter targeting could be confirmed here for prAOX1D (Fig. 12). Interestingly,

results obtained for the promoter of SLAH3, only showed the expected regulation for LBD42 (Supplementary, Fig. 35). This likely makes SLAH3 not a direct target of LBD41, however their activity could potentially affect each other indirectly.

To study a full knockout of this transcriptional regulation, a *lbd40 lbd41 lbd42* line was created prior to this work. When testing this triple mutant, a sequencing of *lbd41* revealed a still intact EAR domain. Measurements conducted in protoplasts then confirmed that the previously used *lbd41* mutant exhibited reduced repression of target expression (Fig. 9). This mutant can therefore be described as a knockdown, and not a knockout. With a already homozygous triple mutant line, the effect of this *lbd41** knockdown and *lbd40 lbd42* knockout was then studied further. In *lbd40 lbd41** *lbd42* seedlings, the only slightly increased target transcripts likely correlate with a mostly functional shortened LBD41* (Fig. 11) (Fig. 21). Under hypoxia, this mutant version appears induced even more strongly, possibly compensating for the reduced activity (Fig. 20). This potentially increased transcription of LBD41 in *lbd40 lbd41** *lbd42* could result from a yet unidentified feedback loop. While a mechanism behind such regulation is unknown, a reproducibility of increased induction can be studied with the new KO lines.

However, a reduced repression was also shown in protoplasts isolated from adult plants, where target promoters showed increased activity in the *lbd40 lbd41** *lbd42* background (Fig. 13) (Fig. 25). Compared to Col-0, *lbd40 lbd41** *lbd42* did not display reduced survivability when submerged or waterlogged (Fig. 22 A) (Fig. 24). However, a possible increased tolerance under starch waterlogging of *lbd40 lbd41** *lbd42* was detected. This result could connect an increased microbial growth under these condtions, to the postulated role of LBD41 in downregulating responses to other stresses (Fig. 22 B). Future experiments should investigate potential advantages of *lbd40 lbd41 lbd42* under short-term flooding and other biotic and abiotic stress situations.

While the triple mutant used here shows reduced activity, the intact EAR domain prevents study of a knockout genotype. To then create a true loss of function mutant, three shortened versions were created using the Crispr/Cas system. Preliminary transcript measurements of *lbd41* Crispr1 and Crispr2 showed a strong induction of LBD40 and elevated levels of PUP10 under hypoxia (Supplementary, Fig. 34). At the same time, *lbd40 lbd41** *lbd42* was backcrossed

with Col-0 to generate *lbd40 lbd42*. Future generation of a new *lbd40 lbd41 lbd42* triple mutant will enable investigation of a full knockout, and the resulting impact on submergence survivability.

4.2.3 Expression of LBD41△EAR:VP16 is possibly counteractive

While morphological changes such as leaf elongation or lack thereof can be identified and classified, metabolic changes are often more elusive. When subjected to flooding stress and subsequent hypoxia, tolerant plants induce transcriptional changes to preserve ATP. Induced in all cell types under hypoxia, the activity of LBD41 is predicted to be part of this ATP conservation mechanism. The N-terminal LOB domain indicative of all LBD proteins grants LBD41 specific target promoter binding. At the same time, the C-terminal EAR motif correlates with a repressive transcriptional function (Kagale et al., 2011). While methods to systemically screen for transcriptional activators are published, studying the effect of a repressor can prove difficult. To identify targets of LBD41, the C-terminus including the EAR motif was removed previously. Replacing this EAR domain, the sequence of a viral VP16 domain was fused to the remaining N-terminus, creating LBD41ΔEAR:VP16. This VP16 domain from *Herpes simplex* was previously identified as a powerful transactivator (Fan et al., 2020) (Jonker et al., 2005). Transcriptomal effects of this mutant were previously studied in a microarray. Subsequently, comparison of DEGs from LBD41ΔEAR:VP16 and native LBD41 overexpression allowed identification of multiple putative target genes (Bäumler, 2020). To then further study the regulation of LBD41, the construct LBD41ΔEAR:VP16 was also inserted into the genome of Col-0. Under constitutive transcription with a 35S promoter, three stable expression lines were identified in this work.

Among them, only the line VP16-2 shows a distinguishable phenotype in shape of seeds and silique (Supplementary, Fig. 32). With the random T-DNA insertion of pr35S:LBD41ΔEAR:VP16, such differences between the lines likely originate from the copy of insertions and their chromosomal location. However, while transcript quantification of seedlings and adults confirmed a hypoxia-independent expression, only a minor variation was measured between the lines. The transcript levels of these mutant variants were also significantly lower than the

hypoxic induction of native LBD41 (Fig. 7). Therefore, only a singular independent insertion of pr35S:LBD41ΔEAR:VP16 can be presumed for each line.

The effect of *in vivo* pr35S:LBD41ΔEAR:VP16 expression was then investigated further. When measuring transcripts of putative target genes in seedlings and adults, only slightly increased levels could be recorded (Fig. 11) (Fig. 21). Simultaneously, no major effect on waterlogging or submergence survival was displayed by the VP16 lines (Fig. 22) (Fig. 24). When detection of the VP16 mutant protein was attempted through western blot, no signal could be obtained from seedlings (Supplementary, Fig. 40). Only heterologous expression in *N. benthamiana* allowed detection of LBD41ΔEAR:VP16, albeit only with limited abundance (Supplementary, Fig. 42).

In contrast to these minor effects through stable expression, *in vitro* pr35S:LBD41ΔEAR:VP16 expression in protoplast displayed substantial activation of targets (Fig. 12) (Fig. 13). Here a strong trans-activating activity was measured for the putative targets PUP10, AOX1D, PAP1 and LBD39. This discrepancy of *in vitro* and *in vivo* expression, possibly results from a difference in copy number. While in both cases overexpression is performed under 35S promoter control, a different ratio of native to mutant LBD41 is present. Based on the transcript results, the stable lines likely feature an equal ratio of native to mutant copies. Meanwhile, in protoplasts, transient expression involves transformation with concentrated pHBTL pr35S:LBD41ΔEAR:VP16 vectors. Presumably, the resulting overexpression is then transcribed from multiple copies for each cell.

Furthermore, previous studies revealed a potential self-targeting of LBD41 and its promoter (Bäumler, 2020). This suggests that LBD41 possess a negative feedback loop of transcriptional self-repression. With the LBD41ΔEAR:VP16 variant containing the identical N-terminal DNA binding domain, mutant proteins should also recognize the native promoter. This leads to the possibility of a weak but constitutive expression of the VP16 variant, which in turn induces transcription of native LBD41. Such a simultaneous expression of native and mutant LBD41 with opposing activity could result in a minimal overall transcriptional outcome. This interaction combined with the difference in copy number, could explain why the VP16 variants shows a strong effect *in vitro* but not *in vivo*. Therefore, continued future work with these VP16

lines requires evaluation of native and mutant transcript levels separately.

4.2.4 Misregulation of LBD41 can impact survival

Although the regulatory knockdown studied in *lbd40 lbd41* lbd42* displayed transcriptional changes to Col-0, an impact on flooding survival could not be discerned. Simultaneously, while LBD41ΔEAR:VP16 showed a strong effect *in vitro*, only minimal influence was recorded for stable expression lines. To then further investigate into misregulation of LBD41, a previously generated pr35S:LBD41 overexpression line was also studied. Unlike the *lbd40 lbd41* lbd42* and LBD41ΔEAR:VP16 lines, constitutive overexpression of LBD41 displayed a strong impact on flooding survival.

Under full submergence, OE plants showed a substantial reduction of long-term survival. Here submerged under short day lighting, Col-0 exhibited an average 50 % survival rate after 28 d of submergence. With the same conditions, OE plants arrive at a 50 % survival rate already between the 21 and 24 d time point. Subsequently after 31 d of submergence, OE plants displayed a less than 5 % survival rate, compared to over 30 % in Col-0 (Fig. 24). When subjected to 14 d of waterlogging, OE plants did not display increased lethality, even if stressed further through added starch (Fig. 22). However, overexpression of LBD41 led to a distinct phenotype which intensifies with waterlogging (Fig. 23). Leaves of OE plants are curled inward and also tilted to the side, giving them the appearance of a turbine in motion. Both aspects of this leaf phenotype are already found under control conditions, but become more apparent with waterlogging. How the constitutive repression of targets in OE plants produces this appearance is difficult to pin down. Of the identified putative targets, no direct correlation to growth or leaf shape has been uncovered. With a already increased seed size of OE plants, this phenotype could arise from misregulation during early development (Fig. 32 D). Furthermore, this leaf phenotype could be connected to the hyponastic response seen in flooded *A. thaliana* (Eysholdt-Derzsó et al., 2019) (Lee et al., 2011).

However, it is possible that this phenotype is unrelated to the native function of LBD41. The construct of native LBD41 expressed in this line features a N-terminal HA-tag and C-terminal GFP. During measurements in protoplasts, it was then uncovered that this N-terminal HA tag

leads to a reduction of transcriptional activity (Fig. 19). This tag likely obstructs promoter recognition and binding of the N-terminal LOB DNA binding domain. When removing the N-terminal HA-tag and attaching it to the C-terminus, a significant increase in activity was recorded. Therefore, it is possible that the phenotype results from overexpression of a partially dysfunctional protein.

Additionally, striking about this construct and plant line is the abundance of resulting protein. Unlike the LBD41ΔEAR:VP16 variant, LBD41 could be detected in seedling extracts, even under control of the same 35S promoter (Supplementary, Fig. 40). Furthermore, when expressed heterologously in *N. benthamiana*, this construct also displayed highly elevated protein abundance (Supplementary, Fig. 42). At a comparable transcript level as pr35S:LBD41'HA, protein content of pr35S:HA'LBD41'GFP was elevated about 100-fold (Supplementary, Fig. 41 A). To investigate whether the encountered phenotype and reduced survivability are specific to this construct in particular, a new overexpression line was created. Future studies of this pr35S:LBD41'HA line should unveil if the acquired results stem from the overexpression of LBD41, or rather the accumulation of a partially defective protein.

4.2.5 LBD41 is involved in germination

So far, induction of LBD41 is mostly associated with flooding acclimation. Here, an additional role during seed ripening and germination is proposed. Transcriptomic data in previous studies already indicates an upregulation of LBD41 at several points during development. Elevated levels were detected during the heart embryo and early cotyledon stages of seed ripening, mostly elevated in the chalazal seed coat (Bassel et al., 2008) (Winter et al., 2007). Furthermore, higher transcripts of LBD41 were detected upon rehydration of dried seeds, accumulating at 24 h after imbibition (Klepikova et al., 2016). In these studies, elevated levels at these developmental stages were also measured for LBD40, although at reduced intensity.

In the work conducted here, seedlings of *lbd40 lbd41* lbd42* already displayed slightly elevated target transcripts without a hypoxic treatment, albeit not significantly (Fig. 11). This could suggest an induction of LBD41 occurs during germination, and independent of flooding. Additionally, seedlings of LBD41ΔEAR:VP16 germinating in liquid medium displayed an

increased content of anthocyanins only at 5 d after transference to the light (Fig. 8 B). With a constitutive pr35S mediated expression of LBD41ΔEAR:VP16, this difference likely stems from reduced regulation by native LBD41. It has to be investigated further if transcription of LBD41 fluctuates within the first week of germination.

The seed phenotypes encountered in this work, further strengthens the argument of an important role of LBD41 in germination. While the small malformed seeds and silique of line VP16-2 was initially attributed to the random insertion of this construct, a relation to the native function of LBD41 is possible. This concept is supported when evaluating seeds of the overexpression line OE(N), which display an enlarged phenotype compared to Col-0 (Supplementary, Fig. 32). Just as the VP16 mutant and native LBD41 enact contrary effects on their target genes, overexpression leads to opposing seed phenotypes. Furthermore, mutants of LBD41 were also investigated on germination rate with increasing salt concentration. Here, all VP16 lines already displayed decreased germination rate to Col-0 under control conditions, further decreasing with increasing salt concentration (Fig. 15). At a total of 100 mM NaCl, germination was recorded for only around 30 % of LBD41ΔEAR:VP16 seeds, compared to over 80 % in the wildtype. With a difference already present under control conditions, early germination is likely affected by the VP16 construct. An upregulation of LBD41 was previously even recorded in transcriptome datasets during stratification (Narsai et al., 2011).

Unfortunately, no available data connects how the regulation imposed by LBD41 influences seed morphology or germination. However, it can be speculated that LBD41 fulfills an ATP conservation function, similar to its role during flooding. Whether this induction is part of a controlled developmental process or the result of transient hypoxic phases during seed development remains unknown (Borisjuk et al., 2009). Besides undergoing stages of transcriptomal changes, substantial chromatin remodelling was detected in germinating seeds (Narsai et al., 2017). As the repressive signal of LBD41 is expected to induce heterochromatin formation, this might play a vital role during early developmental genome remodelling. Through promoting deactivation of inessential genes, germinating plants could potentially prevent starvation during crucial points in development. This pathway might be especially important when germinating under stress conditions. An impact of the newly created *lbd40 lbd41 lbd42* and

LBD41 OE lines should also be investigated in the context of germination. These mutant seeds could be tested with other common stress factors potentially affected by LBD41, such as drought or heat.

4.2.6 Salinity induces LBD41 and affects its targets

When grown outside of a laboratory environment, plants are often subjected to multiple types of stress simultaneously. A heat stressed plant will often experience drought simultaneously, could be infected or suffer from insufficient lighting. Similarly, plants already exposed to high soil salinity might be subjected to hypoxia. Concurrently, plants growing in coastal regions are often exposed to salt water intrusion and subsequent flooding. Such multifactorial stress can have synergistic effects, often impacting survival more strongly than individual stress factors (Zandalinas et al., 2021) (Zandalinas et al., 2022). Although oxidative stress arising from high salinity appears antagonistic to hypoxia, both lead to reduced availability of ATP.

While the mETC is inhibited without oxygen as a terminal electron acceptor, hyperionic conditions also affect ATP synthesis negatively. Additionally to water loss through osmotic potential, high Na^+ concentrations prevents the uptake and transportation of essential K^+ ions. This insufficient K^+ content subsequently also inhibits ATP synthesis (O'Neill et al., 1984) (Hasanuzzaman et al., 2018). To combat this imbalance of Na^+ and K^+, salt tolerant species activate cellular ion transporters. These SALT OVERLY SENSITIVE (SOS) proteins facilitate the excretion of excessive sodium in root cells. At the same time, HIGH AFFINITY K Transporter (HKT) work against the osmotic potential and prevent excessive Na^+ ions from entering the xylem (Gupta et al., 2012) (James et al., 2011). However these transporters are ATP dependent, reducing their effectiveness in already energy-deprived plants (Renziehausen et al., 2024).

Most studies published on the topic of salt flooding, focus on morphological characteristics of tolerant species. For example, a study of the coastal halophyte genus *Salicornia* assigned their tolerance to extensive shallow root growth (Moatabarniya et al., 2022). Especially in less tolerant species such as *A. thaliana*, limited information on hypoxic acclimation of salt stressed plants is available. With some of LBD41's putative targets potentially involved in responses to salt stress, this connection was investigated further. To determine if the transcriptional changes

in *lbd40 lbd41* lbd42* and VP16 lines influences salt responses, germination on salinated medium was tested. A general fitness under salt stress was measured through root length and germination rate. Compared to Col-0, the VP16 lines displayed reduced fitness in both cases, while *lbd40 lbd41* lbd42* only showed reduced growth (Fig. 14) (Fig. 15) (Fig. 16). Surprisingly, when analyzing transcript levels of salt-stressed seedlings, an induction of LBD41 is even recorded in Col-0 (Fig. 18 G and H). Although no previous data connects LBD41 to a salt stress response, other HRGs also show this regulatory overlap. The GVIIERF HRE2 was recently found to contain cis-regulatory elements responding to either salt or hypoxia stress (Seok et al., 2022). A potentially synergistic effect of salt and hypoxia on the regulation of AOX1D, PAP1 and LBD39 was also measured in relative transcripts (Supplementary, Fig. 36). Whether the negative effect on ATP availability of both stressors induces similar energy conservation responses remains to be explored. To characterize the role of LBD41 with salinity, acclimation of *lbd40 lbd41 lbd42* to salt water flooding could uncover further information about this connection.

When germinating seeds on Hoagland medium with 50 mM NaCl, the occurrence of different phenotypes marked an unexpected phenomenon. This effect was recorded in all lines including Col-0, with a reduced variance in the VP16 lines (Fig. 17). These two phenotypes were also visible in independently measured distribution of root length under these conditions (Fig. 16 C). Due to the homozygous nature of these lines, this effect can not be assigned to a genotypic difference. This effect was possibly only recorded for Hoagland and not MS medium due to a difference in trace element availability. Unlike MS, the composition of Hoagland medium used in these assays did not contain any manganese, zinc, boron, copper or molybdenum. Resulting from maternal deposition, the absence of zinc or copper from a medium has not been found to affect the germination of Col-0 (Bouain et al., 2019) (Wintz et al., 2003). While their absence might have a low impact on otherwise unstressed seedlings, it could lead to increased demand under salinity. At least zinc and copper were already found to play a role in anti-oxidative plant responses (Chen et al., 2022) (Kaur et al., 2023). The different phenotypes encountered here might possibly result from an unequal maternal distribution of trace elements during seed maturation. A separate addition of individual trace elements could further highlight their

importance in these stress phenotypes and salt tolerance in general.
As another potential explanation for the seemingly random distribution of salt tolerant and sensitive phenotypes, differences in lighting are proposed. Seedlings on media plates were grown with canopy lighting. The light source used emitted a spectrum of mostly blue, green and red light, with peaks at 440, 550 and 610 nm (Lumilux Cool White L36W/840, Product data sheet, Osram). Through absorption and transmission of light through the environment, some seedlings might be subjected to a increased ratio of longer wavelengths (Linkosalo et al., 2006). With a potentially higher frequency of red and far-red light rays, neighbouring clones could enact different signalling.
An effect likely undetectable in unstressed plants, a similar phenotypic separation to salt stress was recorded before. In this previous study, elevated levels of polyamines were linked to the increased salt tolerance of some plants (Ruiz Carrasco et al., 2007). The positive influence of polyamines on salt tolerance could be confirmed since then, and was shown linked to redox regulation and ion transporter NHX1 expression (Kusano et al., 2007) (Saha et al., 2015) (Shao et al., 2022). Furthermore, increased seed germination was linked to POLYAMINE UPTAKE TRANSPORTER 2 through PHYTOCHROME A (PhyA) regulation (Kim et al., 2019). The red light activated sensor proteins Phy A and B are mostly linked to a shade avoidance response, but are recently investigated in combination with other stress factors (Casal, 2012) (Qiu et al., 2023). A similar effect of red light on salt tolerance was also discovered recently for cucumber (Miao et al., 2023). This would suggest that the salt tolerant phenotype encountered here experienced an increased ratio of longer wavelengths. It has to be tested if the transcriptional differences recorded here for Col-0, can be replicated with red light treatment of salt-stressed plants.

4.2.7 Hypoxia-independent regulation of LBD41

The transcriptional activation of LBD41 as part of the core response has been described in multiple studies, and is often used as a marker for hypoxia. However, an increasing number of data points to further hypoxia-independent regulation. Measurements of transcript levels indicate an even stronger induction in adult plants than in seedlings (Fig. 20). After 24 h of darkness, induction of LBD41 was previously even recorded under normoxia (Bäumler, 2020).

Here, additional induction during germination is proposed, and a potential transcriptional activation through salinity could be shown. Additionally, previous studies showed an upregulation in plants infected with *Botrytis cinerea* and *Phytophthora parasitica* (Thatcher et al., 2012). With many potential influences on transcriptional induction, the repressive function of LBD41 appears to be involved in non-flooding conditions.

However, information on the post-transcriptional regulation of LBD41 is limited. The rate of translation and stability of the resulting protein further impacts activity outcome. Prior to this work, LBD41 was already identified as a potential target of post-translational modification with SUMO (Elrouby et al., 2010). Subsequently, multiple target sites for this SUMOylation were identified in LBD41 using GPS-SUMO (Zhao et al., 2014). Previously, binding of SUMO to LBD41 could be shown in a co-immunoprecipitation, along with a possible removal of this binding through the mutation K105R (Bäumler, 2020). However, in which way SUMOylation affects the regulatory activity of LBD41 remained entirely unknown.

Using the protoplast transactivation system, changes in activity were studied for K105R with native LBD41 and LBD41ΔEAR:VP16 overexpression. Here, LBD41 K105R showed only a slight decrease in activity (Fig. 25). With the other putative binding sites identified, mutants of K135R, K172R, K197R, K221R and K253R were also created and tested. Here neither single (Supplementary, Fig. 39), nor various double or triple lysine to arginine mutants produced distinguishable results (Fig. 26). These tests indicate that a potential SUMOylation does not influence the repressive capabilities of LBD41. However, due to the immense amount of possible combinations of these mutations, only some could be tested. Most importantly, through constitutive overexpression of effectors in a PTA, differences in protein localization or availability are not detectable.

To then further inquire into a potential SUMOylation, protein abundance was studied by western blot. When extracted from OE(N) seedlings, separate proteoforms were detected (Supplementary, Fig. 40). As this line expresses pr35S:HA'LBD41'GFP, the resulting fusion protein is expected at around 55 kDa. However, only a minuscule signal appeared at this size. Instead a strong signal at around 70 kDa is present, likely corresponding to a mono-SUMOylated form. Any potential multimer or non-covalent modification would not be detectable under

denaturating PAGE conditions. Additionally, a signal at 28 kDa possibly represents unmodified LBD41 without the C-terminal GFP, suggesting a digestion at the C-terminus. To achieve a high protein content for improved detection, heterologous expression of LBD41 variants was performed in *N. benthamiana*. Ocurrence of the different proteoforms was also investigated in the context of a 2 h hypoxia treatment with 1 h of reaeration. In these protein extracts, signals for an unmodified LBD41 with fused HA or GFP was again nearly undetectable. In contrary, most variants displayed a strong signal at their theoretical molecular weight with an additional 11 kDa (Fig. 27) (Supplementary, Fig. 42) (Supplementary, Fig. 43). This difference again suggests modification with a single SUMO1 protein. Comparison of heterologous expression and the proteoforms from seedlings then conveys multiple aspects of this regulation.

First of all, *At*LBD41 is apparently recognized as a target for post-translational modification in *N. benthamiana*. Despite the seemingly distant relation of the nightshade and cabbage families, modification of *At*LBD41 orthologs appears conserved. With the newly available genome data of *N. benthamiana*, six putative orthologs could be identified. Overall, these sequences show a highly conserved N-terminal LOB domain, conservation of an EAR motif in all besides Nbe.v1.1.chr02g17130, and conservation of lysine residue K135 in all potential orthologs. Here, Nbe.v1.1.chr19g42470 is identified as the most likely candidate of *Nb*LBD41. With a conservation of the putative SUMOylation lysine residues K105 and K135, the modification site can be narrowed down. Furthermore, upstream of *At*LBD41 K135 a highly conserved DIRH motif was identified. While this sequence can not be linked to a known function, this motif could be related to targeting for post-translational modification of these homologs.

The overall high protein sequence similarity of these *Brassicaceae* and *Solanaceae* orthologs suggests the origin of a LBD41-like protein at least 115 Million years ago, at the early Cretaceous period (Fawcett et al., 2009) (Margelevicius et al., 2010) (Wang et al., 2022). Further investigation into the similarity of these orthologs is required to underline their individual role. To determine their transcriptional similarity, potential weaknesses of a newly created *A. thaliana lbd40 lbd41 lbd42* line can be investigated for rescue with *N. benthamiana* orthologs. Additionally, the exact nature of the post-translational modification has to be determined. Therefore, isolation of the differently sized proteoforms encountered here is required, subsequently

followed by analysis through mass spectrometry.

4.2.8 Post-translational regulation of LBD41 possibly light-mediated

From the heterologous expression of *At*LBD41 in *N. benthamiana* additional aspects of the post-translational modification can be identified. The initial modification with what appears to be single SUMO protein, appears independent of the plants oxygen status. This state seems the most prevalent in all variants, oxygen conditions and both organisms tested here (Fig. 27) (Supplementary, Fig. 42) (Supplementary, Fig. 43). A difference between the environment of *A. thaliana* and *N. benthamiana* is seen in the other proteoforms.

While no higher MW forms than the putative mono-SUMOylated state are seen in seedlings, multiple such signals are detected with heterologous expression in *N. benthamina*. It appears that after this first SUMOylation signal, additional modification of LBD41 takes place. These modifications could be additional SUMOylation, attaching to the first SUMO or a different LBD41 lysine residue. In the native environment of *A. thaliana*, this further modification likely leads to deactivation and degradation of the modified protein. This SUMOylation-regulated pathway of poly-UBIQUITINation and subsequent degradation is the most commonly encountered SUMO-mediated mechanism (Benlloch et al., 2018) (Celen et al., 2020) (Miteva et al., 2010) (Singh et al., 2022).

Perhaps related to the aggregation seen in *N. benthamiana*, a recently described SUMO-based mechanism leads to controlled unfolding of its targets (Lee et al., 2023). In this context, it is possible that the degradation of the poly-modified state happens rapidly in *A. thaliana*, making these forms undetectable in seedlings. Whereas when expressed heterologously in *N. benthamiana*, these forms are not degraded and instead accumulate. These results further conveys the idea of a post-translational regulation of LBD41, but the trigger of this modification remains undefined. When evaluating the blotted proteoforms, an effect of the hypoxic treatment could not be discerned. Especially in the putative native-like variant LBD41'HA, differences between the biological replicates appear stronger than those of the treatment (Fig. 27).

Through the experimental setup, transformed plants were shaded during hypoxia and control

treatment, at random intensity (Supplementary, Fig. 41 B). With no other variation between replicates this suggests that the random shading effect conveys a strong influence on the protein availability of LBD41. A shading effect leads to reduced short-wave blue light and increased red and far-red light. This ratio of far-red to red light then activates PHYTOCHROME A (PhyA) and PHYTOCHROME B (PhyB) (Casal, 2012). Interestingly, the subsequent shading response induces similar elongative growth as seen in LOES plants under flooding, eluding to a potential connection.

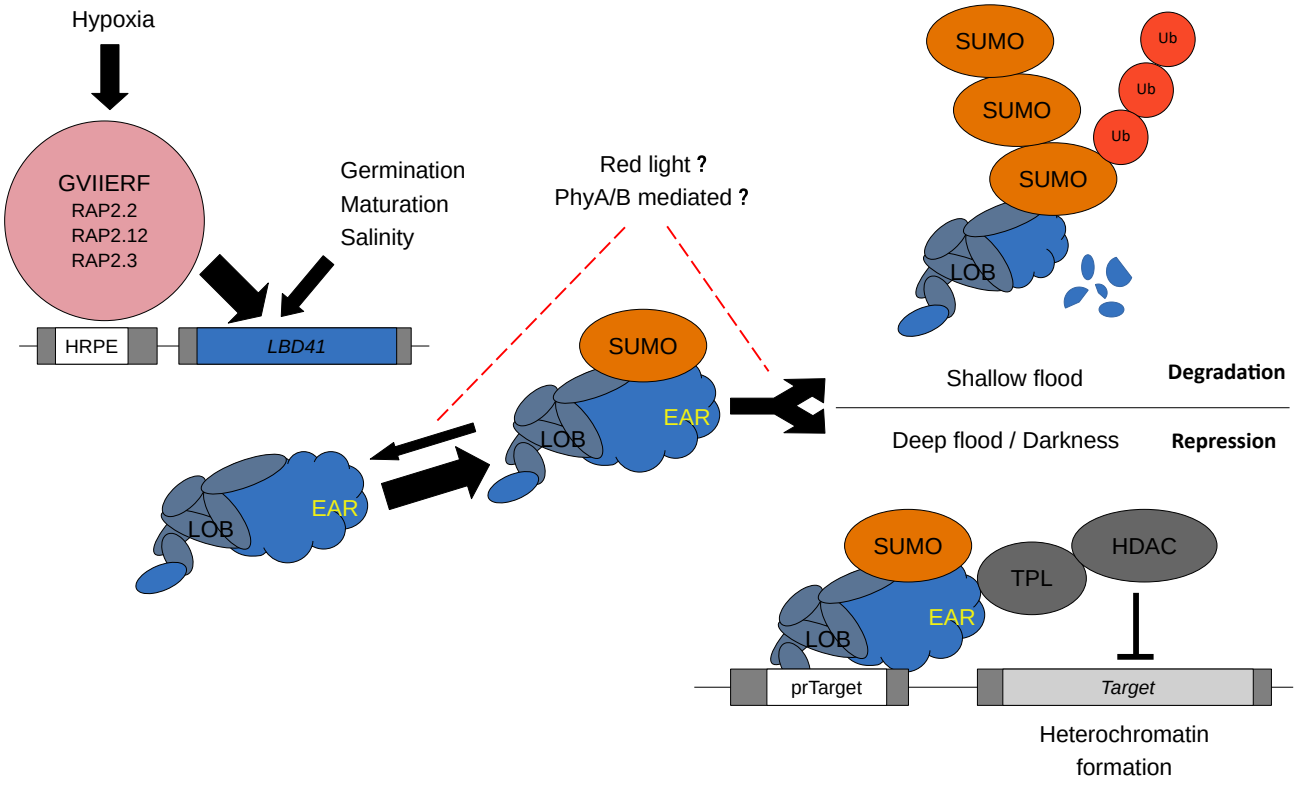

Figure 29: Proposed regulation of LBD41

Updated model of LBD41's putative regulation. Additional transcriptional activation through age and environmental factors was uncovered. Post-translational SUMOylation appears spontaneous and independent of hypoxia. Further protein modifications were detected, likely leading to degradation. Post-translational regulation is proposed to be influenced by red light. This mechanism is hypothesized to differentiate acclimation between shallow flooding and deep dark submergence.

Previously, low light and its negative effect on photosynthesis has already been linked to increased responses to hypoxia (Mommer et al., 2005). Here, a light-mediated post-translational

regulation of LBD41 is hypothesized. Previous work quantified a 3x increased transcription rate in dark flooding (Bäumler, 2020). A potential light regulation of LBD41 was also seen in the *N. officinale* ortholog, where *No*LBD41 was only detected during flooding in darkness (Müller, 2020). Furthermore, the important role of SUMOylation in PHYTOCHROME mediated signalling was shown within the last years (Clark et al., 2022) (Sadanandom et al., 2015) (Zeidler, 2020). In line with the putative role of LBD41 during germination, red light also plays a role in early developmental signalling. Activation of PhyB leads to regulated degradation of PHYTOCHROME INTERACTING FACTOR 3 (PIF3), a necessary process in photomorphogenesis development (Dong et al., 2017) (Kim, 2003). Recently, the importance of SUMOylation in this process was uncovered (Bernula et al., 2021). It is possible that the post-translational regulation of LBD41 is also affected by light-mediated pathways.

Similar to the constitutive expression of the GVIIERFs and their post-translational regulation by oxygen, LBD41 might be ubiquitously transcribed under hypoxia but degraded with available light. As water effectively absorbs longer wavelengths, red light only reaches shallow submerged plants. This mechanism would allow for fine tuning of flooding acclimation, by restricting activity of LBD41 to darkness and deep submergence. Future studies of LBD41's post-transcriptional regulation under hypoxia should investigate potential differences upon treatment with darkness, as well as red and blue light. Additionally, a new *lbd40 lbd41 lbd42* KO lines should be tested for a decreased survival rate under dark submergence. With this context, the ubiquitous transcription of LBD41 in all cell types would suggest a regulatory impact mostly in dark hypoxic tissue. In this hypothesis, a light-mediated degradation would not affect roots, making a regulation imposed by LBD41 possibly much more frequent in this tissue type. The newly created overexpression lines could be used to test for a differential impact on target regulation in root and leaf tissue.

4.3 Conclusion

This work focused on uncovering multiple layers of regulation within acclimation to flooding in *A. thaliana*. The initial hypoxic upregulation of the GVIIERFs RAP2.2, RAP2.12 and RAP2.3, and potential differences between these proteins were investigated. Here, *rap2.12* KO lines displayed slightly lower transcriptional response, reduced ADH activity and survival rate than their *rap2.2* KO line equivalents. Overall however, the equally important function of RAP2.2 and RAP2.12 in flooding acclimation was again confirmed here. Similar to previous results, double KO *rap2.12 rap2.2* leads to substantially reduced transcriptional response to hypoxia. However, despite this seemingly minor activity of RAP2.3, a generally reduced submergence survival rate was not recorded in double KO lines. Furthermore, here plants were subjected to reoccurring hypoxic treatment at the seedling and pre-flowering age. Even three weeks after the treatment, an increased induction of ADH activity was recorded for previously stressed plants. This eludes to the presence of an epigenetic stress memory from flooding events.
Complexity of plant acclimation to flooding was then investigated through the transcriptional repressor LBD41. The studied *lbd40 lbd41* lbd42* contained a still functional EAR motif in *LBD41*, which lead to minimal regulatory differences to Col-0. Subsequently, three *lbd41* KO lines were created, allowing future study of a true *lbd40 lbd41 lbd42* line. Furthermore, expression of pr35S:LBD41ΔEAR:VP16 displayed significant effects when studied *in vitro* in protoplasts. Although, when exploring effects of stable pr35S:LBD41ΔEAR:VP16, this misregulation showed a negligible impact on flooding acclimation. This is attributed to reduced stability and a potential self-deactivating effect of the VP16 mutant variant *in vivo*. Despite their seemingly minor impact, closer investigation of these mutants revealed induction of LBD41 independent of hypoxic treatment.
Here, an increased transcriptional activation was detected in connection with salt stress, resulting in simultaneous regulation of targets AOX1D, PAP1 and LBD39. Furthermore, an increased induction of LBD41 was recorded in adult plants at the age of 4 weeks, alluding to an increased importance of LBD41 during maturation. Most prominently, a role in early development is shown in reduced germination rate of mutants, opposing seed phenotypes of mutant lines VP16-2 and OE(N), as well as previous transcriptomal data. At the same time,

overexpression line OE(N) displayed heavily reduced survival capabilities under submergence, along with a *turbine* leaf phenotype. With high protein abundance and simultaneous reduced activity of the pr35S:HA'LBD41'GFP construct, an effect of LBD41 overexpression requires investigation of the newly created pr35S:LBD41'HA line.

Although the hypoxic induction of LBD41 was uncovered over 15 years ago, regulation of this protein remained mostly elusive. An additional post-translational regulation of LBD41 through SUMO was previously proposed. Similar to preceding assays, the existence of multiple proteoforms could be detected along with a low protein content of the unmodified state. Based on these proteoforms, covalent binding of a putative single SUMO molecule is postulated in overexpressing *A. thaliana*. Additionally, modification of LBD41 was also detected when heterologously expressed in *N. benthamiana*, along with potentially poly-modified proteoforms. Following publication of the *N. benthamiana* genome, high protein sequence conservation between *At*LBD41 and a proposed *Nb*LBD41 can be shown. Furthermore, the modification of LBD41 occurring in both organisms was found to be independent of the internal oxygen status. Here, a role of light mediated signalling is proposed to influence the post-transcriptional abundance of LBD41. An impact of flooding depth and light availability on the ATP-conserving role of LBD41 requires further attention.

Bibliography

Akman, M., A. V. Bhikharie, A. Mustroph, and R. Sasidharan (2014a). "Extreme flooding tolerance in Rorippa". In: *Plant Signaling & Behavior* 9.2, e27847. ISSN: 1559-2324. DOI: 10.4161/psb.27847.

Allawi, H. T. and J. SantaLucia (1997a). "Thermodynamics and NMR of Internal G·T Mismatches in DNA". In: *Biochemistry* 36.34, pp. 10581–10594. ISSN: 0006-2960. DOI: 10.1021/bi962590c.

Anderson, T. R., E. Hawkins, and P. D. Jones (2016a). "CO2, the greenhouse effect and global warming: from the pioneering work of Arrhenius and Callendar to today's Earth System Models". In: *Endeavour* 40.3, pp. 178–187. ISSN: 01609327. DOI: 10.1016/j.endeavour.2016.07.002.

Armstrong, W. (1980). "Aeration in Higher Plants". In: *Advances in Botanical Research*. Vol. 7, pp. 225–332. ISBN: 9780120059072. DOI: 10.1016/S0065-2296(08)60089-0.

Arnosti, D. N., C. M. Preston, M. Hagmann, W. Schaffner, R. Hope, et al. (1993). "Specific transcriptional activation in vitro by the herpes simplex virus protein VP16". In: *Nucleic Acids Research* 21.24, pp. 5570–5576. ISSN: 0305-1048. DOI: 10.1093/nar/21.24.5570.

Baile, F., W. Merini, I. Hidalgo, and M. Calonje (2021a). "EAR domain-containing transcription factors trigger PRC2-mediated chromatin marking in Arabidopsis". In: *The Plant Cell* 33.8, pp. 2701–2715. ISSN: 1040-4651. DOI: 10.1093/plcell/koab139.

Bailey-Serres, J., T. Fukao, D. J. Gibbs, M. J. Holdsworth, S. C. Lee, et al. (2012a). "Making sense of low oxygen sensing". In: *Trends in Plant Science* 17.3, pp. 129–138. ISSN: 13601385. DOI: 10.1016/j.tplants.2011.12.004.

Bailey-Serres, J. and L. Voesenek (2008a). "Flooding Stress: Acclimations and Genetic Diversity". In: *Annual Review of Plant Biology* 59.1, pp. 313–339. ISSN: 1543-5008. DOI: 10.1146/annurev.arplant.59.032607.092752.

Balting, D. F., A. AghaKouchak, G. Lohmann, and M. Ionita (2021b). "Northern Hemisphere drought risk in a warming climate". In: *npj Climate and Atmospheric Science* 4.1, p. 61. ISSN: 2397-3722. DOI: 10.1038/s41612-021-00218-2.

Barker, G. (2006). "Approaches to the Origins of Agriculture". In: *The Agricultural Revolution in Prehistory*. Oxford University Press. DOI: 10.1093/oso/9780199281091.003.0006.

Bassel, G. W., P. Fung, T.-f. F. Chow, J. A. Foong, N. J. Provart, and S. R. Cutler (2008b). "Elucidating the Germination Transcriptional Program Using Small Molecules". In: *Plant Physiology* 147.1, pp. 143–155. ISSN: 1532-2548. DOI: 10.1104/pp.107.110841.

Bäumler, J. (2020). "Charakterisierung der Hypoxie-induzierten Transkriptionsfaktoren AtLBD41 und AtERF#111/ABR1 aus Arabidopsis thaliana". PhD thesis.

Beever, R., E. Mckenzie, S. Pennycook, S. Bellgard, M. Dick, and P. Buchanan (2012b). "Phylum Oomycota water moulds, downy mildews". In: *New Zealand Inventory of Biodiversity*. 1st ed. Vol. 3. Canterebury University Press. Chap. 11, pp. 164–169. ISBN: 978-1-927145-05-0.

Benlloch, R. and L. M. Lois (2018a). "Sumoylation in plants: mechanistic insights and its role in drought stress". In: *Journal of Experimental Botany* 69.19, pp. 4539–4554. ISSN: 0022-0957. DOI: 10.1093/jxb/ery233.

Bensmihen, S., A. To, G. Lambert, T. Kroj, J. Giraudat, and F. Parcy (2004a). "Analysis of an activated ABI5 allele using a new selection method for transgenic Arabidopsis seeds". In: *FEBS Letters* 561.1-3, pp. 127–131. ISSN: 0014-5793. DOI: 10.1016/S0014-5793(04)00148-6.

Bernard, P. and M. Couturier (1992). "Cell killing by the F plasmid CcdB protein involves poisoning of DNA-topoisomerase II complexes". In: *Journal of Molecular Biology* 226.3, pp. 735–745. ISSN: 00222836. DOI: 10.1016/0022-2836(92)90629-X.

Bernula, P., A. Pettkó-Szandtner, A. Hajdu, L. Kozma-Bognár, E.-M. Josse, et al. (2021c). "SUMOylation of PHYTOCHROME INTERACTING FACTOR 3 promotes photomorphogenesis in Arabidopsis thaliana". In: *New Phytologist* 229.4, pp. 2050–2061. ISSN: 0028-646X. DOI: 10.1111/nph.17013.

Borisjuk, L. and H. Rolletschek (2009a). "The oxygen status of the developing seed". In: *New Phytologist* 182.1, pp. 17–30. ISSN: 0028-646X. DOI: 10.1111/j.1469-8137.2008.02752.x.

Borzenkova, I. and Y. Turchinovich (2009b). "HISTORY OF ATMOSPHERIC COMPOSITION". In: *ENVIRONMENTAL STRUCTURE AND FUNCTION: CLIMATE SYSTEM – Vol. II*. Vol. 2, pp. 184–205.

Bouain, N., A. Korte, S. B. Satbhai, H.-I. Nam, S. Y. Rhee, et al. (2019a). "Systems genomics approaches provide new insights into Arabidopsis thaliana root growth regulation under combinatorial mineral nutrient limitation". In: *PLOS Genetics* 15.11, e1008392. ISSN: 1553-7404. DOI: 10.1371/journal.pgen.1008392.

Bradford, M. (1976). "A Rapid and Sensitive Method for the Quantitation of Microgram Quantities of Protein Utilizing the Principle of Protein-Dye Binding". In: *Analytical Biochemistry* 72.1-2, pp. 248–254. ISSN: 00032697. DOI: 10.1006/abio.1976.9999.

Bundesministerium des Innern und für Heimat and Bundesministerium der Finanzen (2022a). *Bericht zur Hochwasserkatastrophe 2021: Katastrophenhilfe, Wiederaufbau und Evaluierungs-prozesse*. Tech. rep.

Cameron, J. and M. J. Carlile (1978). "Fatty acids, aldehydes and alcohols as attractants for zoospores of Phytophthora palmivora". In: *Nature* 271.5644, pp. 448–449. ISSN: 0028-0836. DOI: 10.1038/271448a0.

Cantelon, J. A., J. A. Guimond, C. E. Robinson, H. A. Michael, and B. L. Kurylyk (2022b). "Vertical Saltwater Intrusion in Coastal Aquifers Driven by Episodic Flooding: A Review". In: *Water Resources Research* 58.11. ISSN: 0043-1397. DOI: 10.1029/2022WR032614.

Casal, J. J. (2012). "Shade Avoidance". In: *The Arabidopsis Book* 10, e0157. ISSN: 1543-8120. DOI: 10.1199/tab.0157.

Castaño-Miquel, L., J. Seguí, and L. M. Lois (2011a). "Distinctive properties of Arabidopsis SUMO paralogues support the in vivo predominant role of AtSUMO1/2 isoforms". In: *Biochemical Journal* 436.3, pp. 581–590. ISSN: 0264-6021. DOI: 10.1042/BJ20101446.

Castillo, M.-C., A. Coego, Á. Costa-Broseta, and J. León (2018b). "Nitric oxide responses in Arabidopsis hypocotyls are mediated by diverse phytohormone pathways". In: *Journal of Experimental Botany* 69.21, pp. 5265–5278. ISSN: 0022-0957. DOI: 10.1093/jxb/ery286.

Celen, A. B. and U. Sahin (2020a). *Sumoylation on its 25th anniversary: mechanisms, pathology, and emerging concepts*. DOI: 10.1111/febs.15319.

Cerqueira, J. V. A., M. T. de Andrade, D. D. Rafael, F. Zhu, S. V. C. Martins, et al. (2023a). "Anthocyanins and reactive oxygen species: a team of rivals regulating plant development?" In: *Plant Molecular Biology* 112.4-5, pp. 213–223. ISSN: 0167-4412. DOI: 10.1007/s11103-023-01362-4.

Charng, Y.-y., S. Mitra, and S.-J. Yu (2023b). "Maintenance of abiotic stress memory in plants: Lessons learned from heat acclimation". In: *The Plant Cell* 35.1, pp. 187–200. ISSN: 1040-4651. DOI: 10.1093/plcell/koac313.

Chen, C., J. Wu, Q. Hua, N. Tel-Zur, F. Xie, et al. (2019b). "Identification of reliable reference genes for quantitative real-time PCR normalization in pitaya". In: *Plant Methods* 15.1, p. 70. ISSN: 1746-4811. DOI: 10.1186/s13007-019-0455-3.

Chen, G., J. Li, H. Han, R. Du, and X. Wang (2022c). "Physiological and Molecular Mechanisms of Plant Responses to Copper Stress". In: *International Journal of Molecular Sciences* 23.21, p. 12950. ISSN: 1422-0067. DOI: 10.3390/ijms232112950.

Chen, G., Q. Cheng, T. W. Lyons, J. Shen, F. Agterberg, et al. (2022d). "Reconstructing Earth's atmospheric oxygenation history using machine learning". In: *Nature Communications* 13.1, p. 5862. ISSN: 2041-1723. DOI: 10.1038/s41467-022-33388-5.

Chen, H. and J.-G. Jiang (2010a). "Osmotic adjustment and plant adaptation to environmental changes related to drought and salinity". In: *Environmental Reviews* 18.NA, pp. 309–319. ISSN: 1181-8700. DOI: 10.1139/A10-014.

Chen, X., B. Zhang, Y. Zhao, P. Liu, and Y. Zhou (2013). "EF1α is a suitable housekeeping gene for RT-qPCR analysis during osteogenic differentiation of mouse bone marrow-derived mesenchymal stem cells." In: *Acta biochimica Polonica* 60.3, pp. 381–6. ISSN: 1734-154X.

Clark, L., K. Sue-Ob, V. Mukkawar, A. R. Jones, and A. Sadanandom (2022e). "Understanding SUMO-mediated adaptive responses in plants to improve crop productivity". In: *Essays in Biochemistry* 66.2, pp. 155–168. ISSN: 0071-1365. DOI: 10.1042/EBC20210068.

Coumou, D. and S. Rahmstorf (2012c). "A decade of weather extremes". In: *Nature Climate Change* 2.7, pp. 491–496. ISSN: 1758-678X. DOI: 10.1038/nclimate1452.

Crisp, P. A., D. Ganguly, S. R. Eichten, J. O. Borevitz, and B. J. Pogson (2016b). "Reconsidering plant memory: Intersections between stress recovery, RNA turnover, and epigenetics". In: *Science Advances* 2.2. ISSN: 2375-2548. DOI: 10.1126/sciadv.1501340.

Dabravolski, S. A. and S. V. Isayenkov (2023c). "The Role of Anthocyanins in Plant Tolerance to Drought and Salt Stresses". In: *Plants* 12.13, p. 2558. ISSN: 2223-7747. DOI: 10.3390/plants12132558.

Delden, S. H. van, M. J. Nazarideljou, and L. F. M. Marcelis (2020b). "Nutrient solutions for Arabidopsis thaliana: a study on nutrient solution composition in hydroponics systems". In: *Plant Methods* 16.1, p. 72. ISSN: 1746-4811. DOI: 10.1186/s13007-020-00606-4.

Dijk, M. van, T. Morley, M. L. Rau, and Y. Saghai (2021d). "A meta-analysis of projected global food demand and population at risk of hunger for the period 2010–2050". In: *Nature Food* 2.7, pp. 494–501. ISSN: 2662-1355. DOI: 10.1038/s43016-021-00322-9.

Dissmeyer, N. (2019). "Conditional Protein Function via N-Degron Pathway–Mediated Proteostasis in Stress Physiology". In: *Annual Review of Plant Biology* 70.1, pp. 83–117. ISSN: 1543-5008. DOI: 10.1146/annurev-arplant-050718-095937.

Doench, J. G., N. Fusi, M. Sullender, M. Hegde, E. W. Vaimberg, et al. (2016c). "Optimized sgRNA design to maximize activity and minimize off-target effects of CRISPR-Cas9". In: *Nature Biotechnology* 34.2, pp. 184–191. ISSN: 1087-0156. DOI: 10.1038/nbt.3437.

Dong, J., W. Ni, R. Yu, X. W. Deng, H. Chen, and N. Wei (2017a). “Light-Dependent Degradation of PIF3 by SCFEBF1/2 Promotes a Photomorphogenic Response in Arabidopsis”. In: *Current Biology* 27.16, pp. 2420–2430. ISSN: 09609822. DOI: 10.1016/j.cub.2017.06.062.

Dongen, J. T. van, A. Fröhlich, S. J. Ramírez-Aguilar, N. Schauer, A. R. Fernie, et al. (2009c). “Transcript and metabolite profiling of the adaptive response to mild decreases in oxygen concentration in the roots of arabidopsis plants”. In: *Annals of Botany* 103.2, pp. 269–280. ISSN: 1095-8290. DOI: 10.1093/aob/mcn126.

Dumont, S., N. V. Bykova, A. Khaou, Y. Besserour, M. Dorval, and J. Rivoal (2018c). “Arabidopsis thaliana alcohol dehydrogenase is differently affected by several redox modifications”. In: *PLOS ONE* 13.9, e0204530. ISSN: 1932-6203. DOI: 10.1371/journal.pone.0204530.

Dunn, J.-O., M. Mythen, and M. Grocott (2016d). “Physiology of oxygen transport”. In: *BJA Education* 16.10, pp. 341–348. ISSN: 20585349. DOI: 10.1093/bjaed/mkw012.

Elrouby, N. and G. Coupland (2010b). “Proteome-wide screens for small ubiquitin-like modifier (SUMO) substrates identify Arabidopsis proteins implicated in diverse biological processes”. In: *Proceedings of the National Academy of Sciences* 107.40, pp. 17415–17420. ISSN: 0027-8424. DOI: 10.1073/pnas.1005452107.

Erisman, J. W., M. A. Sutton, J. Galloway, Z. Klimont, and W. Winiwarter (2008c). “How a century of ammonia synthesis changed the world”. In: *Nature Geoscience* 1.10, pp. 636–639. ISSN: 1752-0894. DOI: 10.1038/ngeo325.

Eysholdt-Derzsó, E. and M. Sauter (2019c). “Hypoxia and the group VII ethylene response transcription factor HRE2 promote adventitious root elongation in Arabidopsis”. In: *Plant Biology* 21.S1, pp. 103–108. ISSN: 1435-8603. DOI: 10.1111/plb.12873.

Fan, D., M. Wang, A. Cheng, R. Jia, Q. Yang, et al. (2020c). “The Role of VP16 in the Life Cycle of Alphaherpesviruses”. In: *Frontiers in Microbiology* 11. ISSN: 1664-302X. DOI: 10.3389/fmicb.2020.01910.

FAO United Nations (2023). *The State of Food Security and Nutrition in the World 2023*. FAO; IFAD; UNICEF; WFP; WHO; ISBN: 978-92-5-137226-5. DOI: 10.4060/cc3017en.

Farquhar, G., S. Wong, J. Evans, and K. Hubick (1989). “Photosynthesis and gas exchange”. In: *Plants under Stress*. Cambridge University Press, pp. 47–70. DOI: 10 . 1017 / CBO9780511661587.005.

Fawcett, J. A., S. Maere, and Y. Van de Peer (2009d). “Plants with double genomes might have had a better chance to survive the Cretaceous–Tertiary extinction event”. In: *Proceedings of the National Academy of Sciences* 106.14, pp. 5737–5742. ISSN: 0027-8424. DOI: 10.1073/pnas.0900906106.

Fischer, E. M. and R. Knutti (2015a). “Anthropogenic contribution to global occurrence of heavy-precipitation and high-temperature extremes”. In: *Nature Climate Change* 5.6, pp. 560–564. ISSN: 1758-678X. DOI: 10.1038/nclimate2617.

Food and Agriculture Organization of the United Nations (2023). *The State of Food and Agriculture 2023*. FAO. ISBN: 978-92-5-138167-0. DOI: 10.4060/cc7724en.

Francioli, D., G. Cid, M.-R. Hajirezaei, and S. Kolb (2022f). “Response of the wheat mycobiota to flooding revealed substantial shifts towards plant pathogens”. In: *Frontiers in Plant Science* 13. ISSN: 1664-462X. DOI: 10.3389/fpls.2022.1028153.

Friedlingstein, P., M. O’Sullivan, M. W. Jones, R. M. Andrew, L. Gregor, et al. (2022g). “Global Carbon Budget 2022”. In: *Earth System Science Data* 14.11, pp. 4811–4900. ISSN: 1866-3516. DOI: 10.5194/essd-14-4811-2022.

Fukao, T., B. E. Barrera-Figueroa, P. Juntawong, and J. M. Peña-Castro (2019d). “Submergence and Waterlogging Stress in Plants: A Review Highlighting Research Opportunities and Understudied Aspects”. In: *Frontiers in Plant Science* 10. ISSN: 1664-462X. DOI: 10.3389/fpls.2019.00340.

Fuller, D. Q., T. Denham, M. Arroyo-Kalin, L. Lucas, C. J. Stevens, et al. (2014b). “Convergent evolution and parallelism in plant domestication revealed by an expanding archaeological record”. In: *Proceedings of the National Academy of Sciences* 111.17, pp. 6147–6152. ISSN: 0027-8424. DOI: 10.1073/pnas.1308937110.

Galviz, Y. C. F., R. V. Ribeiro, and G. M. Souza (2020d). “Yes, plants do have memory”. In: *Theoretical and Experimental Plant Physiology* 32.3, pp. 195–202. ISSN: 2197-0025. DOI: 10.1007/s40626-020-00181-y.

Gamelin, B. L., J. Feinstein, J. Wang, J. Bessac, E. Yan, and V. R. Kotamarthi (2022h). "Projected U.S. drought extremes through the twenty-first century with vapor pressure deficit". In: *Scientific Reports* 12.1, p. 8615. ISSN: 2045-2322. DOI: 10.1038/s41598-022-12516-7.

Gasch, P., M. Fundinger, J. T. Müller, T. Lee, J. Bailey-Serres, and A. Mustroph (2016e). "Redundant ERF-VII Transcription Factors Bind to an Evolutionarily Conserved cis-Motif to Regulate Hypoxia-Responsive Gene Expression in Arabidopsis". In: *The Plant Cell* 28.1, pp. 160–180. ISSN: 1040-4651. DOI: 10.1105/tpc.15.00866.

Gasch, P. (2015). "Zentrale Cis- und Transregulation der pflanzlichen Hypoxieantwort ". PhD thesis. Bayreuth: University Bayreuth.

Gibbs, D. J., J. V. Conde, S. Berckhan, G. Prasad, G. M. Mendiondo, and M. J. Holdsworth (2015b). "Group VII Ethylene Response Factors Coordinate Oxygen and Nitric Oxide Signal Transduction and Stress Responses in Plants". In: *Plant Physiology* 169.1, pp. 23–31. ISSN: 0032-0889. DOI: 10.1104/pp.15.00338.

Gibbs, D. J., S. C. Lee, N. Md Isa, S. Gramuglia, T. Fukao, et al. (2011b). "Homeostatic response to hypoxia is regulated by the N-end rule pathway in plants". In: *Nature* 479.7373, pp. 415–418. ISSN: 0028-0836. DOI: 10.1038/nature10534.

Giuntoli, B., S. C. Lee, F. Licausi, M. Kosmacz, T. Oosumi, et al. (2014c). "A Trihelix DNA Binding Protein Counterbalances Hypoxia-Responsive Transcriptional Activation in Arabidopsis". In: *PLoS Biology* 12.9, e1001950. ISSN: 1545-7885. DOI: 10.1371/journal.pbio.1001950.

Giuntoli, B., F. Licausi, H. van Veen, and P. Perata (2017b). "Functional Balancing of the Hypoxia Regulators RAP2.12 and HRA1 Takes Place in vivo in Arabidopsis thaliana Plants". In: *Frontiers in Plant Science* 8. ISSN: 1664-462X. DOI: 10.3389/fpls.2017.00591.

Giuntoli, B. and P. Perata (2018d). "Group VII Ethylene Response Factors in Arabidopsis: Regulation and Physiological Roles". In: *Plant Physiology* 176.2, pp. 1143–1155. ISSN: 0032-0889. DOI: 10.1104/pp.17.01225.

Grant, S. G., J. Jessee, F. R. Bloom, and D. Hanahan (1990). "Differential plasmid rescue from transgenic mouse DNAs into Escherichia coli methylation-restriction mutants." In: *Proceedings of the National Academy of Sciences* 87.12, pp. 4645–4649. ISSN: 0027-8424. DOI: 10.1073/pnas.87.12.4645.

Gupta, K. J., A. U. Igamberdiev, and L. A. J. Mur (2012d). "NO and ROS homeostasis in mitochondria: a central role for alternative oxidase". In: *New Phytologist* 195.1, pp. 1–3. ISSN: 0028-646X. DOI: 10.1111/j.1469-8137.2012.04189.x.

Han, D., J. Lai, and C. Yang (2021e). "SUMOylation: A critical transcription modulator in plant cells". In: *Plant Science* 310, p. 110987. ISSN: 01689452. DOI: 10.1016/j.plantsci.2021.110987.

Hartman, S., Z. Liu, H. van Veen, J. Vicente, E. Reinen, et al. (2019e). "Ethylene-mediated nitric oxide depletion pre-adapts plants to hypoxia stress". In: *Nature Communications* 10.1. ISSN: 20411723. DOI: 10.1038/s41467-019-12045-4.

Hartman, S., R. Sasidharan, and L. A. Voesenek (2021f). *The role of ethylene in metabolic acclimations to low oxygen*. DOI: 10.1111/nph.16378.

Hasanuzzaman, M., M. Bhuyan, K. Nahar, M. Hossain, J. Mahmud, et al. (2018e). "Potassium: A Vital Regulator of Plant Responses and Tolerance to Abiotic Stresses". In: *Agronomy* 8.3, p. 31. ISSN: 2073-4395. DOI: 10.3390/agronomy8030031.

Hattori, Y., K. Nagai, S. Furukawa, X.-J. Song, R. Kawano, et al. (2009e). "The ethylene response factors SNORKEL1 and SNORKEL2 allow rice to adapt to deep water". In: *Nature* 460.7258, pp. 1026–1030. ISSN: 0028-0836. DOI: 10.1038/nature08258.

Hilker, M. and T. Schmülling (2019f). "Stress priming, memory, and signalling in plants". In: *Plant, Cell & Environment* 42.3, pp. 753–761. ISSN: 0140-7791. DOI: 10.1111/pce.13526.

Holdsworth, M. J., J. Vicente, G. Sharma, M. Abbas, and A. Zubrycka (2020e). "The plant N-degron pathways of ubiquitin-mediated proteolysis". In: *Journal of Integrative Plant Biology* 62.1, pp. 70–89. ISSN: 1672-9072. DOI: 10.1111/jipb.12882.

Ingole, K. D., M. Kasera, H. A. van den Burg, and S. Bhattacharjee (2021g). "Antagonism between SUMO1/2 and SUMO3 regulates SUMO conjugate levels and fine-tunes im-

munity". In: *Journal of Experimental Botany* 72.18, pp. 6640–6658. ISSN: 0022-0957. DOI: 10.1093/jxb/erab296.

Ismond, K. P., R. Dolferus, M. De Pauw, E. S. Dennis, and A. G. Good (2003a). "Enhanced Low Oxygen Survival in Arabidopsis through Increased Metabolic Flux in the Fermentative Pathway". In: *Plant Physiology* 132.3, pp. 1292–1302. ISSN: 1532-2548. DOI: 10.1104/pp.103.022244.

Iwakawa, H., Y. Ueno, E. Semiarti, H. Onouchi, S. Kojima, et al. (2002a). "The ASYMMETRIC LEAVES2 Gene of Arabidopsis thaliana, Required for Formation of a Symmetric Flat Leaf Lamina, Encodes a Member of a Novel Family of Proteins Characterized by Cysteine Repeats and a Leucine Zipper". In: *Plant and Cell Physiology* 43.5, pp. 467–478. ISSN: 1471-9053. DOI: 10.1093/pcp/pcf077.

Jabłońska, J. and D. S. Tawfik (2019g). "The number and type of oxygen-utilizing enzymes indicates aerobic vs. anaerobic phenotype". In: *Free Radical Biology and Medicine* 140, pp. 84–92. ISSN: 08915849. DOI: 10.1016/j.freeradbiomed.2019.03.031.

Jackson, M. B. (1985). "Ethylene and Responses of Plants to Soil Waterlogging and Submergence". In: *Annual Review of Plant Physiology* 36.1, pp. 145–174. ISSN: 0066-4294. DOI: 10.1146/annurev.pp.36.060185.001045.

Jain, P. (1993). "Greenhouse effect and climate change: scientific basis and overview". In: *Renewable Energy* 3.4-5, pp. 403–420. ISSN: 09601481. DOI: 10.1016/0960-1481(93)90108-S.

James, R. A., C. Blake, C. S. Byrt, and R. Munns (2011c). "Major genes for Na+ exclusion, Nax1 and Nax2 (wheat HKT1;4 and HKT1;5), decrease Na+ accumulation in bread wheat leaves under saline and waterlogged conditions". In: *Journal of Experimental Botany* 62.8, pp. 2939–2947. ISSN: 0022-0957. DOI: 10.1093/jxb/err003.

Jardine, K. J. and N. McDowell (2023d). "Fermentation-mediated growth, signaling, and defense in plants". In: *New Phytologist* 239.3, pp. 839–851. ISSN: 0028-646X. DOI: 10.1111/nph.19015.

Jethva, J., R. R. Schmidt, M. Sauter, and J. Selinski (2022i). “Try or Die: Dynamics of Plant Respiration and How to Survive Low Oxygen Conditions”. In: *Plants* 11.2, p. 205. ISSN: 2223-7747. DOI: 10.3390/plants11020205.

Jia, W., M. Ma, J. Chen, and S. Wu (2021h). “Plant Morphological, Physiological and Anatomical Adaption to Flooding Stress and the Underlying Molecular Mechanisms”. In: *International Journal of Molecular Sciences* 22.3, p. 1088. ISSN: 1422-0067. DOI: 10.3390/ijms22031088.

Johnson, J. R., B. G. Cobb, and M. C. Drew (1994). “Hypoxic Induction of Anoxia Tolerance in Roots of Adh1 Null Zea mays L”. In: *Plant Physiology* 105.1, pp. 61–67. ISSN: 0032-0889. DOI: 10.1104/pp.105.1.61.

Jonker, H. R. A., R. W. Wechselberger, R. Boelens, G. E. Folkers, and R. Kaptein (2005a). “Structural Properties of the Promiscuous VP16 Activation Domain”. In: *Biochemistry* 44.3, pp. 827–839. ISSN: 0006-2960. DOI: 10.1021/bi0482912.

Kagale, S. and K. Rozwadowski (2011d). “EAR motif-mediated transcriptional repression in plants”. In: *Epigenetics* 6.2, pp. 141–146. ISSN: 1559-2294. DOI: 10.4161/epi.6.2.13627.

Kambona, C. M., P. A. Koua, J. Leon, and A. Ballvora (2023e). “Stress memory and its regulation in plants experiencing recurrent drought conditions”. In: *Theoretical and Applied Genetics* 136.2, p. 26. ISSN: 0040-5752. DOI: 10.1007/s00122-023-04313-1.

Kaneda, T., C. Greenbaum, and C. Haub (2022j). *How Many People Have Ever Lived on Earth?* URL: https://www.prb.org/articles/how-many-people-have-ever-lived-on-earth/.

Karimi, M., D. Inzé, and A. Depicker (2002b). “GATEWAY™ vectors for Agrobacterium-mediated plant transformation”. In: *Trends in Plant Science* 7.5, pp. 193–195. ISSN: 13601385. DOI: 10.1016/S1360-1385(02)02251-3.

Kaufman, D. P., P. F. Kandle, I. V. Murray, and A. S. Dhamoon (2023f). *Physiology, Oxyhemoglobin Dissociation Curve.*

Kaur, S., A. Joshi, K. Gupta, A. Kumar, V. Kumar, et al. (2023g). “Trace Elements and Their Role in Abiotic Stresses”. In: *Biology and Biotechnology of Environmental Stress*

Tolerance in Plants. New York: Apple Academic Press, pp. 67–146. DOI: 10.1201/9781003346203-3.

Kazan, K. and R. Lyons (2016f). "The link between flowering time and stress tolerance". In: *Journal of Experimental Botany* 67.1, pp. 47–60. ISSN: 0022-0957. DOI: 10.1093/jxb/erv441.

Kerfeld, C. A. and K. M. Scott (2011e). "Using BLAST to Teach "E-value-tionary" Concepts". In: *PLoS Biology* 9.2, e1001014. ISSN: 1545-7885. DOI: 10.1371/journal.pbio.1001014.

Kesawat, M. S., N. Satheesh, B. S. Kherawat, A. Kumar, H.-U. Kim, et al. (2023h). "Regulation of Reactive Oxygen Species during Salt Stress in Plants and Their Crosstalk with Other Signaling Molecules—Current Perspectives and Future Directions". In: *Plants* 12.4, p. 864. ISSN: 2223-7747. DOI: 10.3390/plants12040864.

Kim, J. (2003). "Functional Characterization of Phytochrome Interacting Factor 3 in Phytochrome-Mediated Light Signal Transduction". In: *THE PLANT CELL ONLINE* 15.10, pp. 2399–2407. ISSN: 1040-4651. DOI: 10.1105/tpc.014498.

Kim, W., S. Ć. Zeljković, U. Piskurewicz, C. Megies, P. Tarkowski, and L. Lopez-Molina (2019h). "polyamine uptake transporter 2 (put2) and decaying seeds enhance phyA-mediated germination by overcoming PIF1 repression of germination". In: *PLOS Genetics* 15.7, e1008292. ISSN: 1553-7404. DOI: 10.1371/journal.pgen.1008292.

Kittiwongwattana, C. (2019). "Differential effects of synthetic media on long-term growth, starch accumulation and transcription of ADP-glucosepyrophosphorylase subunit genes in Landoltia punctata". In: *Scientific Reports* 9.1, p. 15310. ISSN: 2045-2322. DOI: 10.1038/s41598-019-51677-w.

Klepikova, A. V., A. S. Kasianov, E. S. Gerasimov, M. D. Logacheva, and A. A. Penin (2016g). "A high resolution map of the Arabidopsis thaliana developmental transcriptome based on RNA-seq profiling". In: *The Plant Journal* 88.6, pp. 1058–1070. ISSN: 0960-7412. DOI: 10.1111/tpj.13312.

Klok, E. J., I. W. Wilson, D. Wilson, S. C. Chapman, R. M. Ewing, et al. (2002c). "Expression Profile Analysis of the Low-Oxygen Response in Arabidopsis Root Cultures". In: *The Plant Cell* 14.10, pp. 2481–2494. ISSN: 1532-298X. DOI: 10.1105/tpc.004747.

Kohli, S. K., K. Khanna, R. Bhardwaj, E. F. Abd_Allah, P. Ahmad, and F. J. Corpas (2019i). "Assessment of Subcellular ROS and NO Metabolism in Higher Plants: Multifunctional Signaling Molecules". In: *Antioxidants* 8.12, p. 641. ISSN: 2076-3921. DOI: 10.3390/antiox8120641.

Koncz, C., F. Kreuzaler, Z. Kalman, and J. Schell (1984a). "A simple method to transfer, integrate and study expression of foreign genes, such as chicken ovalbumin and alpha-actin in plant tumors." In: *The EMBO Journal* 3.5, pp. 1029–1037. ISSN: 02614189. DOI: 10.1002/j.1460-2075.1984.tb01923.x.

Kosmacz, M., S. Parlanti, M. Schwarzländer, F. Kragler, F. Licausi, and J. T. Van Dongen (2015c). "The stability and nuclear localization of the transcription factor RAP 2.12 are dynamically regulated by oxygen concentration". In: *Plant, Cell & Environment* 38.6, pp. 1094–1103. ISSN: 0140-7791. DOI: 10.1111/pce.12493.

Kuhlmann, M., K. Horvay, A. Strathmann, T. Heinekamp, U. Fischer, et al. (2003b). "The α-Helical D1 Domain of the Tobacco bZIP Transcription Factor BZI-1 Interacts with the Ankyrin-repeat Protein ANK1 and Is Important for BZI-1 Function, Both in Auxin Signaling and Pathogen Response". In: *Journal of Biological Chemistry* 278.10, pp. 8786–8794. ISSN: 00219258. DOI: 10.1074/jbc.M210292200.

Kump, L. R. (2008). "The rise of atmospheric oxygen". In: *Nature* 451.7176, pp. 277–278. ISSN: 0028-0836. DOI: 10.1038/nature06587.

Kurotani, K.-i., H. Hirakawa, K. Shirasawa, Y. Tanizawa, Y. Nakamura, et al. (2023i). "Genome Sequence and Analysis of Nicotiana benthamiana, the Model Plant for Interactions between Organisms". In: *Plant and Cell Physiology* 64.2, pp. 248–257. ISSN: 0032-0781. DOI: 10.1093/pcp/pcac168.

Kusano, T., K. Yamaguchi, T. Berberich, and Y. Takahashi (2007a). "The Polyamine Spermine Rescues Arabidopsis from Salinity and Drought Stresses". In: *Plant Signaling & Behavior* 2.4, pp. 251–252. ISSN: 1559-2324. DOI: 10.4161/psb.2.4.3866.

Kutty, M. (1987). “Chemical Features of Water”. In: *Site Selection for Aquaculture, United Nations Development Programme*.

Lambers, H. and M. Ribas-Carbo, eds. (2005b). *Plant Respiration*. Vol. 18. Berlin/Heidelberg: Springer-Verlag. ISBN: 1-4020-3588-8. DOI: 10.1007/1-4020-3589-6.

Large, R. R., R. M. Hazen, S. M. Morrison, D. D. Gregory, J. A. Steadman, and I. Mukherjee (2022k). “Evidence that the GOE was a prolonged event with a peak around 1900 Ma”. In: *Geosystems and Geoenvironment* 1.2, p. 100036. ISSN: 27728838. DOI: 10.1016/j.geogeo.2022.100036.

Láruson, Á. J., S. Yeaman, and K. E. Lotterhos (2020f). “The Importance of Genetic Redundancy in Evolution”. In: *Trends in Ecology & Evolution* 35.9, pp. 809–822. ISSN: 01695347. DOI: 10.1016/j.tree.2020.04.009.

Le Gac, A. L. and T. Laux (2019j). “Hypoxia Is a Developmental Regulator in Plant Meristems”. In: *Molecular Plant* 12.11, pp. 1422–1424. ISSN: 17529867. DOI: 10.1016/j.molp.2019.10.004.

Lee, H. G., A. A. Lemmon, and C. D. Lima (2023j). “SUMO enhances unfolding of SUMO–polyubiquitin-modified substrates by the Ufd1/Npl4/Cdc48 complex”. In: *Proceedings of the National Academy of Sciences* 120.1. ISSN: 0027-8424. DOI: 10.1073/pnas.2213703120.

Lee, S. C., A. Mustroph, R. Sasidharan, D. Vashisht, O. Pedersen, et al. (2011f). “Molecular characterization of the submergence response of the Arabidopsis thaliana ecotype Columbia”. In: *New Phytologist* 190.2, pp. 457–471. ISSN: 0028-646X. DOI: 10.1111/j.1469-8137.2010.03590.x.

Lee, S.-Y., E. Y. Hwang, H.-Y. Seok, V. N. Tarte, M. S. Jeong, et al. (2015d). “Arabidopsis AtERF71 HRE2 functions as transcriptional activator via cis-acting GCC box or DRE/CRT element and is involved in root development through regulation of root cell expansion”. In: *Plant Cell Reports* 34.2, pp. 223–231. ISSN: 0721-7714. DOI: 10.1007/s00299-014-1701-9.

Lee, T. A. and J. Bailey-Serres (2021i). "Conserved and nuanced hierarchy of gene regulatory response to hypoxia". In: *New Phytologist* 229.1, pp. 71–78. ISSN: 0028-646X. DOI: 10.1111/nph.16437.

Lee, W. J., C. Y. Jeong, J. Kwon, V. Van Kien, D. Lee, et al. (2016h). "Drastic anthocyanin increase in response to PAP1 overexpression in fls1 knockout mutant confers enhanced osmotic stress tolerance in Arabidopsis thaliana". In: *Plant Cell Reports* 35.11, pp. 2369–2379. ISSN: 0721-7714. DOI: 10.1007/s00299-016-2040-9.

Lehmann, J., M. E. Jørgensen, S. Fratz, H. M. Müller, J. Kusch, et al. (2021j). "Acidosis-induced activation of anion channel SLAH3 in the flooding-related stress response of Arabidopsis". In: *Current Biology* 31.16, pp. 3575–3585. ISSN: 18790445. DOI: 10.1016/j.cub.2021.06.018.

León, J., M. C. Castillo, and B. Gayubas (2021k). *The hypoxia-reoxygenation stress in plants*. DOI: 10.1093/jxb/eraa591.

Licausi, F., B. Giuntoli, and P. Perata (2020g). "Similar and Yet Different: Oxygen Sensing in Animals and Plants". In: *Trends in Plant Science* 25.1, pp. 6–9. ISSN: 13601385. DOI: 10.1016/j.tplants.2019.10.013.

Licausi, F., J. T. Van Dongen, B. Giuntoli, G. Novi, A. Santaniello, et al. (2010c). "HRE1 and HRE2, two hypoxia-inducible ethylene response factors, affect anaerobic responses in Arabidopsis thaliana". In: *Plant Journal* 62.2, pp. 302–315. ISSN: 09607412. DOI: 10.1111/j.1365-313X.2010.04149.x.

Licausi, F., D. A. Weits, B. D. Pant, W. R. Scheible, P. Geigenberger, and J. T. van Dongen (2011g). "Hypoxia responsive gene expression is mediated by various subsets of transcription factors and miRNAs that are determined by the actual oxygen availability". In: *New Phytologist* 190.2, pp. 442–456. ISSN: 0028646X. DOI: 10.1111/j.1469-8137.2010.03451.x.

Linkosalo, T. and M. J. Lechowicz (2006a). "Twilight far-red treatment advances leaf bud burst of silver birch (Betula pendula)". In: *Tree Physiology* 26.10, pp. 1249–1256. ISSN: 0829-318X. DOI: 10.1093/treephys/26.10.1249.

Liu, B., C. Feng, X. Fang, Z. Ma, C. Xiao, et al. (2023k). "The anion channel SLAH3 interacts with potassium channels to regulate nitrogen–potassium homeostasis and the membrane potential in Arabidopsis". In: *The Plant Cell* 35.4, pp. 1259–1280. ISSN: 1040-4651. DOI: 10.1093/plcell/koad014.

Liu, Y., M. Zhang, Z. Meng, B. Wang, and M. Chen (2020h). "Research Progress on the Roles of Cytokinin in Plant Response to Stress". In: *International Journal of Molecular Sciences* 21.18, p. 6574. ISSN: 1422-0067. DOI: 10.3390/ijms21186574.

Livak, K. J. and T. D. Schmittgen (2001). "Analysis of Relative Gene Expression Data Using Real-Time Quantitative PCR and the 2ΔΔCT Method". In: *Methods* 25.4, pp. 402–408. ISSN: 10462023. DOI: 10.1006/meth.2001.1262.

Loreti, E. and P. Perata (2020i). "The Many Facets of Hypoxia in Plants". In: *Plants* 9.6, p. 745. ISSN: 22237747. DOI: 10.3390/plants9060745.

Lynas, M., B. Z. Houlton, and S. Perry (2021l). "Greater than 99% consensus on human caused climate change in the peer-reviewed scientific literature". In: *Environmental Research Letters* 16.11, p. 114005. ISSN: 1748-9326. DOI: 10.1088/1748-9326/ac2966.

MacKay, R. M. and M. A. K. Khalil (2000). "Greenhouse Gases and Global Warming". In: *Trace Gas Emissions and Plants*. Dordrecht: Springer Netherlands, pp. 1–28. DOI: 10.1007/978-94-017-3571-1{_}1.

Mahmoodzadeh, D. and M. Karamouz (2019k). "Seawater intrusion in heterogeneous coastal aquifers under flooding events". In: *Journal of Hydrology* 568, pp. 1118–1130. ISSN: 00221694. DOI: 10.1016/j.jhydrol.2018.11.012.

Majer, C. and F. Hochholdinger (2011h). "Defining the boundaries: structure and function of LOB domain proteins". In: *Trends in Plant Science* 16.1, pp. 47–52. ISSN: 13601385. DOI: 10.1016/j.tplants.2010.09.009.

Manbir, P. Singh, A. Kumari, and K. J. Gupta (2022l). "Alternative oxidase plays a role in minimizing ROS and RNS produced under salinity stress in Arabidopsis thaliana". In: *Physiologia Plantarum* 174.2. ISSN: 0031-9317. DOI: 10.1111/ppl.13649.

Mansoor, S., O. Ali Wani, J. K. Lone, S. Manhas, N. Kour, et al. (2022m). “Reactive Oxygen Species in Plants: From Source to Sink”. In: *Antioxidants* 11.2, p. 225. ISSN: 2076-3921. DOI: 10.3390/antiox11020225.

Maranguit, D., T. Guillaume, and Y. Kuzyakov (2017c). “Effects of flooding on phosphorus and iron mobilization in highly weathered soils under different land-use types: Short-term effects and mechanisms”. In: *CATENA* 158, pp. 161–170. ISSN: 03418162. DOI: 10.1016/j.catena.2017.06.023.

Margelevicius, M. and C. Venclovas (2010d). “Detection of distant evolutionary relationships between protein families using theory of sequence profile-profile comparison”. In: *BMC Bioinformatics* 11.1, p. 89. ISSN: 1471-2105. DOI: 10.1186/1471-2105-11-89.

Masson, N., T. P. Keeley, B. Giuntoli, M. D. White, M. L. Puerta, et al. (2019l). “Conserved N-terminal cysteine dioxygenases transduce responses to hypoxia in animals and plants”. In: *Science* 365.6448, pp. 65–69. ISSN: 0036-8075. DOI: 10.1126/science.aaw0112.

Miao, Y., X. Gao, B. Li, W. Wang, and L. Bai (2023l). “Low red to far-red light ratio promotes salt tolerance by improving leaf photosynthetic capacity in cucumber”. In: *Frontiers in Plant Science* 13. ISSN: 1664-462X. DOI: 10.3389/fpls.2022.1053780.

Mills, B. J., A. J. Krause, I. Jarvis, and B. D. Cramer (2023m). “Evolution of Atmospheric O2 Through the Phanerozoic, Revisited”. In: *Annual Review of Earth and Planetary Sciences* 51.1, pp. 253–276. ISSN: 0084-6597. DOI: 10.1146/annurev-earth-032320-095425.

Mimura, N. (2013). “Sea level rise caused by climate change and its implications for society”. In: *Proceedings of the Japan Academy, Series B* 89.7, pp. 281–301. ISSN: 0386-2208. DOI: 10.2183/pjab.89.281.

Mitchell, M. J., O. E. Jensen, K. A. Cliffe, and M. M. Maroto-Valer (2010e). “A model of carbon dioxide dissolution and mineral carbonation kinetics”. In: *Proceedings of the Royal Society A: Mathematical, Physical and Engineering Sciences* 466.2117, pp. 1265–1290. ISSN: 1364-5021. DOI: 10.1098/rspa.2009.0349.

Miteva, M., K. Keusekotten, K. Hofmann, G. J. K. Praefcke, and R. J. Dohmen (2010f). “Sumoylation as a Signal for Polyubiquitylation and Proteasomal Degradation”. In: pp. 195–214. DOI: 10.1007/978-1-4419-6676-6{_}16.

Moatabarniya, S., A. Chehregani Rad, N. A. Khoshkholgh Sima, H. Askari, M. Zeinalabedini, et al. (2022n). "Morphological and anatomical changes of Salicornia roots are associated with different salinity and nutrients conditions in contrasting genotypes". In: *Rhizosphere* 24, p. 100629. ISSN: 24522198. DOI: 10.1016/j.rhisph.2022.100629.

Molotoks, A., E. Stehfest, J. Doelman, F. Albanito, N. Fitton, et al. (2018f). "Global projections of future cropland expansion to 2050 and direct impacts on biodiversity and carbon storage". In: *Global Change Biology* 24.12, pp. 5895–5908. ISSN: 1354-1013. DOI: 10.1111/gcb.14459.

Mommer, L., H. De Kroon, R. Pierik, G. M. Bögemann, and E. J. W. Visser (2005c). "A functional comparison of acclimation to shade and submergence in two terrestrial plant species". In: *New Phytologist* 167.1, pp. 197–206. ISSN: 0028-646X. DOI: 10.1111/j.1469-8137.2005.01404.x.

Müller, J. T. (2020). "Molekulare und physiologische Charakterisierung der Ueberlebensstrategien von Wildpflanzen der Brassicaceae bei Überflutung ". PhD thesis. Bayreuth: University Bayreuth.

Müller, J. T., H. van Veen, M. M. Bartylla, M. Akman, O. Pedersen, et al. (2021m). "Keeping the shoot above water – submergence triggers antithetical growth responses in stems and petioles of watercress (Nasturtium officinale)". In: *New Phytologist* 229.1, pp. 140–155. ISSN: 0028-646X. DOI: 10.1111/nph.16350.

Mustroph, A., G. A. Barding JR, K. A. Kaiser, C. K. Larive, and J. Bailey-Serres (2014d). "Characterization of distinct root and shoot responses to low-oxygen stress in Arabidopsis with a focus on primary C- and N -metabolism". In: *Plant, Cell & Environment* 37.10, pp. 2366–2380. ISSN: 0140-7791. DOI: 10.1111/pce.12282.

Mustroph, A., S. C. Lee, T. Oosumi, M. E. Zanetti, H. Yang, et al. (2010g). "Cross-Kingdom Comparison of Transcriptomic Adjustments to Low-Oxygen Stress Highlights Conserved and Plant-Specific Responses". In: *Plant Physiology* 152.3, pp. 1484–1500. ISSN: 1532-2548. DOI: 10.1104/pp.109.151845.

Mustroph, A., M. E. Zanetti, C. J. H. Jang, H. E. Holtan, P. P. Repetti, et al. (2009f). "Profiling translatomes of discrete cell populations resolves altered cellular priorities during

hypoxia in Arabidopsis". In: *Proceedings of the National Academy of Sciences* 106.44, pp. 18843–18848. ISSN: 0027-8424. DOI: 10.1073/pnas.0906131106.

Nakamura, M. and K. Noguchi (2020j). "Tolerant mechanisms to O2 deficiency under submergence conditions in plants". In: *Journal of Plant Research* 133.3, pp. 343–371. ISSN: 0918-9440. DOI: 10.1007/s10265-020-01176-1.

Narsai, R., Q. Gouil, D. Secco, A. Srivastava, Y. V. Karpievitch, et al. (2017d). "Extensive transcriptomic and epigenomic remodelling occurs during Arabidopsis thaliana germination". In: *Genome Biology* 18.1, p. 172. ISSN: 1474-760X. DOI: 10.1186/s13059-017-1302-3.

Narsai, R., S. R. Law, C. Carrie, L. Xu, and J. Whelan (2011i). "In-Depth Temporal Transcriptome Profiling Reveals a Crucial Developmental Switch with Roles for RNA Processing and Organelle Metabolism That Are Essential for Germination in Arabidopsis ". In: *Plant Physiology* 157.3, pp. 1342–1362. ISSN: 1532-2548. DOI: 10.1104/pp.111.183129.

Noctor, G. and C. H. Foyer (2016i). "Intracellular Redox Compartmentation and ROS-Related Communication in Regulation and Signaling". In: *Plant Physiology* 171.3, pp. 1581–1592. ISSN: 0032-0889. DOI: 10.1104/pp.16.00346.

Nones, M. (2019). "Dealing with sediment transport in flood risk management". In: *Acta Geophysica* 67.2, pp. 677–685. ISSN: 1895-6572. DOI: 10.1007/s11600-019-00273-7.

Norkunas, K., R. Harding, J. Dale, and B. Dugdale (2018g). "Improving agroinfiltration-based transient gene expression in Nicotiana benthamiana". In: *Plant Methods* 14.1, p. 71. ISSN: 1746-4811. DOI: 10.1186/s13007-018-0343-2.

Nowak, M. A., M. C. Boerlijst, J. Cooke, and J. M. Smith (1997b). "Evolution of genetic redundancy". In: *Nature* 388.6638, pp. 167–171. ISSN: 0028-0836. DOI: 10.1038/40618.

O'Neill, S. D. and R. M. Spanswick (1984b). "Characterization of native and reconstituted plasma membrane H+-ATPase from the plasma membrane ofBeta vulgaris". In: *The Journal of Membrane Biology* 79.3, pp. 245–256. ISSN: 0022-2631. DOI: 10.1007/BF01871063.

O'Sullivan, J. N. (2023). "Demographic Delusions: World Population Growth Is Exceeding Most Projections and Jeopardising Scenarios for Sustainable Futures". In: *World* 4.3, pp. 545–568. ISSN: 2673-4060. DOI: 10.3390/world4030034.

Oberkofler, V., L. Pratx, and I. Bäurle (2021n). "Epigenetic regulation of abiotic stress memory: maintaining the good things while they last". In: *Current Opinion in Plant Biology* 61, p. 102007. ISSN: 13695266. DOI: 10.1016/j.pbi.2021.102007.

Oh, G. G. K., B. M. O'Leary, S. Signorelli, and A. H. Millar (2022o). "Alternative oxidase (AOX) 1a and 1d limit proline-induced oxidative stress and aid salinity recovery in Arabidopsis". In: *Plant Physiology* 188.3, pp. 1521–1536. ISSN: 0032-0889. DOI: 10.1093/plphys/kiab578.

Oras, E., M. Tõrv, K. Johanson, E. Rannamäe, A. Poska, et al. (2023n). "Parallel worlds and mixed economies: multi-proxy analysis reveals complex subsistence systems at the dawn of early farming in the northeast Baltic". In: *Royal Society Open Science* 10.10. ISSN: 2054-5703. DOI: 10.1098/rsos.230880.

Osnato, M. (2022). "The floral transition and adaptation to a changing environment: From model species to cereal crops". In: *The Plant Cell* 34.11, e2.

Pan, J., R. Sharif, X. Xu, and X. Chen (2021o). "Mechanisms of Waterlogging Tolerance in Plants: Research Progress and Prospects". In: *Frontiers in Plant Science* 11. ISSN: 1664-462X. DOI: 10.3389/fpls.2020.627331.

Panchuck, K. (2021). *Physical Geology*. Ed. by S. Earle, J. McBeth, and T. Prokopiuk. H5P Edition. Vol. 7. Victoria: BCcampus, pp. 653–657. ISBN: 978-1-77420-205-0. URL: ttps://opentextbc.ca/physicalgeologyh5p/.

Pandey, S. K. and J. Kim (2018h). "Coiled-coil motif in LBD16 and LBD18 transcription factors are critical for dimerization and biological function in arabidopsis". In: *Plant Signaling & Behavior* 13.1, e1411450. ISSN: 1559-2324. DOI: 10.1080/15592324.2017.1411450.

Park, H. J., W.-Y. Kim, H. C. Park, S. Y. Lee, H. J. Bohnert, and D.-J. Yun (2011j). "SUMO and SUMOylation in plants". In: *Molecules and Cells* 32.4, pp. 305–316. ISSN: 1016-8478. DOI: 10.1007/s10059-011-0122-7.

Pattyn, J., J. Vaughan-Hirsch, and B. Van de Poel (2021p). "The regulation of ethylene biosynthesis: a complex multilevel control circuitry". In: *New Phytologist* 229.2, pp. 770–782. ISSN: 0028-646X. DOI: 10.1111/nph.16873.

Pedersen, O., T. D. Colmer, E. Garcia-Robledo, and N. P. Revsbech (2018i). "CO2 and O2 dynamics in leaves of aquatic plants with C3 or CAM photosynthesis – application of a novel CO2 microsensor". In: *Annals of Botany* 122.4, pp. 605–615. ISSN: 0305-7364. DOI: 10.1093/aob/mcy095.

Péter, C., F. Nagy, and A. Viczián (2021q). "SUMOylation of different targets fine-tunes phytochrome signaling". In: *New Phytologist* 232.3, pp. 1201–1211. ISSN: 0028-646X. DOI: 10.1111/nph.17634.

Petre, B., D. G. O. Saunders, J. Sklenar, C. Lorrain, K. V. Krasileva, et al. (2016j). "Heterologous Expression Screens in Nicotiana benthamiana Identify a Candidate Effector of the Wheat Yellow Rust Pathogen that Associates with Processing Bodies". In: *PLOS ONE* 11.2, e0149035. ISSN: 1932-6203. DOI: 10.1371/journal.pone.0149035.

Phukan, U. J., G. S. Jeena, V. Tripathi, and R. K. Shukla (2017e). "Regulation of Apetala2/Ethylene Response Factors in Plants". In: *Frontiers in Plant Science* 8. ISSN: 1664-462X. DOI: 10.3389/fpls.2017.00150.

Plant, A. R., A. Larrieu, and B. Causier (2021r). "Repressor for hire! The vital roles of TOPLESS-mediated transcriptional repression in plants". In: *New Phytologist* 231.3, pp. 963–973. ISSN: 0028-646X. DOI: 10.1111/nph.17428.

Pombo, M. A., R. N. Ramos, Y. Zheng, Z. Fei, G. B. Martin, and H. G. Rosli (2019m). "Transcriptome-based identification and validation of reference genes for plant-bacteria interaction studies using Nicotiana benthamiana". In: *Scientific Reports* 9.1, p. 1632. ISSN: 2045-2322. DOI: 10.1038/s41598-018-38247-2.

Pope, R. M. and E. S. Fry (1997c). "Absorption spectrum (380–700 nm) of pure water II Integrating cavity measurements". In: *Applied Optics* 36.33, p. 8710. ISSN: 0003-6935. DOI: 10.1364/AO.36.008710.

Pucciariello, C. and P. Perata (2021s). "The Oxidative Paradox in Low Oxygen Stress in Plants". In: *Antioxidants* 10.2, p. 332. ISSN: 2076-3921. DOI: 10.3390/antiox10020332.

Qiu, X., G. Sun, F. Liu, and W. Hu (2023o). "Functions of Plant Phytochrome Signaling Pathways in Adaptation to Diverse Stresses". In: *International Journal of Molecular Sciences* 24.17, p. 13201. ISSN: 1422-0067. DOI: 10.3390/ijms241713201.

Ramakrishnan, M., Z. Zhang, S. Mullasseri, R. Kalendar, Z. Ahmad, et al. (2022p). "Epigenetic stress memory: A new approach to study cold and heat stress responses in plants". In: *Frontiers in Plant Science* 13. ISSN: 1664-462X. DOI: 10.3389/fpls.2022.1075279.

Ranganathan, J., R. Waite, T. Searchinger, and C. Hanson (2018j). *How to Sustainably Feed 10 Billion People by 2050, in 21 Charts*. Tech. rep. World Resources Insitute.

Ratcliffe, P. J., J. F. O'rourke, P. H. Maxwell, and C. W. Pugh (1998a). "Oxygen Sensing, Hypoxia-Inducible Factor-1 and the Regulation of Mammalian Gene Expression". In: *Journal of Experimental Biology* 201.8, pp. 1153–1162. ISSN: 0022-0949. DOI: 10.1242/jeb.201.8.1153.

Rawat, R., F. J. Sandoval, Z. Wei, R. Winkler, and S. Roje (2011k). "An FMN Hydrolase of the Haloacid Dehalogenase Superfamily Is Active in Plant Chloroplasts". In: *Journal of Biological Chemistry* 286.49, pp. 42091–42098. ISSN: 00219258. DOI: 10.1074/jbc.M111.260885.

Rees, T. ap (1985). "The Organization of Glycolysis and the Oxidative Pentose Phosphate Pathway in Plants". In: *Higher Plant Cell Respiration*. Berlin, Heidelberg: Springer Berlin Heidelberg, pp. 391–417. DOI: 10.1007/978-3-642-70101-6{_}14.

Renziehausen, T., S. Frings, and R. Schmidt-Schippers (2024). "'Against all floods': plant adaptation to flooding stress and combined abiotic stresses". In: *The Plant Journal* 117.6, pp. 1836–1855. ISSN: 0960-7412. DOI: 10.1111/tpj.16614.

Rivero L., Scholl R., Holomuzki N., Crist D., Grotewold E., and Brkljacic J. (2014e). "Handling Arabidopsis Plants: Growth, Preservation of Seeds, Transformation, and Genetic Crosses." In: *Arabidopsis Protocols. Methods in Molecular Biology (Methods and Protocols)* 1062.

Romero, E., J. R. Gómez Castellanos, G. Gadda, M. W. Fraaije, and A. Mattevi (2018k). "Same Substrate, Many Reactions: Oxygen Activation in Flavoenzymes". In: *Chemical Reviews* 118.4, pp. 1742–1769. ISSN: 0009-2665. DOI: 10.1021/acs.chemrev.7b00650.

Rosa-Téllez, S., A. D. Anoman, A. Alcántara-Enguídanos, R. A. Garza-Aguirre, S. Alseekh, and R. Ros (2020k). "PGDH family genes differentially affect Arabidopsis tolerance to salt stress". In: *Plant Science* 290, p. 110284. ISSN: 01689452. DOI: 10.1016/j.plantsci.2019.110284.

Rouached, H., A. B. Arpat, and Y. Poirier (2010h). "Regulation of Phosphate Starvation Responses in Plants: Signaling Players and Cross-Talks". In: *Molecular Plant* 3.2, pp. 288–299. ISSN: 16742052. DOI: 10.1093/mp/ssp120.

Rubin, G., T. Tohge, F. Matsuda, K. Saito, and W.-R. Scheible (2009g). "Members of the LBD Family of Transcription Factors Repress Anthocyanin Synthesis and Affect Additional Nitrogen Responses in Arabidopsis". In: *The Plant Cell* 21.11, pp. 3567–3584. ISSN: 1532-298X. DOI: 10.1105/tpc.109.067041.

Ruiz Carrasco, K. B., R. Baroni Fornasiero, A. Tassoni, and N. Bagni (2007b). "Identification of two phenotypes of Arabidopsis thaliana under in vitro salt stress conditions". In: *Biologia plantarum* 51.3, pp. 436–442. ISSN: 00063134. DOI: 10.1007/s10535-007-0093-x.

Růžička, K., K. Ljung, S. Vanneste, R. Podhorská, T. Beeckman, et al. (2007c). "Ethylene Regulates Root Growth through Effects on Auxin Biosynthesis and Transport-Dependent Auxin Distribution". In: *The Plant Cell* 19.7, pp. 2197–2212. ISSN: 1532-298X. DOI: 10.1105/tpc.107.052126.

Rytz, T. C., J. Feng, J. A. S. Barros, and R. D. Vierstra (2023p). "Arabidopsis -expressing lysine-null SUMO1 reveals a non-essential role for secondary SUMO modifications in plants". In: *Plant Direct* 7.7. ISSN: 2475-4455. DOI: 10.1002/pld3.506.

Sadanandom, A., É. Ádám, B. Orosa, A. Viczián, C. Klose, et al. (2015e). "SUMOylation of phytochrome-B negatively regulates light-induced signaling in Arabidopsis thaliana". In: *Proceedings of the National Academy of Sciences* 112.35, pp. 11108–11113. ISSN: 0027-8424. DOI: 10.1073/pnas.1415260112.

Sadigov, R. (2022). "Rapid Growth of the World Population and Its Socioeconomic Results". In: *The Scientific World Journal* 2022, pp. 1–8. ISSN: 1537-744X. DOI: 10.1155/2022/8110229.

Saha, J., E. K. Brauer, A. Sengupta, S. C. Popescu, K. Gupta, and B. Gupta (2015f). "Polyamines as redox homeostasis regulators during salt stress in plants". In: *Frontiers in Environmental Science* 3. ISSN: 2296-665X. DOI: 10.3389/fenvs.2015.00021.

Santer, B. D., C. Mears, F. J. Wentz, K. E. Taylor, P. J. Gleckler, et al. (2007d). "Identification of human-induced changes in atmospheric moisture content". In: *Proceedings of the National Academy of Sciences* 104.39, pp. 15248–15253. ISSN: 0027-8424. DOI: 10.1073/pnas.0702872104.

Sasidharan, R., J. Bailey-Serres, M. Ashikari, B. J. Atwell, T. D. Colmer, et al. (2017f). "Community recommendations on terminology and procedures used in flooding and low oxygen stress research". In: *New Phytologist* 214.4, pp. 1403–1407. ISSN: 0028-646X. DOI: 10.1111/nph.14519.

Sasidharan, R. and A. Mustroph (2011l). "Plant Oxygen Sensing Is Mediated by the N-End Rule Pathway: A Milestone in Plant Anaerobiosis". In: *The Plant Cell* 23.12, pp. 4173–4183. ISSN: 1040-4651. DOI: 10.1105/tpc.111.093880.

Sawyer, J. S. (1972). "Man-made Carbon Dioxide and the "Greenhouse" Effect". In: *Nature* 239.5366, pp. 23–26. ISSN: 0028-0836. DOI: 10.1038/239023a0.

Schachtschabel, P., H.-P. Blume, G. Brümmer, K. Hartge, U. Schwertmann, and M. Renger (1998b). *Lehrbuch der Bodenkunde*. 14th. Stuttgart: Enke.

Schirrmeister, B. E., M. Gugger, and P. C. J. Donoghue (2015g). "Cyanobacteria and the Great Oxidation Event: evidence from genes and fossils". In: *Palaeontology* 58.5, pp. 769–785. ISSN: 0031-0239. DOI: 10.1111/pala.12178.

Schofield, C. J. and P. J. Ratcliffe (2004b). "Oxygen sensing by HIF hydroxylases". In: *Nature Reviews Molecular Cell Biology* 5.5, pp. 343–354. ISSN: 1471-0072. DOI: 10.1038/nrm1366.

Seok, H.-Y., V. N. Tarte, S.-Y. Lee, H.-Y. Park, and Y.-H. Moon (2014f). "Arabidopsis HRE1α, a splicing variant of AtERF73 HRE1, functions as a nuclear transcription activator in hypoxia response and root development". In: *Plant Cell Reports* 33.8, pp. 1255–1262. ISSN: 0721-7714. DOI: 10.1007/s00299-014-1613-8.

Seok, H.-Y., H. T. Tran, S.-Y. Lee, and Y.-H. Moon (2022q). "AtERF71 HRE2, an Arabidopsis AP2 ERF Transcription Factor Gene, Contains Both Positive and Negative Cis-Regulatory Elements in Its Promoter Region Involved in Hypoxia and Salt Stress Responses". In: *International Journal of Molecular Sciences* 23.10, p. 5310. ISSN: 1422-0067. DOI: 10.3390/ijms23105310.

Shao, J., K. Huang, M. Batool, F. Idrees, R. Afzal, et al. (2022r). "Versatile roles of polyamines in improving abiotic stress tolerance of plants". In: *Frontiers in Plant Science* 13. ISSN: 1664-462X. DOI: 10.3389/fpls.2022.1003155.

Sharma, M., P. Kumar, V. Verma, R. Sharma, B. Bhargava, and M. Irfan (2022s). "Understanding plant stress memory response for abiotic stress resilience: Molecular insights and prospects". In: *Plant Physiology and Biochemistry* 179, pp. 10–24. ISSN: 09819428. DOI: 10.1016/j.plaphy.2022.03.004.

Shuai, B., C. G. Reynaga-Peña, and P. S. Springer (2002d). "The Lateral Organ Boundaries gene defines a novel, plant-specific gene family". In: *Plant Physiology* 129.2, pp. 747–761. ISSN: 00320889. DOI: 10.1104/pp.010926.

Singh, M., A. Singh, N. Yadav, and D. K. Yadav (2022t). "Current perspectives of ubiquitination and SUMOylation in abiotic stress tolerance in plants". In: *Frontiers in Plant Science* 13. ISSN: 1664-462X. DOI: 10.3389/fpls.2022.993194.

Smil, V. (1999). "Detonator of the population explosion". In: *Nature* 400.6743, pp. 415–415. ISSN: 0028-0836. DOI: 10.1038/22672.

Someya, S., S. Bando, B. Chen, Y. Song, and M. Nishio (2005d). "Measurement of CO2 solubility in pure water and the pressure effect on it in the presence of clathrate hydrate". In: *International Journal of Heat and Mass Transfer* 48.12, pp. 2503–2507. ISSN: 00179310. DOI: 10.1016/j.ijheatmasstransfer.2004.12.043.

Soyano, T., S. Thitamadee, Y. Machida, and N.-H. Chua (2009h). "ASYMMETRIC LEAVES2-LIKE19/LATERAL ORGAN BOUNDARIES DOMAIN30 and ASL20/LBD18 Regulate Tracheary Element Differentiation in Arabidopsis". In: *The Plant Cell* 20.12, pp. 3359–3373. ISSN: 1532-298X. DOI: 10.1105/tpc.108.061796.

Stemmer, M., T. Thumberger, M. del Sol Keyer, J. Wittbrodt, and J. L. Mateo (2015h). "CCTop: An Intuitive, Flexible and Reliable CRISPR/Cas9 Target Prediction Tool". In: *PLOS ONE* 10.4, e0124633. ISSN: 1932-6203. DOI: 10.1371/journal.pone.0124633.

Stephenson, A., J. W. Adams, and M. Vaccarezza (2017g). "The vertebrate heart: an evolutionary perspective". In: *Journal of Anatomy* 231.6, pp. 787–797. ISSN: 0021-8782. DOI: 10.1111/joa.12687.

Stewart, W. M., D. W. Dibb, A. E. Johnston, and T. J. Smyth (2005e). "The Contribution of Commercial Fertilizer Nutrients to Food Production". In: *Agronomy Journal* 97.1, pp. 1–6. ISSN: 0002-1962. DOI: 10.2134/agronj2005.0001.

Tabari, H. (2020). "Climate change impact on flood and extreme precipitation increases with water availability". In: *Scientific Reports* 10.1, p. 13768. ISSN: 2045-2322. DOI: 10.1038/s41598-020-70816-2.

Tadege, M., R. Brändle, and C. Kuhlemeier (1998c). "Anoxia tolerance in tobacco roots: effect of overexpression of pyruvate decarboxylase". In: *The Plant Journal* 14.3, pp. 327–335. ISSN: 0960-7412. DOI: 10.1046/j.1365-313X.1998.00130.x.

Takeno, K. (2016). "Stress-induced flowering: the third category of flowering response". In: *Journal of Experimental Botany* 67.17, pp. 4925–4934. ISSN: 0022-0957. DOI: 10.1093/jxb/erw272.

Tamura, K. and H. Bono (2022u). "Meta-Analysis of RNA Sequencing Data of Arabidopsis and Rice under Hypoxia". In: *Life* 12.7, p. 1079. ISSN: 2075-1729. DOI: 10.3390/life12071079.

Tang, H., H. Bi, B. Liu, S. Lou, Y. Song, et al. (2021t). "WRKY33 interacts with WRKY12 protein to up-regulate RAP2 . 2 during submergence induced hypoxia response in Arabidopsis thaliana". In: *New Phytologist* 229.1, pp. 106–125. ISSN: 0028-646X. DOI: 10.1111/nph.17020.

Tatham, M. H., M.-C. Geoffroy, L. Shen, A. Plechanovova, N. Hattersley, et al. (2008d). "RNF4 is a poly-SUMO-specific E3 ubiquitin ligase required for arsenic-induced PML degradation". In: *Nature Cell Biology* 10.5, pp. 538–546. ISSN: 1465-7392. DOI: 10.1038/ncb1716.

Tavassoli, M. and A. Kamran-Pirzaman (2023q). “Comparison of effective greenhouse gases and global warming”. In: *2023 8th International Conference on Technology and Energy Management (ICTEM)*. IEEE, pp. 1–5. ISBN: 978-1-6654-5285-4. DOI: 10.1109/ICTEM56862.2023.10083954.

Taylor, C. T. and S. Moncada (2010i). “Nitric Oxide, Cytochrome C Oxidase, and the Cellular Response to Hypoxia”. In: *Arteriosclerosis, Thrombosis, and Vascular Biology* 30.4, pp. 643–647. ISSN: 1079-5642. DOI: 10.1161/ATVBAHA.108.181628.

Taylor, M. and N. Krüger (2019n). “Changes in salinity of a clay soil after a short-term salt water flood event”. In: *Geoderma Regional* 19, e00239. ISSN: 23520094. DOI: 10.1016/j.geodrs.2019.e00239.

Tcherkez, G. and J. Ghashghaie, eds. (2017h). *Plant Respiration: Metabolic Fluxes and Carbon Balance*. Vol. 43. Cham: Springer International Publishing. ISBN: 978-3-319-68701-8. DOI: 10.1007/978-3-319-68703-2.

Thatcher, L. F., K. Kazan, and J. M. Manners (2012e). “Lateral organ boundaries domain transcription factors”. In: *Plant Signaling & Behavior* 7.12, pp. 1702–1704. ISSN: 1559-2324. DOI: 10.4161/psb.22097.

U.N. Department of Economic and Social Affairs Population Division (2022). *World Population Prospects 2022: Summary of Results*. Tech. rep. New York, United Nations,

Uraguchi, S., Y. Ohshiro, Y. Otsuka, H. Tsukioka, N. Yoneyama, et al. (2020l). “Selection of Agar Reagents for Medium Solidification Is a Critical Factor for Metal(loid) Sensitivity and Ionomic Profiles of Arabidopsis thaliana”. In: *Frontiers in Plant Science* 11. ISSN: 1664-462X. DOI: 10.3389/fpls.2020.00503.

Vashisht, D., A. Hesselink, R. Pierik, J. M. H. Ammerlaan, J. Bailey-Serres, et al. (2011m). “Natural variation of submergence tolerance among Arabidopsis thaliana accessions”. In: *New Phytologist* 190.2, pp. 299–310. ISSN: 0028-646X. DOI: 10.1111/j.1469-8137.2010.03552.x.

Voesenek, L. A. C. J. and J. Bailey-Serres (2015i). “Flood adaptive traits and processes: an overview”. In: *New Phytologist* 206.1, pp. 57–73. ISSN: 0028-646X. DOI: 10.1111/nph.13209.

Voinnet, O., S. Rivas, P. Mestre, and D. Baulcombe (2003c). "Retracted: An enhanced transient expression system in plants based on suppression of gene silencing by the p19 protein of tomato bushy stunt virus". In: *The Plant Journal* 33.5, pp. 949–956. ISSN: 0960-7412. DOI: 10.1046/j.1365-313X.2003.01676.x.

Wagner, A. (1996). "Genetic redundancy caused by gene duplications and its evolution in networks of transcriptional regulators". In: *Biological Cybernetics* 74.6, pp. 557–567. ISSN: 0340-1200. DOI: 10.1007/BF00209427.

Wang, Z., J. Yang, F. Cheng, P. Li, X. Xin, et al. (2022v). "Subgenome dominance and its evolutionary implications in crop domestication and breeding". In: *Horticulture Research* 9. ISSN: 2052-7276. DOI: 10.1093/hr/uhac090.

Wehner, N., L. Hartmann, A. Ehlert, S. Böttner, L. Oñate-Sánchez, and W. Dröge-Laser (2011n). "High throughput protoplast transactivation (PTA) system for the analysis of Arabidopsis transcription factor function". In: *Plant Journal* 68.3, pp. 560–569. ISSN: 09607412. DOI: 10.1111/j.1365-313X.2011.04704.x.

Weits, D. A., A. B. Kunkowska, N. C. Kamps, K. M. Portz, N. K. Packbier, et al. (2019o). "An apical hypoxic niche sets the pace of shoot meristem activity". In: *Nature* 569.7758, pp. 714–717. ISSN: 14764687. DOI: 10.1038/s41586-019-1203-6.

Winter, D., B. Vinegar, H. Nahal, R. Ammar, G. V. Wilson, and N. J. Provart (2007e). "An "Electronic Fluorescent Pictograph" Browser for Exploring and Analyzing Large-Scale Biological Data Sets". In: *PLoS ONE* 2.8, e718. ISSN: 1932-6203. DOI: 10.1371/journal.pone.0000718.

Wintz, H., T. Fox, Y.-Y. Wu, V. Feng, W. Chen, et al. (2003d). "Expression Profiles of Arabidopsis thaliana in Mineral Deficiencies Reveal Novel Transporters Involved in Metal Homeostasis". In: *Journal of Biological Chemistry* 278.48, pp. 47644–47653. ISSN: 00219258. DOI: 10.1074/jbc.M309338200.

Wozniak, B. and J. Dera (2006b). *Light Absorption in Sea Water*. Ed. by L. Mysak and K. Hamilton. Volume 33. New York, NY: Springer New York. ISBN: 978-0-387-30753-4. DOI: 10.1007/978-0-387-49560-6.

Xie, L. J., Y. Zhou, Q. F. Chen, and S. Xiao (2021u). *New insights into the role of lipids in plant hypoxia responses*. DOI: 10.1016/j.plipres.2020.101072.

Xing, H.-L., L. Dong, Z.-P. Wang, H.-Y. Zhang, C.-Y. Han, et al. (2014g). "A CRISPR/Cas9 toolkit for multiplex genome editing in plants". In: *BMC Plant Biology* 14.1, p. 327. ISSN: 1471-2229. DOI: 10.1186/s12870-014-0327-y.

Xu, C., F. Luo, and F. Hochholdinger (2016k). "LOB Domain Proteins: Beyond Lateral Organ Boundaries". In: *Trends in Plant Science* 21.2, pp. 159–167. ISSN: 13601385. DOI: 10.1016/j.tplants.2015.10.010.

Xu, K., X. Xu, T. Fukao, P. Canlas, R. Maghirang-Rodriguez, et al. (2006c). "Sub1A is an ethylene-response-factor-like gene that confers submergence tolerance to rice". In: *Nature* 442.7103, pp. 705–708. ISSN: 0028-0836. DOI: 10.1038/nature04920.

Zahnle, K., L. Schaefer, and B. Fegley (2010j). "Earth's Earliest Atmospheres". In: *Cold Spring Harbor Perspectives in Biology* 2.10, a004895–a004895. ISSN: 1943-0264. DOI: 10.1101/cshperspect.a004895.

Zandalinas, S. I. and R. Mittler (2022w). "Plant responses to multifactorial stress combination". In: *New Phytologist* 234.4, pp. 1161–1167. ISSN: 0028-646X. DOI: 10.1111/nph.18087.

Zandalinas, S. I., S. Sengupta, F. B. Fritschi, R. K. Azad, R. Nechushtai, and R. Mittler (2021v). "The impact of multifactorial stress combination on plant growth and survival". In: *New Phytologist* 230.3, pp. 1034–1048. ISSN: 0028-646X. DOI: 10.1111/nph.17232.

Zechmann, B. (2020). "Subcellular Roles of Glutathione in Mediating Plant Defense during Biotic Stress". In: *Plants* 9.9, p. 1067. ISSN: 2223-7747. DOI: 10.3390/plants9091067.

Zeder, M. A. (2011). "The Origins of Agriculture in the Near East". In: *Current Anthropology* 52.S4, S221–S235. ISSN: 0011-3204. DOI: 10.1086/659307.

Zeidler, M. (2020). "Fine Tuning by the Touch of Big Dudes: SUMOs Role in Light Signaling". In: *Molecular Plant* 13.7, pp. 943–945. ISSN: 16742052. DOI: 10.1016/j.molp.2020.06.001.

Zhang, Y., Z. Li, B. Ma, Q. Hou, and X. Wan (2020m). *Phylogeny and functions of LOB domain proteins in plants*. DOI: 10.3390/ijms21072278.

Zhao, Q., Y. Xie, Y. Zheng, S. Jiang, W. Liu, et al. (2014h). "GPS-SUMO: a tool for the prediction of sumoylation sites and SUMO-interaction motifs". In: *Nucleic Acids Research* 42.W1, W325–W330. ISSN: 1362-4962. DOI: 10.1093/nar/gku383.

Supplementary

Table 4: Oligonucleotides used

Name	Sequence
attB1_fw	GGGGACAAGTTTGTACAAAAAAGCAGGCT
attB2_rev	GGGGACCACTTTGTACAAGAAAGCTGGGT
sgGGT4_fw	AACTTCACCACGATCAATGGC
sgGGT4_rev	AGCTCATGTCCTCTCTCTGCT
sgLBD39_fw	TGAACTCCAACGTCCTGCTTT
sg_LBD39_rev	ATACGTGCCAGTTCCTGGTC
sgPGDH_fw	AGGTGGAATTGTCGTCAGTCA
sgPGDH_rev	CGACGAGAGATACACCGACG
sgPUP10_fw	ACGGCGGATCAAGAACTACAAA
sg_PUP10_rev	TGTATATAAAGTCACCCTGAGCCA
qPCR-EF-INA-fw	TGAGCACGCTCTTCTTGCTTTCA
qPCR-EF-INA-rev	GGTGGTGGCATCCATCTTGTTACA
VP16_cloning_fw	TCCGGAATTCCGTATGGCAATG
VP16_cloning_rev	TAGATCTAGATCATGTTTGACAGCTTATC
LBD42_fw3	TGCCTTCAATGGATCAAATC
LBD42_rev3	GTAGCACTAGAACTTGGGAG
Rap2.2B_fw	GTGTGGAGGAGCTATAATCTC
Rap2.2B_rev	CTTAGTAGTTGCGGTGAAGA
Rap2.2C_fw	TAAGGTGAATTTTCCCGAGG
Rap2.2C_rev	TATCCATTGTTACCTCCAGC
AOX1D_fw3_qPCR	AACGAGCGATTGTGTTCACG
AOX1D_rev3_qPCR	ACGATGAGCAAGTTTGGGTGA
PGDH_fw2_qPCR	GCGAGAAGAGCCAAAGGTCT

Table 4: Oligonucleotides used

Name	**Sequence**
PGDH_rev2_qPCR	AAATCGGCGGTGGAGATAGC
PAP1_fw_qPCR	CTGGTCGGACCGAAATGA
PAP1_rev_qPCR	GGTGTTGTAGGAATGGGCGT
AtLBD41_K135R_fw	CATCCGACATATCTCCAGGGATGATAACTCTGCCGC
AtLBD41_K135R_rev	GCGGCAGAGTTATCATCCTTGGAGATATGTCGGATG
AtLBD41_K172R_fw	GCGGAATCGGAGGGAAGGTCTGACGAGGC
AtLBD41_K172R_rev	GCCTCGTCAGACCTTCCCTCCGATTCCGC
AtLBD41_K197R_fw	CATGAAGGAGAGAGCAGGGAATCCGAGAGCAATG
AtLBD41_K197R_rev	CATTGCTCTCGGATTCCCTGCTCTCTCCTTCATG
AtLBD41_K221_fw	GGCTCCGGCGAGATAAGGCTTGACCTAACTTTAAG
AtLBD41_K221_rev	CTTAAAGTTAGGTCAAGCCTTATCTCGCCGGAGCC
AtLBD41_K253_fw	GTTTGGCACGTGTCAGAGGGAGAGCACGTGTAAG
AtLBD41_K253_rev	CTTACACGTGCTCTCCCTCTGACACGTGCCAAAC
LBD41rev_mut_mitStop	AGAAAGCTGGGTTTACACCACATGATACGCACG
SLAH3_qPCR_fw	GGCGTACACCTTTCCGATGA
SLAH3_qPCR_rev	AGCAGTGCGAACACGACTAA
AtLBD41_Crispr1_fw	ATTGAAAACCACTAACCAGGACGA
AtLBD41_Crispr1_rev	AAACTCGTCCTGGTTAGTGGTTTT
AtLBD41_Crispr2_fw	ATTGGCTTTGTCAAGACGCCGTGG
AtLBD41_Crispr2_rev	AAACCCACGGCGTCTTGACAAAGC
AtLBD41_Crispr3_fw	ATTGTCCAGCACGGCCATAGAACT
AtLBD41_Crispr3_rev	AAACAGTTCTATGGCCGTGCTGGA
prSLAH3_rev_NcoI	AGTGCCATGGTTTTTTCTTCTTTTTAATTTC
prSLAH3_fw_BamHI	ATTAGGATCCAGATCTTTTTTGGGTTTTTTC
prSLAH3seq_fw	GCAAAGTCTAGTGGTGTTGCC
LBD41_fw4	CGGATGAGCTGTAATGGATGC

Table 4: Oligonucleotides used

Name	**Sequence**
LBD41_rev4	CTAGCCTCGTCAGACTTTCCC
LBD41_rev	ACGCCGATCCTTCTCTTCTTA
LBD41_fw_realtime	GTTCTTCGGAAAGGGTGTAGTGAG
HADLH_fw_qPCR	CGCTGCGTCTAACAATTCCG
HADLH_rev_qPCR	GGCGTTTTGGGAAGTGAACC
AtADH1_qPCR_fw	TCACTTCTCTCTGTCACACCG
AtADH1_qPCR_rev	TCATGGCCGAAGATACGTGG
PAP1_semi_fw	CCATGGAGGGTTCGTCCAAA
PAP1_semi_rev	TCGTCGCTTCAGGAACCAAA
pBT10_Seq	ATTCCGCGTACGTGATGTTC
pHBTL_fw_seq	ATGACGCACAATCCCACTATC
pHBTL_rev_seq	TGCGCGCTATATTTTGTTTTC
LBD41fw_mitStart	AAAAAGCAGGCTTAATGCGGATGAGCTGTAATG
LBD41rev_short_ohneStop	AGAAAGCTGGGTTCTTCACAGCCGGAGGCGAGA
LBD41rev_short_mitStop	AGAAAGCTGGGTTTACTTCACAGCCGGAGGCGAG
LBD41rev_ohneStop	AGAAAGCTGGGTTGAGCATAAGCTCAGTCTTAC
LBD40_fw_realtime	AACAAGCTTTGCGACATAAGACAC
LBD40_rev_realtime	TGACTCAAAGACCTCACGTTTCTC
LBD41_fw_realtime	GTTCTTCGGAAAGGGTGTAGTGAG
LBD41_rev_realtime	CATAGAACTTGGCGAGAAAGACAG
LBD41_fwRT2	CGTGCTGGACTCATGAACCTCATC
LBD41_revRT2	GATCGGAAAATCCCAGGACGAAGG
Tub_ATH_fw	CTCAAGAGGTTCTCAGCAGTA
Tub_ATH_rev	TCACCTTCTTCATCCGCAGTT
qPCR_NbUbe35_fw	CTTCAGATTCGCACCGTTCT
qPCR_NbUbe35_rev	CCAATGCTTCGCAATGTTCTC

Table 5: Plasmids used

Name	Cloned by	Content
pDONR221	(Invitrogen, 2003)	attP flanked ccdB
pDONR221: LBD41	Judith Bäumler	attL flanked LBD41
pDONR221: LBD41 K105R (K2R)	Judith Bäumler	attL flanked LBD41 K105R
pDONR221: LBD41 K135R	Marvin Hönle	attL flanked LBD41 K135R
pDONR221: LBD41 K172R	Marvin Hönle	attL flanked LBD41 K172R
pDONR221: LBD41 K197R	Marvin Hönle	attL flanked LBD41 K197R
pDONR221: LBD41 K221:R	Marvin Hönle	attL flanked LBD41 K221R
pDONR221: LBD41 K253R	Marvin Hönle	attL flanked LBD41 K253R
pDONR221: LBD41 K105R K135R	Marvin Hönle	attL flanked LBD41 K105R K135R
pDONR221: LBD41 K105R K172R	Marvin Hönle	attL flanked LBD41 K105R K172R
pDONR221: LBD41 K105R K197R	Marvin Hönle	attL flanked LBD41 K105R K197R
pDONR221: LBD41 K105R K221R	Marvin Hönle	attL flanked LBD41 K105R K221R
pDONR221: LBD41 K105R K253R	Marvin Hönle	attL flanked LBD41 K105R K253R
pDONR221: LBD41 K105R K221R K135R	Marvin Hönle	attL flanked LBD41 K105R K221R K135R

Table 5: Plasmids used

Name	Cloned by	Content
pDONR221: LBD41 K105R K221R K172R	Marvin Hönle	attL flanked LBD41 K105R K221R K172R
pDONR221: LBD41 K105R K221R K197R	Marvin Hönle	attL flanked LBD41 K105R K221R K197R
pDONR221: LBD41 K105R K221R K253R	Marvin Hönle	attL flanked LBD41 K105R K221R K253R
pDONR221: prSLAH3	Marvin Hönle	attL flanked Promoter of AtSLAH3
pHBTL:GW:C'HA	(Kuhlmann et al., 2003)	pr35S attR flanked ccdB C'HA
pHBTL: HA:GW	Philipp Gasch	pr35S: attR flanked ccdB N'HA
pHTBL:GW:VP16 C'HA	Philipp Gasch	pr35S: attR flanked ccdB VP16 C'HA
pHBTL: LBD41 C'HA	Judith Bäumler	pr35S: LBD41 C-term. HA tag
pHBTL: LBD41 N'HA	Marvin Hönle	pr35S: LBD41 N-term. HA tag
pHBTL: LBD41-VP16 C'HA	Judith Bäumler	pr35S: LBD41ΔEAR:VP16 C-term. HA tag
pHBTL: LBD40 C'HA	Judith Bäumler	pr35S: LBD40 C-term. HA tag
pHBTL: LBD40-VP16 C'HA	Judith Bäumler	pr35S: LBD40ΔEAR:VP16 C-term. HA tag
pHBTL: LBD42 C'HA	Judith Bäumler	pr35S: LBD42 C-term. HA tag
pHBTL: LBD42-VP16 C'HA	Judith Bäumler	pr35S: LBD42ΔEAR:VP16 C-term. HA tag
pHBTL: LBD41_short_mut C'HA	Marvin Hönle	pr35S: AtLBD41* (early STOP, as in lbd41*)
pHBTL: LBD41 K105R C'HA	Marvin Hönle	pr35S: LBD41 K105R C-term. HA tag

Table 5: Plasmids used

Name	**Cloned by**	**Content**
pHBTL: LBD41-VP16 K105R C'HA	Marvin Hönle	pr35S: LBD41ΔEAR:VP16 K105R C-term. HA tag
pHBTL: LBD41 K135R C'HA	Marvin Hönle	pr35S: LBD41 K135R C-term. HA tag
pHBTL: LBD41 K172R C'HA	Marvin Hönle	pr35S: LBD41 K172R C-term. HA tag
pHBTL: LBD41 K197R C'HA	Marvin Hönle	pr35S: LBD41 K197R C-term. HA tag
pHBTL: LBD41 K221R C'HA	Marvin Hönle	pr35S: LBD41 K221R C-term. HA tag
pHBTL: LBD41 K253R C'HA	Marvin Hönle	pr35S: LBD41 K253R C-term. HA tag
pHBTL: LBD41 K105R K135R C'HA	Marvin Hönle	pr35S: LBD41 K105R K135R C-term. HA tag
pHBTL: LBD41 K105R K172R C'HA	Marvin Hönle	pr35S: LBD41 K105R K172R C-term. HA tag
pHBTL: LBD41 K105R K197R C'HA	Marvin Hönle	pr35S: LBD41 K105R K197R C-term. HA tag
pHBTL: LBD41 K105R K221R C'HA	Marvin Hönle	pr35S: LBD41 K105R K221R C-term. HA tag
pHBTL: LBD41 K105R K253R C'HA	Marvin Hönle	pr35S: LBD41 K105R K253R C-term. HA tag
pHBTL: LBD41 K105R K221R K135R C'HA	Marvin Hönle	pr35S: LBD41 K105R K221R K135R C-term. HA tag
pHBTL: LBD41 K105R K221R K172R C'HA	Marvin Hönle	pr35S: LBD41 K105R K221R K172R C-term. HA tag

Table 5: Plasmids used

Name	Cloned by	Content
pHBTL: LBD41 K105R K221R K197R C'HA	Marvin Hönle	pr35S: LBD41 K105R K221R K197R C-term. HA tag
pHBTL: LBD41 K105R K221R K253R C'HA	Marvin Hönle	pr35S: LBD41 K105R K221R K253R C-term. HA tag
pBT10: GAL4 UAS LUC	Judith Bäumler	attR flanked ccdB: Firefly Luciferase
pBT10: pRUC	Judith Bäumler	pr35S: Renilla Luciferase
pBT10: prPAP1: LUC	Judith Bäumler	prPAP1: Firefly Luciferase
pBT10: prLBD39: LUC	Judith Bäumler	prLBD39: Firefly Luciferase
pBT10: prAOX1D: LUC	Judith Bäumler	prAOX1D: Firefly Luciferase
pBT10: prPUP10: LUC	Judith Bäumler	prPUP10: Firefly Luciferase
pBT10 prSLAH3: LUC	Marvin Hönle	prSLAH3: Firefly Luciferase
pK7FWG2	(Karimi et al., 2002)	RB/LB flanked: pr35S: attR flanked ccdB
pK7FWG2: C'GFP	Angelika Mustroph	RB/LB flanked: pr35S: C-term. GFP
pK7FWG2: LBD41 C-term. GFP	Judith Bäumler	RB/LB flanked: pr35S: LBD41 C-term. GFP
pK7FWG2: LBD40 C'GFP	Judith Bäumler	RB/LB flanked: pr35S: LBD40 C-term. GFP
pK7FWG2: LBD41-VP16 C'HA	Judith Bäumler	RB/LB flanked: pr35S: LBD41ΔEAR:VP16 C-term. HA
pK7FWG2: HA-LBD41 C'GFP	Judith Bäumler	RB/LB flanked: pr35S: N-term. HA LBD41ΔEAR:VP16 C-term. GFP
pK7FWG2: LBD41 C'HA	Marvin Hönle	RB/LB flanked: pr35S: LBD41 C-term. HA
pKSE401: Crispr1	Marvin Hönle	guide strain LBD41 Crispr1, pr35S:Cas9

Table 5: Plasmids used

Name	Cloned by	Content
pKSE401: Crispr2	Marvin Hönle	guide strain LBD41 Crispr2, pr35S:Cas9
pKSE401: Crispr3	Marvin Hönle	guide strain LBD41 Crispr3, pr35S:Cas9

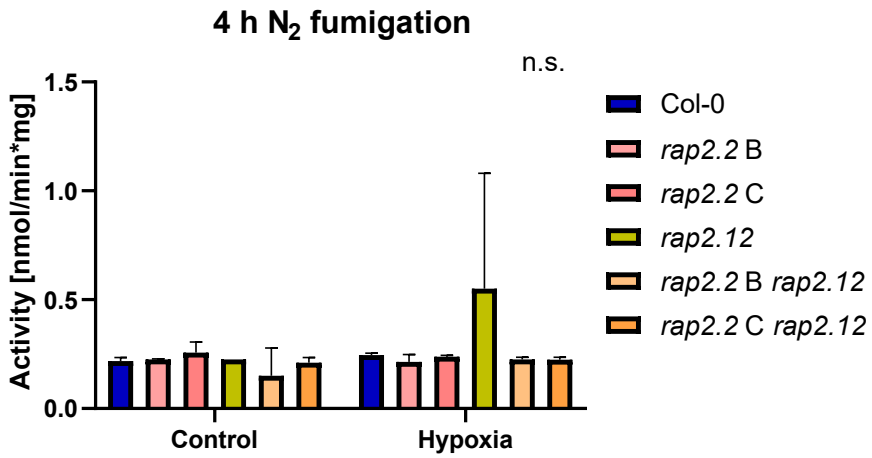

Figure 30: No ADH activity after 4 h of hypoxia

ADH activity of 7 d old seedlings. Plants were treated with N_2 (Hypoxia) or air (Control) for 4 h. Protein samples were extracted, quantified by Bradford and their ADH activity measured. Graphs show the average ±standard deviation of 3 biological replicates. No significant differences were calculated in a statistical analysis (Two-way ANOVA, Tukey post-hoc). Data was collected by Sabrina Teubner.

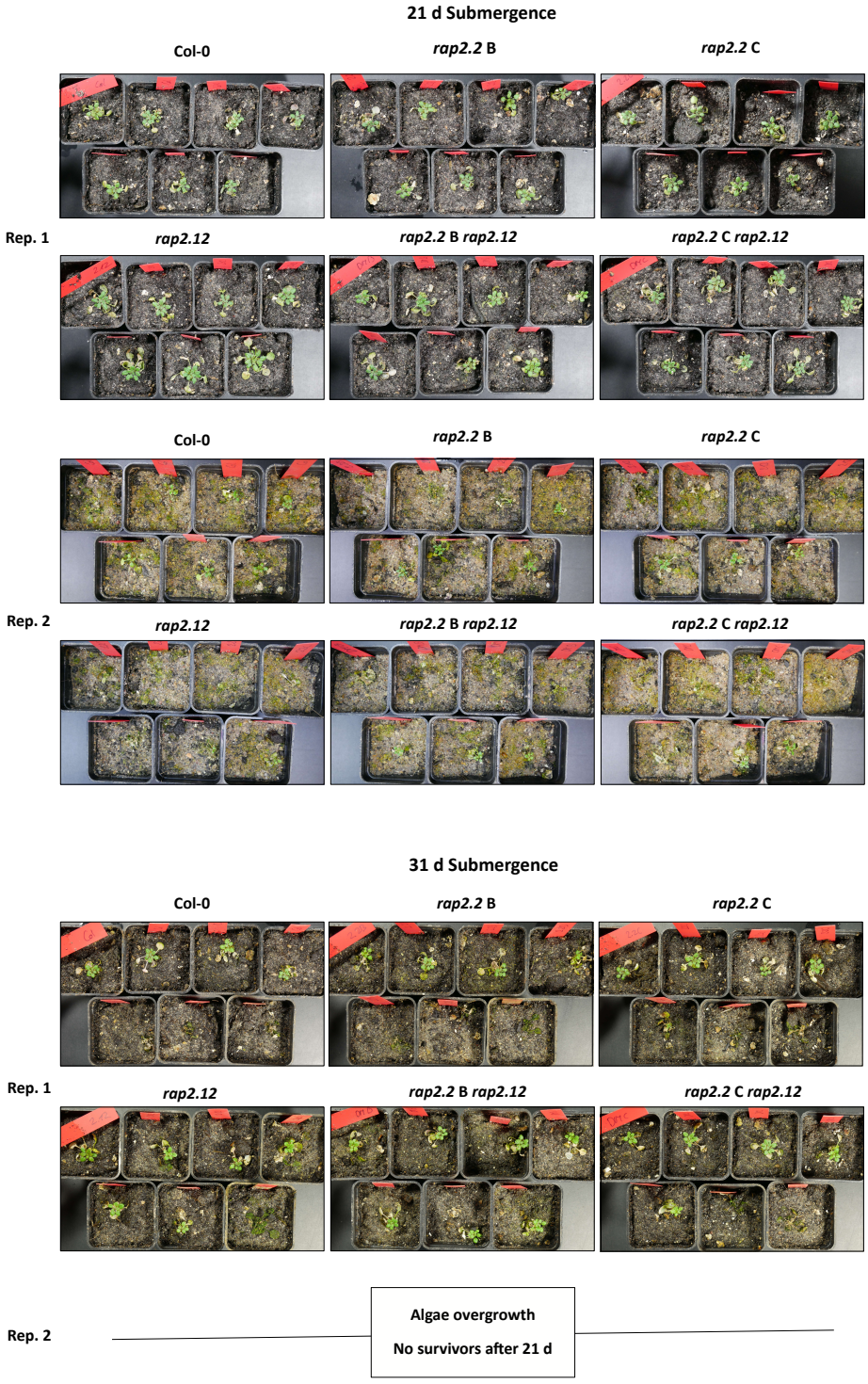

Figure 31: Submergence phenotype of RAP mutants
Pictures of submerged plants after recovery. Plants were germinated on MS agar, transferred to soil and grown under short day conditions until 21 d old. Plants were fully submerged for 21 to 31 d, followed by subsequent recovery for 14 d. Figure shows no visual differences between genotypes of *rap2.2* and *rap2.12* mutants. Different intensity of algae growth between replicates is depicted. Pictures are representative of 4 biological replicates, 7 plants each time point.

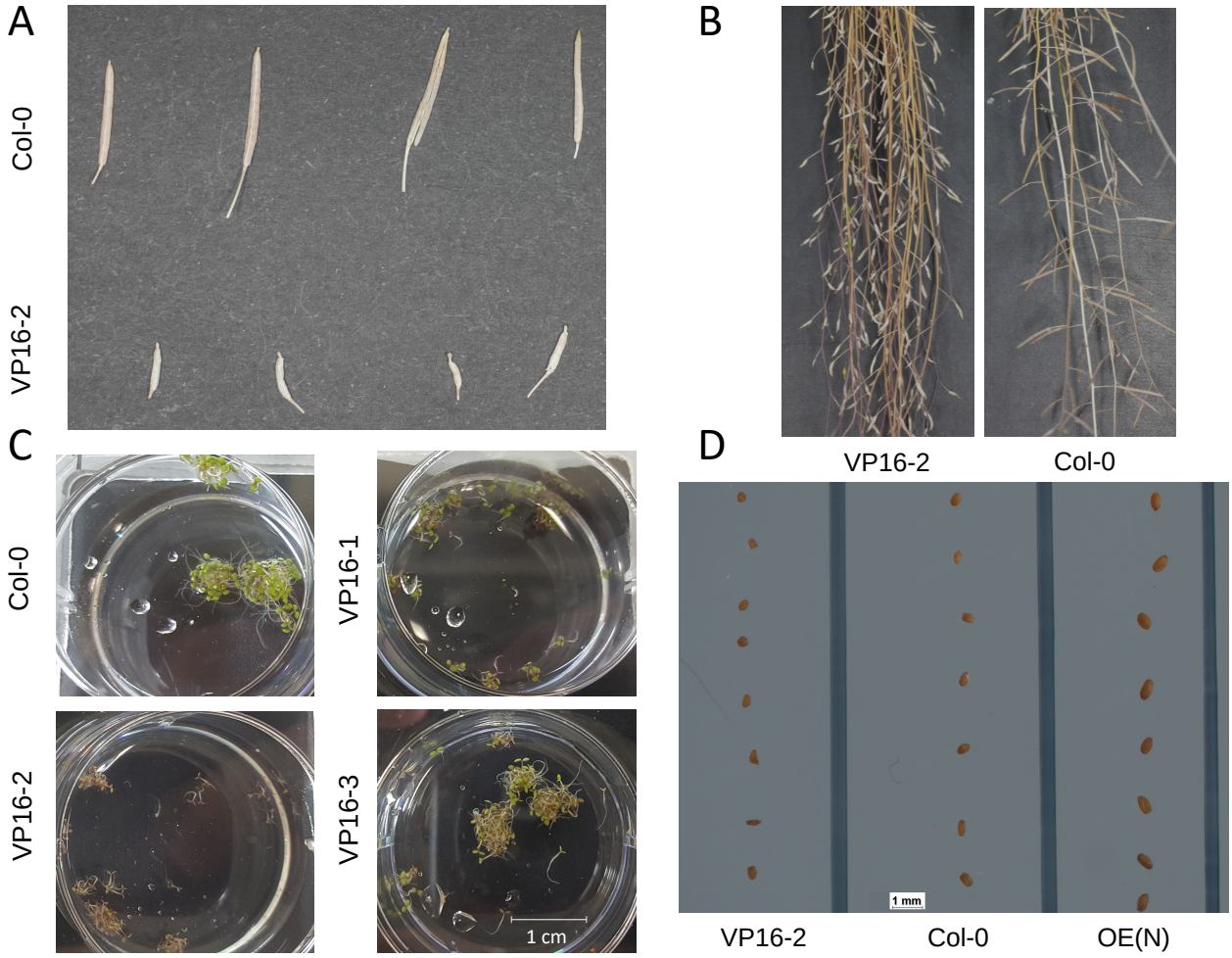

Figure 32: Phenotypes of LBD41 misregulation

Various phenotypic effects displayed in overexpression lines of native LBD41 or LBD41ΔEAR:VP16. Pictures display a seed pod phenotype encountered in VP16-2, leading to short, malformed silique (A and B). All VP16 lines showed visibly increased anthocyanin content during liquid germination, reduced size of VP16-2 (C). Seeds of VP16-2 were also affected, showing decreased size and misshapen development. Contrary, the overexpression line of HA'LBD41'GFP (OE(N)) displayed increased seed size compared to Col-0 (D). Seed phenotype of OE(N) was not analyzed for repeatability.

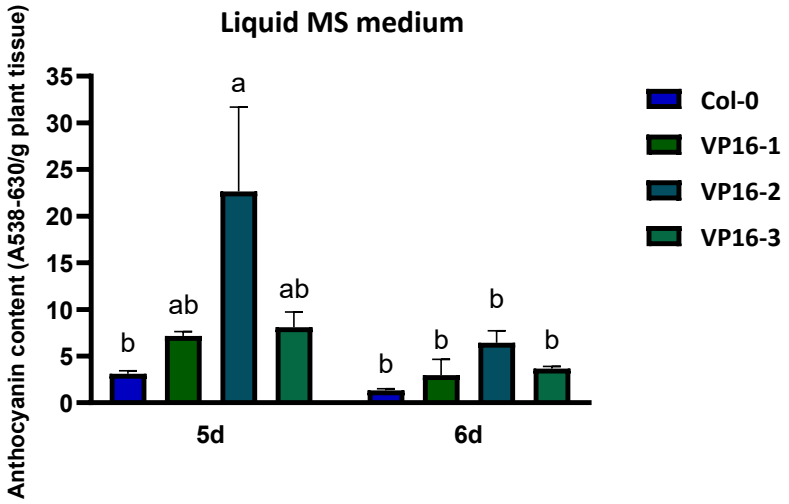

Figure 33: Anthocyanin content decrease

Seedlings of Col-0 or three independent pr35S:LBD41ΔEAR:VP16 lines 1, 2 and 3 were germinated in liquid MS medium. All growth took place under long day conditions. Samples were harvested at 5 or 6 d after transferal to long day growth conditions, followed by determination of their fresh weight. Anthocyanin content was calculated from photometrically measured difference of A_{538}-A_{630}, per g of tissue fresh weight. Graphs show the average with standard deviation of 3 biological replicates. Letters indicate significant differences ($p<0.05$) calculated from a statistical analysis (Two-way ANOVA, Tukey post-hoc test).

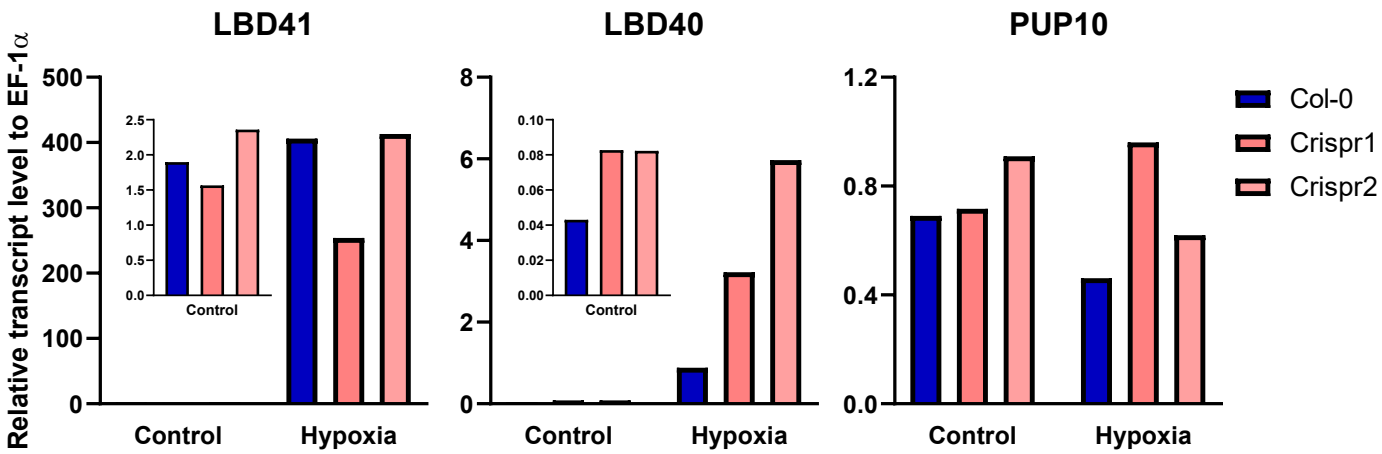

Figure 34: Preliminary qPCR results of Crispr *lbd41*

Seedlings of presumably homozygous *lbd41* lines of Crispr1 and Crispr2 were germinated on MS Agar. At 7 d old, seedlings were fumigated with N_2 or air for 8 h under long day conditions. Seedling samples were collected, RNA extracted and reverse transcribed. Transcript level was analyzed in a qPCR and referenced to EF1α. Transcript levels of LBD41, LBD40 and PUP10 were measured for mutant and wildtype samples. Graphs shows the result of a single biological replicate. Primers for LBD41 align in the unedited N-terminal LOB motif. Data was collected by Robin Bär.

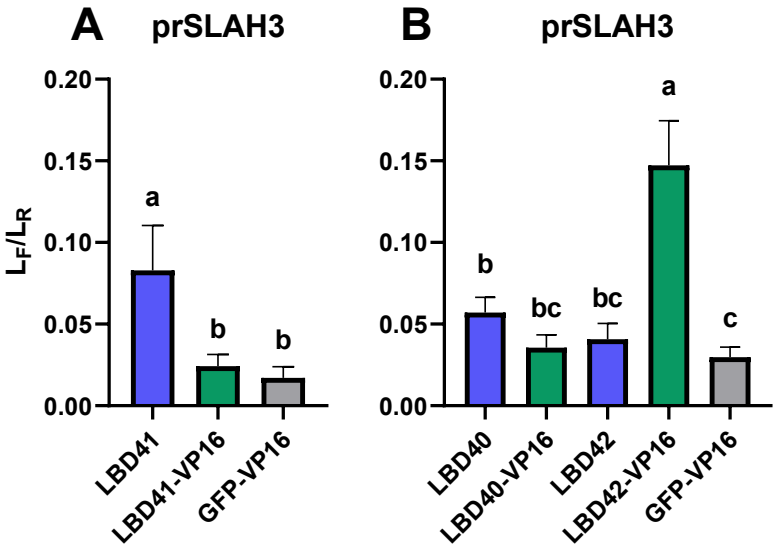

Figure 35: SLAH3 promoter activity of LBD41 homologs

Protoplasts were isolated from 4-6 week old Col-0 plants grown under short day conditions. Cells were transformed with a pBT10 prSLAH3:luc reporter and pr35S:luc normalization plasmid. Co-transformation of pHBTL pr35S: of LBD41, the ΔEAR:VP16 mutant or a GFP-VP16 control (A) or their homologs (B). Graphs represent average ±standard deviation of 3 biological replicates, with 2 technical replicates each. Letters indicate significant differences $p<0.05$ calculated in a statistical analysis (One-way ANOVA, Tukey post-hoc).

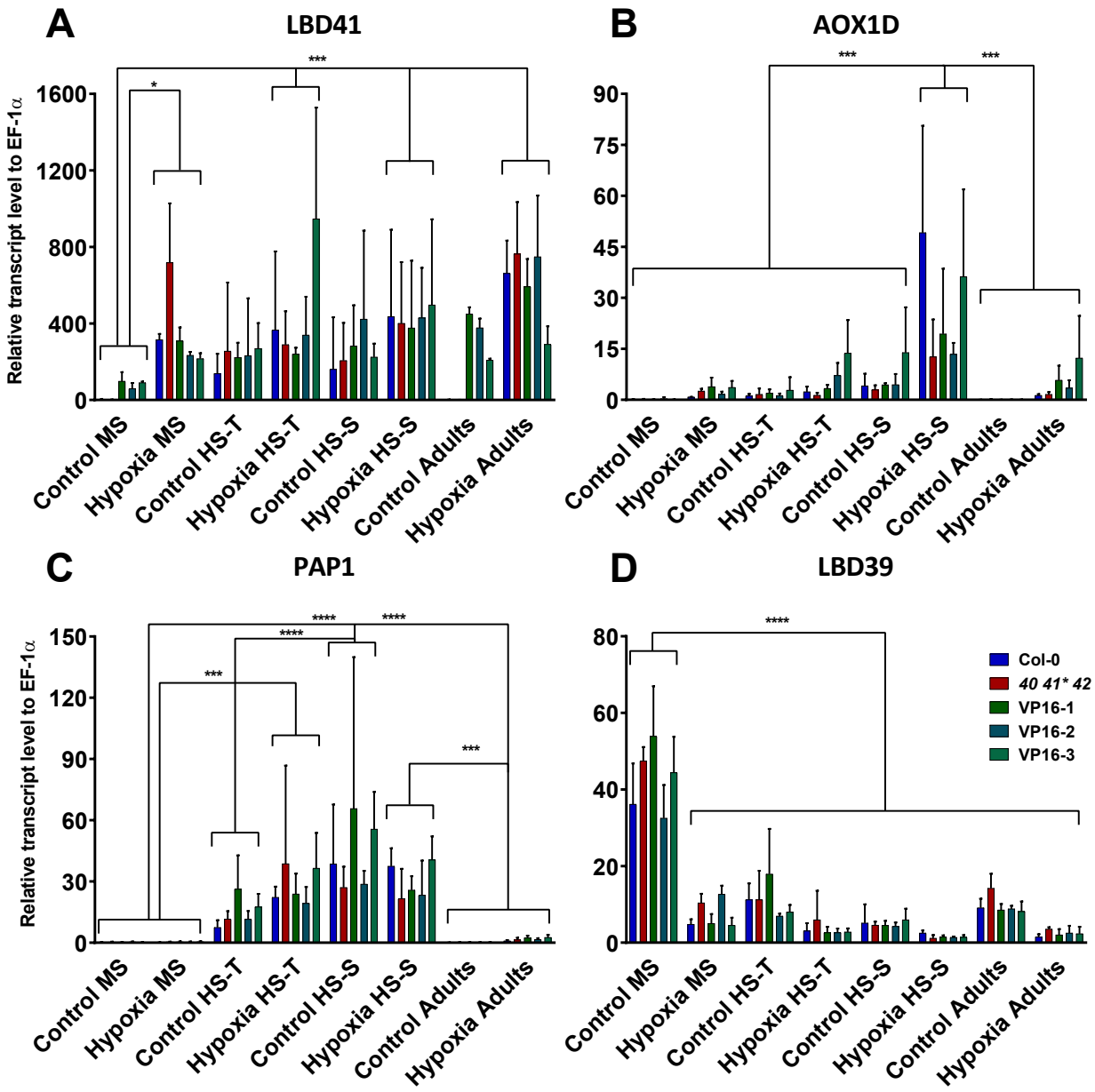

Figure 36: Comparison of transcript levels across treatments

Plants of Col-0, *lbd40 lbd41* lbd42* and VP16 lines 1, 2 and 3 were treated at 7 d old on MS medium or Hoagland with 50 mM NaCl (HS). Seedlings grown on HS medium were separated based on phenotype into salt tolerant (HS-T) or sensitive (HS-S). Adults were germinated on MS, then transferred to soil and treated at 28 d old. Plants were treated with either air (Control) or N_2 (Hypoxia) for 8 h. Total RNA was extracted, reverse transcribed and quantified by qPCR. Transcripts of LBD41 (A) AOX1D (B) PAP1 (C) and LBD39 (D) are analyzed. Transcript levels were calculated relative to EF-1α. Graphs show the average ±standard deviation of 3-4 biological replicates. Asterisks represent significant differences between treatments, calculated in a statistical analysis (Two-way ANOVA, Tukey post-hoc).

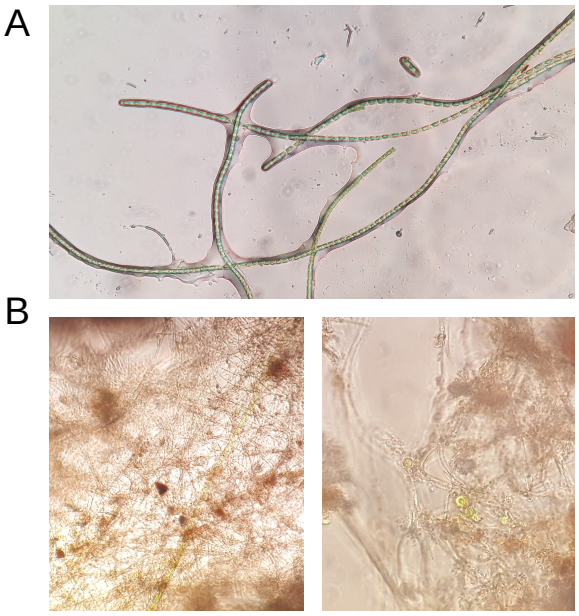

Figure 37: Algae encountered during submergence

Microscopic pictures of algae species during contained flooding experiments. Identified were a common fresh water green algae, likely of the *Zygnema* genus (A). Overgrowth originating from the soil during submergence could not be identified (B). Pictures were taken using a DPlan 10x, 0.25, 160/0.17 lens.

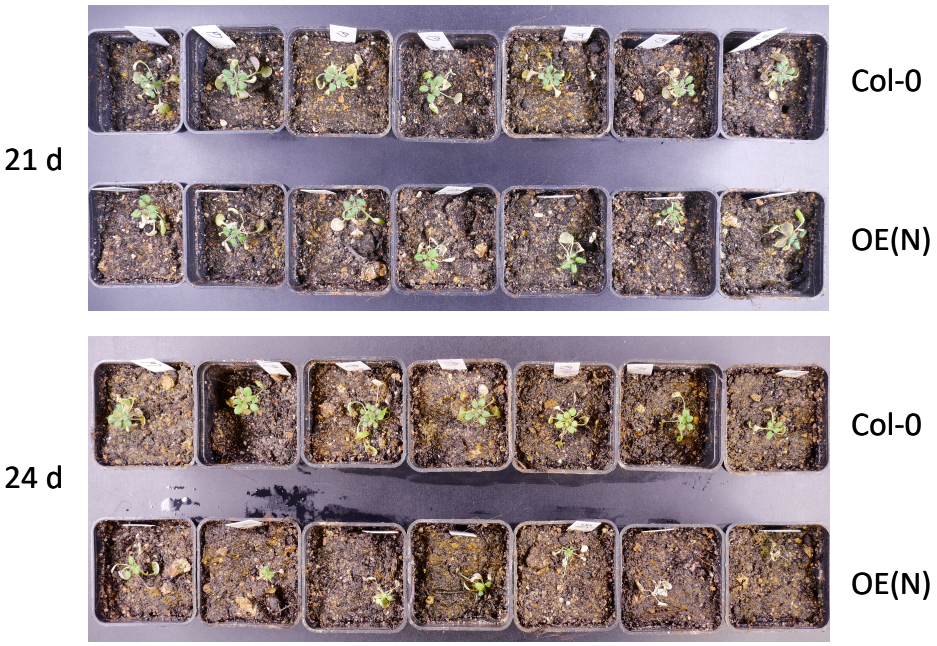

Figure 38: LBD41 OE recovery difference after submergence

Pictures of submerged plants after recovery. Plants were germinated on MS agar, transferred to soil and grown under short day conditions until 28 d old. Plants were fully submerged for 21 to 31 d, followed by subsequent recovery for 14 d. Figure shows the differences between Col-0 and OE(N) after 21 and 24 d of stress. Pictures are representative of 4 biological replicates, 7 plants each time point.

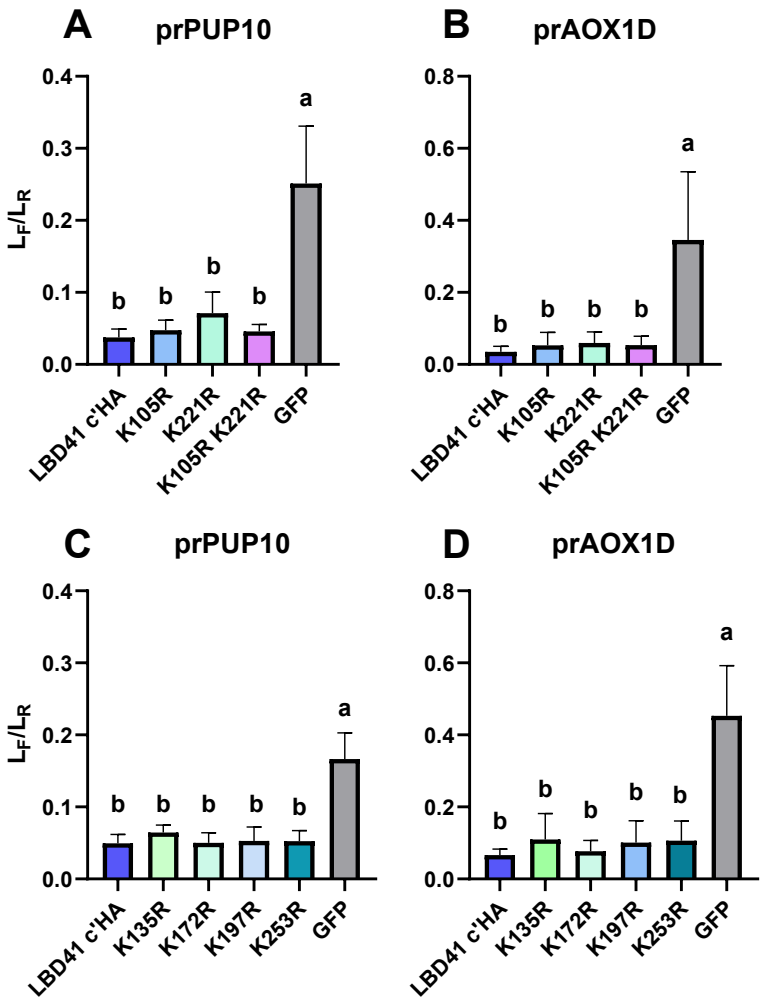

Figure 39: Protoplast activity assay of single SUMO mutants and K105R K221R

Protoplasts were isolated from 4-6 week old Col-0 plants grown under short day conditions. Cells were transformed with pBT10:luc reporter and pr35S:luc normalization plasmid. Co-transformation of pHBTL pr35S:LBD41 with various lysine to arginine mutations. Target reporter vectors were tested with promoters of PUP10 (A and C) or AOX1D (B and D). Graphs represent average ±standard deviation of 3 biological replicates, with 2 technical replicates each. Letters indicate significant differences $p<0.05$ calculated in a statistical analysis (One-way ANOVA, Tukey post-hoc). Data was collected by Carolin Schnedermann.

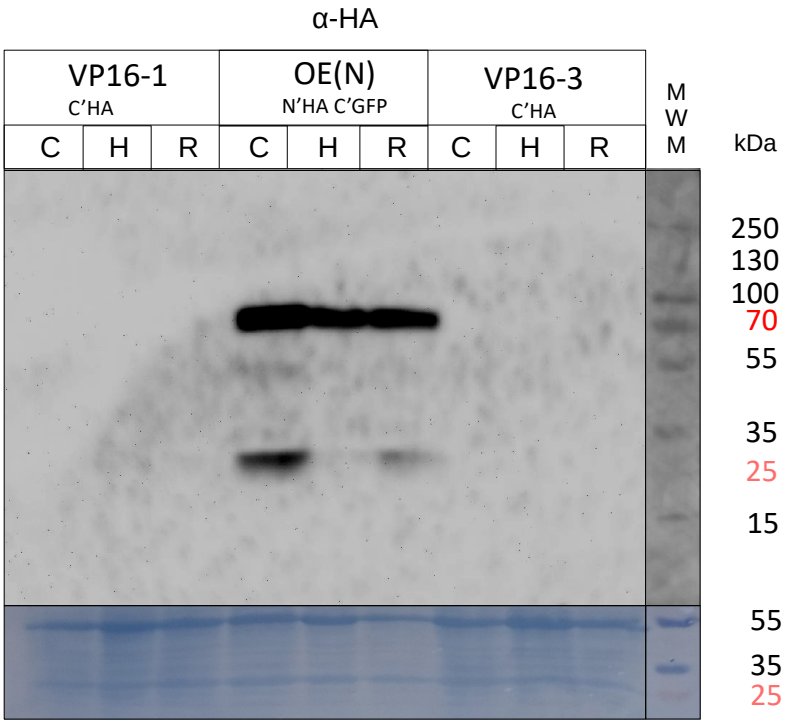

Figure 40: Western blot of seedlings

Seedlings of HA-tagged native LBD41 and LBD41-VP16 overexpressing lines were grown on MS Agar. At 7 d old under long day conditions, seedlings were treated with 8 h of fumigation with air (C), N_2 gas (H) or N_2 followed by 1 h of reaeration with air (R). Proteins were extracted with the alternative extraction buffer, separated by SDS-PAGE and detected by western blot using α-HA primary and anti-Mouse-HRG secondary antibodies. Image is representative of two biological replicates.Detection of chemiluminescent signal was performed with 10 min exposure. Molecular weight marker (MWM) was applied as PageRuler Prestained Protein Ladder (Thermo Fisher Scientific Inc.) which contained standards for 250, 130, 100, 70, 55, 35, 25, 15 and 10 kDa. Blots were stained with coomassie brilliant blue after signal detection.

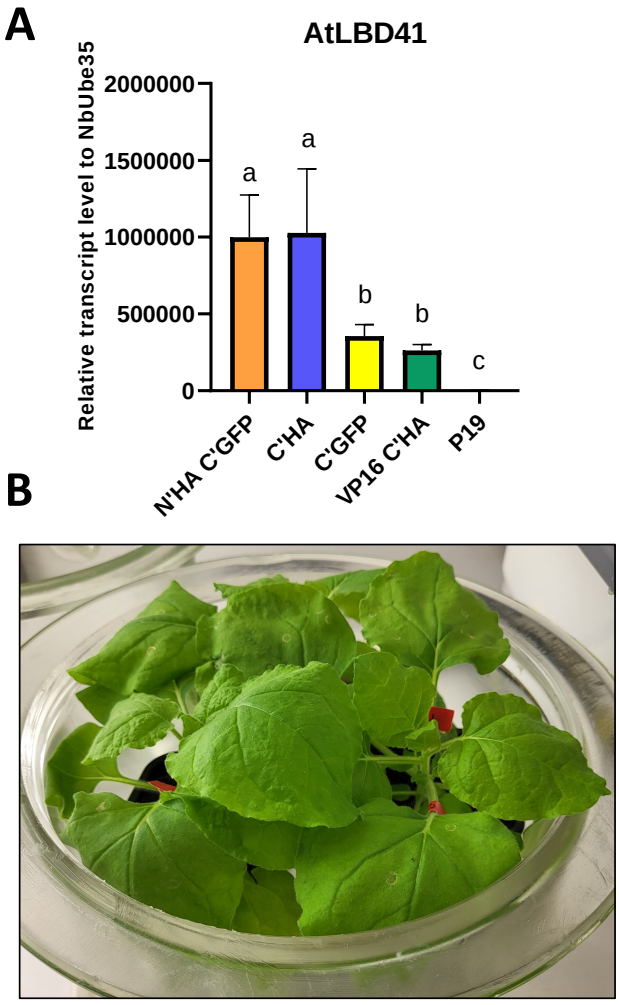

Figure 41: Heterologous expression transcripts and treatment setup

Transcript levels of heterologously expressed *At*LBD41 in *N. benthamiana*. Plants were infiltrated with pK7FWG2 pr35S:LBD41 variants carried by *A. tumefaciens* Samples had their RNA extracted, reverse transcribed and analyzed by qPCR. Transcript levels were referenced to *Nb*UBE35. Graphs represent the average ±standard deviation of 4 biological replicates, extracted from 3 leaf discs per replicate. Data shows the transcripts of plants used for protein detection through western blot (Supplementary, Fig. 42 and Fig. 43 Rep. 3 - Rep. 6). Letters represent significant differences calculated in a statistical analysis (Two-way ANOVA, Tukey post hoc) Data collected by Emma Düthorn (A). Also depicted is the setup for hypoxia treatment of *N. benthamiana* inside a desiccator. Picture is representative of the random shading effect during nitrogen fumigation (B).

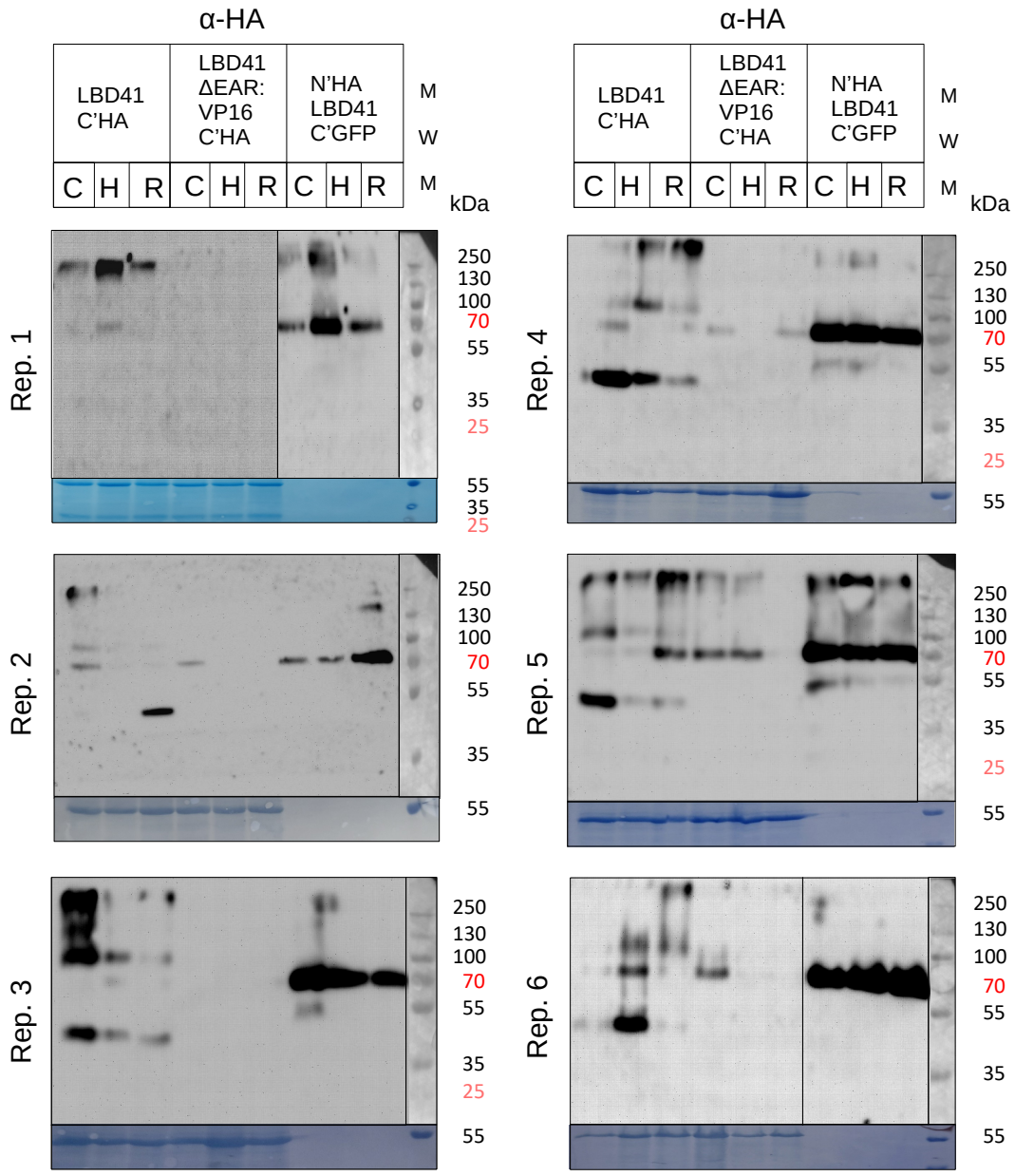

Figure 42: Western blot of HA-tagged LBD41 variants

Leaves of 3 w old *N.benthamiana* were co-infiltrated using transformed *A. tumefaciens* carrying a pBin19 anti-silencing plasmid and pK7FWG2 expression vector. Heterologous expression of HA-tagged LBD41 was performed with a constitutive 35S promoter under long day conditions for 65 h. Plants were then subjected to 2 h of fumigation with air (C), N_2 (H) or N_2 followed by 1 h of reaeration with air (R). Proteins were extracted, separated by SDS-PAGE and detected by western blot using α-HA primary and anti-Mouse-HRG secondary antibodies. Images represent 6 biological replicates for infiltration and treatment, with an alternative extraction buffer used for the first two replicates. Detection of chemiluminescent signal was performed with 10 min exposure. Molecular weight marker (MWM) was applied as PageRuler Prestained Protein Ladder (Thermo Fisher Scientific Inc.) which contained standards for 250, 130, 100, 70, 55, 35, 25, 15 and 10 kDa. Blots were stained with coomassie brilliant blue after signal detection.

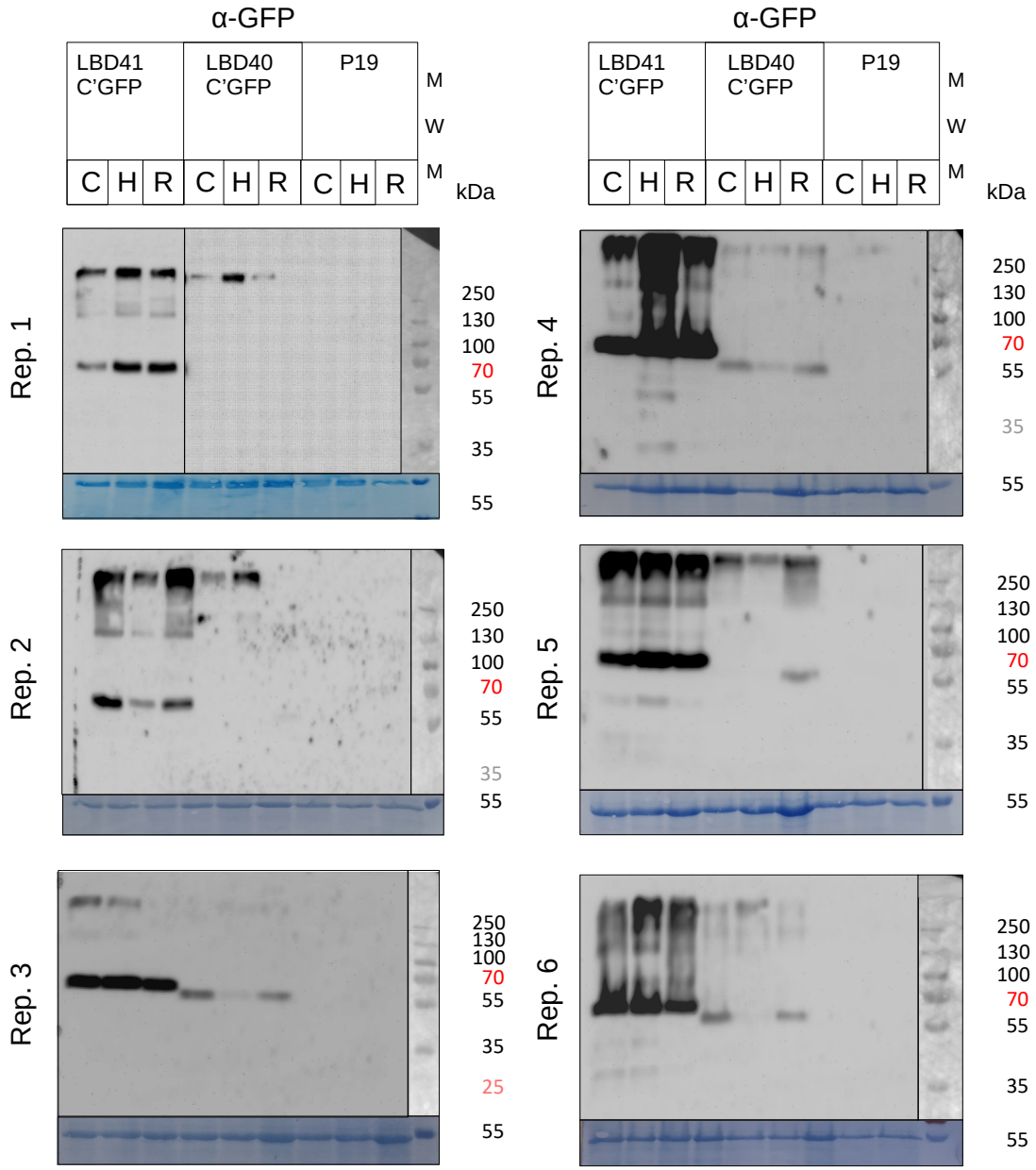

Figure 43: Western blot of GFP-tagged LBD41 and LBD40

Leaves of 3 w old *N.benthamiana* were co-infiltrated using transformed *A. tumefaciens* carrying a pBin19 anti-silencing plasmid and pK7FWG2 expression vector. Heterologous expression of GFP-tagged LBD41 was performed with a constitutive 35S promoter under long day conditions for 65 h. Plants were then subjected to 2 h of fumigation with air (C), N_2 (H) or N_2 followed by 1 h of reaeration with air (R). Proteins were extracted, separated by SDS-PAGE and detected by western blot using α-GFP primary and anti-Mouse-HRG secondary antibodies. Images represent 6 biological replicates for infiltration and treatment, with a different extraction buffer used after the second replicate. Detection of chemiluminescent signal was performed with 10 min exposure. Molecular weight marker (MWM) was applied as PageRuler Prestained Protein Ladder (Thermo Fisher Scientific Inc.) which contained standards for 250, 130, 100, 70, 55, 35, 25, 15 and 10 kDa. Blots were stained with coomassie brilliant blue after signal detection.

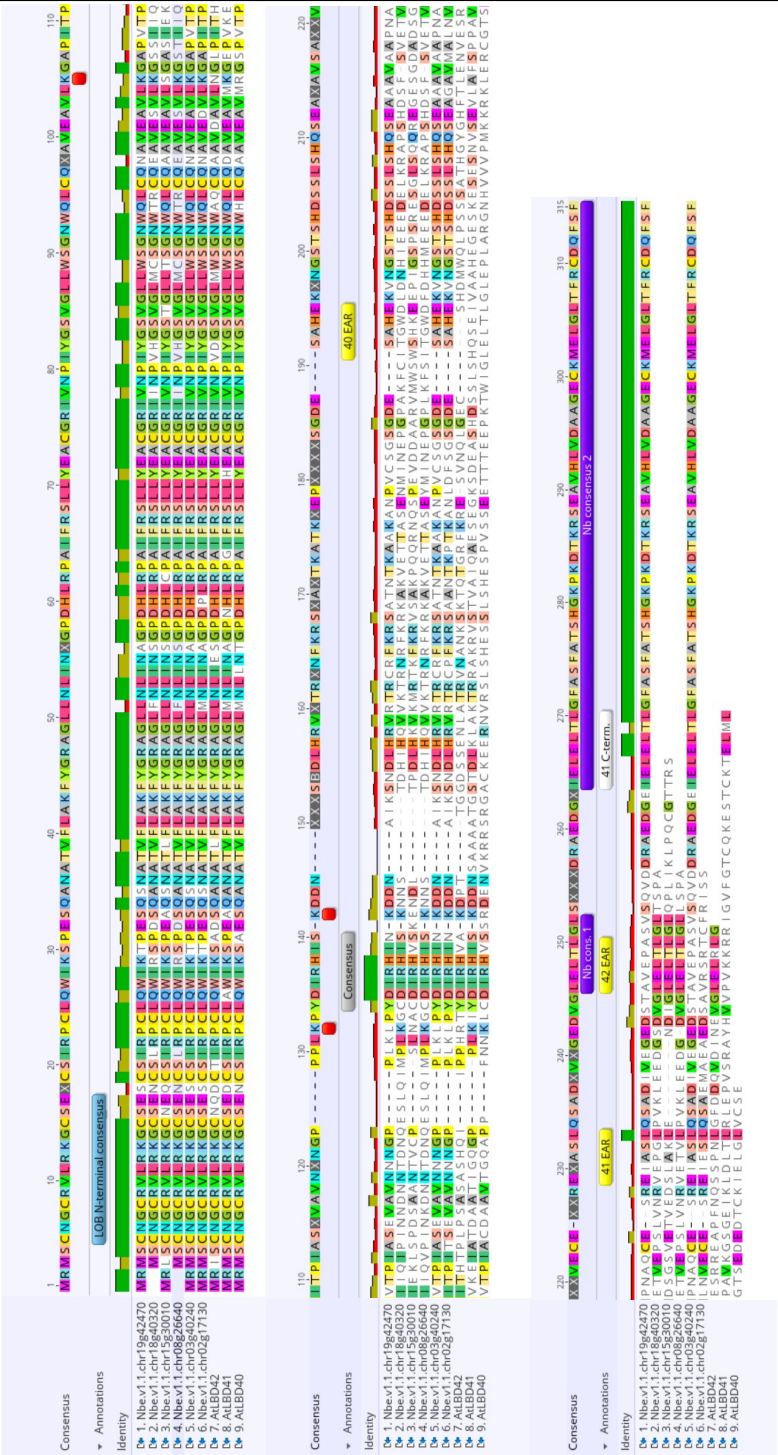

Figure 44: Protein Alignment of *At*LBD41 homologs with *N. benthamiana*

Amino acid sequences of *At*LBD41, *At*LBD40 and *At*LBD42 aligned with six putative homologs identified in *N. benthamiana*. Alignment performed in Geneious2024 with the Blosum62 matrix, gap open penalty 12, extension penalty and refinement iterations of 3. Conserved residues are highlighted. Annotated are the LOB consensus motif (blue), conserved lysine residues (red) and connecting consensus (grey). Also marked are the EAR motifs of *A. thaliana* homologs (yellow) and two *N. benthamiana* consensus sites containing EAR domains (purple).

List of Figures

List of Tables

They merely adopted the hypoxia. I was born in it, moulded by it. I couldn't take a deep breath until I was already a man.

– This asthmatic Author (Modified from The Dark Knight Rises, 2012)

Acknowledgement

For the supervision of this work, special thanks go to Prof. Dr. Angelika Mustroph. Without her constant feedback, availability for questions and in-depth knowledge, this work would not have been possible. I'm especially grateful for the organisation of and invitation to the ISPA 2022 conference.

Further thanks for their constructive feedback go to the entire chair of Plant Physiology, particularly Prof. Dr. Stephan Clemens, Dr. Michael Weber, Dr. Fabrizio Barozzi and Dr. Maria Klecker. Special thanks to Maria for her method of protein extraction, general lab and life advice. Additional thanks go to Ursula Ferrera, who provided invaluable help when dealing with bureaucracy. Further thanks go to my predecessors Dr. Phillip Gasch and Dr. Judith Bäumler, who advanced this topic and generated multiple constructs used here.

Thanks go to Alina Hieber, Sabrina Teubner, Miriam Prinzler, Carolin Schnedermann, Konrad Buchholz, Hayat Kopkin, Kathrin Döhla, Max Bauer, Emma Düthorn and Robin Bär, who performed some of the experiments shown in this Dissertation.

Further thanks go to my office- and lab mates Colleen Rafferty, Malte Bartylla, Lukas Ackermann, Alina Hieber and Sarah Nitsche. Especially, to Sarah who has been a great friend throughout my entire journey as a PhD-Student, and showed incredible strength during the Covid-19 pandemic.

Finally, my eternal gratitude goes to my family, who supported me all my life. To my grandparents, my parents Alfred and Ines, and my brother Yannic. Without their encouragement, I would not have made it this far.

Eidesstattliche Versicherungen und Erklärungen

(§ 8 Satz 2 Nr. 3 PromO Fakultät)
Hiermit versichere ich eidesstattlich, dass ich die Arbeit selbstständig verfasst und keine anderen als die von mir angegebenen Quellen und Hilfsmittel benutzt habe
(vgl. Art. 97 Abs. 1 Satz 8 BayHIG).

(§ 8 Satz 2 Nr. 3 PromO Fakultät)
Hiermit erkläre ich, dass ich die Dissertation nicht bereits zur Erlangung eines akademischen Grades eingereicht habe und dass ich nicht bereits diese oder eine gleichartige Doktorprüfung endgültig nicht bestanden habe.

(§ 8 Satz 2 Nr. 4 PromO Fakultät)
Hiermit erkläre ich, dass ich Hilfe von gewerblichen Promotionsberatern bzw. –vermittlern oder ähnlichen Dienstleistern weder bisher in Anspruch genommen habe noch künftig in Anspruch nehmen werde.

(§ 8 Satz 2 Nr. 7 PromO Fakultät)
Hiermit erkläre ich mein Einverständnis, dass die elektronische Fassung der Dissertation unter Wahrung meiner Urheberrechte und des Datenschutzes einer gesonderten Überprüfung unterzogen werden kann.

(§ 8 Satz 2 Nr. 8 PromO Fakultät)
Hiermit erkläre ich mein Einverständnis, dass bei Verdacht wissenschaftlichen Fehlverhaltens Ermittlungen durch universitätsinterne Organe der wissenschaftlichen Selbstkontrolle stattfinden können.

Ort *Datum* *Unterschrift*